PARTICLE KINETICS OF
GAS - SOLID PARTICLE MIXTURES

Thesis by

Roger Allison Haas

In Partial Fulfillment of the Requirements

For the Degree of

Doctor of Philosophy

California Institute of Technology

Pasadena, California

1969

(Submitted May 26, 1969)

DEDICATED TO MY FATHER

Mr. Allison Franklin Haas

ACKNOWLEDGMENTS

It is a pleasure to express my deep gratitude to Professor Frank E. Marble for suggesting this problem and for his advice, guidance, and encouragement during the course of this study.

I am also very grateful to Mrs. Virginia Conner and Mrs. Roberta Duffy for their excellent work in preparing this manuscript. I also wish to thank Mr. Frank T. Linton for helping prepare the figures.

Financial support from the California Institute of Technology, the Robert O. Law Foundation, the Florence and Daniel Guggenheim Foundation, the Alfred P. Sloan Foundation, the Ford Foundation, and the National Science Foundation is gratefully acknowledged.

Finally, I am particularly grateful to my wife, Donna, for her continuing understanding, cooperation, and encouragement.

ABSTRACT

In this thesis the interaction of a normal gas dynamic shock wave with a gas containing a distribution of small solid spherical particles of two distinct radii, σ_1 and σ_2, is studied (1) to demonstrate that the methods of kinetic theory can be extended to treat solid particle collision phenomena in multidimensional gas-particle flows; (2) to elucidate some of the essential physical characteristics associated with particle-particle collision processes; and (3) to give some indication regarding the importance of particle collisions in particle-laden gas flows. It is assumed that upstream of the shock wave particles σ_1 are uniformly distributed while particles σ_2 are non-uniformly distributed parallel to the shock face and in much smaller numbers than particles σ_1. Under these conditions the gas-particle σ_1 flow downstream of the shock wave is very nearly one-dimensional and independent of the presence of particles σ_2. The usual shock relaxation zone is established by the interaction of particles σ_1 and the gas downstream of the shock wave. The collisional model proposed by Marble[3] is then extended and used with a modified form of the mean free path method of kinetic theory to calculate the macroscopic distribution and velocity of particles σ_2 as determined by the particle σ_1 - particle σ_2 and particle σ_2-gas interactions. Within the condition that the random velocity imparted to a particle σ_2 by a collision is damped by its viscous interaction with the gas before it suffers another collision, the kinetic theory method established here may be extended to include more general particle-particle and particle-gas interaction laws than those used by Marble. However, the

collisional model employed is particularly important because the criteria for its application are easy to establish and because it admits a wide class of physically interesting situations.

Within the restrictions of this collision model, it is possible to analyze the macroscopic motion of particles σ_2 in three important limiting cases: $(\sigma_2/\sigma_1)^2 >> 1$, $(\sigma_2/\sigma_1)^2 << 1$ and $(\sigma_2/\sigma_1)^2 \sim 1$. It is found that when $(\sigma_2/\sigma_1)^2 >> 1$ there is essentially no redistribution of particles σ_2 normal to the gas flow. The only effect of particle σ_1 -particle σ_2 encounters is a drag force acting to slow down particles σ_2. When $(\sigma_2/\sigma_1)^2 << 1$ it is found that particles σ_2 may have many collisions during their passage through the shock relaxation zone. As a consequence there may be a substantial redistribution of particles σ_2 downstream of the shock wave. The physical features of this process are studied in detail together with the range of validity of this diffusion model. The case $(\sigma_2/\sigma_1)^2 \sim 1$ is analyzed under the condition particles σ_2 have at most one collision during their passage through the shock relaxation zone. It is found that when the gas or particle σ_1 density is low, the single collision effects may be important even when σ_2/σ_1 differs significantly from unity and the particles are not very small.

Under most conditions of practical significance, because there is invariably a distribution of particles sizes present in a dusty gas, the calculation of the particle distribution in the shock relaxation zone should account for the effects of particle-particle encounters. It is suggested that an experimental observation of particle size distribution

in a shock relaxation zone can yield significant information on particle-particle and particle-gas interaction laws.

TABLE OF CONTENTS

TABLE OF CONTENTS (Continued)

I. INTRODUCTION

If phase change and chemical reaction do not occur and external forces are neglected, then the dynamics of solid particle clouds transported by gases is governed by the viscous forces exerted on the particles by the gas and by collisions between individual particles. The gas - particle and particle - particle interactions are not always distinguishable from one another, since the interaction of two or more particles is characterized not only by the collision of their surfaces but also by the coupling of their individual flow fields.

If the number density of the particles is very high, the flow fields of many individual particles may be coupled together continuously as the mixture evolves, for example, as in a gas - fluidized bed. In this situation, the gas - particle mixture behaves almost as a fluid with modified properties since the particles and the gas are strongly locked to each other. On the other hand, if the average distance between particles within the gas is much greater than the characteristic dimensions of their individual flow fields, the particles may move significant distances during which they interact only with the gas, and collisions involving more than two particles will be rare. Under these circumstances, a collision between two particles, when viewed on a macroscopic time scale, is characterized by a rapid and very complicated transfer of momentum and energy between the particles.

This investigation will deal exclusively with dilute particulate suspension. For a general discussion of methods applicable to the treatment of gas - particle flows in which the particle densities are high, the reader is referred to the books by Zenz and Othmer[1] and

Soo[2].

With the exception of Marble's work[3], previous investigations[4-8] into the dynamics of gas-particle mixtures, in which the particle densities were not large, have neglected the effects of particle-particle interactions. This approach is valid only if the particle number densities are quite small or if the particles are very nearly the same size so the particles have little tendency to collide.

Since these circumstances do not generally occur in nature or in problems of practical significance, the effect of particle-particle interactions must usually be accounted for in describing the macroscopic motion of the gas-particle system. Fortunately, it seems that in many problems of practical significance the gas-particle and particle-particle interactions are sufficiently independent phenomena, with regard to the motion of a particle through the mixture, that the methods of kinetic theory may be used in principle to compute the macroscopic motion of the particles. The complexity and considerable lack of knowledge regarding the particle-particle and gas-particle interaction laws, however, prohibit a comprehensive treatment of the dynamics of dilute particulate suspensions. There do exist circumstances, however, under which the gas-particle and particle-particle interactions are simplified and the viscous damping of the particle motion between collisions simplifies the treatment of the collision process so that a detailed solution to the problem is possible. These circumstances were first studied by Marble[3] for one-dimensional gas-particle flows. The present work proposes: first, to demonstrate, by generalizing Marble's collision model, that

the methods of kinetic theory can indeed be extended to treat solid particle collision phenomena in multi-dimensional gas-particle flows; second, to elucidate some of the fundamental physical characteristics of the dispersion of particles in a gas-particle flow field due to particle-particle encounters; and finally, to assess the importance of particle collisions in particle-laden gas flows. To attain these objectives, this study is divided into two parts. Because of the general complexity of this subject, it is appropriate to first establish a good qualitative understanding of the physical aspects of gas-particle flows. The foundation is particularly important here, because the kinetic theory method is considerably simplified if use is made of the underlying symmetry principles that govern particle-gas motion and interaction. Therefore, the first part of this study presents a qualitative discussion of the essential physical features of gas-particle flows. Important dimensionless parameters are introduced and their general physical significance is indicated.

The analysis is broken into four parts. First, a reasonably general model for the gas-particle system to be used throughout this thesis is outlined. Then the fundamental characteristics of single particle motion in gas flows commensurate with this model are described. Third, a particularly important particle-particle interaction model and conditions required for its validity are presented. Some experimental results obtained by McLaughlin[9] which tend to support this model are also described. These general concepts of single particle motion and particle-particle interaction are then combined to treat qualitatively the motion of a test particle in a gas-

particle flow including collisions.

In part two, the interaction of a normal gasdynamic shock wave with a dusty gas is studied with appropriate mathematical rigor by using the powerful methods of kinetic theory together with ideas generated in part one. Throughout the calculation, an effort is made to ascertain the validity of the computational model in order to establish the physical significance of the results. This approach also serves to point out ways of increasing the quantitative accuracy of the calculation. It should also become evident as we proceed that the necessary conditions for the application of kinetic theory procedures to the study of gas-particle flows are sufficiently weak that, in addition to the shock wave problem, they admit a wide class of physically interesting problems.

Finally, it should be noted that the study of shock waves passing through gas-particle mixtures appears to have fundamental as well as practical implications. For instance, this investigation reveals that the study of shock waves in gas-particle suspensions may be particularly suited as a means for investigating particle-particle interactions and other non-equilibrium phenomena in solid particle - gas flows. This is an important result, since at the present time there is little experimental evidence regarding gas - particle and particle - particle interactions and their effect on the dynamics of gas -particle systems.

II. FUNDAMENTALS OF PARTICLE MOTION IN A GAS

1. Some Fundamental Considerations

Consider a perfect gas containing a dilute distribution of small, solid, spherical particles of two distinct radii, σ_1 and σ_2. In principle, it is straightforward to extend the following considerations to treat particle distributions that consist of more than two distinct particle sizes.

Suppose that the state of the gas and the composition of the particles are such that the following assumptions are valid. Individual particles do not vaporize, condense, agglomerate, or chemically react with the gas during their motion through it. Then the mechanical properties of the particles are dynamical invariants. The particles have a large thermal conductivity, so their internal temperature is uniform. Furthermore, heat exchange occurs only by thermal transfer between particles and gas; radiative heat transfer is neglected. The distribution of particles is dilute in the sense that the average distance between particles, within any region in the gas, is much greater than the characteristic dimensions of their individual flow fields. In general, the flow fields of individual particles do not overlap continuously during their motion through the gas. In fact, the particles may travel significant distances during which they interact only with the gas.

A collisional encounter between particles occurs when they approach sufficiently close that the force exerted by the gas upon each particle is significantly altered. In essence, a collision occurs when

there is a substantial coupling of the flow fields of the individual particles involved. Consequently, if the particle number densities are not too large, collision events involving more than two particles will be rare.

To be more specific, suppose m_1, m_2 are the masses, n_{p1}, n_{p2} are the local number densities, and $\rho_{p1} = m_1 n_{p1}$, $\rho_{p2} = m_2 n_{p2}$ are the local mass densities of particles of radius σ_1 and σ_2, respectively. The local average distance between particles of radius σ_j is then approximately $\delta_j \cong n_{pj}^{-1/3}$, and the local average distance between particles of radius σ_1 and particles of radius σ_2 is $\delta_{12} \cong (n_{p1} + n_{p2})^{-1/3}$. Now if Σ_i is the characteristic radial dimension of the flow field of an isolated particle of radius σ_i, the distribution is called dilute if the following inequalities are satisfied throughout the flow;

$$\delta_1 \cong n_{p1}^{-1/3} >> 2\Sigma_1 \tag{2.1}$$

$$\delta_2 \cong n_{p2}^{-1/3} >> 2\Sigma_2 \tag{2.2}$$

$$\delta_{12} \cong (n_{p1} + n_{p2})^{-1/3} >> \Sigma_1 + \Sigma_2 \tag{2.3}$$

The length Σ_i depends upon the local particle Reynolds number $Re_i = \rho \sigma_i |\underline{u} - \underline{v}_{pi}| / \mu$, Mach number $M_{pi} = |\underline{u} - \underline{v}_{pi}| / a$ and Knudsen number $K_{pi} = \lambda_c / \sigma_i$, where ρ, μ, $\underline{u}$, and a are the local gas density, viscosity, velocity, and sonic speed, respectively; λ_c is the molecular mean free path, and $\underline{v}_{pi}$ is the local average velocity of particles of radius σ_i. Since the

Knudsen number can generally be expressed as a function of Mach number, $\Sigma_i = \Sigma_i (Re_i, M_{pi})$.

If $\lambda_c << \sigma_i$ corresponds to $K_{pi} << 1$, the gas behaves as a continuum with regard to its interaction with the particles. When $\lambda_c >> \sigma_i$ corresponding to $K_{pi} >> 1$, the gas-particle interaction may be described by the methods of rarefied gas dynamics. In this case, if the particle velocity and mass are sufficiently small, Brownian motion of the particles may be important.

Cases where the effects of slip flow, transition flow, and free molecule flow are significant will not be discussed. It will be assumed that $K_{pi} << 1$ and that the motion of the gas and the particle can be computed on the basis of continuum mechanics. When the velocity of individual particles relative to the gas is much less than the sound speed, the gas behaves as an incompressible medium in response to the particle motion, and $\Sigma_i \cong \Sigma_i (Re_i)$.

The disturbance created in the gas by the motion of a particle is usually spatially anisotropic, emphatically so when a wake is formed. The significance of Σ_i is illustrated by the data of Taneda[10] presented in Figure 1. For the steady motion of a sphere for $10 < Re_i < 300$, the particle motion is accompanied by a wake. This wake consists of a vortex ring, $Re_i > 24$, that grows in size and decreases in stability as Re_i increases. For $Re_i > 130$ it oscillates and gives rise to time dependent forces on the particle.

Generally, we will assume Σ_i to be the maximum radial characteristic dimension of the particle disturbance unless, as in the case of a large wake, Σ_i has no useful significance.

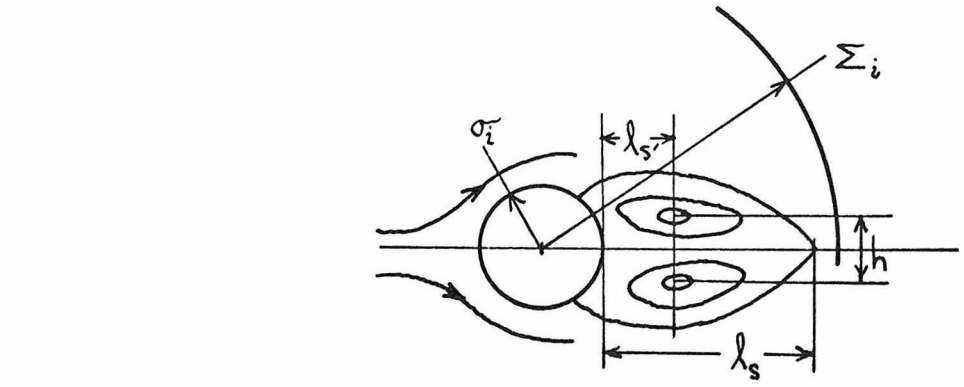

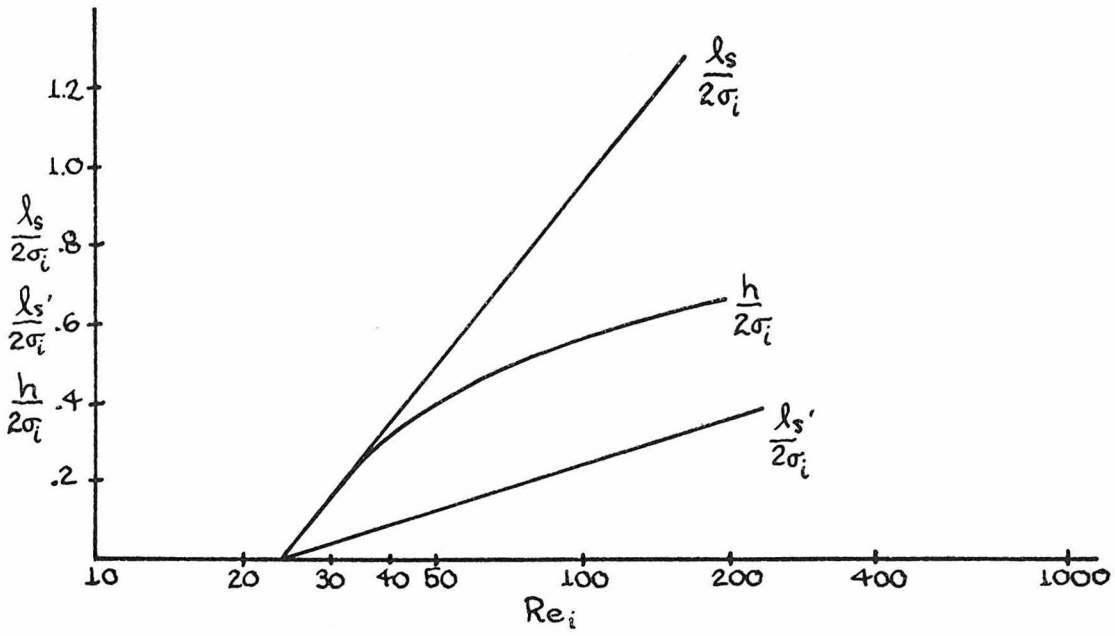

Figure 1. Sphere wake dimensions as a function of particle Reynolds number (Taneda).[10] Note; $\Sigma_i \sim \sigma_i$

Using the previous results, we can rewrite (2. 3) in the form

$$\frac{1}{\left(\frac{\rho_{p1}}{m_1}+\frac{\rho_{p2}}{m_2}\right)^{1/3}} \gg \Sigma_1+\Sigma_2 \qquad (2.4)$$

If all particles are composed of material of density ρ_s, then $m_1=\frac{4}{3}\pi\rho_s\sigma_1^3$ and $m_2=\frac{4}{3}\pi\rho_s\sigma_2^3$. Then, defining $K_i \equiv \rho_{pi}/\rho$, the ratio of the mass density of particles of radius σ_i to the mass density of the gas, and supposing for convenience $\sigma_1 > \sigma_2$, we can rewrite (2. 4):

$$\frac{\sigma_1}{\left[\frac{3}{4\pi}\left(K_1+K_2\left(\frac{\sigma_1}{\sigma_2}\right)^3\right)\left(\frac{\rho}{\rho_s}\right)\right]^{1/3}} \gg (\Sigma_1+\Sigma_2) \qquad (2.5)$$

or

$$\left(\frac{\rho_s}{\rho}\right)^{1/3}\left\{\frac{3}{4\pi}\left(K_1+K_2\left(\frac{\sigma_1}{\sigma_2}\right)^3\right)\right\}^{-1/3} \gg \frac{(\Sigma_1+\Sigma_2)}{\sigma_1} \qquad (2.6)$$

In a similar fashion, relations (2. 2) and (2. 3) become:

$$\left(\frac{\rho_s}{\rho}\right)^{1/3}\left(\frac{4\pi}{3K_1}\right)^{1/3} \gg 2\Sigma_1/\sigma_1 \qquad (2.7)$$

and

$$\left(\frac{\rho_s}{\rho}\right)^{1/3}\left(\frac{4\pi}{3K_2}\right)^{1/3} \gg 2\Sigma_2/\sigma_2 \qquad (2.8)$$

The quantity K_i is a measure of the local total interaction force per unit mass between the particles of radius σ_i and the gas.

If $K_i << 1$, the presence of particles of radius σ_i has negligible effect on the dynamics of the gas. If $K_i >> 1$, the particle density may be very high, a situation with which we are not presently concerned. When, however, $K_i \sim 1$, the gas and particles of radius σ_i are coupled together and local gas properties are modified by the momentum, energy, and heat transfer between the particles and the gas. The situation $K_i \lesssim 1$ occurs, for instance, in the passage of shock waves through dusty atmospheres[5-7] and in the exhaust plume of metallized solid propellant rocket motors.[8] If local gas density, ρ, is less than or on the same order as the standard atmospheric density, and the particles are composed of solid material, $\rho_s/\rho \gtrsim 10^3$. Usually, $\Sigma_1 \sim \sigma_1$, $\Sigma_2 \sim \sigma_2$, and there would appear to be no difficulty in satisfying (2.6), (2.7), and (2.8) if σ_1/σ_2 is not too large. For particles in liquids, since ρ_s/ρ is not large, conditions (2.6), (2.7), and (2.8) are much more restrictive. These considerations suggest that there exist physically interesting gas - solid particle flows in which the particles modify local gas properties but may travel substantial distances between interactions.

The system is defined to be in its equilibrium state when the density, temperature, and velocity of the gas are uniform and the particles move with the gas and have the same temperature as the gas. The particles may be non-uniformly distributed throughout the gas.

The dynamical evolution of a non-equilibrium state of such a heterogeneous system depends on the following time scales or their corresponding characteristic lengths:

(a) τ_o , duration of a collision between two molecules within the gas. For gases at standard conditions, $\tau_o \simeq 10^{-12}$ sec.

(b) τ_c , the average time between successive molecular collisions within the gas. For gases at standard conditions, $\tau_c \simeq 10^{-9}$ sec.

(c) τ_{oij} , the time of a collision between particles of radius σ_i and particles of radius σ_j , which is characterized by the time during which there is a significant interaction between the flow field of particle σ_i and the flow field created by σ_j . "Bonding" of one particle to another is explicitly neglected. Note: $\tau_{oij} = \tau_{oji}$ for particles with $\sigma_i \sim 10\mu$ and relative velocity $\sim .1a$ at standard conditions $\tau_{oij} \sim 10^{-5} - 10^{-6}$ sec.

(d) τ_{vi} , the velocity equilibration time for particles of radius σ_i , a measure of the time required for the motion of a particle to respond to changes in local gas flow. For particles with $\sigma_i \sim 10\mu$ in gases at standard conditions, $\tau_{vi} \sim 10^{-2}$ sec.

(e) τ_{Ti} , the thermal equilibration time for particles of radius σ_i , a measure of the time required for the temperature of a particle to respond to changes in the local gas temperature. For most gases, $\tau_{vi} \simeq \tau_{Ti}$.

(f) τ_{cij} , the average time between encounters for particles of radius σ_i with particles of radius σ_j . Generally, τ_{cij} is the same magnitude as $\tau_{\sigma i}$, $\tau_{\sigma j}$.

(g) τ , the time over which the entire flow system changes appreciably. Generally, $\tau > 10^{-4}$ sec.

Associated with these relaxation times are the following length scales:

(a) $\lambda_o \sim \tau_o a$ is approximately the range of the intermolecular potential, where a is the local sonic speed and is nearly the gaseous thermal speed. In gases at standard conditions, $\lambda_o \sim 10^{-8}$ cm.

(b) $\lambda_c \sim \tau_c a$ is the molecular mean free path within the gas. In gases at standard conditions, $\lambda_c \sim 10^{-5}$ cm.

(c) $\lambda_{\sigma_{ij}} \simeq \tau_{\sigma_{ij}} |\underline{v}_{pi} - \underline{v}_{pj}|$ is the range of the particle-particle interaction, where $\underline{v}_{pi}$ and $\underline{v}_{pj}$ are the local characteristic velocities of particles σ_i and σ_j respectively. $\lambda_{\sigma_{ij}} \sim 10^{-3}$ cm.

(d) $\lambda_{v_i} \simeq \tau_{v_i} |\underline{v}_{pi}|$, the velocity equilibration length, is a measure of the distance covered by a particle during its response to changes in the local gas velocity; provided $|\underline{v}_{pi}| \sim .1a$ in gases at standard conditions, $\lambda_{v_i} \sim 10$ cm.

(e) $\lambda_{T_i} \simeq \tau_{T_i} |\underline{v}_{pi}|$, the thermal equilibration length, is a measure of the distance covered by a particle during its response to changes in the local gas temperature. Generally, $\lambda_{T_i} \simeq \lambda_{v_i}$

(f) $\lambda_{c_{ij}} \simeq \tau_{c_{ij}} |\underline{v}_{pi}|$ is the average distance traveled by particles of radius σ_i between successive collisions with particles of radius σ_j.

(g) $|\underline{L}| \simeq \tau |\underline{u}|$ is the characteristic geometric dimension of the entire gas particle flow system and $|\underline{u}|$ is the characteristic velocity of the system. Generally, $|\underline{L}| \gtrsim 10^{-1}$ cm.

If the number density of the particles becomes too large and (2.1) - (2.3) are no longer satisfied, the particle relaxation times

and lengths will in general be well-defined no longer. When the flow fields of many individual particles are coupled together, the time of a particle-particle collision and the average time between successive collisions lose their meaning. We shall assume that characteristic times and lengths are well defined and that conditions (2. 1), (2. 2), and (2. 3) are satisfied.

For sufficiently dilute gas-particle mixtures, the characteristic parameters are related in the following manner:

$$\left.\begin{aligned} &\tau_o \ll \tau_c \ll \tau_{oij} \ll \tau_{v_i}, \tau_{cij}, \tau \\ &\lambda_o \ll \lambda_c \ll \lambda_{oij} \ll \lambda_{v_i}, \lambda_{cij}, L \end{aligned}\right\} \quad (2.9)$$

In relations (2. 9) it is assumed that the gas behaves as a continuum in its interaction with particles.

Because ρ_s/ρ is large and the particles are small, it is reasonable to suppose that, when $K_i \lesssim 1$, the volume occupied by the particles is negligible compared to that of the gas. When treating the average macroscopic motion of the gas, it is assumed that, on the scale of particles, disturbances caused by the particle motions may be neglected. This implies that the momentum defect on the particle scale introduced into the gas is immediately diffused to a neighborhood of the particle spacing scale. The same assumption applies to the energy dissipated in the gas by the particle motion through it. In microscopic detail, of course, the energy first appears in the particle wake as a velocity disturbance which is, in turn, dissipated to thermal energy. In our approximation, the energy is

dissipated immediately and uniformly throughout a local volume of particle spacing dimensions. Provided no large gradients in gas properties are present, such as gasdynamic shocks, we assume that the gas is inviscid except for the drag it exerts on the particles. The specific heats of the gas and particles are assumed constant. As a consequence of these assumptions, the particles move through a gas with "smoothed" properties.

Since $\tau_{o_{ij}} << \tau_{c_{ij}}$ corresponding to $\lambda_{o_{ij}} << \lambda_{c_{ij}}$, the dynamics of particles can be computed using the averaged gas properties. Specifically, the dynamics of an encounter between two particles within the gas may be studied approximately by assuming "smoothed" local properties of the gas. Large gradients may, however, be created within the gas during an encounter between two particles. Therefore, on the microscopic scale of particle-particle interactions, viscous effects cannot be ignored.

2. Particle - Gas Interaction

The motion of a single small, solid, spherical particle in a non-uniform gas flow is governed by the viscous forces exerted upon the particle by the relative gas motion and by heat transfer between the particle and the surrounding gas. This problem has been discussed in some detail by Torobin and Gauvin[10], Hoglund[8], Fuks[11], Marble[4], and Soo.[2]

If the temperature of the particle is different from the temperature of the gas through which it is moving, there will be a variation in fluid viscosity around the particle because of heat transfer

and the corresponding temperature distribution. Variations in viscosity alter the velocity field of the gas and, hence, the viscous drag on the particle. Fortunately, the slow variation of viscosity with temperature exhibited by gases makes this effect fairly minor if the temperature of the particle does not differ greatly from the temperature of the gas. We shall assume that the particle resistance may be computed utilizing the local viscosity coefficient, neglecting local thermal effects of the particle.

If we neglect non-steady effects upon the particle resistance, the equations for particle motion are

$$m \frac{d}{dt} \underline{u}_p(t) = \frac{1}{2} C_D(Re, M) \rho(\underline{x}_p(t)) \pi \sigma^2 (\underline{u}(\underline{x}_p(t)) - \underline{u}_p(t)) \left| \underline{u}(\underline{x}_p(t)) - \underline{u}_p(t) \right| \tag{2.10}$$

$$\frac{d\underline{x}_p(t)}{dt} = \underline{u}_p(t) \tag{2.11}$$

where $\underline{x}_p(t)$ and $\underline{u}_p(t)$ are the position and velocity of the particle at time t. The drag coefficient, C_D, is a function of the particle Reynolds number $Re = \rho(\underline{x}_p(t)) \sigma \left| \underline{u}(\underline{x}_p(t)) - \underline{u}_p(t) \right| / \mu$ and Mach number $M = \left| \underline{u}(\underline{x}_p(t)) - \underline{u}_p(t) \right| / a(\underline{x}_p(t))$, where ρ, a, and μ are the gas density, sonic speed, and viscosity, respectively. For low values of M, the medium may be considered incompressible and the drag coefficient is a function of only the particle Reynolds number.

For simplicity, we shall assume that the individual particle motion obeys the classical Stokes law and that the heat transfer between the particle and the gas takes place with a Nusselt number of unity based on the particle radius. Although these drag and heat

transfer laws hold strictly for a single sphere in steady motion through a uniform medium, the errors involved in applying them to a dilute suspension are minor. Moreover, the significant physical features of the collective gas-particle motion do not depend strongly on the details of the drag law.

Consider the motion of a particle of mass m and radius σ in a steady, one-dimensional gas flow of velocity $u(x)\underline{e}_x$. The position, $\underline{x}_p(t)$, velocity, $\underline{u}_p(t)$, and temperature, $T_p(t)$, of the particle satisfy, using Stokes Drag Law and Nusselt Number of unity,

$$m \frac{d\underline{u}_p(t)}{dt} = 6\pi\mu\sigma \left(u(x_p(t))\underline{e}_x - \underline{u}_p(t)\right) \tag{2.12}$$

$$m c_s \frac{dT_p(t)}{dt} = \left(\frac{k}{\sigma}\right) 4\pi\sigma^2 \left(T(x_p(t)) - T_p(t)\right) \tag{2.13}$$

and

$$\frac{d\underline{x}_p(t)}{dt} = \underline{u}_p(t) \tag{2.14}$$

In equations (2.12) - (2.14), μ is the local gas viscosity, c_s the specific heat of the solid, and k the thermal conductivity of the gas. Define the velocity equilibration time

$$\tau_v = \frac{m}{6\pi\mu\sigma} \tag{2.15}$$

and the thermal equilibration time

$$\tau_T = \frac{m c_p}{4\pi\sigma k} = \frac{3}{2}\left(\frac{c_p \mu}{k}\right)\tau_v \qquad (2.16)$$

where c_p is the specific heat of the gas at constant pressure. Since the Prandtl number, $Pr = c_p \mu / k$, for most gases is approximately two-thirds, the velocity and thermal equilibration times are about equal.

Rewriting (2.12) and (2.13) using the definitions (2.15) and (2.16),

$$\frac{d\underline{u}_p}{dt} = \frac{1}{\tau_v}\left(u\,\underline{e}_x - \underline{u}_p\right) \qquad (2.17)$$

$$\frac{dT_p}{dt} = \left(\frac{c_p}{c_s}\right)\frac{1}{\tau_T}\left(T - T_p\right) \qquad (2.18)$$

In most situations for solid particles $c_s \sim c_p$. From the form of (2.17) we see that τ_v is approximately the time required for the velocity of the particle to respond to changes in the local gas velocity. If the gas is uniform, it becomes the time required for the particle slip velocity $\underline{u}_s = u\,\underline{e}_x - \underline{u}_p$ to decay to e^{-1} of its initial value. A similar interpretation of τ_T is useful to describe the variation of particle temperature. The spatial relaxation of the particle velocity and temperature is characterized by the velocity and thermal equilibration lengths, respectively. They are usually defined as:

$$\lambda_v = \tau_v u_o \qquad (2.19)$$

$$\lambda_T = \tau_T u_o \qquad (2.20)$$

where u_0 is a velocity characterizing the gas flow. The parameters λ_v and λ_T are measures of the distance that a particle of radius σ will be transported before its velocity and temperature equilibrate reasonably with those of the gas stream.

If ρ is the mass density of the gas, ρ_s the mass density of the particle, and ν the kinematic viscosity of the gas, then the equilibration parameters may be written

$$\lambda_v = \frac{2}{9}\left(\frac{\rho_s}{\rho}\right)\left(\frac{\sigma u_0}{\nu}\right)\sigma \tag{2.21}$$

$$\lambda_T = \frac{1}{3} Pr \left(\frac{\rho_s}{\rho}\right)\left(\frac{\sigma u_0}{\nu}\right)\sigma \tag{2.22}$$

For metallic solids in gases at standard atmospheric conditions, ρ_s/ρ is on the order of 10^3. For a typical particle of radius $\sigma \sim 10^{-4}$ cm the velocity equilibrationtime at standard atmospheric conditions in air is $\tau_v \sim 10^{-4}$ sec, and increases as the square of the particle radius. When the viscosity of the gas, μ, is nearly constant over the gas flow, τ_v is also nearly constant. Under this condition, it is apparent from equation (2.17) that the motion of the particle normal to the gas flow direction is independent of its motion parallel to the gas flow. This transverse motion is damped in a time of order τ_v.

Suppose at time $t=0$ and position $\underline{x} = 0$ a particle is injected into the gas flow with a velocity

$$\underline{u}_p(0) = u_p(0)\,\underline{e}_x + \underline{u}_{p\perp}(0) \tag{2.23}$$

different from the local gas velocity. The velocity components of the

particle are governed by

$$\frac{du_p(t)}{dt} = \frac{1}{\tau_v}\left(u(x_p(t)) - u_p(t)\right) \tag{2.24}$$

$$\frac{du_{p\perp}}{dt} = -\frac{1}{\tau_v}\, u_{p\perp}(t) \tag{2.25}$$

$$\frac{dx_p(t)}{dt} = u_p(t) \tag{2.26}$$

$$\frac{dx_{p\perp}(t)}{dt} = u_{p\perp}(t) \tag{2.27}$$

Equations (2.25) and (2.27) are readily solved, and the motion of the particle perpendicular to the direction of gas flow is given by:

$$u_{p\perp}(t) = u_{p\perp}(0)\, e^{-t/\tau_v} \tag{2.28}$$

$$x_{p\perp}(t) = u_{p\perp}(0)\, \tau_v \left(1 - e^{-t/\tau_v}\right) \tag{2.29}$$

The velocity of the particle normal to the gas flow is damped exponentially in a time of order τ_v so that it reaches a limiting transverse position

$$x_{p\perp}(\infty) = u_{p\perp}(0)\, \tau_v \tag{2.30}$$

The length $x_{p\perp}(\infty)$ is called the transverse range of the particle; it is the maximum distance the particle can move across the gas flow field if its initial transverse velocity component is $u_{p\perp}(0)$. The value of $x_{p\perp}(\infty)$ depends on the particle's initial transverse veloc-

ity and is independent of variations in parallel velocity components. The concept of a transverse range may be extended to circumstances where τ_v varies with x.

The motion of a particle parallel to the gas flow is generally complicated and is most conveniently treated within the framework of a given problem. The dynamics of the particle depend strongly on the magnitude of $(\lambda_v/L) \sim (\tau_v/\tau)$ where L is the characteristic geometric length of the gas flow field and $\tau \sim u_o L$ is approximately the time it takes a particle to travel a distance L.

When $\tau_v >> \tau$ corresponding to $\lambda_v >> L$, Figure 2, the particle motion is relatively unaffected by local changes in the gas flow field. The force acting between the particle and the gas is small compared with particle inertial forces and may be treated as a perturbation on the motion the particle would have in the absence of the gas. The particle motion through a region of length L within the gas is determined principally by its motion at the time it enters the region and, in the absence of external forces, the particle trajectory will be nearly linear.

On the other hand, if $\tau_v << \tau$, corresponding to $\lambda_v << L$, the particle adjusts rapidly to the local gas velocity. Referring to Figure 3, the particle motion is strongly coupled to the gas motion because its relaxation time is much less than the time over which significant changes in the flow field occur. Because the initial motion of the particle across the gas flow is damped out in a time of order τ_v, its motion is nearly parallel to the direction of the one-dimensional gas flow for times larger than τ_v. Under these con-

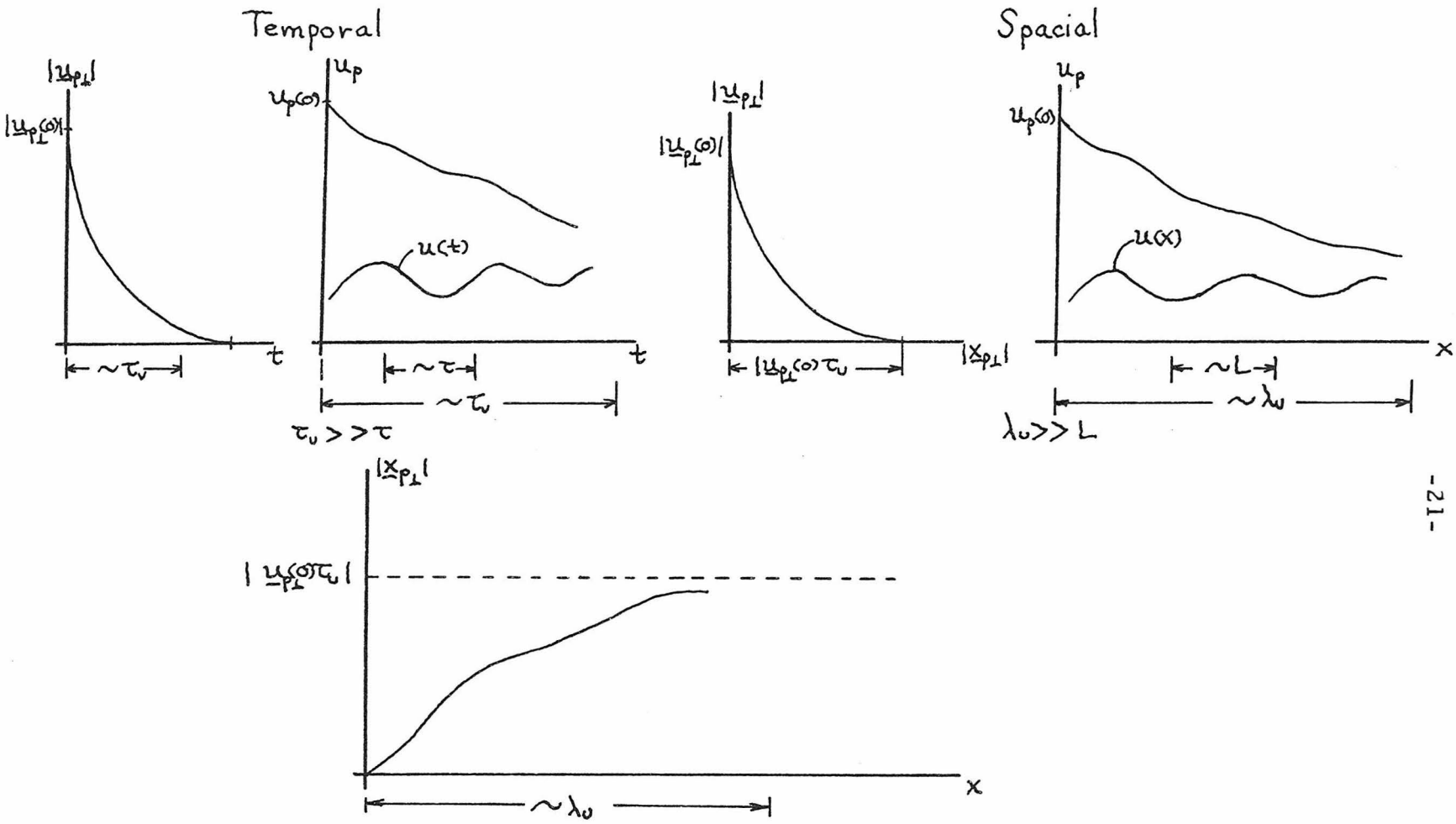

Figure 2. Particle relaxation effects; motion of a particle through a region of the gas when $\tau_v/\tau = \lambda_v/L >> 1$

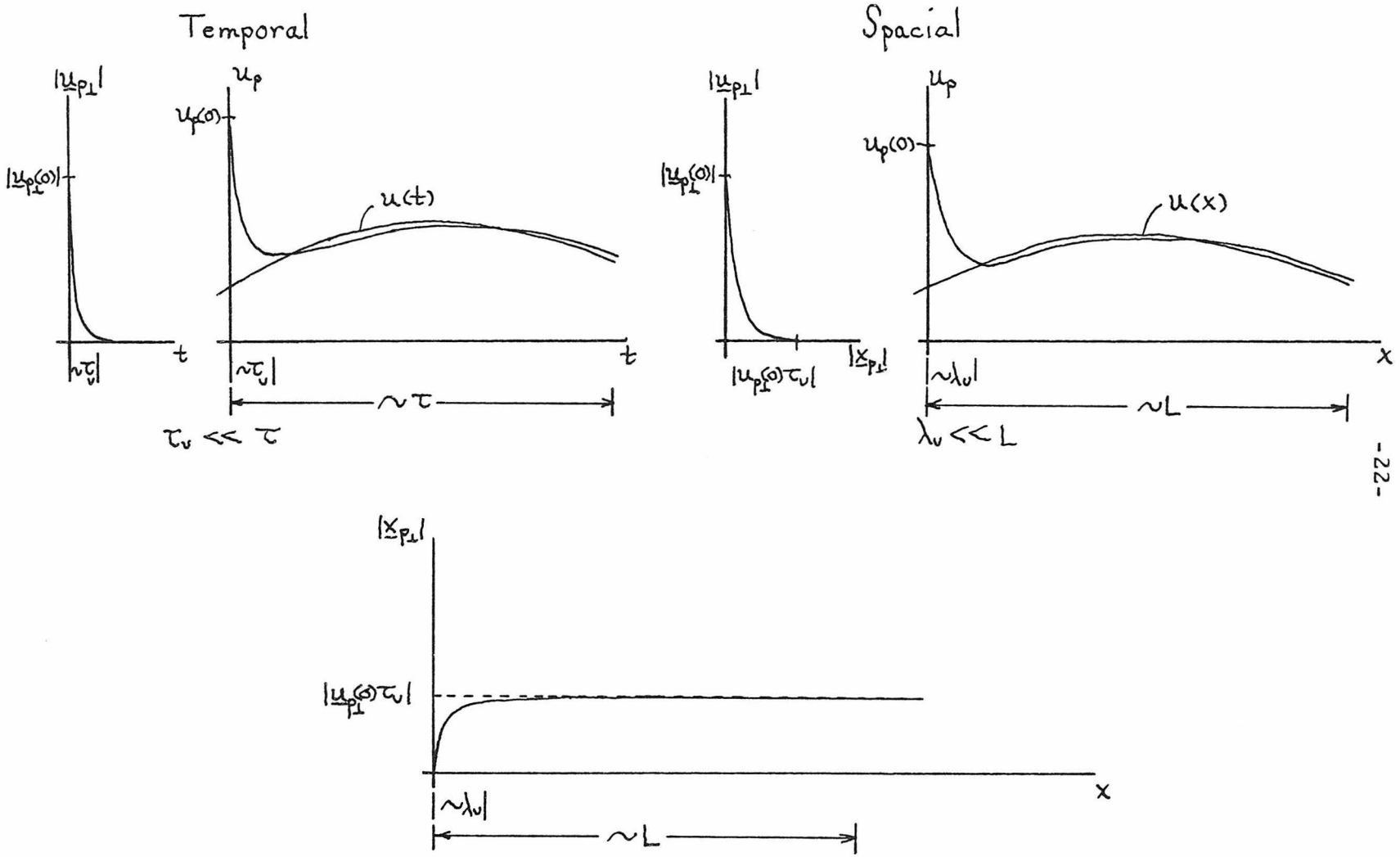

Figure 3. Particle relaxation effects; motion of a particle through a region of the gas when $\tau_v/\tau = \lambda_v/L \ll 1$

ditions, Marble[4] has shown that after its initial rapid relaxation for $t \gtrsim \tau_v$, $x_p(t) \gtrsim \lambda_v$, the particle adjusts itself to the one-dimensional gas motion by taking on a velocity relative to the gas, the slip velocity, that provides the force to accelerate or decelerate the particle at nearly the local rate of acceleration or deceleration of the gas. Then, for $t >> \tau_v$ corresponding to $x_p(t) >> \lambda_v$, the state of motion of the particle is approximately given by

$$u_p(t) \simeq u(x_p(t)) + \tau_v \frac{du}{dt}(x_p(t)) \qquad (2.31)$$

$$\underline{u}_{p\perp}(t) \simeq 0 \qquad (2.32)$$

and

$$\underline{x}_{p\perp}(t) \simeq \underline{u}_{p\perp}(0)\tau_v \qquad (2.33)$$

The particle has essentially lost its memory of its state of motion at time $t=0$; its motion is relatively independent of its previous history.

When $\tau_v/\tau \sim \lambda_v/L$ is neither large nor small, the motion of the particle depends on the entire history of its motion through regions within the gas of dimension L . Apparently, Figure 4, no great simplifications may be made in treating the particle motion parallel to the flow. The transverse displacement, however, has almost reached its limiting value.

A similar discussion holds for the relationship between the local particle and gas temperatures. For a more detailed discussion of the gas-particle interaction, the reader is referred to the work by

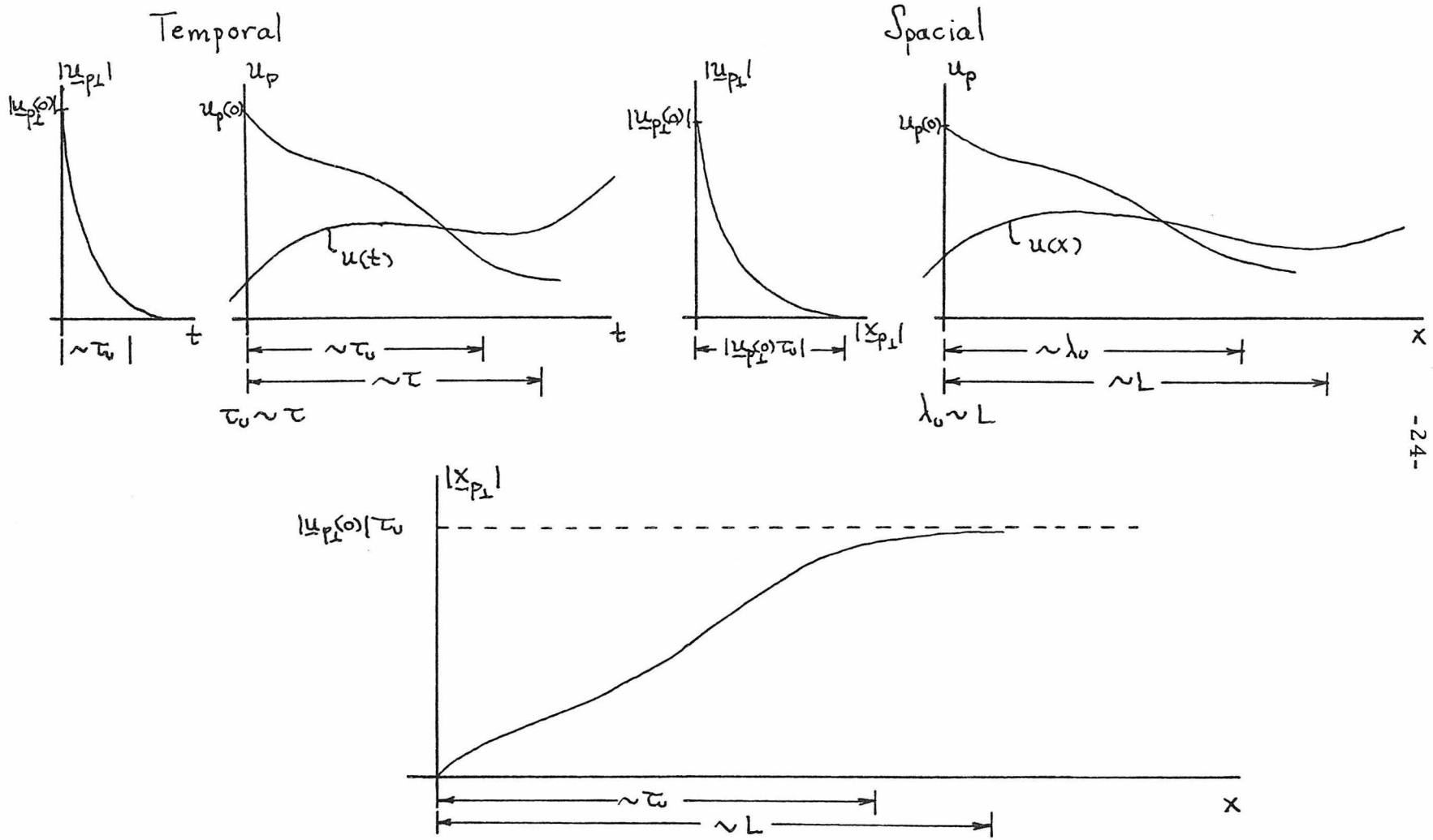

Figure 4. Particle relaxation effects; motion of a particle through a region of the gas when $\tau_v/\tau = \lambda_v/L \sim 1$.

Marble[4], which also includes some illuminating examples of the physical significance of τ_0/τ .

3. Particle-Particle Interaction

The collision of two spherical particles in a viscous fluid is complicated by the fact that, during collision, the distance between particle surfaces in relative motion becomes so small that viscous forces dominate. The problem is further complicated when the particle Reynolds numbers are so large that wakes are formed. Then the interaction mechanism loses its symmetry; this is probably of importance when particles collide while moving parallel to each other through the fluid.

In spite of these complexities, it is reasonable to expect conditions under which the particle-particle collision is nearly elastic and is characterized primarily by the particles' properties. When two particles approach each other, their individual flow fields interact and the force exerted by the gas upon each particle is altered. If this viscous force had a negligible effect upon the collision, the momentum and energy exchange between the particles then depends on the nature of their contact. Marble[3] has suggested that a necessary condition for this behavior is that the time required for each particle to traverse the flow field of the other must be small in comparison with the velocity equilibration time. This condition is reasonable since, if it were not satisfied, the particle would have sufficient time during the encounter to respond to the flow field of the other particle.

To make this criterion quantitative, let Σ_i be the characteristic radial dimension of the flow field of the particle whose radius

is σ_i and $\underline{u}_{pi}$ be the local collisionless velocity. The time during which particles of radii σ_i and σ_j interact is of the order $\Sigma_i / |\underline{u}_{pi} - \underline{u}_{pj}|$. Consequently, in order that the collision between particles of radius σ_1 and σ_2 be nearly independent of the structure of their flow fields, it is necessary that

$$\frac{\tau_{v_1}}{\Sigma_2 / |\underline{u}_{p1} - \underline{u}_{p2}|} >> 1 \tag{2.34}$$

$$\frac{\tau_{v2}}{\Sigma_1 / |\underline{u}_{p1} - \underline{u}_{p2}|} >> 1 \tag{2.35}$$

Utilizing the definition of the velocity equilibration time τ_{v_j} of a particle of radius σ_j and assuming the particles are composed of the same material so $\rho_{s_1} = \rho_{s2} = \rho_s$, this may be written

$$\frac{2}{9}\left(\frac{\sigma_1}{\Sigma_2}\right)\left(\frac{\rho \sigma_1 |\underline{u}_{p1} - \underline{u}_{p2}|}{\mu}\right)\left(\frac{\rho_s}{\rho}\right) >> 1 \tag{2.36}$$

$$\frac{2}{9}\left(\frac{\sigma_2}{\Sigma_1}\right)\left(\frac{\rho \sigma_2 |\underline{u}_{p1} - \underline{u}_{p2}|}{\mu}\right)\left(\frac{\rho_s}{\rho}\right) >> 1 \tag{2.37}$$

The second bracketed term is a Reynolds number based upon the relative velocity of the two particles and will generally be of order unity. For our purposes here, it will suffice to take $\Sigma_1 \sim \sigma_1$ and $\Sigma_2 \sim \sigma_2$, and conditions (2.36) and (2.37) become

$$\frac{2}{9}\left(\frac{\sigma_1}{\sigma_2}\right)\left(\frac{\rho\sigma_1|\underline{u}_{p1}-\underline{u}_{p2}|}{\mu}\right)\left(\frac{\rho_s}{\rho}\right) >> 1 \qquad (2.38)$$

$$\frac{2}{9}\left(\frac{\sigma_2}{\sigma_1}\right)\left(\frac{\rho\sigma_2|\underline{u}_{p1}-\underline{u}_{p2}|}{\mu}\right)\left(\frac{\rho_s}{\rho}\right) >> 1 \qquad (2.39)$$

For solid particles in gases, the density ratio ρ_s/ρ is large and, for particles having Reynolds numbers of relative motion of order unity, expressions (2.38) and (2.39) are of magnitude 10^3.

Further information is required to determine just how large expressions (2.38) and (2.39) must be to assure that a collision is essentially elastic.

Toward this end, a detailed experimental investigation has been made by McLaughlin[9] into the momentum and energy losses resulting from the collision of spherical particles with an infinite wall in the presence of a viscous fluid. This is a geometry which tends to maximize the energy and momentum losses of the sphere. The experiments were performed using steel spheres in glycerin-water mixtures.

His results, most conveniently given in terms of $\rho_s u\sigma/\mu$, showed two definite interaction regimes. For $\rho_s u\sigma/\mu$ less than about 30, the kinetic energy of the particle was dissipated in approaching the wall and no rebound occurred. Above $\frac{\rho_s u\sigma}{\mu} \sim 10^2$, over two-thirds of the energy dissipation of the sphere occurred within a tenth of a sphere radius from the wall.

At higher $\rho_s u\sigma/\mu$, the sphere rebounded from the wall,

and as $\rho_s u \sigma / \mu$ was increased, the loss became a smaller fraction of the kinetic energy of the sphere. At $\rho_s u \sigma / \mu \simeq 5 \times 10^4$, the loss had been reduced to approximately eleven percent. Furthermore, as the Reynolds number was increased, the length scale over which the momentum loss occurred was observed to decrease. Table I shows the variation of momentum loss with the $\rho_s u \sigma / \mu$ as indicated by selected examples of McLaughlin's experiment. At $\rho_s u \sigma / \mu \sim 10^4$ the collision is reasonably elastic.

TABLE I

Radius, cm	Viscosity poise	Velocity cm/sec	$\frac{\rho_s u \sigma}{\mu}$	Momentum Loss, %
0.318	9.25	12.75	8.7	100
0.476	9.25	26.9	28.6	100
0.476	2.40	55.3	214	69
0.476	0.59	95.3	1475	39
0.238	0.096	103	40300	18

The experimental results point to a thin-film energy loss mechanism over a wide range of $\rho_s u \sigma / \mu$. To confirm this mechanism, McLaughlin also performed experiments to measure the loss of a sphere rebounding from a wall covered by only a thin film of the liquid. These results showed that a critical film thickness existed, above which the energy loss did not significantly increase with increasing film thickness. The critical thickness for a particular case was $\frac{1}{5}\sigma$, considerably smaller than the particle radius.

The experimental results of McLaughlin suggest that flows

generated by colliding particles exhibit high pressure gradients perpendicular to the line of approach, supported by high shear stresses generated by squeezing liquid from between the surfaces. For values of $\rho u \sigma / \mu > 10^4$, elastic deformation of the solid occurs to such an extent that the collision may be considered elastic.

4. Motion of a Test Particle

Let us now consider some qualitative aspects of the effects of particle collisions on the motion of particles within a gas. Consider a perfect gas containing number densities n_{p1} and n_{p2} of particles having radii σ_1 and σ_2 , respectively. The dynamic behavior of this complete system is intimately related to the relative magnitudes of the several characteristic time scales or their associated lengths. Assume that the gas behaves as a continuum and that the particle number densities are low enough that only binary collisions between particles are important. Finally, assume that the average time of an encounter is much less than the velocity equilibration time of either particle, the average times between encounters and the time over which the flow field changes significantly.

Under these conditions, an encounter between two particles appears as an almost discontinuous transfer of momentum and energy between the particles. Between encounters, the particles interact only with the gas. In terms of characteristic time scales described previously,

$$\tau_o << \tau_c << \tau_{o_{12}} << \left\{ \begin{matrix} \tau_{o_1} & \tau_{c_{11}} & \tau_{c_{12}} \\ \tau_{o_2} & \tau_{c_{21}} & \tau_{c_{22}} \end{matrix} \right\} < \tau$$

The dynamics of this system may be described in terms of (i) the momentum and energy transfer in particle-particle encounters, and (ii) the motion of the particles between encounters.

Suppose that the particle-particle interaction law is known and we wish to consider the motion of the particles between encounters. The particles respond to local changes in the gas flow field through the viscous force exerted upon them. There is a transfer of momentum between the particles and the gas. The magnitude of this momentum transfer and its overall effect on the motion of the particles depends on the time between encounters. Consequently, the relative importance of these momentum and energy transfer processes, and therefore the motion of the particles due to collisions, is dependent upon the ratios $\tau_{v1}/\tau_{c11} \sim \lambda_{v1}/\lambda_{c11}$, $\tau_{v1}/\tau_{c12} \sim \lambda_{v1}/\lambda_{c12}$, $\tau_{v2}/\tau_{c21} \sim \lambda_{v2}/\lambda_{c21}$, and $\tau_{v2}/\tau_{c22} \sim \lambda_{v2}/\lambda_{c22}$.

These ratios will depend strongly on the particle radius ratio σ_1/σ_2 and the number densities of the two particle species. The velocity equilibration time of a particle depends on the particle radius because it is a factor in the drag law; in the Stokes regime, $\tau_{vj} \sim \sigma_j^2$. The average time, τ_{cij} , between successive encounters depends on the sum of the radial dimensions of their flow fields, $\Sigma_i + \Sigma_j$, their relative velocity, $|\underline{v}_{pi} - \underline{v}_{pj}|$, and the number density of particles. In practical problems a wide distribution of particle sizes occurs, and one should expect a corresponding variation of velocity equilibration and collision parameters.

Suppose that $n_{p1} >> n_{p2}$ so that τ_{c22} , τ_{c11} , $\tau_{c12} >> \tau$; the effect of collisions on the motion of particles

of radius σ_1 can be neglected. Particles of radius σ_1 may, however, have a significant effect on the character of the gas flow field. Consequently, the gas-particle flow field will remain one-dimensional provided the mass density of particles of radius σ_2 is also much less than the mass density of the gas. Under these circumstances, the motions of σ_2 particles, caused by gas-particle and particle-particle interactions, may be studied without consideration of their effect on the gas or particles of radius σ_1 .

For the purposes of discussion, suppose that $\sigma_1 > \sigma_2$; particles of radius σ_1 and σ_2 will have different collisionless velocities u_{p1} and u_{p2} and different slip velocities $u_{s_1} = u - u_{p1}$ and $u_{s_2} = u - u_{p2}$. The particle velocities u_{p1} and u_{p2} will indicate local collisionless velocity of the particles. The local collisionless velocity is the local velocity that particles would have if there were no collisions. Now if the gaseous acceleration is negative in the direction of the positive x axis $u_{p1} > u_{p2}$ The relative velocity of these two particle sizes will lead to collisions between particles of radius σ_2 and particles of radius σ_1. If the velocity equilibration time of particles of radius σ_2 is short in comparison with the time between collisions, $\tau_{v_2} < \tau_{c_{21}}$, a particle of radius σ_2 that is disturbed from its local slip velocity by a collision will return to its local slip velocity before it encounters another particle.

The collision frequency $\nu_{c_{21}}$ computed in the classical manner is

$$\nu_{c_{21}} \cong n_{p_1} \pi (\Sigma_1 + \Sigma_2)^2 |u_{p1} - u_{p2}| \qquad (2.52)$$

and the mean free path between collisions

$$\lambda_{c_{21}} \sim \frac{u_{p2}}{\nu_{c_{21}}} = \frac{u_{p2}}{n_{p_1}\pi(\Sigma_1+\Sigma_2)^2|u_{p_1}-u_{p2}|} \qquad (2.53)$$

Collisions may be neglected if $\tau_{c_{21}} >> \tau$, corresponding to $\lambda_{c_{21}} >> L$.

The approximate time $\tau_{c_{21}}$ to be expected between encounters experienced by a particle σ_2 is

$$\tau_{c_{21}} \sim \frac{1}{\nu_{c_{21}}} \qquad (2.54)$$

and it is of interest to compare this time with the effective velocity equilibration time τ'_{u_2} , for a particle σ_2. Using

$$\tau'_{u_2} \simeq \frac{2m_2}{C_D(Re_2, M_2)\rho\pi\sigma_2^2|u-u_{p2}|} \qquad (2.55)$$

where local particle Reynolds number and Mach number are given by

$$Re_2 = \rho\sigma_2|u-u_{p2}|/\mu \qquad \text{and} \qquad M_2 = |u-u_{p2}|/a$$

respectively we have as the ratio of the characteristic times;

$$\frac{\tau'_{u_2}}{\tau_{c_{21}}} \sim \left(\frac{2m_2}{C_D(Re_2, M_2)\rho\pi\sigma_2^2|u-u_{p2}|}\right)\left(n_{p_1}\pi(\Sigma_1+\Sigma_2)^2|u_{p_1}-u_{p2}|\right) \qquad (2.56)$$

$$\frac{\tau'_{u_2}}{\tau_{c_{21}}} \sim \left(\frac{2}{C_D(Re_2, M_2)}\right)\left(\frac{\rho_{p1}}{\rho}\right)\left(\frac{|u_{p_1}-u_{p2}|}{|u-u_{p2}|}\right)\left(\frac{m_2}{m_1}\left(\frac{\Sigma_1+\Sigma_2}{\sigma_2}\right)^2\right) \qquad (2.57)$$

The magnitude of each of the bracketed terms may be estimated. If the local Reynolds number and Mach number are sufficiently small, $C_D(Re_2, M_2) \sim 12/Re_2$, $\Sigma_1 \sim \sigma_1$, $\Sigma_2 \sim \sigma_2$ and equation 2.57 becomes

$$\frac{\tau'_{v_2}}{\tau_{c_{21}}} \simeq \frac{1}{6}\left(\frac{\rho(\sigma_1+\sigma_2)|u_{p1}-u_{p2}|}{\mu}\right)\left(\frac{\rho_{p1}}{\rho}\right)\left(\frac{(\sigma_1+\sigma_2)\sigma_2^2}{\sigma_1^3}\right) \quad (2.58)$$

The quantity $\rho(\sigma_1+\sigma_2)|u_{p1}-u_{p2}|/\mu$ is the Reynolds number of particles based on their relative motion and in the Stokes law regime is less than or of order unity. The quantity ρ_{p1}/ρ is generally less than unity. The last term involves only the two particle radii and becomes small as σ_2/σ_1 becomes small. Therefore it is not restrictive to assume that

$$\frac{\tau'_{v_2}}{\tau_{c_{21}}} \lesssim 1 \quad (2.59)$$

where relative particle velocities are not large.

Outside the Stokes regime for particle Reynolds numbers greater than unity and Mach numbers less than or on the same order as unity, the drag coefficient of a sphere is of order unity. Except for unusual situations such as particle shock waves or extended turbulent wakes, experimental evidence[10] suggests that $\Sigma_1 \sim \sigma_1$ and $\Sigma_2 \sim \sigma_2$. Consequently even outside the Stokes regime there seems to be no difficulty in satisfying condition (2.59) if the density of particles of radius σ_1 is not too large and σ_2/σ_1 is sufficiently small.

Consider the motion of a test particle of radius σ_2, $\tau_{v_2}/\tau_{c_{21}} < 1$. If the particle were subject only to interaction with the gas, it would, after an initial transient, slip relative to the gas at a rate such that the viscous drag force accelerates the particle at very nearly the local gas acceleration rate. When the particle is disturbed from this state, it will return to the appropriate local state

of slip within a time of order τ_{v_2} . Now the collisions experienced by the test particle disturb the particle from the local equilibrium slip condition. The scattering velocities that result from collisions will have components normal and tangential to the directions of average gas velocity.

Consider first the scattering velocity component normal to the average motion as indicated in Figure 5 . Following a collision the normal velocity component decays toward zero with a time constant τ_{v_2} . Consequently if the time interval $\tau_{c_{21}}$ between successive collisions is larger than its velocity equilibration time τ_{v_2} , the particle enters into each collision with negligible velocity normal to the direction of gas flow. Furthermore, the particle has moved across the flow field, its transverse range based on the scattering velocity $u_{p_\perp}(0)$ normal to the gas flow. The transverse range, in the Stokes regime, is approximately $u_{p_\perp}(0)\,\tau_{v_2}$.

The scattering velocity parallel to the gas motion, see Figure 5 , is a bit more complicated. Prior to a collision the test particle is moving with its local collisionless slip velocity. After a collision, the parallel components of the particle velocity decays toward its collisionless slip velocity with time constant τ_{v_2} . Consequently the restriction insures that particles of radii σ_1 and σ_2 are moving at very nearly their local collisionless velocities prior to each collision.

We conclude that when $\tau_{v_2}/\tau_{c_{21}} \ll 1$ particles of radius σ_2 will "diffuse" across the gas flow. There is an interesting analogy with the manner in which a low density, weakly ionized plasma diffuses across a strong magnetic field, Figure 6 . The guiding center

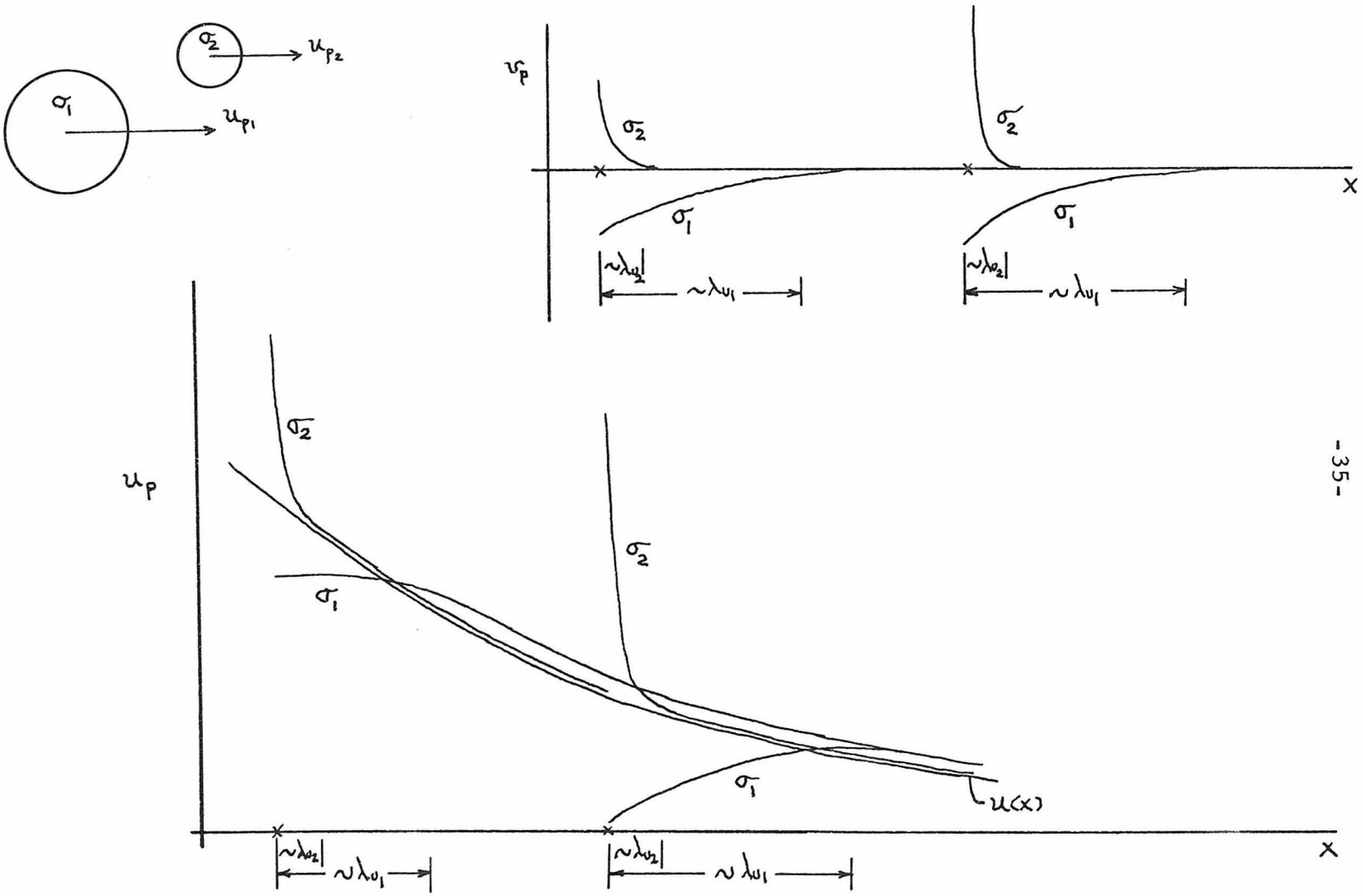

Figure 5. The positions of successive collisions for test particle σ_2 are marked along the x axis

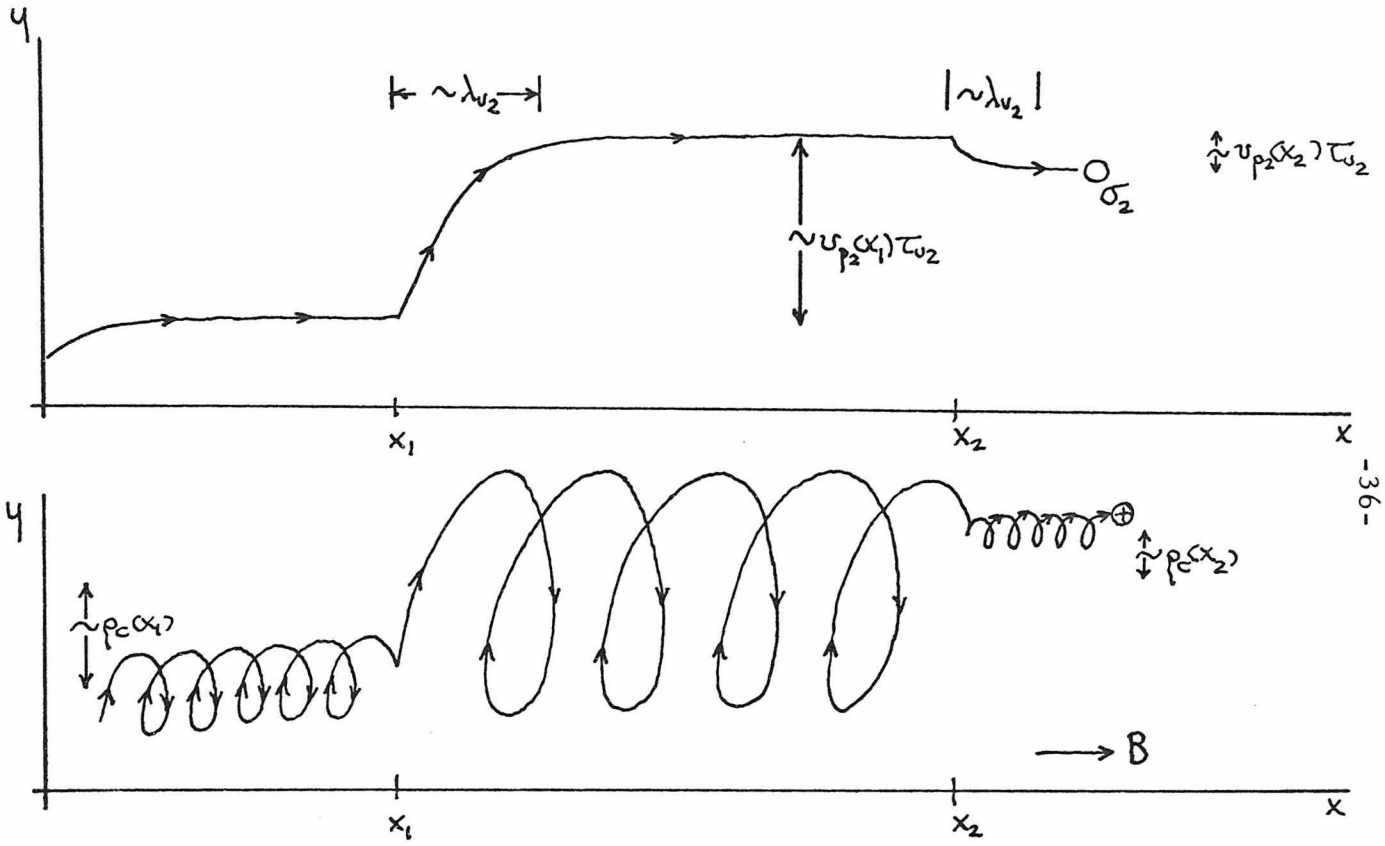

Figure 6. If a particle of radius σ_2 undergoes many collisions it will "diffuse" across the gas flow much like an ion diffuses across a weakly ionized low density plasma that is confined by a strong magnetic field.

of a typical ion in the plasma can move only a finite distance across the magnetic field due to collisions. This distance is characterized by its cyclotron radius $\rho_c \sim u_1(0)\,\tau_c$ where τ_c is the cyclotron period. The requirement that $\rho_{p1}, \rho >> \rho_{p2}$ so that collisions had a negligible effect on the dynamics of particles of radius σ_1, was a matter of convenience only. It assured that the initially one-dimensional gas flow would remain one-dimensional; if $\rho_{p1} \sim \rho_{p2} \sim \rho$ the gas flow will usually deviate from one-dimensionality.

The following physical picture of the gas-particle flow process will hold: If $\rho_{p1}, \rho_{p2} \lesssim O(\rho)$

and

$$\tau_{v2} < \tau_{c21}, \tau_{c22} < \tau$$

$$\tau_{v1} < \tau_{c11}, \tau_{c12} < \tau ,$$

then

(1) the collisionless slip velocities of the particles are determined by the local acceleration of the equilibrium gas-particle flow field.

(2) the random particle velocities resulting from inter-particle collisions have essentially decayed to zero before the next collision takes place.

(3) all collisions take place with a relative velocity equal to the difference between the local collisionless velocities of the two particle sizes and with a direction parallel to the local gas acceleration. Consequently collisions between like particles are unimportant.

(4) collisions between particles result in a transfer of momentum, due to viscous interaction, from the particles to the gas in the

direction normal to the local gas acceleration. A gas flow that is initially one-dimensional if $\rho_{p1} \sim \rho_{p2} \sim \rho$ will most likely deviate from one-dimensionality as a consequence of particle-particle interactions.

III. NORMAL SHOCK WAVE IN A GAS-PARTICLE MIXTURE

The considerations of Chapter II suggest that there exist a fairly wide class of physically interesting gas-particle flows for which conditions

$$\tau_o << \tau_c << \tau_{oij} << \tau_{vi}, \tau_{cij}, \tau$$

$$\lambda_o << \lambda_c << \lambda_{oij} << \lambda_{vi}, \lambda_{cij}, L$$

hold. Collisions between particles within the gas are well-defined events so that particle-gas and particle-particle interactions, which govern the evolution of the system, are readily distinguished. Between collisions, the particles interact primarily with the gas. In addition, the experiments suggest that when $\tau_{oij} << \tau_{vi}, \tau_{vj}$, the collisions between particles are nearly elastic and the effect of the gas is relatively negligible.

Throughout the remainder of the analysis we shall consider the encounter to be elastic, recognizing that even with its weakness, this assumption is the most reasonable within the present state of our knowledge. Indeed, it will turn out that many of our results, if compared with a suitable experiment, should provide insight into the true character of the particle-particle interaction law in a dilute gas-particle system.

With the picture of the physical phenomena which we have formed, let us consider the passage of a normal shock wave through a gas containing a distribution of small, solid, spherical particles. This example is intended:

(1) to demonstrate that the principles of kinetic theory may be extended to treat quantitatively the dynamics of dilute gas-particle flows in which particle-particle interactions are important;

(2) to determine novel physical features introduced by particle-particle collisions; and

(3) to ascertain the general importance of collisions in the dynamics of dilute gas-particle suspensions.

We shall suppose the dust is composed of particles of two distinct sizes with radii σ_1 and σ_2. To insure simplicity at a later stage of the calculation, we shall let particles of radius σ_1 be distributed uniformly upstream of the shock wave. On the other hand, particles with radius σ_2 are non-uniformly distributed in a direction parallel to the face of the normal shock wave with a density much less than that of particles σ_1. Under these conditions, particles of radius σ_2 have little effect on the motion of the gas and particles σ_1. The motions of the gas and particles with radius σ_1, however, are strongly coupled. These circumstances permit us to examine the effect of collisions on the motion of the cloud of particles σ_2 downstream of the normal shock wave.

We shall compute first the dynamics of the gas-particle mixture due to the presence of the shock wave, neglecting the presence of particles σ_2. Then, using these results, we shall analyze in detail the motions of particles σ_2 in the known gas-particle flow field.

Finally, primarily to simplify the analysis, we shall make several restrictive assumptions regarding the gas-particle and

particle-particle interactions. Stokes drag law will be used to describe the gas-particle interaction. The collisions between particles will be approximated by collisions between rigid elastic spheres, considering the gas to have negligible effect on the particle-particle interaction. Throughout the discussion, every effort will be made to ascertain the validity of these assumptions and their general effect on the solution. It will be shown, quite clearly, that their primary effect on the results is quantitative. Qualitatively, they do not alter the essential physical features of the gas-particle flow downstream of the gasdynamic shock wave.

1. Passage of a Normal Shock Wave through a Uniform Distribution of Particles of a Single Size.

Consider a normal shock wave in a mixture of perfect gas and a collection of small, solid, spherical particles of essentially uniform radius σ_1 . So long as the solid particles are large with respect to the molecular mean free path of the gas, $\sigma_1 >> \lambda_c$, the thickness of a gasdynamic shock is negligible in comparison with the momentum and thermal ranges of the particles. Thus, the structure of a normal shock wave in a dilute particle-gas mixture may be thought of as a conventional gasdynamic shock which produces temperature and velocity conditions of the gas different from those of the particles. Following this essentially discontinuous variation of the gas properties is a relaxation zone in which equilibrium between the particles σ_1 and the gas is gradually re-established through the mechanisms of particle drag and heat transfer. If the particles represent a significant frac-

tion of the mass of the gas-particle σ_l mixture, their response to changes in the gas, in turn, modifies the state of the gas.

The statement and analysis equations of this problem were apparently first given by Carrier[5]. Various aspects of the relaxation process were also studied by other investigators, for instance, Marble[4], Rudinger[6], and Kriebel.[7] In the present presentation we will follow the analysis by Marble[4] since his approximations are consistent with ours.

The number density of particles σ_l is sufficiently low that pairs or groups of particles may be considered non-interacting. The volume occupied by the particulate matter is assumed negligible. At any point in space not occupied by a particle, the state of the gas is defined by its local pressure, density, temperature, and three components of velocity. The properties of the gas are assumed to be smoothed; only the average effects of particle motions are accounted for. The energy and momentum present in the particle wakes are assumed to be dissipated immediately and uniformly through a volume with dimension of the order of particle spacing. The gas is treated as inviscid except for its interaction with the particles. The state of any particle is defined by its velocity components and its temperature, both generally differing from those of the gas. As a consequence of these assumptions, it is admissible to employ the known behavior of isolated particles in uniform gas fields to calculate the interaction between the two phases. The shock wave and shock structure are stationary in the reference frame employed.

Under these restrictions, the method presented by Marble[4]

may be used to establish the equations of motion for this gas-particle σ_1 mixture. Denote the gas velocity and density by u and ρ, respectively, and designate the average velocity and density of particles σ_1 by u_{p1} and ρ_{p1}, respectively. The mass flow of each phase is conserved, so

$$\rho u = \dot{m} \tag{3.1}$$

$$\rho_{p1} u_{p1} = K_1 \dot{m} \tag{3.2}$$

where $\dot{m}$ is the gas mass flow rate per unit area and $K_1\dot{m}$ is the mass flow rate of the solid particles σ_1 per unit area. Likewise, the momentum equations for the two phases are

$$\rho u \frac{du}{dx} + \frac{dp}{dx} = F_{p1} \tag{3.3}$$

$$\rho_{p1} u_{p1} \frac{du_{p1}}{dx} = -F_{p1} \tag{3.4}$$

where p is the local gas pressure and F_{p1} is the force exerted upon a unit volume of the gas by the particles. The partial pressure of the particle σ_1 cloud is negligible. For a number density n_{p1} of non-interacting particles σ_1, assuming that the particles obey Stokes drag law, F_{p1} is given by

$$F_{p1} = \frac{\rho_{p1} a}{\lambda_{v_1}} (u_{p1} - u) \tag{3.5}$$

Since the particles are non-interacting, u_{p1} may be interpreted as the local collisionless velocity of particles with radius σ_1. Furthermore, $\lambda_{v_1} \equiv m_1 a / 6\pi\mu\sigma_1$ is defined as the velocity

equilibration length of particles σ and a is the local gaseous sound speed. It will be assumed that the local gas viscosity $\mu \sim T^{1/2}$, so that the ratio μ/a is a constant, and consequently λ_{v_1} is also constant.

The first law of thermodynamics for the gas is

$$\rho u c_p \frac{dT}{dx} - u \frac{dp}{dx} = (u_{p_1} - u) F_{p_1} + Q_{p_1} \quad (3.6)$$

where Q_{p_1} is the heat transferred per unit volume per second from the particles to the gas; the term $(u_{p_1} - u) F_{p_1}$ represents the dissipative work done on the gas by the particles passing through the gas. The specific heat, c_p, at constant pressure, is assumed constant. To the same approximation as Stokes law, we assumed the heat transfer between the particles and the gas takes place at a Nusselt number (based on particle radius) of unity, and Q_{p_1} may be written as

$$Q_{p_1} = \frac{\rho_{p_1} c_p a}{\lambda_{T_1}} (T_{p_1} - T) \quad (3.7)$$

where $$\lambda_{T_1} \equiv c_p m_1 a / 4\pi k \sigma_1 = \frac{3}{2} Pr \lambda_{v_1}$$

is the thermal equilibration length for particles σ_1. Usually, the value of the Prandtl number, $Pr \equiv c_p \mu / k$, is assumed to be a constant and is essentially equal to 2/3, so that λ_{v_1} and λ_{T_1} are considered equal.

The first law of thermodynamics for the solid phase is

$$\rho_{p1} u_{p1} c_s \frac{dT_{p1}}{dx} = -\varphi_{p1} \tag{3.8}$$

where c_s is the constant specific heat of the solid material. Together with the equation of state for a perfect gas,

$$p = \rho R T \tag{3.9}$$

the above equations provide a complete description of the non-equilibrium gas-particle σ_1 flow downstream of the gasdynamic shock wave.

Equations (3.3), (3.4), (3.6), and (3.8) together with the equations of continuity (3.1) and (3.3) may be combined and integrated directly to give the conservation laws

$$\rho u^2 + \rho_{p1} u_{p1}^2 + p = C_1 \tag{3.10}$$

$$\rho u \left\{ c_p T + \frac{u^2}{2} \right\} + \rho_{p1} u_{p1} \left\{ c_s T_{p1} + \frac{u_{p1}^2}{2} \right\} = C_2 \tag{3.11}$$

where C_1 and C_2 are constants. The conservation laws (3.1), (3.2), (3.10), and (3.11) are sometimes referred to as the mass, momentum, and energy integrals of the flow. They are valid even across the shock wave.

We now denote, as indicated in Figure 7, the conditions upstream of the shock, where the gas and particles σ_1 are in mechanical and thermal equilibrium, by 1; the conditions immediately downstream of the gasdynamic shock by 2; and by ∞, the condition far

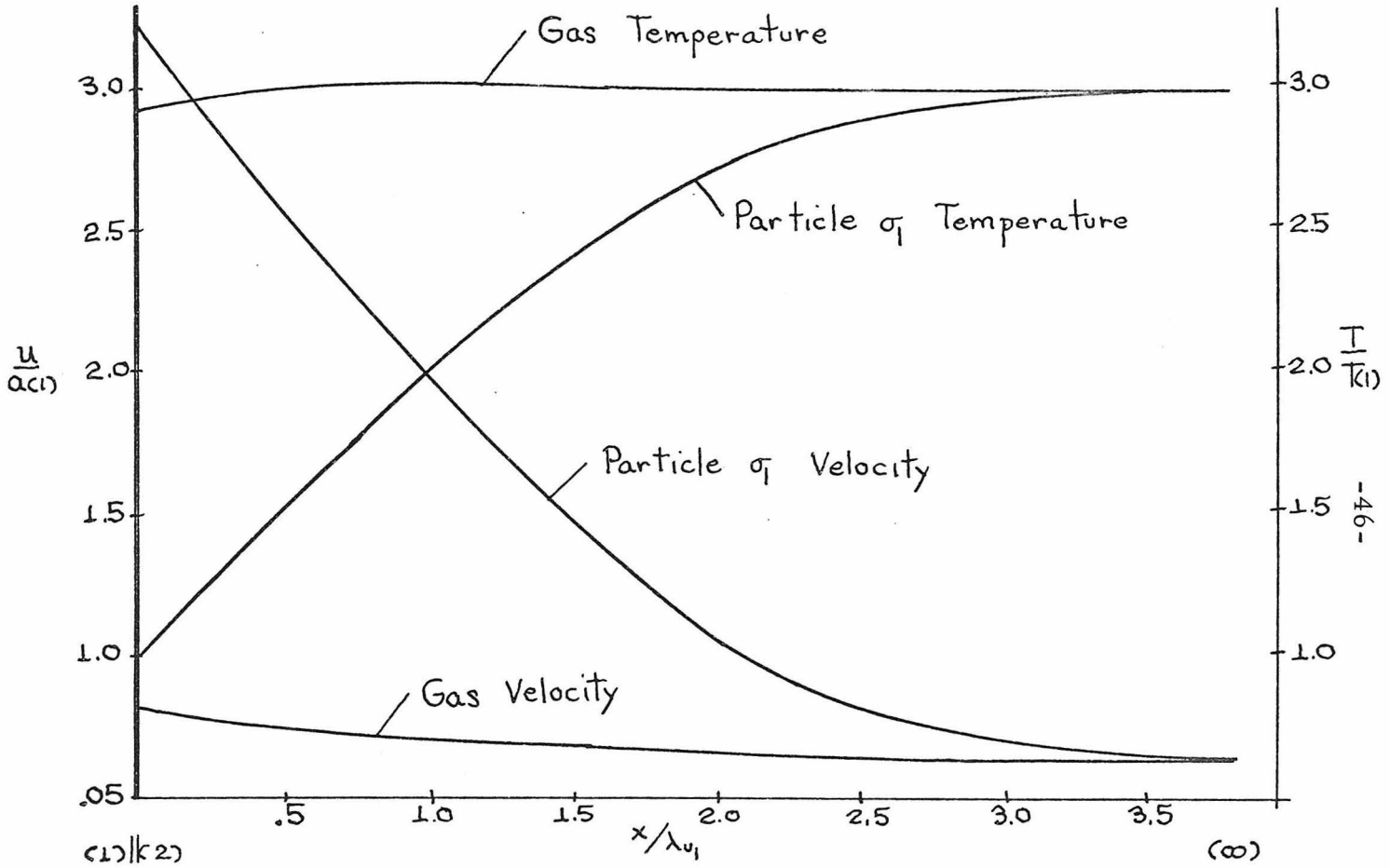

Figure 7. Spatial non-equilibrium of a gas-particle σ_1 flow downstream of a gas dynamic shock wave $M_1 = 3.2$, $\gamma = 1.4$, $K_1 = .25$, $c_s/c_p = \lambda_{u_1}/\lambda_{T_1} = 1$

downstream where velocity and thermal equilibrium has been re-established between the solid particles and the gas. Then, since the particles do not affect the structure of the gasdynamic shock, the change in state of the gas from 1 to 2 is given by the conventional gasdynamic shock relations

$$\frac{\rho(1)}{\rho(2)} = \frac{u(2)}{u(1)} = \frac{2}{(\gamma+1)M_1^2}\left\{1 + \frac{(\gamma-1)}{2}M_1^2\right\} \qquad (3.12)$$

$$\frac{T(2)}{T(1)} = \left(\frac{a(2)}{a(1)}\right)^2 = \left(1 + \frac{2\gamma}{\gamma+1}(M_1^2-1)\right)\left(1 - \frac{2}{(\gamma+1)M_1^2}(M_1^2-1)\right) \qquad (3.13)$$

where $M_1 \equiv u(1)/a(1)$ is the Mach number of the shock relative to the gas and $\gamma = c_p/c_v$ is the specific heat ratio of the gas.

The equilibrium conditions far downstream of the shock wave are altered by the particles and may be related to the conditions upstream of the shock wave by applying the mass, momentum, and energy integrals of the gas-particle σ_1 mixture between these two points. For simplicity, if we set $c_p/c_s = 1$, then

$$\frac{u(\infty)}{u(1)} = \frac{1}{\left(1 + k_1\left(\frac{2\gamma}{\gamma+1}\right)\right)}\left(\frac{2}{\gamma+1}\right)\left\{\frac{1 + \frac{(\gamma-1)}{2}M_1^2}{M_1^2}\right\} = \frac{u_{p_1}(\infty)}{u_{p_1}(1)} = \frac{\rho_{p_1}(1)}{\rho_{p_1}(\infty)} \qquad (3.14)$$

$$= \frac{\rho(1)}{\rho(\infty)}$$

By comparison of these results with (3.12), we have a relation between the gas velocity immediately downstream of the shock wave and the gas velocity far downstream:

$$\frac{u(\infty)}{u(2)} = \frac{1}{\left(1 + K_1\left(\frac{2\gamma}{\gamma+1}\right)\right)} \qquad (3.15)$$

This relation indicates the general effect of the particles on the gas; the significance of K_1 . For situations of interest in this thesis, $K_1 \lesssim 1$; consequently, for $\gamma \sim 1.4$ corresponding to a diatomic gas, $u(\infty)/u(2) \lesssim 1/2$.

The detailed variations of the properties of the gas and particles σ_1 are determined by numerical evaluation of equations (3.1), (3.2), (3.4), (3.8), (3.10), and (3.11), utilizing C_1 and C_2 evaluated upstream of the shock wave. The appropriate initial conditions at $X = 0$ for the evaluation of the particle equations of motion are $u_{p_1}(0) \simeq u(1)$ and $T_{p_1}(0) \simeq T(1)$. When solving (3.10) and (3.11) for T and u , care must be taken to assure that as $X \to 0$ from downstream of the shock wave, $u \to u(2)$ and $T \to T(2)$.

A typical solution, which illustrates the general character of the relaxation zone downstream of the gasdynamic shock wave, is presented in Figure 7. Downstream of the shock wave the particles and the gas are out of equilibrium. Because of their greater velocity, the particles do work on and transfer momentum to the gas; as a result, they are decelerated. The force applied to the gas tends to establish a positive pressure gradient in the gas as well as to increase its momentum flux. The dissipation and heat transfer associated with the particles decrease and increase its density, respectively. Generally, the properties of the gas and particles are such that the gas velocity is reduced downstream of the shock wave.

Rudinger[6] has investigated the variations in structure of the relaxation zone when different assumptions are made for the drag and heat transfer laws which govern the gas-particle σ_1 interaction. His results show that quantitatively both the particle velocity and gas pressure are significantly affected by the assumption for the drag coefficient. As should be expected, the Stokes law produces a relatively large zone. In contrast, the assumptions for the heat transfer law have only a small effect. In general, however, the essential physical features of the relaxation zone are qualitatively correct in all cases using the Stokes drag law and heat transfer law with Nusselt number unity.

2. Problem of a Shock Wave Passing through a Gas Containing Particles of Two Distinct Sizes.

When particles of a different size, σ_2, are present in the gas under the condition that $\rho_{p_2} << \rho, \rho_{p_1}$, the shock relaxation zone is established solely by the interaction of particles σ_1 and the gas. The motion of particles σ_2 is then governed by their interaction with the gas and collisions with particles of radius σ_1. This situation may be studied by considering the magnitude of the particle size ratio, σ_2/σ_1.

When $\sigma_2/\sigma_1 >> 1$, the length of the shock relaxation zone, established by the interaction of particles σ_1 and the gas, is small compared to the velocity equilibration length, λ_{v_2}, of the particles σ_2. Consequently, throughout most of the relaxation zone, particles σ_2 are moving through a uniform distribution

composed of much smaller particles. This phenomenon is similar to the motion of a steel ball through still air. There will be a drag force exerted on the particle of radius σ_2 due to encounters with particles σ_1 in addition to the viscous drag associated with its motion relative to the gas. On the other hand, there will be essentially no redistribution of particles σ_2 in the directions parallel to the shock face. We shall not consider this case in further detail.

When $\sigma_2/\sigma_1 \ll 1$, the length of the relaxation zone of the shock wave is large compared to the velocity equilibration length of particles σ_2. Under these conditions, the redistribution of particles σ_2 is collision dominated. When the distribution of particles σ_1 is dilute, binary collisions $\sigma_2 - \sigma_1$ are important, and because of the large momentum transferred to particles σ_2 during collision there may be a substantial spreading of the cloud of particles σ_2 downstream of the shock wave. This situation is studied in detail in Chapter IV.

When $\sigma_2/\sigma_1 \sim 1$, the particles have very nearly the same velocity, and consequently have at most one collision during their passage through the shock relaxation zone. The particles collide while moving at their local collisionless velocities. The particles are of nearly the same size, so their velocity equilibration lengths, λ_{v_1} and λ_{v_2}, are approximately equal. Following a collision σ_2 particles move a distance of order λ_{v_2} normal to the gas flow field, relative to the characteristic length λ_{v_1} of the shock relaxation zone. Therefore, a substantial redistribution of particles σ_2 due to single collisions is possible. This case will be considered in detail

in Chapter V.

IV. PARTICLE-PARTICLE SCATTERING IN A SHOCK WAVE; $\sigma_2/\sigma_1 \ll 1$, NON-UNIFORM DISTRIBUTION OF SMALL PARTICLES

When $\sigma_2/\sigma_1 \ll 1$, a particle of radius σ_2 may have many collisions with particles of radius σ_1 satisfying the conditions

$$\tau_o \ll \tau_c \ll \tau_{o21} \ll \tau_{v_2} < \tau_{c21} \ll \tau_{v_1}$$
$$\lambda_o \ll \lambda_c \ll \lambda_{o21} \ll \lambda_{v_2} < \lambda_{c21} \ll \lambda_{v_1} \qquad (4.1)$$

during its motion through the shock relaxation zone of thickness of order λ_{v_1}. It will become evident later that since $\rho_{p2} \ll \rho_{p1} \sim \rho$ conditions (4.1) can be met, provided the particles are sufficiently small, namely $\sigma_1 \lesssim 10\text{-}100\,\mu$. The large difference between the collisionless velocities of the two types of particles is indicated in Figure 8. Under conditions (4.1), only binary encounters are important and, between successive collisions with particles σ_1, particles σ_2 relax to their local collisionless velocities. Therefore, the macroscopic motion of the non-uniform distribution of particles of radius σ_2, downstream of the gasdynamic shock, is expected to be diffusive or collision dominated. Consequently, there may be a substantial redistribution of the cloud of particles of radius σ_2 in directions normal to the gas flow. Let us now analyze the process in detail, supposing that conditions (4.1) are satisfied throughout the relaxation zone and that the particle-gas interaction is governed by Stokes law.

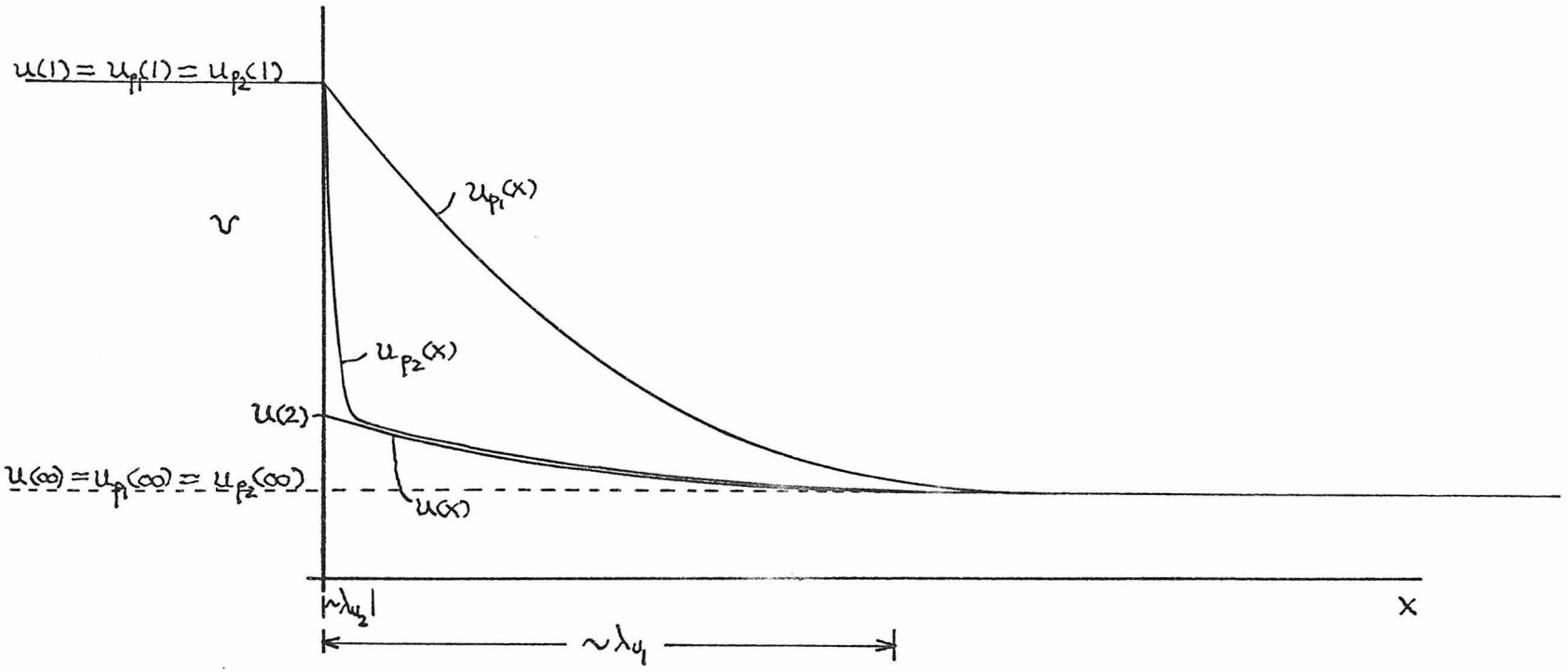

Figure 8. Collisionless velocity relaxation conditions when $\sigma_2/\sigma_1 \ll 1$

1. Macroscopic Motion of Particles σ_2.

The dynamics of particle cloud σ_2 will be computed by assuming $\rho_{p1} \ , \rho >> \rho_{p2}$ so that the presence of particles σ_2 has essentially no effect on the motion of the gas and the cloud of particles σ_1 downstream of the shock wave.

Upstream of the shock wave, all particles are in mechanical and thermal equilibrium with the gas, but particles of radius σ_2 are non-uniformly distributed in a direction parallel to the shock face, while particles of radius σ_1 are uniformly distributed. If we denote by 1 conditions upstream of the shock wave; by 2, conditions immediately downstream of the shock; and by ∞, conditions far downstream where mechanical and thermal equilibrium between the particles and the gas has been re-established, then upstream of the gasdynamic shock,

$$\begin{aligned} u_{p_1}(1) &= u_{p_2}(1) = u(1) \\ T_{p_1}(1) &= T_{p_2}(1) = T(1) \\ \rho_{p_1}(1) &= K_1 \rho(1) \ ; \ \rho_{p_2}(1) = \rho_{p_2}^{(1)}(y,z) \end{aligned} \tag{4.2}$$

Throughout the calculation the right-handed Cartesian coordinate system xyz is oriented so x measures distances normal to the shock face, y and z measure distances parallel to the shock face, Figure 9. The origin of xyz is located on the downstream side of the mathematically infinitely thin shock wave.

Because of their size and mass, the particles are unaffected by passing through the gasdynamic shock, while the gas undergoes a compressive change of state. The change in the state of the gas is

computed from the usual gasdynamic jump conditions. The macroscopic properties of the particles are continuous across the shock wave. Consequently, immediately downstream of the shock wave, at $X = 0$, the states of the gas and particles are related to their conditions upstream of the shock by

$$\frac{\rho(2)}{\rho(1)} = \frac{u(1)}{u(2)} = \frac{2}{(\gamma+1)M_1^2}\left\{1 + \frac{(\gamma-1)}{2} M_1^2\right\}$$

$$\frac{T(2)}{T(1)} = \left(\frac{a(2)}{a(1)}\right)^2 = \left(1 + \frac{2\gamma}{\gamma+1}(M_1^2-1)\right)\left(1 - \frac{2}{\gamma+1}\frac{(M_1^2-1)}{M_1^2}\right)$$

$$T_{p_2}(2) = T_{p_1}(2) = T(1) \qquad (4.3)$$

$$u_{p_2}(2) = u_{p_1}(2) = u(1)$$

$$\rho_{p_1}(2) = K_1\rho(1) \quad ; \quad \rho_{p_2}(2) = \rho_{p2}^{(1)}(y,z)$$

By changing the state of the gas, the gasdynamic shock has established a non-equilibrium situation between the particles and the gas. The relaxation of this gas-particle mixture to a new equilibrium state, where the particles and the gas are again in mechanical and thermal equilibrium, is governed by the following considerations.

Because the number density of particles of radius σ_2 is very small, the particles σ_2 have no effect on the dynamics of the gas or the particles of radius σ_1. The gas-particle σ_1 flow remains one-dimensional downstream of the shock and is governed by

the exchange of momentum and energy between the gas and particles of radius σ_1 . This gas-particle σ_1 problem has been treated in detail in Chapter III. Henceforth, we will assume that ρ , u , T , ρ_{p1} , u_{p1} , and T_{p1} are known functions of x derived by numerical solution of the problem formulated in Chapter III. Within this approximation, the equilibrium state achieved by the gas and particles of radius σ_1 is independent of the presence of particles of radius σ_2 .

On the other hand, the motion of particles σ_2 downstream of the gasdynamic shock is governed by viscous interaction with the gas and by collisions with particles σ_1 . The dynamics of the cloud of particles of radius σ_2 downstream of the shock can be viewed as the spreading of a non-uniform stream or beam of particles moving perpendicularly away from the shock face. The spreading or redistribution of this beam is due to collisions between particles of radius σ_2 and the particles of radius σ_1 which are unaffected by the beam. Consequently, the final distribution in the beam of particles σ_2 will depend on their complete interaction with the gas-particle σ_1 mixture.

The macroscopic states of particles of radius σ_2 are continuous across the gasdynamic shock wave and are therefore known at $x = 0$. Although the distribution of particles σ_2 is dilute, the number density is sufficiently high that fluctuations in the macroscopic properties of the particle cloud may be neglected and the methods of continuum mechanics are applicable. This assumption implies that within an infinitesimal volume element there are suffi-

cient particles σ_2 that particle density n_{p2} and other macroscopic properties of the σ_2 particle cloud are well defined.

The equation of continuity for particles σ_2 is established in the usual manner. Consider a fixed element of volume V whose surface is of arbitrary shape, but closed, with area A. The mass of particles of radius σ_2 within this volume is

$$\int_V \rho_{p2}\, dV \tag{4.4}$$

where $\rho_{p2} = m_2 n_{p2}$ is the mass density of particles σ_2 and the integration is over the volume V. The mass of particles σ_2 flowing in unit time through an element $d\underline{A}$ of the surface bounding the volume V is $\underline{\mathcal{F}}_{p2} \cdot d\underline{A}$ where $\underline{\mathcal{F}}_{p2}$ is the local mass flux density of particles of radius σ_2. Its direction is that of the average motion of the particles, while its magnitude equals the mass of particles of radius σ_2 flowing in unit time through a unit area perpendicular to the average velocity, $\underline{v}_{p2}$, of the particles; $\underline{\mathcal{F}}_{p2} = \rho_{p2}\underline{v}_{p2}$. The magnitude of the vector $d\underline{A}$ is equal to the area of the surface element and its direction is along the local normal. By convention we take $d\underline{A}$ positive along the outward normal. Then $\underline{\mathcal{F}}_{p2} \cdot d\underline{A}$ is positive if the particles are flowing out of the volume V, and negative if they are flowing into the volume. Consequently, the total mass of particles σ_2 flowing out of the volume V in unit time is

$$\int_A \underline{\mathcal{F}}_{p2} \cdot d\underline{A} \tag{4.5}$$

where the integration is over the whole closed surface A surrounding the volume V.

Since the mechanical properties of particles σ_2 are invariants of their motion through the gas and during encounters with particles σ_1, the decrease per unit time in the mass of particles σ_2 in the volume V

$$-\frac{\partial}{\partial t}\int_V \rho_{p2}\,dV \tag{4.6}$$

must equal the total mass of particles σ_2 flowing out of the volume V in unit time. Therefore, equating (4.5) and (4.6),

$$-\frac{\partial}{\partial t}\int_V \rho_{p2}\,dV = \int_A \underline{\varphi}_{p2}\cdot d\underline{A} \tag{4.7}$$

we establish the integral form of the conservation of mass for particles of radius σ_2. The surface integral can be transformed by Green's Theorem to a volume integral; then equation (4.7) becomes

$$\int_V \left\{ \frac{\partial \rho_{p2}}{\partial t} + \nabla\cdot\underline{\varphi}_{p2} \right\} dV = 0 \tag{4.8}$$

Since the particular choice of V is completely arbitrary, the integrand in equation (4.8) must vanish everywhere in the shock relaxation zone. Therefore, in differential form, the equation of continuity of particles σ_2 is

$$\frac{\partial \rho_{p2}}{\partial t} + \nabla\cdot\underline{\varphi}_{p2} = 0 \tag{4.9}$$

where $\underline{\varphi}_{p2} = \rho_{p2}\underline{v}_{p2}$ is the local mass flux density of particles of radius σ_2. Since there are no oscillations or other time-dependent phenomena present in the shock relaxation zone, $\frac{\partial}{\partial t}\rho_{p2} = 0$ and equation (4.9) becomes

$$\nabla \cdot \underline{\varphi}_{f_{p2}} = 0 \tag{4.10}$$

Define $\underline{u}_{p2} = u_{p2}(x)\, \underline{e}_x$ as the local collisionless velocity of particles σ_2 ; u_{p2} is the velocity particles σ_2 would have if they passed through the shock relaxation zone without encountering any particles of radius σ_1 . Then, since we have assumed that the particles interact with the gas according to the first order Stokes law, u_{p2} is given by

$$u_{p2} \frac{du_{p2}}{dx} = \frac{a}{\lambda_{v_2}} (u - u_{p2}) \tag{4.11}$$

where immediately behind the shock wave at $x=0$, $u_{p2}(0) = u(1)$, $\lambda_{v_2} \equiv m_2 a / 6\pi\mu\sigma_2$ is the velocity equilibration length for particles σ_2 and is a constant since we assumed a/μ , the ratio of the gaseous sound speed to the gas viscosity, is a constant. Without loss of generality, the local mass flux density of particles of radius σ_2 , $\underline{\varphi}_{f_{p2}}$, may be written

$$\underline{\varphi}_{f_{p2}}(\underline{x}) = \rho_{p2}(\underline{x})\, u_{p2}(x)\, \underline{e}_x + \underline{\varphi}^{(r)}_{f_{p2}}(\underline{x}) \tag{4.12}$$

This decomposition simplifies the treatment of the motion of particles σ_2 between collisions and allows $\underline{\varphi}^{(r)}_{f_{p2}}$ to be computed by kinetic theory methods.

Now $\underline{\varphi}^{(r)}_{f_{p2}}$ is the local mass flux density of particles σ_2 at the origin of a non-inertial reference frame which is moving at the local collisionless velocity of particles σ_2 . In the absence of collisions, $\underline{\varphi}_{f_{p2}} = \rho_{p2}\, u_{p2}\, \underline{e}_x$; consequently, $\underline{\varphi}^{(r)}_{f_{p2}}$ is the flux of particles σ_2 due to collision of particles σ_2 with particles σ_1.

In general, $\underline{\varphi}_{p2}^{(r)}$ depends on ρ_{p1}, u_{p1}, ρ, u, ρ_{p2}, u_{p2}, and their spatial derivatives, namely, $\underline{\varphi}_{p2}^{(r)} = \underline{\varphi}_{p2}^{(r)}(\rho_{p1}, u_{p1}, \rho, u, \rho_{p2}, u_{p2})$ When $\underline{\varphi}_{p2}^{(r)}$ is known in this form, equation (4. 10) leads to an equation for ρ_{p2}, the mass density of particles σ_2. The values of ρ_{p1}, u_{p1}, ρ, and u are known from the solution of the gas-particle σ_1 problem, and u_{p2} is obtained from (4. 11). Therefore, ρ_{p2} satisfies

$$\frac{\partial}{\partial x}\left(\rho_{p2}(x)\, u_{p2}(x)\right) + \nabla \cdot \underline{\varphi}_{p2}^{(r)}(\rho_{p1}, u_{p1}, \rho, u, \rho_{p2}, u_{p2}, x) = 0 \qquad (4.13)$$

together with appropriate boundary conditions.

In the present problem, $\underline{\varphi}_{p2}^{(r)}$ can be found, with good approximation, by a straightforward extension of the "mean free path"[12] method of kinetic theory.

The particle flux $\underline{\varphi}_{p2}^{(r)}$ depends fundamentally on the σ_1 particle - σ_2 particle interaction law and the characteristics of the motion of particles σ_2 between collisions. It will prove convenient to view this motion as an observer at rest in a reference frame moving at the local collisionless velocity.

2. Motion of a Particle Impulsively Disturbed from Its Local Collisionless Motion

Before proceeding with the detailed calculation of $\underline{\varphi}_{p2}^{(r)}$, consider the motion of a particle σ_2, following a collision with a particle of radius σ_1, as viewed from a reference frame moving at the local collisionless velocity of particles of radius σ_2. Since $\tau_{v_2} < \tau_{z_1}$, the particle σ_2 is nearly at rest in this reference frame if the collision takes place near the origin. For simplicity, we will assume

that the origin of this reference frame is coincident with the center of the particle σ_2 prior to the encounter. The Cartesian axes $x_c y_c z_c$ are taken parallel to the xyz axes which define the rest frame of the gasdynamic shock, Figure 9. At time $t=0$, the position and velocity of reference frame $x_c y_c z_c$ relative to the shock wave are $x=0$, $y=y_0$, $z=z_0$, and $u_{p_2}(0)=u(1)$. The calculation of the local collisionless velocity of particles σ_2 may be carried out using either Eulerian or Lagrangian coordinates. Both are useful for our purposes.

In Eulerian coordinates, the local collisionless velocity, $u_{p_2}(x)$, of particles of radius σ_2, since the flow is steady, is determined by the solution of

$$m_2 u_{p_2}(x) \frac{du_{p_2}(x)}{dx} = 6\pi\mu(x)\sigma_2 (u(x)-u_{p_2}(x)) \quad (4.14)$$

together with the condition immediately downstream of the gasdynamic shock wave; at $x=0$, $u_{p_2}(0)=u(1)$. The solution of (4.14) defines a velocity field $u_{p_2}(x)$.

In Lagrangian coordinates, the local collisionless velocity, $u^{(c)}_{p_2}(s)$, is given by the solution of the pair of coupled differential equations

$$m_2 \frac{du^{(c)}_{p_2}(s)}{ds} = 6\pi\mu(x^{(c)}_{p_2}(s))(u(x^{(c)}_{p_2}(s)) - u^{(c)}_{p_2}(s)) \quad (4.15)$$

and

$$\frac{dx^{(c)}_{p_2}(s)}{ds} = u^{(c)}_{p_2}(s) \quad (4.16)$$

where s is a dummy time parameter. At time $s=0$, the position

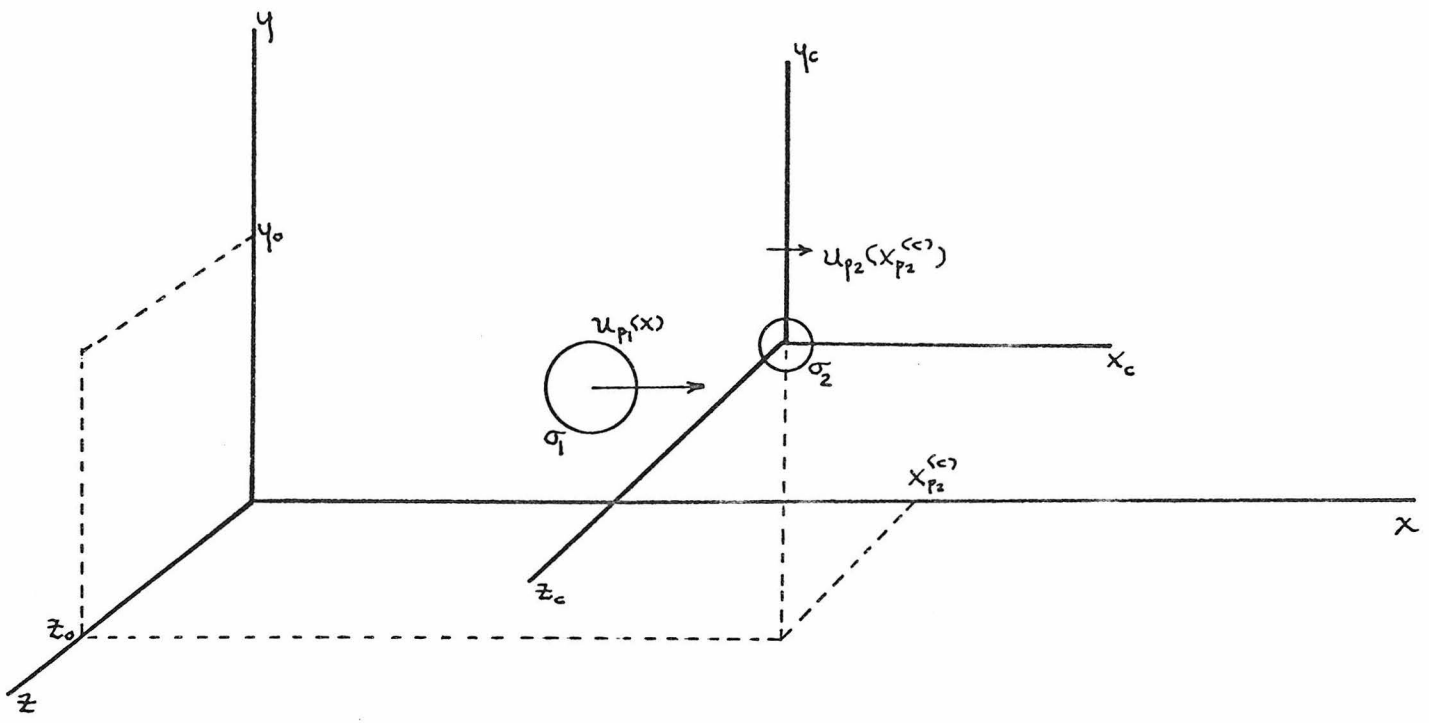

Figure 9. Definition of reference frames. The shock wave is stationary in xyz and is located at $x=0$. The cartesian reference frame xyz together with clocks is an inertial reference frame. The reference frame $x'y'z'$, moving at the local collisionless velocity, $u_{p_2}(x)$, of particles σ_2, is decelerating relative to xyz.

of the particle is $X^{(c)}_{p_2}(0) = 0$ and its velocity is $u^{(c)}_{p_2}(0) = u(1)$. Equations (4. 15) and (4. 16) are the characteristic equations of (4. 14). They describe the trajectory of a particle that at $S=0$ is immediately downstream of the gasdynamic shock. Since the gas flow is steady, the subsequent motion of the particle is such that at time $S=S_1$ the particle will be at position $X = X^{(c)}_{p_2}(S_1)$ and its velocity will be $u_{p_2} = u^{(c)}_{p_2}(S_1) = u_{p_2}(X^{(c)}_{p_2}(S_1))$. Consequently, the link between the two descriptions is simply

$$u_{p_2}(X^{(c)}_{p_2}) = u^{(c)}_{p_2}(S(X^{(c)}_{p_2})) \tag{4. 17}$$

or

$$u_{p_2}(X) = u^{(c)}_{p_2}(S(X)) \tag{4. 18}$$

The position of the origin of the reference frame $x_c y_c z_c$ for $t>0$ may be computed from (4. 15) and (4. 16) by simply replacing S by t. Furthermore, the velocity of this reference frame is related to the collisionless velocity field, $u_{p_2}(X)$, of particles σ_2 by (4. 17) and (4. 18).

Let us now calculate the motion of particle σ_2, initially at rest at the origin of $x_c y_c z_c$ following a collision with a particle σ_1. The encounter between the two particles occurs in the relaxation zone of the shock wave at time $t=t_0$ when the origin of $x_c y_c z_c$ is located at $\underline{X} = (x_0, y_0, z_0)$ and its velocity is $u_{p_2}(x_0) = u^{(c)}_{p_2}(t_0)$. At $t=t_0$, when its position was $\underline{X}^{(c)}_{p_2} = (x_0, y_0, z_0)$, the particle received an impulse from its encounter with particle σ_1, giving it an instantaneous increment

in velocity without changing its physical position. During this encounter, the effect of the gas on the interaction of the two particles is negligible. The details of such an encounter are classical and are given in Appendix A-1. Following the impulse, $t > t_o$, the motion of the particle may be described in Lagrangian coordinates relative to the inertial rest frame of the shock wave

$$m_2 \frac{d\underline{v}_{p2}(t)}{dt} = 6\pi\mu(x_{p2}(t))\sigma_2 \left(u(x_{p2}(t))\,\underline{e}_x - \underline{v}_{p2}(t)\right) \tag{4.19}$$

$$\frac{d\underline{x}_{p2}(t)}{dt} = \underline{v}_{p2}(t) \tag{4.20}$$

where $\underline{x}_{p2}(t)$ and $\underline{v}_{p2}(t)$ are the position and velocity of the particle relative to the xyz frame. In many cases of interest, the viscosity μ of the gas may be treated as constant.

If the velocity equilibration time $\tau_{v_2} = m_2/6\pi\mu\sigma_2$ and length $\lambda_{v_2} = a\tau_{v_2}$ are introduced, equation (4.19) may be rewritten

$$\frac{d\underline{v}_{p2}(t)}{dt} = \frac{a(x_{p2}(t))}{\lambda_{v_2}} \left(u(x_{p2}(t))\,\underline{e}_x - \underline{v}_{p2}(t)\right) \tag{4.21}$$

Immediately after the impulse, the particle at $\underline{x}_{p2} = (x_o, y_o, z_o)$ will have a velocity

$$\underline{v}_{p2}(t_o) = \overset{(c)}{u}_{p2}(t_o)\,\underline{e}_x + \overset{(f)}{\underline{u}}_{p2}(x_o) \tag{4.22}$$

where $\overset{(f)}{\underline{u}}_{p2}(x_o)$ is given by (A1.5 - A1.8), evaluated at $x = x_o$, and is the velocity increment due to the collision. All

values of the impact parameter for the collision are considered equally likely.

The subsequent motion of the particle σ_2 is complicated by variation in the gas flow field in the region of the shock relaxation zone through which the particle moves. Fortunately, the approximate motion of the particle σ_2 is particularly simple when viewed in the $x_c y_c z_c$ reference frame. Since $x_c y_c z_c$ is a non-inertial reference frame, the apparent acceleration effects on the particle must be accounted for in determining the motion of the σ_2 particle relative to this frame. This is simply done by decomposing the velocity and position of the particle into the sums,

$$\underline{v}_{p_2}(t) = u_{p_2}^{(c)}(t)\, \underline{e}_x + \underline{u}_{p_2}^{(r)}(t) \qquad (4.23)$$

$$\underline{x}_{p_2}(t) = \underline{x}_{p_2}^{(c)}(t) + \underline{x}_{p_2}^{(r)}(t) \qquad (4.24)$$

where $u_{p_2}^{(c)}(t)$ and $\underline{x}_{p_2}^{(c)}(t)$ are the velocity and position of the origin of the $x_c y_c z_c$ reference frame at time t. Physically, they are the velocity and position which the particle σ_2 would have had at time t if there had been no collision at time $t = t_o$. Consequently, $u_{p_2}^{(c)}(t)$ and $\underline{x}_{p_2}^{(c)}(t)$ are appropriate solutions of equations (4.15) and (4.16) with, at $t = 0$, $\underline{x}_{p_2}^{(c)}(0) = (0, y_0, z_0)$ and $u_{p_2}^{(c)}(0) = u(1)$. Evidently $\underline{x}_{p_2}^{(r)}(t)$ and $\underline{u}_{p_2}^{(r)}(t)$ are the position and velocity of particle σ_2 relative to the origin of the $x_c y_c z_c$ frame at time $t > t_o$ following the collision. The geometry of the conditions (4.23) and (4.24) is presented in Figure 10.

Substituting (4.23) and (4.24) into (4.20) and (4.21), one obtains

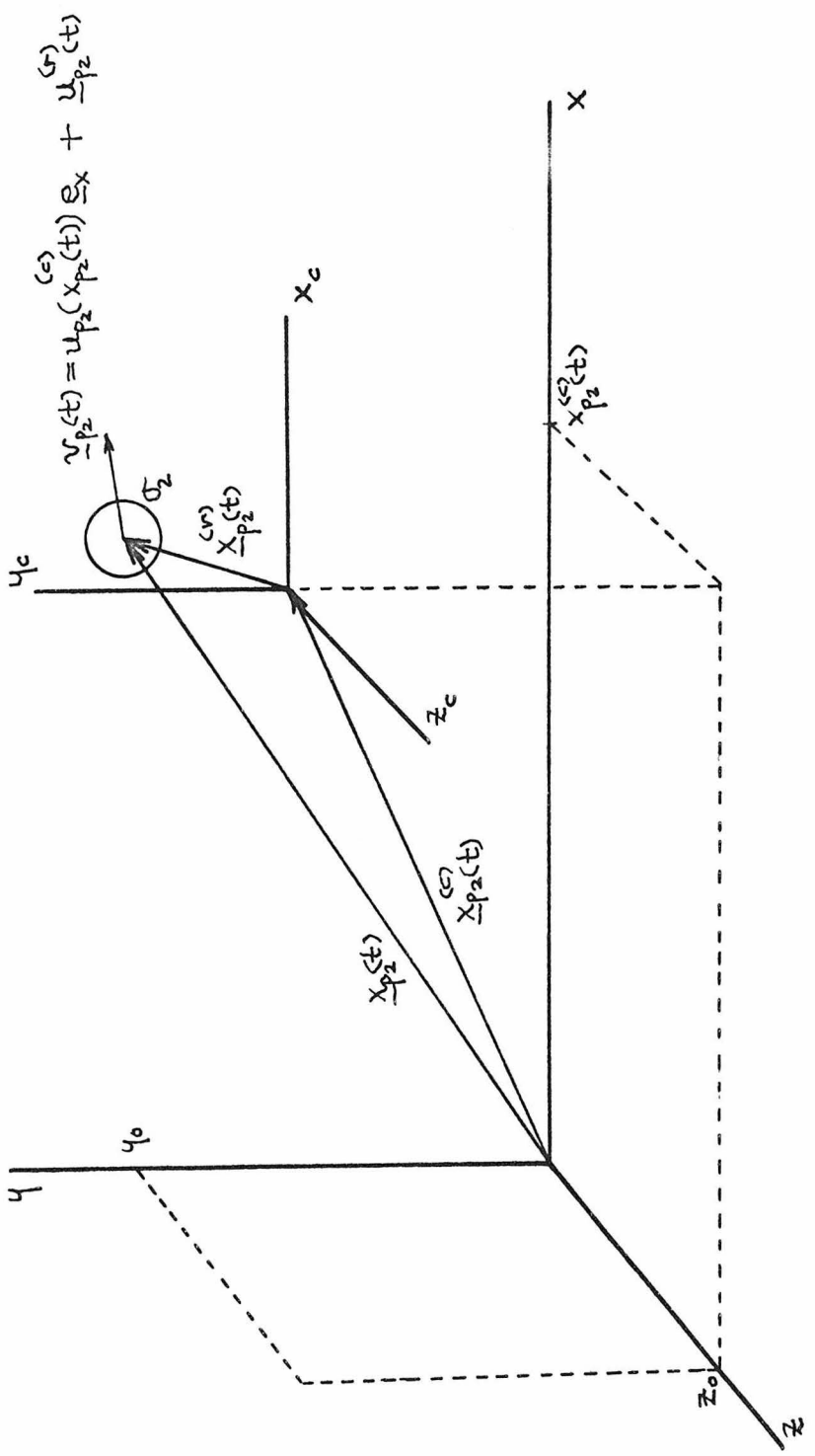
$\underline{v}_{p_2}(t) = u_{p_2}(x^{(c)}_{p_2}(t))\,\underline{e}_x + \underline{u}^{(c)}_{p_2}(t)$
σ_2
$\underline{x}^{(c)}_{p_2}(t)$
$x^{(c)}_{p_2}(t)$
$\underline{x}_{p_2}(t)$
$x_{p_2}(t)$
y_c
x_c
z_c
y_o
z_o
y
x
z

Figure 10.

$$\frac{d\underline{u}_{p_2}^{(c)}(t)}{dt}\underline{e}_x + \frac{d\underline{u}_{p_2}^{(r)}(t)}{dt} = \frac{a(x_{p_2}^{(c)}(t) + x_{p_2}^{(r)}(t))}{\lambda_{v_2}}\left(u(x_{p_2}^{(c)}(t) + x_{p_2}^{(r)}(t)) - u_{p_2}(t)\underline{e}_x - \underline{u}_{p_2}^{(r)}(t)\right) \quad (4.25)$$

$$\frac{d\,x_{p_2}^{(c)}(t)}{dt}\,\underline{e}_x + \frac{d\underline{x}_{p_2}^{(r)}(t)}{dt} = u_{p_2}^{(c)}(t)\,\underline{e}_x + \underline{u}_{p_2}^{(r)}(t) \quad (4.26)$$

Now if the particle σ_2 does not move "far" from the origin of the decelerating reference frame $x_c y_c z_c$ following the encounter, we may expand a and u in a Taylor series about the collisionless position $\underline{x}_{p_2}^{(c)}(t)$, the origin of $x_c y_c z_c$ at time t.

$$a(x_{p_2}^{(c)}(t) + x_{p_2}^{(r)}(t)) \simeq a(x_{p_2}^{(c)}(t)) + x_{p_2}^{(r)}(t)\frac{da}{dx}(x_{p_2}^{(c)}(t)) + \cdots \quad (4.27)$$

$$u(x_{p_2}^{(c)}(t) + x_{p_2}^{(r)}(t)) \simeq u(x_{p_2}^{(c)}(t)) + x_{p_2}^{(r)}(t)\frac{du}{dx}(x_{p_2}^{(c)}(t)) + \cdots \quad (4.28)$$

Since λ_{v_1} is the characteristic length over which a and u change, $x_{p_2}^{(r)}(t)$, the x component of the distance moved by the particle relative to the origin of the $x_c y_c z_c$ frame, is not "far" if $|x_{p_2}^{(r)}(t)| << \lambda_{v_1}$. In this case, the first terms in (4.27) and (4.28) are really adequate. Substituting (4.27) and (4.28) into equations (4.25) and (4.26), we have

$$\frac{d\underline{u}_{p_2}^{(c)}(t)}{dt}\,\underline{e}_x + \frac{d\underline{u}_{p_2}^{(r)}(t)}{dt} = \frac{a(x_{p_2}^{(c)}(t))}{\lambda_{v_2}}\left(u(x_{p_2}^{(c)}(t))\underline{e}_x - u_{p_2}(t)\,\underline{e}_x\right) - \frac{a(x_{p_2}^{(c)}(t))}{\lambda_{v_2}}\,\underline{u}_{p_2}^{(r)}(t) + O\left(\frac{x_{p_2}^{(r)}}{\lambda_{v_1}}\right) \quad (4.29)$$

Since $u_{p_2}^{(c)}(t)$ and $x_{p_2}^{(c)}(t)$ are solutions of equations (4.15) and (4.16) together with appropriate initial conditions as discussed earlier, we find the velocity, $\underline{u}_{p_2}^{(r)}(t)$, and position, $\underline{x}_{p_2}^{(r)}(t)$, of particle σ_2 relative to $x_c y_c z_c$ due to the collision impulse at $t=t_o$ are determined by

$$\frac{d\underline{u}_{p_2}^{(r)}(t)}{dt} = -\frac{a(x_{p_2}^{(c)}(t))}{\lambda_{u_2}} \underline{u}_{p_2}^{(r)}(t) + O\left(\frac{x_{p_2}^{(r)}}{\lambda_{u_1}}\right) \qquad (4.30)$$

$$\frac{d\underline{x}_{p_2}^{(r)}(t)}{dt} = \underline{u}_{p_2}^{(r)}(t) \qquad (4.31)$$

with the initial conditions at time $t=t_o$; $\underline{x}_{p_2}^{(r)}(t_o) = 0$,
$u_{p_2}^{(r)}(t_o) = u_{p_2}^{(f)}(x_o)$.

In many cases of interest, $a \propto \mu \simeq$ constant in the shock relaxation zone, as pointed out in previous calculations. Assuming that the local variation of a and μ and hence τ_{u_2} may be neglected, the solution of (4.30) and (4.31) is

$$\underline{u}_{p_2}^{(r)}(t) \cong \underline{u}_{p_2}^{(f)}(x_o)\, e^{-\frac{a}{\lambda_{u_2}}(t-t_o)} + O\left(\frac{x_{p_2}^{(r)}}{\lambda_{u_1}}\right) \qquad (4.32)$$

and

$$\underline{x}_{p_2}^{(r)}(t) \cong \underline{u}_{p_2}^{(f)}(x_o)\,\tau_{u_2}\left(1 - e^{-\frac{a}{\lambda_{u_2}}(t-t_o)}\right) + O\left(\frac{x_{p_2}^{(r)}}{\lambda_{u_1}}\right) \qquad (4.33)$$

Introducing the velocity equilibration time, $\tau_{u_2} = \lambda_{u_2}/a$, we can rewrite (4.32) and (4.33) as

$$\underline{u}_{p_2}^{(r)}(t) \simeq \underline{u}_{p_2}^{(f)}(x_o)\, e^{-(t-t_o)/\tau_{v_2}} + O\left(\frac{x_{p_2}^{(r)}}{\lambda_{v_1}}\right) \qquad (4.34)$$

$$\underline{x}_{p_2}^{(r)}(t) \simeq \underline{u}_{p_2}^{(f)}(x_o)\,\tau_{v_2}\left(1 - e^{-(t-t_o)/\tau_{v_2}}\right) + O\left(\frac{x_{p_2}^{(r)}}{\lambda_{v_1}}\right) \qquad (4.35)$$

Furthermore, there is no difficulty in showing that for gas flow in the relaxation zone of a gasdynamic shock, $0 \le (t-t_o) \ll \tau_{v_1}$, that $x_{p_2}^{(r)}/\lambda_{v_1} \sim \lambda_{v_2}/\lambda_{v_1} << 1$. Consequently, relative to the collisionless motion, the gas appears locally uniform to particles σ_2 and the increment in velocity of a σ_2 particle due to a collision is damped exponentially.

From (4.35) we reach the important conclusion that, following the collision, the trajectory of particle σ_2 as seen in $x_c y_c z_c$ is linear to order $\lambda_{v_2}/\lambda_{v_1} << 1$. From (4.35) it is also apparent that for $0 \le (t-t_o) << \tau_{v_1}$ the particle σ_2 moves only a finite distance relative to the origin of $x_c y_c z_c$ before it comes to rest. Furthermore, since this limiting position is reached in a time $(t-t_o) \sim \tau_{v_2}$ and $\tau_{v_2} < \tau_{c_{21}} << \tau_{v_1}$, it is very unlikely that the particle will have a collision before it has reached this limiting position. The fact that $\tau_{v_2} < \tau_{c_{12}} << \tau_{v_1}$ makes it unnecessary to include higher order terms in the computation of $\underline{x}_{p_2}^{(r)}(t)$ and $\underline{u}_{p_2}^{(r)}(t)$ than those contained in (4.34) and (4.35).

The particle will have another collision before (4.34) and (4.35) are significantly invalidated. Under these conditions, the finite distance moved by the particle σ_2 based on (4.34) and (4.35) is of particular significance, and we shall refer to it as the range,

$\underline{R}_{p2}(X_0)$, of the particle σ_2 . We might note that equations (4.34) and (4.35) are exact for particle σ_2 motion normal to the gas flow, and the approximation enters only in the motion parallel to the direction of gas flow. The range for particle σ_2 is obtained from (4.35) under the condition $\tau_{v_2} << (t-t_0) << \tau_{v_1}$ and is given by

$$\underline{R}_{p2}(X_0) = \underline{u}^{(f)}_{p2}(X_0)\,\tau_{v_2} \tag{4.36}$$

We note that the range of particle σ_2 , $\underline{R}_{p2}(X_0)$, depends only on τ_{v_2} and the initial velocity increment received from the collision with particle σ_1 . Since $\tau_{v_2} = \frac{2}{9}\left(\frac{\rho_s}{\rho}\right)\left(\frac{\sigma_2^2}{\nu}\right)$, large, dense particles move the farthest for a given velocity increment.

In general, it is expected that $|\underline{u}^{(f)}_{p2}(X_0)| \lesssim a$. Then from (4.36) and the definition $\lambda_{v_2} \equiv a\,\tau_{v_2}$, $|\underline{R}_{p2}(X_0)| \lesssim \lambda_{v_2}$. Consequently, the condition $|\underline{x}^{(r)}_{p2}(t)| << \lambda_{v_1}$ is well satisfied when $0 < (t-t_0) << \tau_{v_1}$.

Using equations (A1.5), (A1.6), and (A1.8), the components of the σ_2 particle range are

$$(\underline{R}_{p2})_{x_c} = \frac{m_1 \tau_{v_2}}{m_1+m_2}\,|u_{p1}(X_0) - u_{p2}(X_0)|\,(1+\cos 2\psi') \tag{4.37}$$

$$(\underline{R}_{p2})_{y_c} = \frac{m_1 \tau_{v_2}}{m_1+m_2}\,|u_{p1}(X_0) - u_{p2}(X_0)|\,\cos\varphi' \sin 2\psi' \tag{4.38}$$

$$(\underline{R}_{p2})_{z_c} = \frac{m_1 \tau_{v_2}}{m_1+m_2}\,|u_{p1}(X_0) - u_{p2}(X_0)|\,\sin\varphi' \sin 2\psi' \tag{4.39}$$

Specifically, these are the components of the range of particle σ_2 due to a collision with a particle of radius σ_1 whose impact parameter was $b' = (\sigma_1 + \sigma_2) \sin\psi'$ and azimuthal angle φ'. The geometry of the collision is depicted in Appendix A, Figure A1. Following the collision, particle σ_2 can only move in the positive x_c direction. This is a direct consequence of the manner in which momentum was transferred in the collision, since $u_{p_1}(x) > u_{p_2}(x)$ throughout the shock relaxation zone.

In analogy with the distribution of particle σ_2 recoil velocities over a sphere in the velocity space of the $x_c y_c z_c$ reference frame, we also have a distribution of particle ranges over a similar sphere in the $x_c y_c z_c$ reference frame, Figure 11.

Now suppose that a collision between a particle of radius σ_2 and a particle of radius σ_1 occurs at time $t = t_0$ at a position different from the $x_c = 0$ plane in the $x_c y_c z_c$ system. Following the collision, the trajectory of particle σ_2 is, by simple modification of previous arguments, linear to first order in $\lambda_{o_2}/\lambda_{o_1}$ and of essentially finite length on the time scales of interest. This conclusion is accurate so long as $x_e/\lambda_{o_1} \ll 1$ where x_e is the x_c position of the encounter relative to the origin of the $x_c y_c z_c$ reference frame. However, the tips of the velocity $u_{p_2}^{(f)}(x_0 + x_e)$ and range $R_{p_2}(x_0 + x_e)$ vectors for particle σ_2 are no longer distributed over a perfectly spherical surface because of the variation of the relative velocity of particles along the direction of the gas flow. The surface is, however, nearly spherical because of the slow variation of the relative velocity of the particles compared to the ap-

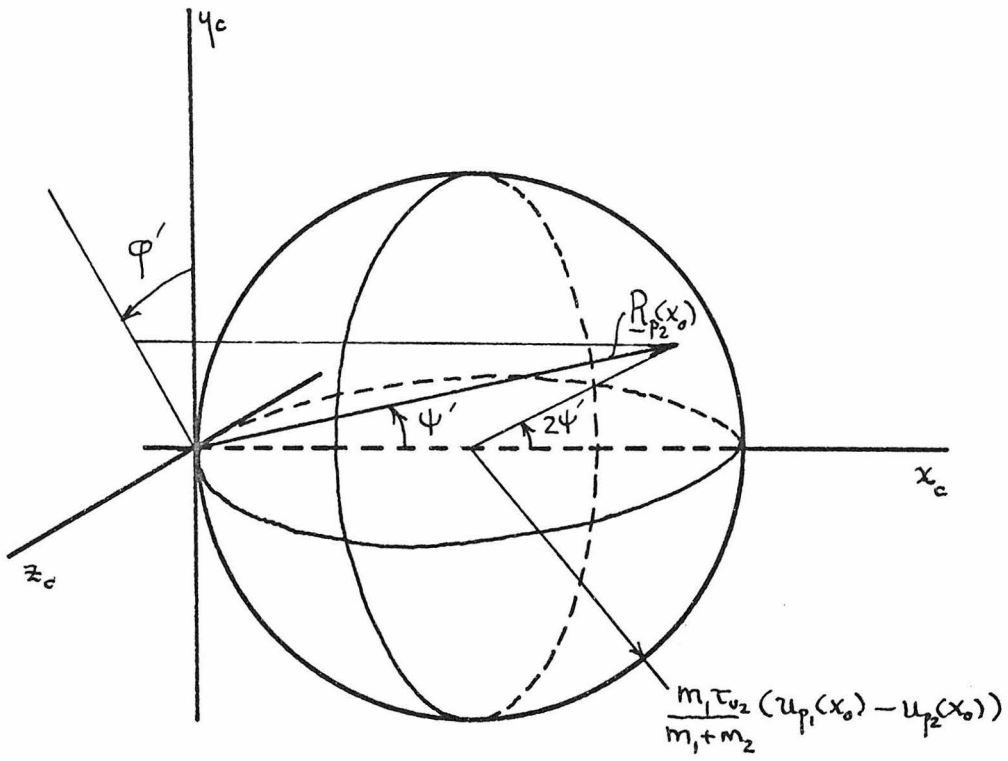

Figure 11. Range sphere for particles σ_2 due to collisions with particles σ_1. Reference frame $x_c y_c z_c$ moves at the local collisionless velocity of particles σ_2.

proximate radius of the range sphere. Upstream of the origin of $X_c Y_c Z_c$ the range sphere is slightly larger and elongated, and downstream it is slightly smaller and compressed in the X_c direction. Note, however, that the scattering is still entirely in the forward or positive X_c direction. The situation is sketched in Figure 12.

It should also be noted that the previous results can be extended to three-dimensional flows and different drag laws. The concept of particle range, which we will use often in the following analysis, is independent of the form of the drag law. The linear Stokes law has been used because of its computational simplicity, and serves well in elucidating the fundamental physical features of the collisional process.

Summarizing, we can make the following general statement which, provided $\tau_{o_{21}} \ll \tau_{v_2} < \tau_{c_{21}} \ll \tau_{v_1}$, is essentially independent of the particle-particle and gas-particle interaction laws. As viewed in a reference frame moving at the local collisionless velocity of particles σ_2, between successive collisions with particles of radius σ_1, a particle σ_2 moves along a linear trajectory whose maximum length, the range $R_{p_2}(X)$ of particles σ_2, depends on the momentum transferred to particle σ_2 during collision and its velocity equilibration time. Furthermore, it should be clear that the previous results hold for encounters between particles σ_1 and σ_2 throughout the shock relaxation zone as viewed from local reference frames moving at the collisionless velocity of particles of radius σ_2; $U_{p_2}(X)$.

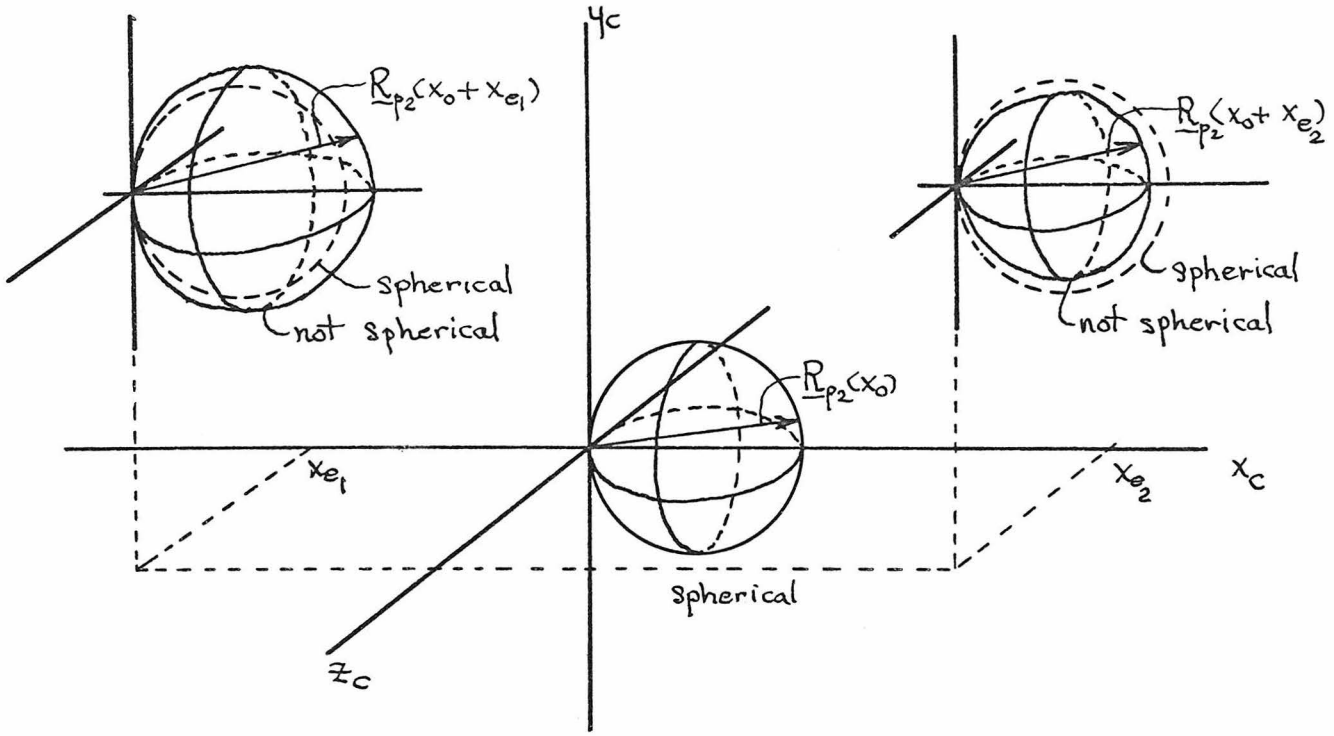

Figure 12. Variation in the range of particles σ_2 near the origin of $x_c y_c z_c$ assuming collisions producing the different surfaces occur at $t = t_o$ with the origin of $x_c y_c z_c$ at x position x_o relative to the shock front.

With these results, by appropriate superposition of the motions of particles σ_2, due to collisions with particles σ_1, we can calculate $\underline{\mathcal{J}}_{\rho 2}^{(r)}$. The quantity $\underline{\mathcal{J}}_{\rho 2}^{(r)}$ is the mass flux density of particles of radius σ_2 at the origin of a non-inertial reference frame which is moving at the local collisionless velocity, $u_{\rho 2}(x)$, of particles σ_2.

3. Calculation of the Scattering Flux.

In the reference frame $\bar{x}\bar{y}\bar{z}$, moving at the local collisionless velocity of particles σ_2, $\underline{\mathcal{J}}_{\rho 2}^{(r)}$ is the mass flux density of particles of radius σ_2 at the origin of $\bar{x}\bar{y}\bar{z}$ due to collisions between particles σ_1 and σ_2 in the vicinity of the origin. Since particles σ_2 move a finite distance, $\underline{R}_{\rho 2}$, in $\bar{x}\bar{y}\bar{z}$ following an encounter, only encounters within a small region touching the origin of $\bar{x}\bar{y}\bar{z}$ can contribute to $\underline{\mathcal{J}}_{\rho 2}^{(r)}$.

Consider a small volume element dV located near the origin of $\bar{x}\bar{y}\bar{z}$. Assume particles σ_2 are at rest before a collision. In order to describe events relative to dV, erect a Cartesian reference frame, $\bar{x}'\bar{y}'\bar{z}'$, with origin centered within dV. The $\bar{x}'\bar{y}'\bar{z}'$ frame is fixed with respect to the $\bar{x}\bar{y}\bar{z}$ reference frame and its axes are parallel to the corresponding axes of the $\bar{x}\bar{y}\bar{z}$ frame as described in Figure 13.

From Appendix A, equation (A2.3), the number per second, $\frac{dN_{\rho 2}(\underline{x}_v)}{dt}$, of particles σ_2 scattered into a solid angle $d\Omega'$ by collisions within the element dV, located at position $\underline{x}_v$ relative to the shock face, is

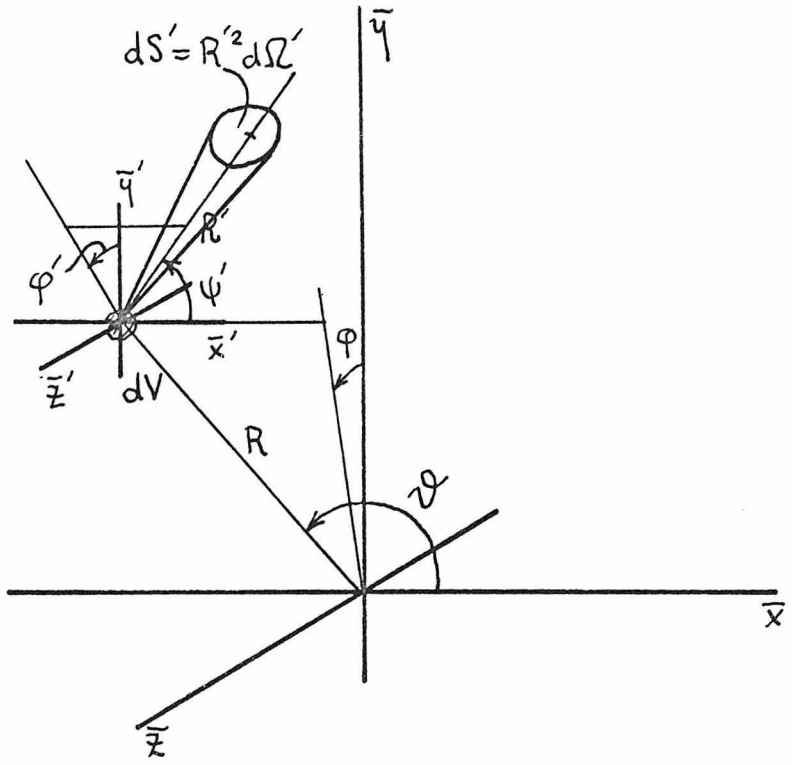

Figure 13.

$$\frac{dN_{p2}(\underline{x}_v)}{dt} = n_{p_1}(x_v)\, n_{p_2}(\underline{x}_v)\,(u_{p_1}(x_v) - u_{p_2}(x_v))(\sigma_1+\sigma_2)^2 \cos\psi' d\Omega' dV \tag{4.40}$$

The element of solid angle is $d\Omega' = \sin\psi' d\psi' d\varphi'$.

In the absence of collisions and neglecting, for the moment, transit time effects, the number per second of particles σ_2 passing through an element of area dS', subtended by solid angle $d\Omega'$, on the surface of a sphere of radius R' centered on dV due to the linearity of the particle trajectories, is equal to (4.40). It is explicitly assumed here that R' is less than the range of particles σ_2 scattered out of dV into solid angle $d\Omega'$. The element of surface cut out by the solid angle is

$$\underline{e}_{R'} \cdot d\underline{S}' = dS' = R'^2 d\Omega' \tag{4.41}$$

where $\underline{e}_{R'}$ is a unit vector in the R' direction. The basis vectors for a polar coordinate system in $\bar{x}'\bar{y}'\bar{z}'$ are $(\underline{e}_{R'}, \underline{e}_{\psi'}, \underline{e}_{\varphi'})$. Using (4.41) we may rewrite (4.40) as

$$\frac{dN_{p2}(\underline{x}_v)}{dt} = d\underline{\Gamma}_{p2}(\underline{x}_v) \cdot d\underline{S} = d\Gamma_{p2}\, \underline{e}_{R'} \cdot d\underline{S}' \tag{4.42}$$

where

$$d\Gamma_{p2}(\underline{x}_v) = n_{p_1}(x_v)\, n_{p_2}(\underline{x}_v)\,(u_{p_1}(x_v) - u_{p_2}(x_v))(\sigma_1+\sigma_2)^2 \frac{\cos\psi' dV}{R'^2} \tag{4.43}$$

is the flux of particles of radius σ_2 at the point (R', ψ', φ'), relative to $\bar{x}'\bar{y}'\bar{z}'$, due to collisions in dV. Since dS' is small, we have assumed $d\Gamma_{p2}$ is constant over dS'. We note that $d\underline{\Gamma}_{p2}(x_v)$

has the units of particles/cm^{2}sec and is directly radially outward from dV since particle trajectories are linear. The volume element dV may be viewed as a source of particles. However, there is no component of $d\underline{\Gamma}_{p2}(\underline{x}_v)$ in the negative $\bar{x}'$ direction relative to dV since the scattering of particles σ_2 out of dV occurs only in the forward $\bar{x}'$ direction.

Let us now discuss the transit time effect. Now the reference frames $\bar{x}'\bar{y}'\bar{z}'$ and $\bar{x}\bar{y}\bar{z}$, while stationary with respect to each other, are in motion parallel to the direction of gas flow in the shock relaxation zone. Consequently, the position $\underline{x}_v$ in (4.40) and (4.43) is changing with time, and there is a time dependence associated with $\frac{dN_{p2}}{dt}$ and $d\underline{\Gamma}_{p2}(\underline{x}_v)$. Since the time required for $\bar{x}\bar{y}\bar{z}$ to move a significant distance through the shock relaxation zone is τ_{v_1} , then the characteristic time over which n_{p1} , n_{p2} , u_{p1} , u_{p2} , $\frac{dN_{p2}}{dt}$, and $d\Gamma_{p2}$ vary significantly, as viewed by an observer fixed in $\bar{x}\bar{y}\bar{z}$, is also τ_{v_1} . Now the flux, $d\underline{\Gamma}_{p2}$, of particles is non-zero only over distances of order λ_{v_2} in the direction downstream of dV because of their finite range. Generally, the time required for these particles to trace out their range is of order τ_{v_2} . Consequently, since $\tau_{v_2}/\tau_{v_1} \ll 1$, the flux of particles $d\underline{\Gamma}_{p2}(\underline{x})$ at a distance R' from dV varies slowly compared to the time required for particles σ_2 to transverse the distance R' from dV . Then, as an approximation which has a correction of order $\tau_{v_2}/\tau_{v_1} \ll 1$, we may neglect the motion of reference frame $\bar{x}\bar{y}\bar{z}$ in the shock relaxation zone to simplify the calculation of $\underline{\Phi}^{(r)}_{p2}$. Note that the transit time effect re-

quires a correction that is of the same order as the correction required for the particle trajectory curvature effect. We have neglected collisions under the assumption τ_{v_2} is sufficiently less than $\tau_{c_{21}}$. Almost all the particles trace out their range between successive collisions.

From this point on, the calculation is relatively straightforward and parallels to some extent the mean free path method of kinetic theory.

Consider an element of volume dV of the gas-particle mixture located at R, ϑ, and φ with respect to $\bar{x}\bar{y}\bar{z}$ (see Figure 14). The flux of particles of radius σ_2 in the positive $\bar{x}$-direction at the origin due to collisions in dV, neglecting collisions and transit time effects, is the component of $d\underline{\Gamma}_{p_2}(\underline{x}_v)$ parallel to the $\bar{x}$-axis, $d\vec{\Gamma}_{p_2\bar{x}}(\underline{x}_v)$, which is given by

$$d\vec{\Gamma}_{p_2\bar{x}}(\underline{x}_v) = -d\underline{\Gamma}_{p_2}(\underline{x}_v)\cos\vartheta \tag{4.44}$$

where $\pi/2 \leq \vartheta \leq \pi$. There is no component of $d\underline{\Gamma}_{p_2}(\underline{x}_v)$ in the negative $\bar{x}$-direction due to scattering of particles σ_2 from volume elements in the region $\bar{x} > 0$, since the scattering of particles σ_2 out of a given volume element located in $\bar{x}\bar{y}\bar{z}$ is always forward.

Using equation (4.43) for $d\underline{\Gamma}_{p_2}(\underline{x}_v)$,

$$d\vec{\Gamma}_{p_2\bar{x}}(\underline{x}_v) = -n_{p_1}(x_v)\, n_{p_2}(\underline{x}_v)(u_{p_1}(x_v) - u_{p_2}(x_v))(\sigma_1+\sigma_2)^2 \frac{\cos\psi\, dV\cos\vartheta}{R^2} \tag{4.45}$$

Expressing dV in spherical polar coordinates with respect to $\bar{x}\bar{y}\bar{z}$,

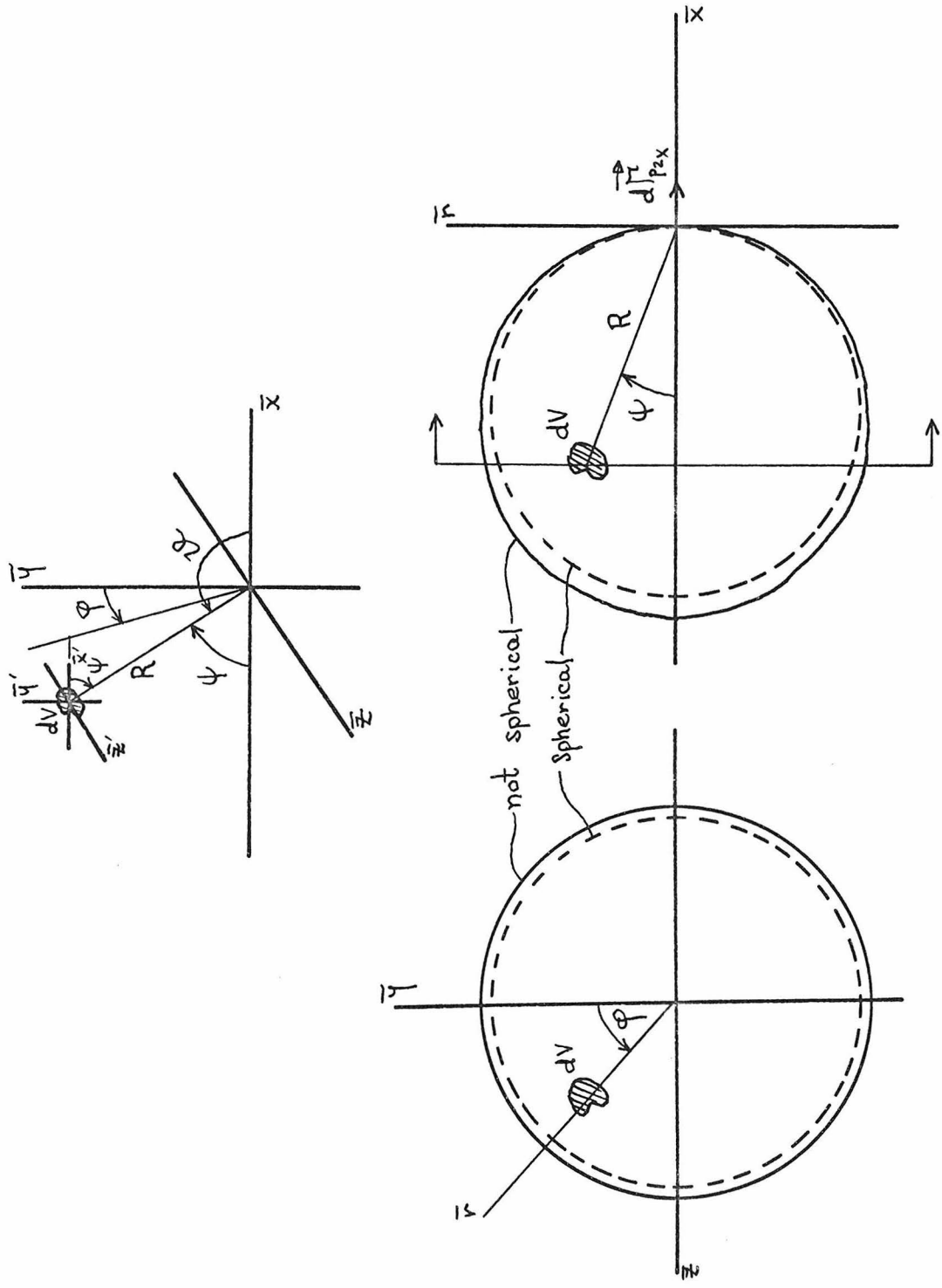

Figure 14.

$$dV = R^2 \sin\vartheta \, d\vartheta \, d\varphi \, dR \tag{4.46}$$

We rewrite (4.45) as

$$d\vec{\Gamma}_{p_2\bar{x}}(\underline{x}_v) = -n_{p_1} n_{p_2} (u_{p_1} - u_{p_2}) (\sigma_1 + \sigma_2)^2 \cos\psi \cos\vartheta \sin\vartheta \, d\vartheta \, d\varphi \, dR \tag{4.47}$$

where we understand that $\psi = \pi - \vartheta$.

The total flux in the positive $\bar{x}$ -direction due to collisions in volume elements located in $\bar{x} < 0$ is then

$$\vec{\Gamma}_{p_2\bar{x}} = \int_{\bar{x}<0} d\vec{\Gamma}_{p_2\bar{x}} = -(\sigma_1 + \sigma_2)^2 \int_{\pi/2}^{\pi} \cos\psi \cos\vartheta \sin\vartheta \, d\vartheta \int_0^{2\pi} d\varphi \int_0^{R_{p_2}^{(m)}(\psi,\varphi)} n_{p_1} n_{p_2} (u_{p_1} - u_{p_2}) dR \tag{4.48}$$

where we note that $\underline{x}_v$ depends on R, ψ , φ in general, as noted earlier, because of the variation of particle properties across the flow.

As should be expected, from the considerations of Chapter V-2, the integral summation is over a nearly spherical region upstream of the origin of $\bar{x}\,\bar{y}\,\bar{z}$, see Figure 14. The region is not spherical simply because $(u_{p_1} - u_{p_2})$ varies locally, and consequently the particle ranges are not independent of the position of the scattering event in $\bar{x}\bar{y}\bar{z}$. In (4.28), $R_{p_2}^{(m)}(\psi,\varphi)$ is a measure of the maximum particle range along the direction ψ, φ . Only particles within a distance $R_{p_2}^{(m)}(\psi,\varphi)$ in direction ψ, φ have sufficient momentum following a collision to overcome the viscous forces exerted upon them by the gas and reach the origin $\bar{x}\bar{y}\bar{z}$. Changing variables from ϑ to ψ , we obtain from (4.48)

$$\vec{\Gamma}_{p_2\bar{x}} = (\sigma_1+\sigma_2)^2 \int_0^{\pi/2} \cos^2\psi \sin\psi \, d\psi \int_0^{2\pi} d\varphi \int_0^{R_{p_2}^{(m)}(\psi,\varphi)} n_{p_1} n_{p_2} (u_{p_1} - u_{p_2}) \, dR \qquad (4.49)$$

Since there is no contribution from scattering events in the region $\bar{x} > 0$, $\overleftarrow{\Gamma}_{p_2\bar{x}} = 0$. Then the net flux of particles of radius σ_2 in the positive $\bar{x}$-direction at the origin of $\bar{x}\bar{y}\bar{z}$ is

$$\Gamma_{p_2\bar{x}} = \vec{\Gamma}_{p_2\bar{x}} = (\sigma_1+\sigma_2)^2 \int_0^{\pi/2} \cos^2\psi \sin\psi \, d\psi \int_0^{2\pi} d\varphi \int_0^{R_{p_2}^{(m)}(\psi,\varphi)} n_{p_1} n_{p_2} (u_{p_1} - u_{p_2}) \, dR \qquad (4.50)$$

where $R_{p_2}^{(m)}(\psi, \varphi)$ will be determined subsequently.

The flux of particles of radius σ_2 parallel to the $\bar{y}$-axis at the origin of $\bar{x}\bar{y}\bar{z}$ is calculated in a similar manner. The flux, $d\Gamma_{p_2\bar{y}}\downarrow$, of particles σ_2 in the negative $\bar{y}$-direction at the origin of $\bar{x}\bar{y}\bar{z}$ due to collisions in a volume element dV located at R, ψ, and φ in the half space $\bar{y} > 0$, is given by the component of $d\underline{\Gamma}_{p_2}(\underline{x}_v)$ parallel to the $\bar{y}$-axis. Taking this component of $d\underline{\Gamma}_{p_2}$ we have

$$d\Gamma_{p_2\bar{y}}(\underline{x}_v)\downarrow = d\Gamma_{p_2}(\underline{x}_v) \sin\vartheta \cos\varphi \qquad (4.51)$$

and using (4.43) and (4.46) we obtain

$$d\Gamma_{p_2\bar{y}}(\underline{x}_v)\downarrow = n_{p_1}(x_v) \, n_{p_2}(x_v) (u_{p_1}(x_v) - u_{p_2}(x_v)) (\sigma_1+\sigma_2)^2 \cos\psi \sin^2\vartheta \cos\varphi \, d\psi \, d\vartheta \, d\varphi \, dR \qquad (4.52)$$

The total downward flux is found by summing over all elements whose particles have ranges long enough so that they reach the origin of $\bar{x}\bar{y}\bar{z}$, see Figure 15(i). The region is found to be nearly hemispherical, the deviation being due to the variation of $(u_{p_1}-u_{p_2})$ across the flow. Application of these considerations to (4.52) yields

$$\Gamma_{p_2\bar{y}}^{\downarrow} = \int_{\bar{y}>0} d\Gamma_{p_2\bar{y}}^{\downarrow} = (\sigma_1+\sigma_2)^2 \int_{\pi/2}^{\pi} \cos\psi \sin^2\vartheta d\vartheta \int_{-\pi/2}^{\pi/2} \cos\varphi d\varphi \int_0^{R_{p_2}^{(m)}(\psi,\varphi)} n_{p_1} n_{p_2} (u_{p_1}-u_{p_2}) dR \quad (4.53)$$

Changing variables of integration from ϑ to ψ ,

$$\Gamma_{p_2\bar{y}}^{\downarrow} = (\sigma_1+\sigma_2)^2 \int_0^{\pi/2} \cos\psi \sin^2\psi d\psi \int_{-\pi/2}^{\pi/2} \cos\varphi d\varphi \int_0^{R_{p_2}^{(m)}(\psi,\varphi)} n_{p_1} n_{p_2} (u_{p_1}-u_{p_2}) dR \quad (4.54)$$

The upward flux of particles parallel to $\bar{y}$ due to scattering events in the region $\bar{y}<0$ is obtained by taking the component of $d\underline{\Gamma}_{p_2}(\underline{x}_v)$ in this direction:

$$d\Gamma_{p_2\bar{y}}^{\uparrow}(\underline{x}_v) = -d\underline{\Gamma}_{p_2}(\underline{x}_v) \sin\vartheta \cos\varphi \quad (4.55)$$

Using (4.43) and (4.46) one obtains

$$d\Gamma_{p_2\bar{y}}^{\uparrow}(\underline{x}_v) = -n_{p_1}(x_v)\, n_{p_2}(\underline{x}_v)\left(u_{p_1}(x_v)-u_{p_2}(x_v)\right)(\sigma_1+\sigma_2)^2 \cos\psi \sin^2\vartheta d\vartheta \cos\varphi d\varphi dR \quad (4.56)$$

The total upward flux of particles of radius σ_2 at the origin of $\bar{x}\bar{y}\bar{z}$ is then found by integrating (4.56) over the nearly hemispherical region sketched in Figure 15(ii). Again, this is a consequence of the

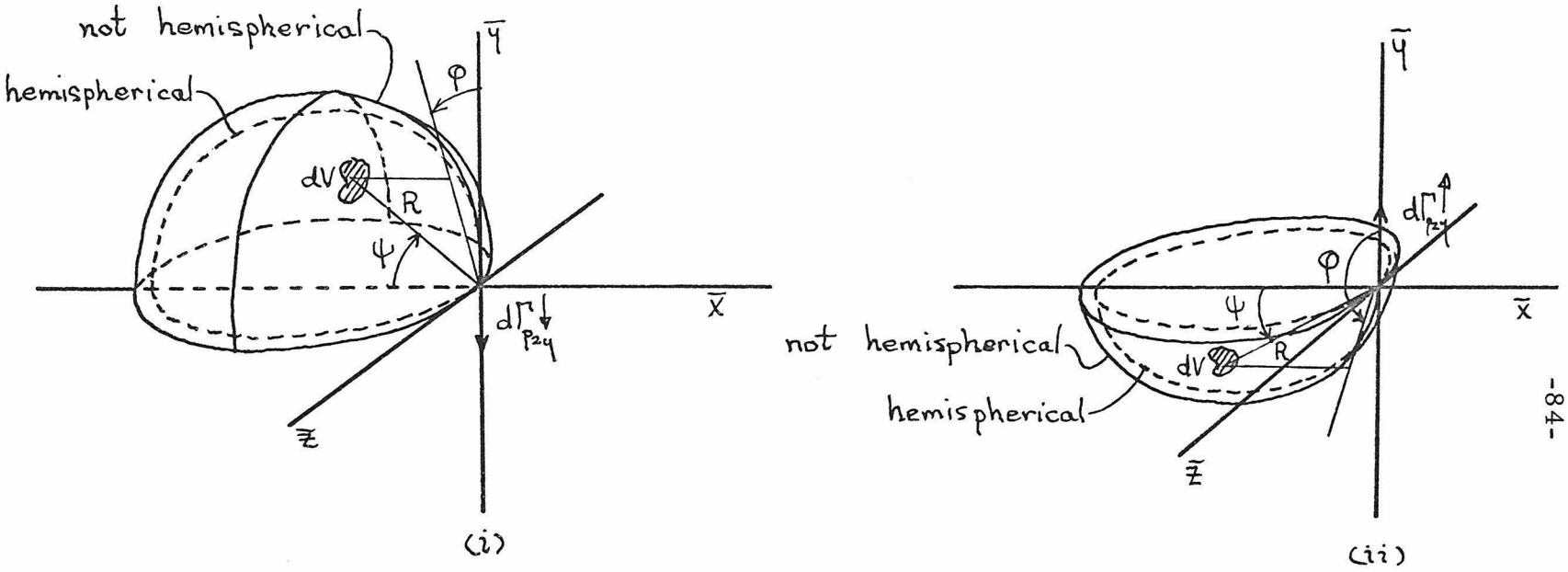
not hemispherical
hemispherical
$\bar{y}$
φ
dV
R
ψ
$d\Gamma_{P_2 q}$
$\bar{x}$
$\bar{z}$
(i)
$\bar{y}$
$d\Gamma_{P_2 q}$
φ
ψ
$\bar{x}$
not hemispherical
dV
R
hemispherical
$\bar{z}$
(ii)

Figure 15.

finite range of particles σ_2 . From (4. 56),

$$\Gamma^{\uparrow}_{p_2\bar{y}} = \int_{\bar{y}<0} d\Gamma^{\uparrow}_{p_2\bar{y}} = -(\sigma_1+\sigma_2)^2 \int_{\pi/2}^{\pi} \cos\psi \sin^2\vartheta \, d\vartheta \int_{\pi/2}^{3\pi/2} \cos\varphi \, d\varphi \int_0^{R_{p_2}^{(m)}(\psi,\varphi)} n_{p_1} n_{p_2} (u_{p_1} - u_{p_2}) \, dR \quad (4.57)$$

which may be simplified by changing variables from ϑ to ψ .

$$\Gamma^{\uparrow}_{p_2\bar{y}} = -(\sigma_1+\sigma_2)^2 \int_0^{\pi/2} \cos\psi \sin^2\psi \, d\psi \int_{\pi/2}^{3\pi/2} \cos\varphi \, d\varphi \int_0^{R_{p_2}^{(m)}(\psi,\varphi)} n_{p_1} n_{p_2} (u_{p_1} - u_{p_2}) \, dR \quad (4.58)$$

The new upward flux of particles of radius σ_2 at the origin of $\bar{x}\bar{y}\bar{z}$ due to collisions in the neighborhood of this origin is given simply by

$$\Gamma_{p_2\bar{y}} = \Gamma_{p_2\bar{y}}^{\uparrow} - \Gamma_{p_2\bar{y}}^{\downarrow} \quad (4.59)$$

Substituting (4. 58) for $\Gamma_{p_2\bar{y}}^{\uparrow}$ and (4. 54) for $\Gamma_{p_2\bar{y}}^{\downarrow}$, we obtain

$$\Gamma_{p_2\bar{y}} = -(\sigma_1+\sigma_2)^2 \int_0^{\pi/2} \cos\psi \sin^2\psi \, d\psi \int_0^{2\pi} \cos\varphi \, d\varphi \int_0^{R_{p_2}^{(m)}(\psi,\varphi)} n_{p_1} n_{p_2} (u_{p_1} - u_{p_2}) \, dR \quad (4.60)$$

The region of integration is the almost spherical volume described in Figure 14.

In a similar manner, the net flux of particles of radius σ_2 in the $\bar{z}$ -direction is given by

$$\Gamma_{p_2\bar{z}} = -(\sigma_1+\sigma_2)^2 \int_0^{\pi/2} \cos\psi \sin^2\psi d\psi \int_0^{2\pi} \cos\varphi d\varphi \int_0^{R_{p_2}^{(m)}(\psi,\varphi)} n_{p_1} n_{p_2} (u_{p_1} - u_{p_2}) dR \quad (4.61)$$

It is appropriate to note that the expressions (4.50), (4.60), and (4.61) for the fluxes of the particles σ_2 at the origin of $\bar{x}\bar{y}\bar{z}$, due to collisions, are accurate to zeroth order of $\tau_{v_2}/\tau_{v_1} = \lambda_{v_2}/\lambda_{v_1}$ where $\tau_{v_2}/\tau_{v_1} << 1$ since $(\sigma_2/\sigma_1)^2 << 1$. The $\bar{x}\bar{y}\bar{z}$ reference frame is located at $\underline{X}$ with respect to the shock wave and moving at the local collisionless velocity of particles σ_2, $u_{p_2}(x)$.

Let us now evaluate the expressions (4.50), (4.60), and (4.61) for $\Gamma_{p_2\bar{x}}(\underline{X})$, $\Gamma_{p_2\bar{y}}(\underline{X})$, and $\Gamma_{p_2\bar{z}}(\underline{X})$, respectively, taking account of the slow variation of the particle properties in the region of integration. The procedure to be employed necessitates approximations that involve the transit time and the curvature of particle trajectories. It will be shown that this approximation is of the same order as those made previously.

The upper limit, $R_{p_2}^{(m)}(\psi,\varphi)$, on the radial integral $\int_0^{R_{p_2}^{(m)}} n_{p_1} n_{p_2} (u_{p_1} - u_{p_2}) dR$ is a measure of the maximum particle range for particles σ_2 scattered toward the origin of $\bar{x}\bar{y}\bar{z}$ along the direction ψ, φ. This limit may be estimated by expanding $|\underline{R}_{p_2}(\underline{X}_v)|$ about the origin. Using the components of velocity, $u_{p_2}^{(f)}(\underline{X}_v)$, of a particle σ_2 that has had a collision at $\underline{X}_v$ as given by (A1.5), (A1.6), and (A1.8) together with the definition of the particle range

$$\underline{R}_{p_2}(\underline{x}_v) = \underline{u}_{p_2}(\underline{x}_v)\,\tau_{v_2} \qquad (4.62)$$

then

$$|\underline{R}_{p_2}| = \sqrt{(\underline{R}_{p_2})_{\bar{x}}^2 + (\underline{R}_{p_2})_{\bar{y}}^2 + (\underline{R}_{p_2})_{\bar{z}}^2} \qquad (4.63)$$

or

$$|\underline{R}_{p_2}| = \frac{m_1}{m_1+m_2}(u_{p_1} - u_{p_2})\,2\tau_{v_2}\cos\psi \;\equiv R_{p_2} \qquad (4.64)$$

For small variations of $(u_{p_1} - u_{p_2})$ and short particle ranges, as indicated in Chapter V-2, the maximum range is nearly the same as the range in a uniform system. We suppose that a suitable approximation to $R_{p_2}^{(m)}(\psi, \varphi)$ is a Taylor expansion of (4.64) about the range for a uniform system. This is the range $\underline{R}_{p_2}$ evaluated at the origin of $\bar{x}\bar{y}\bar{z}$, $\underline{R}_{p_2}(\underline{x})$. Therefore, we approximate $R_{p_2}^{(m)}(\psi, \varphi)$ by

$$R_{p_2}^{(m)}(\psi,\varphi) \simeq R_{p_2}(\underline{x}) + \frac{\partial}{\partial x}R_{p_2}(x)\,(\underline{R}_{p_2}(x))_{\bar{x}} + \frac{\partial}{\partial y}R_{p_2}(x)\,(\underline{R}_{p_2}(x))_{\bar{y}} + \frac{\partial}{\partial z}R_{p_2}(x)\,(\underline{R}_{p_2}(x))_{\bar{z}} + \cdots \qquad (4.65)$$

where $\underline{x}$ refers to the position of $\bar{x}\bar{y}\bar{z}$ with respect to the shock wave and is independent of ψ or φ. Then using equations (A1.5), (A1.6), and (A1.8) together with (4.62), we obtain

$$(\underline{R}_{p_2}(\underline{x}))_{\bar{x}} = -\frac{m_1\tau_{v_2}}{m_1+m_2}(u_{p_1}(x) - u_{p_2}(x))(1+\cos 2\psi) \qquad (4.66)$$

$$\left(\underline{R}_{p_2}(\underline{x})\right)_{\bar{y}} = \frac{m_1 \tau_{v2}}{m_1+m_2}\left(u_{p_1}(x) - u_{p_2}(x)\right) \sin 2\psi \cos\varphi \tag{4.67}$$

$$\left(\underline{R}_{p_2}(\underline{x})\right)_{\bar{z}} = \frac{m_1 \tau_{v2}}{m_1+m_2}\left(u_{p_1}(x) - u_{p_2}(x)\right) \sin 2\psi \sin\varphi \tag{4.68}$$

and

$$\frac{\partial}{\partial x} R_{p_2}(\underline{x}) = \frac{m_1 \tau_{v2}}{m_1+m_2} \frac{\partial}{\partial x}\left(u_{p_1}(x) - u_{p_2}(x)\right) \cos\psi \tag{4.69}$$

$$\frac{\partial R_{p_2}(\underline{x})}{\partial y} = 0 = \frac{\partial R_{p_2}(\underline{x})}{\partial z} \tag{4.70}$$

The radial integral may be written by defining

$$F(\underline{x}, R, \psi, \varphi) = n_{p_1}(x_v)\, n_{p_2}(\underline{x}_v)\left(u_{p_1}(x_v) - u_{p_2}(x_v)\right) \tag{4.71}$$

as

$$I_R(\underline{x}, \psi, \varphi) = \int_0^{R_{p_2}^{(m)}(\psi,\varphi)} F(\underline{x}, R, \psi, \varphi)\, dR \tag{4.72}$$

Because of the slow variation of particle properties across the gas flow field, to a good approximation, we may expand F in a Taylor series about the origin of $\bar{x}\bar{y}\bar{z}$:

$$F(\underline{x}, R, \psi, \varphi) = F(\underline{x}, \bar{x}, \bar{y}, \bar{z}) \simeq F(\underline{x}) + \frac{\partial F(\underline{x})}{\partial x}\bar{x} + \frac{\partial F}{\partial y}(\underline{x})\bar{y} + \frac{\partial F}{\partial z}(\underline{x})\bar{z} + \cdots \tag{4.73}$$

Expressing $\bar{x}$, $\bar{y}$, and $\bar{z}$ in spherical polar coordinates R, ψ, and φ, namely,

$$\bar{x} = R\cos\vartheta = -R\cos\psi \tag{4.74}$$

$$\bar{y} = R\sin\vartheta\cos\varphi = R\sin\psi\cos\varphi \tag{4.75}$$

$$\bar{z} = R\sin\vartheta\sin\varphi = R\sin\psi\cos\varphi \tag{4.76}$$

and using them, we substitute (4.73) together with (4.65) into (4.72) to obtain

$$I_R \cong \int_0^{R_{p_2}(\underline{x}) + \frac{\partial R_{p_2}(\underline{x})}{\partial x}(R_{p_2}(\underline{x}))_x} \left\{ F(\underline{x}) + \frac{\partial F(\underline{x})}{\partial x}(-R\cos\psi) + \frac{\partial F(\underline{x})}{\partial y}(R\sin\psi\cos\varphi) + \frac{\partial F(\underline{x})}{\partial z}(R\sin\psi\cos\varphi) \right\} dR \tag{4.77}$$

Since the gradients are of second order, we neglect products of them and (4.77) becomes

$$I_R \cong F(\underline{x})\left\{ R_{p_2}(\underline{x}) + \frac{\partial}{\partial x}R_{p_2}(\underline{x})\,(R_{p_2}(\underline{x}))_{\bar{x}} \right\} + \int_0^{R_{p_2}(\underline{x})} \left\{ \frac{\partial F(\underline{x})}{\partial x}(-R\cos\psi) + \frac{\partial F(\underline{x})}{\partial y}(R\sin\psi\cos\varphi) + \frac{\partial}{\partial z}F(\underline{x})\,(R\sin\psi\sin\varphi) \right\} dR \tag{4.78}$$

Carrying out the integral in (4.78) over R, recognizing that $\underline{x}$, ψ, and φ are independent of R and using the definition of $R_{p_2}(\underline{x})$ given in (4.64), it is straightforward to show that

$$I_R \cong F(\underline{x})\, R_{p_2}(\underline{x}) + F(\underline{x}) \left\{ \frac{\partial}{\partial x} R_{p_2}(\underline{x})\, (\underline{R}_{p_2})_{\bar{x}} \right\}$$

$$+ \frac{R_{p_2}(\underline{x})}{2} \left\{ \frac{\partial F(\underline{x})}{\partial x} (\underline{R}_{p_2})_{\bar{x}} + \frac{\partial F(\underline{x})}{\partial y} (\underline{R}_{p_2})_{\bar{y}} + \frac{\partial F(\underline{x})}{\partial z} (\underline{R}_{p_2})_{\bar{z}} \right\} \quad (4.79)$$

which may also be rewritten

$$I_R \cong F(\underline{x})\, R_{p_2}(\underline{x}) + \frac{1}{2} \left\{ F(\underline{x}) \frac{\partial R_{p_2}(\underline{x})}{\partial x} + \frac{\partial}{\partial x} \left(R_{p_2}(\underline{x})\, F(\underline{x}) \right) \right\} (\underline{R}_{p_2})_{\bar{x}}$$

$$+ \frac{1}{2} \left\{ \frac{\partial}{\partial y} \left(R_{p_2}(\underline{x})\, F(\underline{x}) \right) \right\} (\underline{R}_{p_2})_{\bar{y}}$$

$$+ \frac{1}{2} \left\{ \frac{\partial}{\partial z} \left(R_{p_2}(\underline{x})\, F(\underline{x}) \right) \right\} (\underline{R}_{p_2})_{\bar{z}} \quad (4.80)$$

where $I_R = I_R(\underline{x}, \psi, \varphi)$ since $\underline{R}_{p_2} = \underline{R}_{p_2}(\underline{x}, \psi, \varphi)$.

Using the definition (4.72), the fluxes (4.50), (4.60), and (4.61) may be written as

$$\Gamma_{p_2 \bar{x}}(\underline{x}) = (\sigma_1 + \sigma_2)^2 \int_0^{\pi/2} d\psi \int_0^{2\pi} d\varphi \left\{ \sin\psi \cos^2\psi\, I_R(\underline{x}, \psi, \varphi) \right\} \quad (4.81)$$

$$\Gamma_{p_2 \bar{y}}(\underline{x}) = -(\sigma_1 + \sigma_2)^2 \int_0^{\pi/2} d\psi \int_0^{2\pi} d\varphi \left\{ \cos\psi \sin^2\psi \cos\varphi\, I_R(\underline{x}, \psi, \varphi) \right\} \quad (4.82)$$

and

$$\Gamma_{p_2 \underline{z}}(\underline{x}) = -(\sigma_1+\sigma_2)^2 \int_0^{\pi/2} d\psi \int_0^{2\pi} d\varphi \left\{ \cos\psi \sin^2\psi \sin\varphi \, I_R(\underline{x},\psi,\varphi) \right\} \quad (4.83)$$

Substituting (4.80) into (4.81), (4.82), and (4.83) and then carrying out the somewhat tedious integrations, one obtains

$$\Gamma_{p_2 \underline{x}}(\underline{x}) = \pi(\sigma_1+\sigma_2)^2 \frac{m_1 \tau_{v_2}}{(m_1+m_2)} n_{p_1}(x)\, n_{p_2}(\underline{x}) \left(u_{p_1}(x) - u_{p_2}(x)\right)^2$$

$$- \frac{2}{3}\pi(\sigma_1+\sigma_2)^2 \left(\frac{m_1}{m_1+m_2}\right)^2 \tau_{v_2}^2 \frac{\partial}{\partial x} \left\{ n_{p_1}(x)\, n_{p_2}(\underline{x}) \left(u_{p_1}(x) - u_{p_2}(x)\right)^3 \right\} \quad (4.84)$$

$$\Gamma_{p_2 \underline{y}}(\underline{x}) = -\frac{\pi}{6}(\sigma_1+\sigma_2)^2 \left(\frac{m_1}{m_1+m_2}\right)^2 \tau_{v_2}^2 \frac{\partial}{\partial y} \left\{ n_{p_1}(x)\, n_{p_2}(\underline{x}) \left(u_{p_1}(x) - u_{p_2}(x)\right)^3 \right\} \quad (4.85)$$

$$\Gamma_{p_2 \underline{z}}(\underline{x}) = -\frac{\pi}{6}(\sigma_1+\sigma_2)^2 \left(\frac{m_1}{m_1+m_2}\right)^2 \tau_{v_2}^2 \frac{\partial}{\partial z} \left\{ n_{p_1}(x)\, n_{p_2}(\underline{x}) \left(u_{p_1}(x) - u_{p_2}(x)\right)^3 \right\} \quad (4.86)$$

Then the random flux, $\underline{\Gamma}_{p_2}(\underline{x})$, of particles of radius σ_2 at the point $\underline{x}$ relative to the collisionless flux of particles σ_2, $n_{p_2}(\underline{x})\, u_{p_2}(x)$ is given by

$$\underline{\Gamma}_{p_2}(\underline{x}) = \Gamma_{p_2 \underline{x}}(\underline{x})\, \underline{e}_x + \Gamma_{p_2 \underline{y}}(\underline{x})\, \underline{e}_y + \Gamma_{p_2 \underline{z}}(\underline{x})\, \underline{e}_z$$

The character of the components of $\underline{\Gamma}_{p_2}(\underline{x})$ as given by (4.84), (4.85), and (4.86) may be accounted for by the following considera-

tions. Because $\tau_{v_2} < \tau_{c_{21}}$, the particles collide, on the average, only when moving at their local collisionless velocities. Since $\tau_{v_2}/\tau_{v_1} = \lambda_{v_2}/\lambda_{v_1} << 1$ in the relaxation zone of the shock wave, $u_{p_1}(x) > u_{p_2}(x)$ for all x . Consequently, collisions are characterized by particles σ_1 overtaking particles σ_2 and hitting them from behind. Particles σ_2 are always scattered forward, and this increases their flux in the x -direction and accounts for the first term on the right hand side of (4. 84).

However, because of the variation of the particle properties across the gas-particle flow field when particles σ_2 which are scattered out of different regions in the flow come together, they are out of phase. A net flux of particles thus arises.

There is a certain randomness introduced into the system by the encounters and the variation of the particle properties. This is the essential origin of the second term in (4. 84). The variation in the particle σ_2 density normal to the gas-particle σ_1 flow accounts for the net flux of particles in this direction. These terms are similar in effect to the second term of (4. 84). These statements are rather brief. Later, we will take a much closer look at the interpretation of the character of the particle fluxes.

The random mass flux density $\underline{\varphi}^{(r)}_{p_2}$ can be derived from (4. 84), (4. 85), and (4. 86) by multiplying by the mass of a particle σ_2. Each particle σ_2 by its motion through the gas transports a mass m_2 , $\underline{\varphi}^{(r)}_{p_2} = \varphi^{(r)}_{p_{2\bar{x}}}\,\underline{e}_x + \varphi^{(r)}_{p_{2\bar{y}}}\,\underline{e}_y + \varphi^{(r)}_{p_{2\bar{z}}}\,\underline{e}_z$ where $\varphi^{(r)}_{p_{2\bar{x}}} = m_2 \Gamma_{p_{2\bar{x}}}(\underline{x})$, $\varphi^{(r)}_{p_{2y}} = m_2 \Gamma_{p_{2y}}(\underline{x})$, and $\varphi^{(r)}_{p_{2\bar{z}}} = m_2 \Gamma_{p_{2\bar{z}}}(\underline{x})$.

4. Physical Significance of Expression for $\underset{\sim}{\mathcal{F}}^{(r)}_{p_2}$

In terms of the mass densities of the two particle clouds, $\rho_{p_1} = m_1 n_{p_1}$ and $\rho_{p_2} = m_2 n_{p_2}$, the components of the mass flux density of particles of radius σ_2 relative to their local collisionless mass flux

$$\left(\underset{\sim}{\mathcal{F}}^{(r)}_{p_2}\right)_x = \pi(\sigma_1+\sigma_2)^2 \frac{\tau_{v_2}}{(m_1+m_2)} \rho_{p_1} \rho_{p_2} (u_{p_1}-u_{p_2})^2$$

$$-\frac{2}{3}\pi(\sigma_1+\sigma_2)^2 \frac{m_1 \tau_{v_2}^2}{(m_1+m_2)^2} \frac{\partial}{\partial x}\left(\rho_{p_1} \rho_{p_2} (u_{p_1}-u_{p_2})^3\right) \tag{4.87}$$

$$\left(\underset{\sim}{\mathcal{F}}^{(r)}_{p_2}\right)_y = -\frac{\pi}{6}(\sigma_1+\sigma_2)^2 \frac{m_1 \tau_{v_2}^2}{(m_1+m_2)^2} \frac{\partial}{\partial y}\left(\rho_{p_1} \rho_{p_2} (u_{p_1}-u_{p_2})^3\right) \tag{4.88}$$

and

$$\left(\underset{\sim}{\mathcal{F}}^{(r)}_{p_2}\right)_z = -\frac{\pi}{6}(\sigma_1+\sigma_2)^2 \frac{m_1 \tau_{v_2}^2}{(m_1+m_2)^2} \frac{\partial}{\partial z}\left(\rho_{p_1} \rho_{p_2} (u_{p_1}-u_{p_2})^3\right) \tag{4.89}$$

Derivation of these relations involved assumptions, some of them concerning the kinetic theory method, others the particle-gas and particle-particle interaction laws. Because of the large numbers of particles involved, the restrictions introduced by the kinetic theory method are minor. Therefore, any inaccuracies stem from the validity of the particular gas-particle and particle-particle interaction laws and the assumptions introduced to facilitate their application.

Consider two important approximations: (i) to neglect the curvature of particle σ_2 trajectories in reference frame $\bar{x}\bar{y}\bar{z}$

caused by viscous interaction of particles with the gas, and (ii) transit time effects in $\bar{x}\bar{y}\bar{z}$ resulting from the finite velocity of reference frame $\bar{x}\bar{y}\bar{z}$ in the shock relaxation zone.

The trajectory of particle σ_2 in the $\bar{x}\bar{y}\bar{z}$ frame will have a curvature correction of order $(\lambda_{v_2}/\lambda_{v_1})$ to the linear motion. The transit time effects are expected to be of order τ_{v_2}/τ_{v_1}. Because $(\sigma_2/\sigma_1)^2 << 1$, these effects are small and of the same order. Since the expression (4.87) is the sum of two terms, the first of which is larger than the second, it is important to compare their relative magnitudes.

Let us define, for purposes of examination,

$$\left(\underline{f}_{p_2}^{(r)}\right)_x = f_1 + f_2 \tag{4.90}$$

where

$$f_1 = \pi(\sigma_1+\sigma_2)^2 \frac{\tau_{v_2}}{(m_1+m_2)} \rho_{p_1}\rho_{p_2}(u_{p_1}-u_{p_2})^2 \tag{4.91}$$

and

$$f_2 = -\frac{2}{3}\pi(\sigma_1+\sigma_2)^2 \frac{m_1\tau_{v_2}^2}{(m_1+m_2)^2} \frac{\partial}{\partial x}\left(\rho_{p_1}\rho_{p_2}(u_{p_1}-u_{p_2})^3\right) \tag{4.92}$$

The characteristic length over which ρ_{p_1} and $(u_{p_1}-u_{p_2})$ vary in the relaxation zone is of order λ_{v_1}. It is also to be expected that, because of collisional coupling of particles σ_2 and σ_1, the density of particles σ_2 will vary significantly over the same characteristic length. Consequently, it is to be expected that

$$\frac{\partial}{\partial x}\left(\rho_{p_1}\rho_{p_2}(u_{p_1}-u_{p_2})^3\right) \sim \frac{\rho_{p_1}\rho_{p_2}(u_{p_1}-u_{p_2})^3}{\lambda_{v_1}}$$

so that

$$\left|\frac{\mathcal{F}_2}{\mathcal{F}_1}\right| = \left| \frac{\frac{-2}{3}\pi(\sigma_1+\sigma_2)^2 m_1 \tau_{v_2}^2}{(m_1+m_2)^2} \frac{\partial}{\partial x}\left(\rho_{p_1}\rho_{p_2}(u_{p_1}-u_{p_2})^3\right)}{\pi(\sigma_1+\sigma_2)^2 \frac{\tau_{v_2}}{(m_1+m_2)}\rho_{p_1}\rho_{p_2}(u_{p_1}-u_{p_2})^2} \right|$$

$$\left|\frac{\mathcal{F}_2}{\mathcal{F}_1}\right| \sim \left|\frac{2}{3}\left(\frac{m_1}{m_1+m_2}\right)\frac{\tau_{v_2}}{\lambda_{v_1}}(u_{p_1}-u_{p_2})\right| = \left|\frac{2}{3}\left(\frac{m_1}{m_1+m_2}\right)\left(\frac{\lambda_{v_2}}{\lambda_{v_1}}\right)\frac{(u_{p_1}-u_{p_2})}{a}\right| \quad (4.93)$$

Since $(u_{p_1}-u_{p_2})/a \lesssim O(1)$ we conclude that

$$\left|\frac{\mathcal{F}_2}{\mathcal{F}_1}\right| \sim O\left(\frac{\lambda_{v_2}}{\lambda_{v_1}}\right) \quad (4.94)$$

Therefore, relative to $\mathcal{F}_1$ the flux term $\mathcal{F}_2$ represents a correction of order $(\sigma_2/\sigma_1)^2$, the same order as that to be expected from particle trajectory curvature and transit time effects. Hence, $\mathcal{F}_2$ contains only part of the term of order $(\lambda_{v_2}/\lambda_{v_1})$ relative to $\mathcal{F}_1$. Therefore, to make this calculation correct to first order in $(\lambda_{v_2}/\lambda_{v_1})$, further restrictions are required.

The relative magnitudes of $\mathcal{F}_2$ with respect to $\left(\underline{\mathcal{F}}_{p_2}^{(r)}\right)_y$ and $\left(\underline{\mathcal{F}}_{p_2}^{(r)}\right)_z$ become important in the equation of continuity, and therefore it is appropriate to compare $\frac{\partial \mathcal{F}_2}{\partial x}$ with $\frac{\partial(\underline{\mathcal{F}}_{p_2})_y}{\partial y}$, $\frac{\partial(\underline{\mathcal{F}}_{p_2})_z}{\partial z}$. Suppose that λ_y and λ_z are the characteristic lengths of the density distribution of particles of radius σ_2 in the y and z directions, respectively. Therefore $\frac{\partial^2 \rho_{p_2}}{\partial y^2} \sim \frac{\rho_{p_2}}{\lambda_y^2}$ and $\frac{\partial^2 \rho_{p_2}}{\partial z^2} \sim \frac{\rho_{p_2}}{\lambda_z^2}$ since

only ρ_{p_2} depends on y and z in (4.87-4.89). Using these approximations,

$$\left|\begin{array}{c}\dfrac{\partial \varphi_2}{\partial x} \\ \dfrac{\partial\left(\varphi_{p_2}^{(r)}\right)}{\partial y}_{y}\end{array}\right| = \left|\begin{array}{c}-\dfrac{2}{3}\pi(\sigma_1+\sigma_2)^2 \dfrac{m_1\tau_{v_2}^2}{(m_1+m_2)^2}\dfrac{\partial^2}{\partial x^2}\left(\rho_{p_1}\rho_{p_2}(u_{p_1}-u_{p_2})^3\right) \\ \dfrac{\pi}{6}(\sigma_1+\sigma_2)^2 \dfrac{m_1\tau_{v_2}^2}{(m_1+m_2)^2}\rho_{p_1}(u_{p_1}-u_{p_2})^3\dfrac{\partial^2\rho_{p_2}}{\partial y^2}\end{array}\right|$$

$$\left|\begin{array}{c}\dfrac{\partial \varphi_2}{\partial x} \\ \dfrac{\partial\left(\varphi_{p_2}^{(r)}\right)}{\partial y}_{y}\end{array}\right| \sim O\left(\left(\frac{\lambda_y}{\lambda_{v_1}}\right)^2\right) \tag{4.95}$$

similarly,

$$\left|\begin{array}{c}\dfrac{\partial \varphi_2}{\partial x} \\ \dfrac{\partial\left(\varphi_{p_2}^{(r)}\right)}{\partial z}_{z}\end{array}\right| \sim O\left(\left(\frac{\lambda_z}{\lambda_{v_1}}\right)^2\right) \tag{4.96}$$

From (4.95) and (4.96) we can conclude that, provided

$$\left(\frac{\lambda_y}{\lambda_{v_1}}\right)^2 \ll 1 \qquad \left(\frac{\lambda_z}{\lambda_{v_1}}\right)^2 \ll 1 \quad , \tag{4.97}$$

corrections to φ_1 of order $(\lambda_{v_2}/\lambda_y)$ can be properly neglected. The detailed evaluation of λ_y and λ_z depends on the upstream density profile, $\rho_{p_2}^{(1)}(y,z)$, of particles σ_2 and the collisional spreading of this profile downstream of the gas dynamic shock wave. Therefore, the rigorous justification for neglecting φ_2 must usually be established after calculating ρ_{p_2}.

We shall restrict ourselves to circumstances such that, when $(\lambda_{v_2}/\lambda_{v_1}) << 1$ and transverse gradients in density ρ_{p_2} of particles σ_2 are not small, we may write the components of mass flux density

$$\left(\underset{\sim}{\varphi}^{(r)}_{p_2}\right)_x \cong \pi(\sigma_1+\sigma_2)^2 \frac{\tau_{v_2}}{(m_1+m_2)} \rho_{p_1}\rho_{p_2}(u_{p_1}-u_{p_2})^2\left(1+O\left(\frac{\lambda_{v_2}}{\lambda_{v_1}}\right)\right) \quad (4.98)$$

$$\left(\underset{\sim}{\varphi}^{(r)}_{p_2}\right)_y \cong -\frac{\pi}{6}(\sigma_1+\sigma_2)^2 \frac{\tau_{v_2}^2 m_1}{(m_1+m_2)} \rho_{p_1}(u_{p_1}-u_{p_2})^3 \frac{\partial \rho_{p_2}}{\partial y}\left(1+O\left(\frac{\lambda_{v_2}}{\lambda_{v_1}}\right)\right) \quad (4.99)$$

and

$$\left(\underset{\sim}{\varphi}^{(r)}_{p_2}\right)_z \cong -\frac{\pi}{6}(\sigma_1+\sigma_2)^2 \frac{\tau_{v_2}^2 m_1}{(m_1+m_2)^2} \rho_{p_1}(u_{p_1}-u_{p_2})^3 \frac{\partial}{\partial z}\rho_{p_2}\left(1+O\left(\frac{\lambda_{v_2}}{\lambda_{v_1}}\right)\right) \quad (4.100)$$

Then the total mass flux density of particles σ_2 at a given point in the relaxation zone is given by;

$$\underset{\sim}{\varphi}_{p_2} = \rho_{p_2}\left\{ u_{p_2} + \pi(\sigma_1+\sigma_2)^2 \frac{\tau_{v_2}}{(m_1+m_2)} \rho_{p_1}(u_{p_1}-u_{p_2})^2 \right\} \underline{e}_x$$

$$-\frac{\pi}{6}(\sigma_1+\sigma_2)^2 \frac{\tau_{v_2}^2 m_1}{(m_1+m_2)^2} \rho_{p_1}(u_{p_1}-u_{p_2})^3 \nabla_\perp \rho_{p_2} = \underset{\sim}{\varphi}_{p_2 x} \underline{e}_x + \underset{\sim}{\varphi}_{p_2 \perp} \quad (4.101)$$

or in component form

$$\underset{\sim}{\varphi}_{p_2 x} = \rho_{p_2}\left\{ u_{p_2} + \pi(\sigma_1+\sigma_2)^2 \frac{\tau_{v_2}}{(m_1+m_2)} \rho_{p_1}(u_{p_1}-u_{p_2})^2 \right\} \quad (4.102)$$

and

$$\underline{\mathcal{F}}_{p_2\perp} = \mathcal{F}_{p_2 y}\underline{e}_y + \mathcal{F}_{p_2 z}\underline{e}_z = -\frac{\pi}{6}(\sigma_1+\sigma_2)^2\frac{\tau_{v_2}^2 m_1}{(m_1+m_2)^2}\rho_{p_1}(u_{p_1}-u_{p_2})^3\nabla_\perp \rho_{p_2} \quad (4.103)$$

The symbol

$$\nabla_\perp = \frac{\partial}{\partial y}\underline{e}_y + \frac{\partial}{\partial z}\underline{e}_z$$

denotes the transverse gradient operator. The representation of $\underline{\mathcal{F}}_{p_2\perp}$ in other coordinate systems, for instance cylindrical polars, is readily obtained by expressing $\nabla_\perp$ in this coordinate system. (See Appendix B for treatment for the representation in a cylindrical coordinate system.)

Equations (4.102) and (4.103) express the mass flux density of particles of radius σ_2 as a function of several known quantities and the mass density ρ_{p_2} of particles σ_2. Consequently, by substituting (4.102) and (4.103) into (4.10) we obtain an equation for ρ_{p_2} which, together with appropriate boundary conditions, determines ρ_{p_2} throughout the shock relaxation zone.

Before proceeding with this calculation, let us consider our results in terms of more familiar kinetic theory ideas. Introduce the quantities λ and ν where $\lambda(x)$ is a measure of the maximum distance moved by a particle of radius σ_2, following a collision, in excess of the distance it would have moved without collisions.

$$\lambda(x) \equiv \frac{m_1\tau_{v_2}}{m_1+m_2}\left(u_{p_1}(x) - u_{p_2}(x)\right) \quad (4.104)$$

The quantity $\nu(x)$ is approximately the local frequency of collisions between particles of radius σ_2 and σ_1 i.e. $\tau_{c_{21}} = \nu^{-1}(x)$ is the local average time between successive collisions. This may be written

$$\nu(x) = \pi(\sigma_1+\sigma_2)^2 n_{p_1} (u_{p_1} - u_{p_2}) = \pi(\sigma_1+\sigma_2)^2 \frac{\rho_{p_1}}{m_1} (u_{p_1} - u_{p_2}) \tag{4.105}$$

Physically, the length $\lambda(x)$ is the maximum distance that a particle σ_2 can move normal to the gas flow following a collision at x. In fact, it is the transverse range of particle σ_2. Using the definitions of λ and ν, Eqs. (4.104) and (4.105), the components of the mass flux density of particles σ_2, Eq. (4.102) and Eq. (4.103), may be written in the form;

$$(\underline{\underline{\varphi}}_{p_2})_x = \rho_{p_2} \left\{ u_{p_2} + \lambda\nu \right\} \underline{e}_x \tag{4.106}$$

and

$$\underline{\underline{\varphi}}_{p_2 \perp} = -\frac{1}{6} \lambda^2 \nu \, \nabla_\perp \rho_{p_2} \tag{4.107}$$

The motion of the particle cloud σ_2 is characterized by an average convection with velocity $v_{p_2} = u_{p_2} + \lambda\nu$ parallel to the gas flow accompanied by a diffusive spreading of the particles σ_2 across the gas flow. Evidently the average convective velocity of particles σ_2, from Eq. (4.106), is a sum consisting of the local collisionless velocity, u_{p_2}, of particles σ_2 and a local diffusion velocity, $\lambda\nu$, due to the collisions between particles of radius σ_2 and particles of radius σ_1.

Marble[3] has pointed out that these collisional effects may be interpreted as a force per unit volume existing between the particle

clouds. In other words there exists a "dynamical friction" between the cloud of particles σ_1 and the cloud of particles σ_2. The effect of this interaction is to increase the average velocity of particles σ_2 toward u_{p1}, the local collisionless velocity of particles σ_1. The degree to which v_{p2} approaches u_{p1} depends upon the relative magnitudes of τ_{v_2} and τ_{c21}. The circumstance such that the average time, τ_{c21}, a particle σ_2 spends between successive collisions with particles σ_1 exceeds its velocity equilibration time, τ_{v_2}, is of special interest. Before a collision particles σ_2 are moving at their local collisionless velocity, u_{p2}, which may differ significantly from u_{p1}, the local collisionless velocity of particles σ_1. Following a collision the momentum and energy received by the particle σ_2 during the collision are damped by the viscous forces exerted on the particle σ_2 by the gas. The particle returns to its local collisionless velocity u_{p2} before it has another encounter. Consequently the viscous force exerted on the particles σ_2 during their motion between successive collisions tends to force particles of radius σ_2 to take on their local collisionless velocity which is near the velocity of the gas, since $\lambda_{v_2}/\lambda_{v_1}$ is small. Therefore, the dynamical friction force competes with the viscous drag force. It is the interaction of these two forces which determines the average convective velocity of particles σ_2, $v_{p2} \cong u_{p2} + \lambda\nu$, parallel to the gas-particle σ_1 flow.

Let us compute the dynamical friction force, $\underline{F}_{DF}$, acting on particle cloud σ_2 and compare it with the Stokes drag force. Denote by $\underline{F}_{DF}$ the force per unit volume exerted on particle cloud σ_2 due to collisions between particles σ_2 and σ_1. $\underline{F}_{DF}$ depends on the rate

of transfer of momentum from particles σ_1 to particles σ_2 resulting from collisions; its jth component may be written;

$$\left(\underline{F}_{DF}(\underline{x})\right)_j = \int_{4\pi} \Delta\left(m_2 \underline{v}_{p_2}(\underline{x},\Omega)\right)_j \frac{dN_{p_2}(\underline{x},\Omega)}{dt\,dV} \tag{4.108}$$

where $\Delta\left(m_2 \underline{v}_{p_2}(\underline{x},\Omega)\right)_j$ is the jth component of momentum change of a particle σ_2 that scatters it into a solid angle $\Omega - \Omega + d\Omega$. $\frac{dN_{p_2}}{dt\,dV}(\underline{x},\Omega)$ is the number of particles σ_2 per second, per unit volume, at $\underline{x}$ that experience a collision and are scattered into a solid angle $\Omega - \Omega + d\Omega$. Now since $\Delta(m_2 \underline{v}_{p_2}(\Omega))_j$ is proportional to a velocity difference and $\frac{dN_{p_2}(\Omega)}{dt\,dV}$ is independent of the reference frame from which the collisions are viewed, the reference frame in which the integral (4.108) is evaluated is irrelevant. We choose the local collisionless velocity frame for particles σ_2 since they are at rest in this reference frame prior to a collision. Therefore from (A1.5), (A1.6), (A1.8), and (A2.5) of Appendix A we have;

$$\Delta\left(m_2 \underline{v}_{p_2}(\underline{x},\Omega)\right)_x = \frac{m_1 m_2}{(m_1+m_2)}\left(u_{p_1}(x) - u_{p_2}(x)\right)(1+\cos 2\psi) \tag{4.109}$$

$$\Delta\left(m_2 \underline{v}_{p_2}(\underline{x},\Omega)\right)_y = \frac{m_1 m_2}{(m_1+m_2)}\left(u_{p_1}(x) - u_{p_2}(x)\right)\sin 2\psi \cos\varphi \tag{4.110}$$

$$\Delta\left(m_2 \underline{v}_{p_2}(\underline{x},\Omega)\right)_z = \frac{m_1 m_2}{(m_1+m_2)}\left(u_{p_1}(x) - u_{p_2}(x)\right)\sin 2\psi \sin\varphi \tag{4.111}$$

and

$$\frac{dN_{p_2}(\underline{x},\Omega)}{dt\,dV} = n_{p_1}(x)\, n_{p_2}(\underline{x})\left|u_{p_1}(x) - u_{p_2}(x)\right|(\sigma_1+\sigma_2)^2 \cos\psi\, d\Omega \tag{4.112}$$

Then by substituting (4.109) and (4.112) into (4.108) the force per unit volume exerted on particle cloud σ_2 due to collisions with particles σ_1 is;

$$(\underline{F}_{DF}(\underline{x}))_x = \frac{m_1 m_2}{(m_1+m_2)} n_{p_1} n_{p_2} (\sigma_1+\sigma_2)^2 (u_{p_1}-u_{p_2}) |u_{p_1}-u_{p_2}| \int_0^{2\pi} d\varphi \int_0^{\pi/2} d\psi \left\{ (1+\cos 2\psi) \frac{\sin 2\psi}{2} \right\} \tag{4.113}$$

or

$$(\underline{F}_{DF}(\underline{x}))_x = \frac{\rho_{p_1}(x)\rho_{p_2}(x)}{(m_1+m_2)} \pi (\sigma_1+\sigma_2)^2 (u_{p_1}(x)-u_{p_2}(x)) |u_{p_1}(x)-u_{p_2}(x)| \tag{4.114}$$

This result is valid for all values of σ_2/σ_1 when $\tau_{U_2} < \tau_{CZ_1}$. The following discussion, however, is restricted to the present case where $\sigma_2/\sigma_1 << 1$.

An equal and opposite force, $-(\underline{F}_{DF}(\underline{x}))_x$, is exerted per unit volume on particle cloud σ_1 . However, since $\rho_{p_1} >> \rho_{p_2}$ this force is negligible compared to the viscous drag force acting on particles σ_1 . In a similar manner, using (4.110) and (4.111), one finds, by carrying out the integral in (4.108)

$$(\underline{F}_{DF}(\underline{x}))_y = (\underline{F}_{DF}(\underline{x}))_z = 0 \tag{4.115}$$

This result is not surprising since in the calculation of $\frac{dN_{p_2}}{dtdV}$ all impact parameters for collisions within the volume element dV were taken equally probable. Under this condition there can be no net transfer of momentum normal to the X axis which is parallel to the direction of relative motion of the particles prior to an encounter.

Consequently the dynamical force, $\underline{F}_{DF}(\underline{x}) = F_{DF}(\underline{x})\,\underline{e}_x$, exerted upon particle cloud σ_2 , acts only in the positive x direction and tends to increase the convective velocity of particles σ_2 as they pass through the relaxation zone. This result is consistent with expressions 4.106, 4.107 for the mass flux density, $\underline{\Psi}_{p2}$, of particles σ_2.

We are now in a position to investigate the relative magnitudes of collisional interaction force and viscous forces acting on particles σ_2 . Under the assumption of Stokes law, the viscous drag force per unit volume acting on particles σ_2 is

$$\underline{F}_S = F_S\,\underline{e}_x = \frac{\rho_{p2}\,a}{\lambda v_2}(u-u_{p2})\underline{e}_x = \frac{\rho_{p2}}{\tau_{v_2}}(u-u_{p2})\underline{e}_x \qquad (4.116)$$

Then using (4.114) and (4.116);

$$\frac{F_{DF}}{F_S} = \left(\frac{\tau_{v2}}{\tau_{c21}}\right)\left(\frac{m_1}{m_1+m_2}\right)\left(\frac{u_{p1}-u_{p2}}{u-u_{p2}}\right) \qquad (4.117)$$

where $\tau_{c_{21}} = \nu^{-1}$ is the average time between successive collisions for particles σ_2 . Consequently since $\sigma_1 > \sigma_2$ and $m_1 > m_2$, the collisional to viscous force ratio depends essentially on the product of the ratio, τ_{v2}/τ_{c21} , of the velocity equilibration time to collisional time and the ratio, $(u_{p1}-u_{p2})/(u-u_{p2})$, of the difference in the local collisionless velocities of the two particle sizes to the slip velocity of particles σ_2 . For the simplified collision model employed here, τ_{v2}/τ_{c21} is less than or equal to unity. From Figure 8 it is evident that, when $\sigma_2/\sigma_1 \ll 1$, the ratio $(u_{p2}-u_{p1})/(u-u_{p2})$ becomes large downstream of the shock wave. The solution for u_{p1}, u_{p2} and u , Figure 8., show that, immediately downstream of the shock, $u_{p1} \sim u_{p2}$ and $u-u_{p2}$ is large; therefore viscous forces

dominate. For $x \gtrsim \lambda_{v_2}$, however, the local collisionless velocity of particles σ_2 has decreased nearly to its small slip value;

$$u - u_{p_2} \sim \lambda_{v_2} \frac{u}{a} \frac{du}{dx} \tag{4.118}$$

and consequently $(u_{p_1} - u_{p_2})$ may be large $\sim (u(1) - u(2))$. In this region the collision forces dominate.

We may conclude, therefore, that there exist conditions, when $\tau_{v_2}/\tau_{c_{21}} < O(1)$, under which collisions dominate viscous forces in determining the macroscopic motion of the particle cloud σ_2. Then $F_{DF}/F_S \gtrsim 1$ under most circumstances when $\sigma_2/\sigma_1 \ll 1$.

It is interesting to rewrite (4.114) using expressions (4.104) and (4.105) for λ and ν;

$$F_{DF} = \rho_{p_2} \left(\frac{\lambda \nu}{\tau_{v_2}} \right) \tag{4.119}$$

This suggests that the rate of increase of the diffusion velocity of particles σ_2 is limited by the relaxation time, τ_{v_2}, of particles σ_2. In addition, dividing (4.114) by the Stokes force (4.116), we obtain,

$$\frac{F_{DF}}{F_S} = \frac{\lambda \nu}{(u - u_{p_2})} \tag{4.120}$$

Since F_{DF}/F_S may be significantly greater than unity, the effective diffusion velocity, $\lambda\nu$, exceeds the slip velocity of particles σ_2.

Expression (4.107), which gives the mass flux of particles σ_2 normal to the direction of gas flow, indicates their motion to be diffusive but not in the sense that the collisions are completely random. The reason for this is the fact that collisions take place only when particles σ_2 are overtaken by particles σ_1 and always recoil in

the direction downstream of the collision site. Within this restriction, all impact parameters are equally probable and consequently the normal scattering introduces some random character into the transverse motion of particles σ_2.

The numerical effect of the anisotropy in the scattering may be seen by rewriting (4.107)

$$\frac{\varphi}{p_{z_1}} = -D \nabla_\perp \rho_{p_z} \tag{4.121}$$

where $D = \frac{1}{6}\lambda^2 \nu$ is the effective diffusion (4.122) constant for the transverse dispersion of particles σ_2. If there were complete randomness we would expect a numerical factor of 1/3 instead of 1/6. It seems appropriate to interpret D as a diffusion constant, recognizing that the analogy is not complete.

When a diffusion process is purely random the diffusion constant is given by;[12, 13]

$$D_D \sim L^2 \nu_c \tag{4.123}$$

where L is the characteristic step size of the diffusing particle and ν_c is the number of collisions per second. The motion of the particle appears as a random walk due to collisions. For instance the diffusion of gas molecules of a given species, i, through a much more dense uniform distribution of gas molecules of another species, j, is described by the diffusion constant;

$$D_i \sim \lambda_{ij}^2 \nu_{ij} \tag{4.124}$$

where λ_{ij} is the average distance moved by a molecule of species i between successive collisions with molecules of type j and ν_{ij} is the local collision frequency for collision. This process is sketched in Fig. 16a.

A contrasting example exhibiting anisotropy is the diffusion of a weakly ionized gas which is drifting parallel to a strong uniform magnetic field B. The charged particles are nonuniformly distributed. Because the gas is weakly ionized, only charged particle-neutral collisions are important. In a reference frame drifting with the gas, the magnetic field causes the diffusion process to be anisotropic.

Because the magnetic field is strong, the cyclotron radius ρ_c of the ions, is much less than the mean free path for ion-neutral collisions, λ_{in}. Under these conditions the diffusion of ions across the magnetic field is determined by

$$D_{i_\perp} \sim (\rho_c)^2 \nu_{in} \tag{4.125}$$

where $\rho_c = \frac{v_\perp}{\nu_c}$; $\nu_c = \frac{eB}{m_i}$. $v_\perp$ is the average velocity of ions perpendicular to the magnetic field, e/m_i the charge to mass ratio of the ion, and ν_{in} the collision frequency for ion-neutral collisions. The magnetic field does not affect the diffusion of ions parallel to it and consequently

$$D_{i_{||}} \sim \lambda_{in}^2 \nu_{in} \tag{4.126}$$

The diffusion of a test ion is depicted in Figure 16b. Since $\rho_c << \lambda_{in}$ the motion of the ion across the magnetic field is constrained. The ion moves normal to the field only by colliding with a

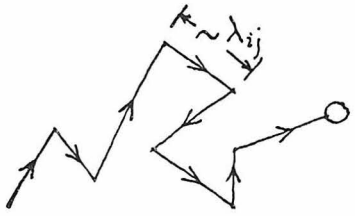

(a)

diffusion of a molecular test particle of species i. Characteristic stepsize of particle diffusion is mean free path λ_{ij}

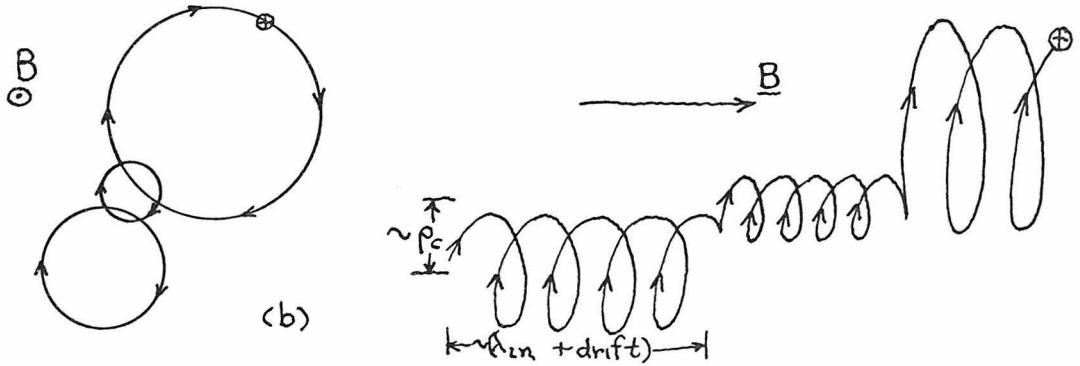

diffusion of an ion in a magnetic field B. Characteristic stepsize for motion across the flow is ρ_c, The cyclotron radius, parallel to the flow in a drifting reference frame it is λ_{in} the ion-neutral collision mean free path.

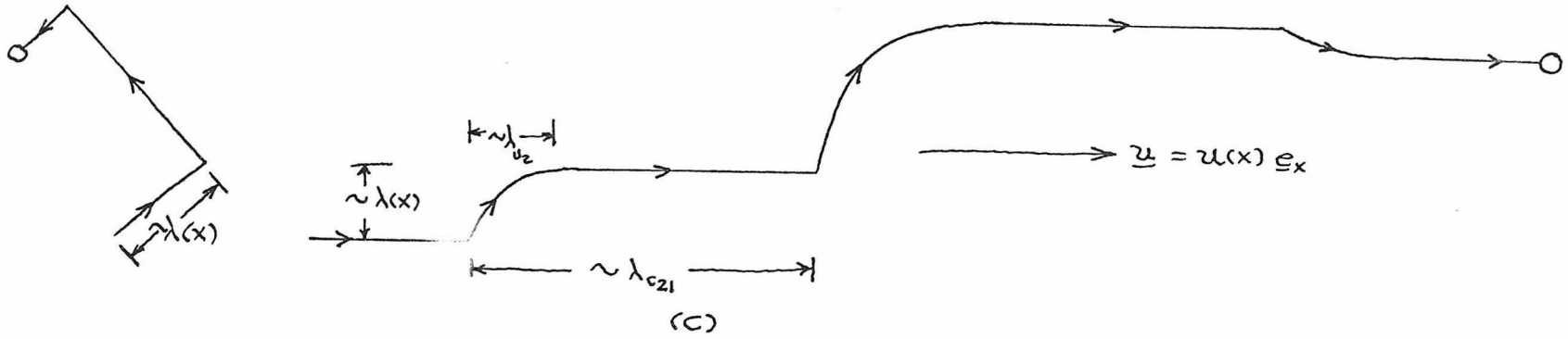

Figure 16. Diffusion of a solid particle σ_2 across a decelerating gas-particle σ_1 flow in shock relaxation zone, $\sigma_2/\sigma_1 \ll 1$, characteristic stepsize across flow is λ the transverse range.

neutral molecule. The characteristic step size for the displacement is the cyclotron radius

$$\rho_c = \frac{v_\perp}{\nu_c} = v_\perp \tau_c \tag{4.127}$$

In light of this result, the correspondence of (4.122) and (4.123) suggest the following analogy. The motion of particles of radius σ_2 across the gas flow, due to encounters with particles σ_1, is a diffusion process in the sense that $\lambda(x)$ may be interpreted as the characteristic step size of the dispersion when $\tau_{v_2}/\tau_{c_{21}} \sim \lambda_{v_2}/\lambda_{c_{21}} < 1$ (See Figure 16c). In this sense λ corresponds to ρ_c for ion diffusion in a magnetic field and τ_{v_2} corresponds to τ_c. Following a collision, a particle σ_2 moves a distance $\lambda = u^{(f)}_{p_{2\perp}} \tau_{v_2}$ across the gas flow where $u^{(f)}_{p_{2\perp}}$ is the component of its scattering velocity normal to the direction of the gas flow. The gas, through the action of viscous forces, constrains the perpendicular motion of particles σ_2 analogous to the magnetic field-ion interaction.

5. Solution for the Particle Density ρ_{p2}.

The equation of continuity (4.10) and the expressions (4.102) and (4.103) for the mass flux density, $\underline{\Phi}_{p2}$, of particles of radius may be written;

$$\nabla \cdot \underline{\Phi}_{p2} = 0 \tag{4.128}$$

and

$$\underline{\Phi}_{p2} = \Phi_{p2x}\,\underline{e}_x + \underline{\Phi}_{p2\perp} \tag{4.129}$$

with;

$$\mathcal{F}_{p_2 x} = \rho_{p_2} v_{p_2} = \rho_{p_2}\left\{ u_{p_2} + \lambda\nu \right\} \tag{4.130}$$

$$\mathcal{F}_{p_2 \perp} = -\frac{1}{6}\lambda^2 \nu \, \nabla_\perp \rho_{p_2} = -D(x) \nabla_\perp \rho_{p_2} \tag{4.131}$$

In Equation 4.131 $\nabla_\perp$ is the gradient operator of the coordinate system used to describe the distribution in a plane parallel to the shock face, ρ_{p_2} is the average density of particles of radius σ_2, u_{p_2} the local collisionless velocity of particles of radius σ_2, λ and ν are given by (4.104) and (4.105).

$$\lambda(x) = \frac{m_1 \tau_{u_2}}{m_1 + m_2} \left(u_{p_1}(x) - u_{p_2}(x) \right) \tag{4.132}$$

and

$$\nu(x) = \pi (\sigma_1 + \sigma_2)^2 \frac{\rho_{p_1}(x)}{m_1} \left(u_{p_1}(x) - u_{p_2}(x) \right) \tag{4.133}$$

Substituting (4.131) and (4.130) into (4.128) using (4.129) we obtain;

$$\frac{\partial}{\partial x}\left(\rho_{p_2}(\underline{x}) v_{p_2}(x) \right) - D(x) \nabla_\perp^2 \rho_{p_2}(\underline{x}) = 0 \tag{4.134}$$

where only $\rho_{p_2} = \rho_{p_2}(\underline{x})$ is a function of transverse coordinates. Since $v_{p_2}(x)$ is independent of these coordinates, (4.134) may be rewritten;

$$\frac{\partial}{\partial x}\left(\rho_{p_2}(\underline{x}) v_{p_2}(x) \right) - K(x) \nabla_\perp^2 \left(\rho_{p_2}(\underline{x}) v_{p_2}(x) \right) = 0 \tag{4.135}$$

where $K(x) \equiv D(x) / v_{p_2}(x)$. Now, as remarked earlier, ρ_{p_1}, u_{p_1}, u_{p_2} and τ_{u_2} are known functions of x obtained by solution of Eqs. (3.1)-(3.9) and Eq. (4.11) together with conditions (4.3). Equation (4.135) determines $\rho_{p_2} = \rho_{p_2}(\underline{x})$ when supplied with appropriate boundary and

initial conditions. Using 4.130, the mass flux density $\mathcal{F}_{p_2x}$ satisfies a diffusion equation;

$$\frac{\partial \mathcal{F}_{p_2x}(\underline{x})}{\partial x} - K(x)\,\nabla_\perp^2 \mathcal{F}_{p_2x}(\underline{x}) = 0 \tag{4.136}$$

with diffusion coefficient $K(x) = D(x)/n_{p_2}(x)$. Since $K(x) \geq 0$ for $x > 0$, Eq. (4.136) is parabolic. The mathematical problem[14] for $\mathcal{F}_{p_2x}$ is properly posed when $\mathcal{F}_{p_2}(\underline{x})$ is given at $x = 0$, for all $\underline{x}_\perp$, and $\mathcal{F}_{p_2x}(0, \underline{x}_\perp)$ is bounded for $-\infty < |\underline{x}_\perp| < \infty$. These conditions are met by our physical knowledge of the problem.

To establish $\mathcal{F}_{p_2}(0, \underline{x}_\perp)$ we observe that particles σ_1 and σ_2 pass unaffected through the gas dynamic shock. All particle properties are continuous across the shock. Then if $\mathcal{F}_{p_2x}$ is the mass flux density of particles σ_2 in the x direction and $\underline{\mathcal{F}}_{p_2\perp}$ is the mass flux density of particles σ_2 in the directions perpendicular to x,

$$\begin{aligned} \mathcal{F}_{p_2x}(1) &= \mathcal{F}_{p_2x}(2) \\ \underline{\mathcal{F}}_{p_2\perp}(1) &= \underline{\mathcal{F}}_{p_2\perp}(2) = 0 \end{aligned} \tag{4.137}$$

Here, 1 denotes conditions immediately upstream of the shock wave and 2 denotes conditions immediately downstream. Using conditions (4.3), expressions (4.106) and (4.107) for $\mathcal{F}_{p_2x}$ and $\underline{\mathcal{F}}_{p_2\perp}$, respectively, and taking the limit of $\mathcal{F}_{p_2x}$, $\underline{\mathcal{F}}_{p_2\perp}$ as $x \to 0$ from downstream of the shock wave, it follows that conditions (4.137) are satisfied. In addition the density, ρ_{p_2}, of particles σ_2 is continuous through the shock wave and this situation is consistent with continuity of particle fluxes as examined earlier.

The mass flux density of particles σ_2 is determined by

$$\frac{\partial}{\partial x}\varphi_{p_2x}(\underline{x}) - k(x)\nabla_\perp^2 \varphi_{p_2x}(\underline{x}) = 0 \tag{4.138}$$

together with;

$$\varphi_{p_2x}(0,\underline{x}_\perp) = \rho^{(1)}_{p_2}(\underline{x}_\perp)\, u(1) \tag{4.139}$$

Since $\varphi_{p_2x}(\underline{x}) = \rho_{p_2}(\underline{x})\, v_{p_2}(x)$ and $v_{p_2}(x) = u_{p_2}(x) + \lambda(x)\nu(x)$ the values of $\rho_{p_2}(\underline{x})$ downstream of the gas dynamic shock wave are

$$\rho_{p_2}(\underline{x}) = \frac{\varphi_{p_2x}(\underline{x})}{v_{p_2}(x)} = \frac{\varphi_{p_2x}(\underline{x})}{u_{p_2}(x) + \lambda(x)\nu(x)} \tag{4.140}$$

where $v_{p_2}(x) \neq 0$ for all $x \geq 0$.

Consider the variation of φ_{p_2x} with respect to the xyz cartesian system oriented such that the plane $x=0$ contains the shock face. Then (4.138) and (4.139) become;

$$\frac{\partial}{\partial x}\varphi_{p_2x}(x,y,z) - k(x)\left\{\frac{\partial^2 \varphi_{p_2x}(x,y,z)}{\partial y^2} + \frac{\partial^2 \varphi_{p_2x}(x,y,z)}{\partial z^2}\right\} = 0 \tag{4.141}$$

and;

$$\varphi_{p_2x}(0,y,z) = \rho^{(1)}_{p_2}(y,z)\, u(1) \tag{4.142}$$

Transform (4.141) to canonical form by writing

$$\zeta(x) = \int_0^x k(x')\,dx' \quad ; \quad x \geq 0 \tag{4.143}$$

$$\frac{\partial}{\partial \zeta}\varphi_{p_2x}(\zeta,y,z) - \frac{\partial^2 \varphi_{p_2x}(\zeta,y,z)}{\partial y^2} - \frac{\partial^2}{\partial z^2}\varphi_{p_2x}(\zeta,y,z) = 0 \tag{4.144}$$

Because $\zeta = 0$ when $x = 0$ the boundary condition (4.142) holds when $\zeta = 0$.

The particular solution

$$\mathcal{F}^{(f)}_{p_2 x}(x,y,z) = \frac{m_2 N_{p_2} u(1)}{4\pi s(x)} e^{-(y^2+z^2)/4s(x)} \tag{4.145}$$

corresponds to a delta function distribution of particles σ_2 upstream of the gas-dynamic shock wave

$$\rho^{(1)}_{p_2}(y,z) = m_2 N_{p_2} \delta(y)\,\delta(z) \tag{4.146}$$

where the delta function has the properties

$$\delta(\alpha-\alpha_0) = \lim_{\beta\to 0} \frac{e^{-(\alpha-\alpha_0)^2/4\beta}}{\sqrt{4\pi\beta}}$$

$$\int_{-\infty}^{\infty} \delta(\alpha-\alpha_0)\,d\alpha = 1 \tag{4.147}$$

Consequently; $\frac{1}{m_2}\int_{-\infty}^{\infty} \rho^{(1)}_{p_2}(y,z)\,dy\,dz = N_{p_2}$ and we interpret N_{p_2} as the number of particles of radius σ_2 in a cross section of unit thickness in the X direction of the distribution of particles σ_2 upstream of the gas-dynamic shock wave. We call this the fundamental beam solution.

Because (4.144) is linear, we may write the general beam solution of (4.144) as a superposition of fundamental beams

$$\mathcal{F}_{p_2 x}(x,y,z) = \frac{1}{4\pi s(x)} \int_{-\infty}^{\infty}\int \mathcal{F}_{p_2 x}(0,y',z')\, e^{-\{(y-y')^2+(z-z')^2\}/4s(x)}\,dy'dz' \tag{4.148}$$

Using (4.140) and (4.145) the density of particles σ_2, for a delta function distribution of particles σ_2 upstream, is;

$$\rho_{p_2}^{(f)}(x,y,z) = m_2 N_{p_2}\left(\frac{u(1)}{v_{p_2}(x)}\right)\frac{e^{-(y^2+z^2)/4\zeta(x)}}{4\pi\zeta(x)} \tag{4.149}$$

so that, for a general density distribution, $\rho_{p_2}^{(1)}(y,z)$, we have;

$$\rho_{p_2}(x,y,z) = \left(\frac{u(1)}{v_{p_2}(x)}\right)\frac{1}{4\pi\zeta(x)}\int_{-\infty}^{\infty}\int_{-\infty}^{\infty}\rho_{p_2}^{(1)}(y',z')\,e^{-\{(y-y')^2+(z-z')^2\}/4\zeta(x)}\,dy'dz' \tag{4.150}$$

utilizing previous results,

$$\zeta(x) = \int_0^x \frac{D(x')}{v_{p_2}(x')}dx' = \frac{1}{6}\int_0^x \lambda(x')\left(\frac{\lambda(x')\nu(x')}{v_{p_2}(x')}\right)dx' \tag{4.151}$$

$$v_{p_2}(x) = u_{p_2}(x) + \lambda(x)\nu(x) \tag{4.152}$$

$$\lambda(x) = \frac{m_1\tau_{v_2}}{m_1+m_2}\left(u_{p_1}(x) - u_{p_2}(x)\right) \tag{4.153}$$

and

$$\nu(x) = \pi(\sigma_1+\sigma_2)^2\frac{\rho_{p_1}(x)}{m_1}\left(u_{p_1}(x) - u_{p_2}(x)\right) \tag{4.154}$$

As x becomes large u_{p_1}, u_{p_2} and u all reach the same limiting value $u(\infty)$. Therefore because of the functional dependence of v_{p_2} and K on u_{p_2} and u_{p_1}, $\zeta(x) \to$ constant as x becomes large. Consequently the density of particles σ_2 always reaches a limiting distribution far downstream of the shock wave. There is a "freezing" of the density distribution of particles of radius σ_2. Later we will show that this final distribution is essentially reached when $x > O(\lambda_{v_1})$. The final equilibrium state of this gas-particle mixture is therefore

$$u(\infty) = u_{p_1}(\infty) = u_{p_2}(\infty) = v_{p_2}(\infty)$$

$$T(\infty) = T_{p_1}(\infty) = T_{p_2}(\infty)$$

$$\rho(\infty) = \rho(1)\left(\frac{u(1)}{u(\infty)}\right) \qquad \rho_{p_1}(\infty) = K_1 \rho(\infty)$$

and

$$\rho^{(f)}_{p_2}(\infty, y, z) = m_2 N_{p_2}\left(\frac{u(1)}{u(\infty)}\right)\frac{e^{-(y^2+z^2)/4\Sigma(\infty)}}{4\pi\Sigma(\infty)}$$

or

$$\rho(\infty, y, z) = \frac{u(1)}{u(\infty)}\frac{1}{4\pi\Sigma(\infty)}\int_{-\infty}^{\infty}\int \rho^{(1)}_{p_2}(y', z')\, e^{-\left\{(y-y')^2+(z-z')^2\right\}/4\Sigma(\infty)}\, dy'\, dz'$$

where;

$$\Sigma(\infty) = \int_0^{\infty} K(x')\, dx'$$

In this state the particles and the gas are in velocity and thermal equilibrium but particles σ_2 are nonuniformly distributed normal to the X axis.

For the present, restrict the analysis to a two-dimensional problem, that is one where particle σ_2 distributions are independent of z. The appropriate fundamental and general beam solutions for this case may be obtained from (4.144) or by integration in (4.149);

$$\rho_{p_2}^{(f)}(x,y) = m_2 \bar{N}_{p2} \left(\frac{u(1)}{v_{p_2}(x)}\right) \frac{e^{-y^2/4\Im(x)}}{\sqrt{4\pi\Im(x)}} \tag{4.155}$$

and

$$\rho_{p_2}(x,y) = \left(\frac{u(1)}{v_{p_2}(x)}\right) \frac{1}{\sqrt{4\pi\Im(x)}} \int_{-\infty}^{\infty} \rho_{p_2}^{(1)}(y') e^{-(y-y')^2/4\Im(x)} dy' \tag{4.156}$$

In the present case $\bar{N}_{p_2} = \frac{1}{m_2}\int_{-\infty}^{\infty} \rho_{p_2}^{(1)}(y')dy'$ is the number of particles in a cross section of unit thickness in the x and z direction upstream of the shock wave.

Analytical evaluation of $\Im(x)$ is not possible because λ, ν, and v_{p_2} are obtained from numerical solutions of (3.1) to (3.9) and (4.11). Consequently further analysis must also be done numerically. Before presenting results of such calculations, let us review the conditions for the validity of our solutions.

Introduce the dimensionless variables;

$$\begin{aligned}
&x = \lambda_{v_1}\tilde{x} \qquad y = \lambda_{v_1}\tilde{y} \\
&\rho = \rho(1)\tilde{\rho} \qquad \rho_{p1} = \rho(1)\tilde{\rho}_{p1} \qquad \rho_{p2} = \rho_{p2}(1)\tilde{\rho}_{p2} \qquad \rho_{p2}^{(1)} = \rho_{p2}(1)\tilde{\rho}_{p2}^{(1)} \\
&u = a(1)\tilde{u} \qquad u_{p1} = a(1)\tilde{u}_{p1} \qquad u_{p2} = a(1)\tilde{u}_{p2} \qquad a = a(1)\tilde{a} \\
&T = T(1)\tilde{T} \qquad T_{p1} = T(1)\tilde{T}_{p1} \qquad T_{p2} = T(1)\tilde{T}_{p2}
\end{aligned} \tag{4.157}$$

and

$$\lambda = \lambda(2)\tilde{\lambda} \qquad \nu = \nu(2)\tilde{\nu} \qquad v_{p_2} = a(1)\tilde{v}_{p_2} \tag{4.158}$$

where $\rho_{p_2}(1)$ is the characteristic magnitude of $\rho_{p_2}^{(1)}(y)$. The characteristic transverse range, $\lambda(2)$, and collision frequency, $\nu(2)$, are

given by;

$$\lambda(2) = \frac{m_1 \tau_{v_2}}{m_1+m_2} \left(u(1)-u(2)\right) \tag{4.159}$$

$$\nu(2) = \pi(\sigma_1+\sigma_2)^2 \frac{\rho_{p_1}(1)}{m_1} \left(u(1)-u(2)\right) = \pi(\sigma_1+\sigma_2)^2 \frac{K_{p_1}(1)}{m_1} \left(u(1)-u(2)\right) \tag{4.160}$$

Substituting (4.157) and (4.158) into (4.155) and (4.156) we obtain;

$$\tilde{\rho}^{(f)}_{p_2}(\tilde{x},\tilde{y}) = \left(\frac{M_1}{\tilde{v}_{p_2}(\tilde{x})}\right) \frac{e^{-\tilde{y}^2/4D\tilde{S}(\tilde{x})}}{\sqrt{4\pi D\tilde{S}(\tilde{x})}} \tag{4.161}$$

and

$$\tilde{\rho}_{p_2}(\tilde{x},\tilde{y}) = \left(\frac{M_1}{\tilde{v}_{p_2}(\tilde{x})}\right) \frac{1}{\sqrt{4\pi D\tilde{S}(\tilde{x})}} \int_{-\infty}^{\infty} \tilde{\rho}^{(1)}_{p_2}(\tilde{y}')\, e^{-(\tilde{y}-\tilde{y}')^2/4D\tilde{S}(\tilde{x})}\, d\tilde{y}' \tag{4.162}$$

where we have taken $\rho^{(f)}_{p_2} = m_2 \frac{\bar{N}_{p_2}}{\lambda v_1}$ $\tilde{\rho}^{(f)}_{p_2} = \rho_{p_2}(0)\, \tilde{\rho}^{\nu(f)}_{p_2}$ since $m_2 \bar{N}_{p_2} / \lambda v_1$ has dimensions of a density, and

$$D \equiv \frac{D(2)}{\lambda v_1} \equiv \frac{1}{6} \left(\frac{\lambda(2)}{\lambda v_1}\right) \left(\frac{\lambda(2)\nu(2)}{a(1)}\right) \tag{4.163}$$

In addition rewrite (4.151) and (4.152) using (4.157)-(4.160);

$$\tilde{S}(\tilde{x}) = S/\lambda_1^2 D = \int_0^{\tilde{x}} \tilde{K}(\tilde{x})\, d\tilde{x} = \int_0^{\tilde{x}} \frac{\tilde{D}(\tilde{x})}{\tilde{v}_{p_2}(\tilde{x})}\, d\tilde{x} = \int_0^{\tilde{x}} \tilde{\lambda}(\tilde{x}') \left(\frac{\tilde{\lambda}(\tilde{x}')\tilde{\nu}(\tilde{x}')}{\tilde{v}_{p_2}(\tilde{x}')}\right) d\tilde{x}' \tag{4.164}$$

and

$$\tilde{v}_{p_2}(\tilde{x}) = \tilde{u}_{p_2}(\tilde{x}) + V(2)\, \tilde{\lambda}\tilde{\nu} \tag{4.165}$$

where;

$$V(2) \equiv \frac{\lambda(2)\,\nu(2)}{a(1)} \tag{4.166}$$

The dimensionless quantities D and V characterize the relative dispersion of the density of particles σ_2 downstream of the shock wave. Using Figure 8, the definitions (4.151), (4.153), (4.154), (4.159) and (4.160), Figure 17 indicates the approximate variation of the u_{p1}, u_{p2}, u, $\nu/\nu(2)$, and $\lambda/\lambda(2)$ with x. The dependence of $\nu/\nu(2)$ and $\lambda/\lambda(2)$ on $(u_{p1} - u_{p2})$ stems directly from the collisions model valid when $\tau_{u_2} < \tau_{c_{21}}$. They reach a maximum at $x \sim \lambda_{u_2}$ and since $\lambda_{u_2}/\lambda_{u_1} << 1$, the maxima occur close to the shock wave. Because of the relatively slow variation of the properties of the gas and particles σ_1 in this region, $(\nu(x))_{max} \sim \nu(2)$ and $(\lambda(x))_{max} \sim \lambda(2)$ where $\nu(2)$ and $\lambda(2)$ are defined by (4.159) and (4.160). Consequently $\nu(2)$ is approximately the maximum collision frequency for particle σ_1 - particle σ_2 encounters within the shock relaxation zone. Similarly $\lambda(2)$ is the maximum value of λ, the transverse range of particles σ_2, throughout the shock relaxation zone.

The physical conditions underlying the validity of the collision model and its consequences, Equations (4.149) and (4.150) are as follows:

(a) The region over which the gas flow field varies significantly, λ_{u_1}, is much larger than the velocity equilibration length of particles σ_2

$$\frac{\lambda_{u_2}}{\lambda_{u_1}} = \frac{\tau_{u_2}}{\tau_{u_1}} = \left(\frac{\sigma_2}{\sigma_1}\right)^2 << 1 \tag{4.167}$$

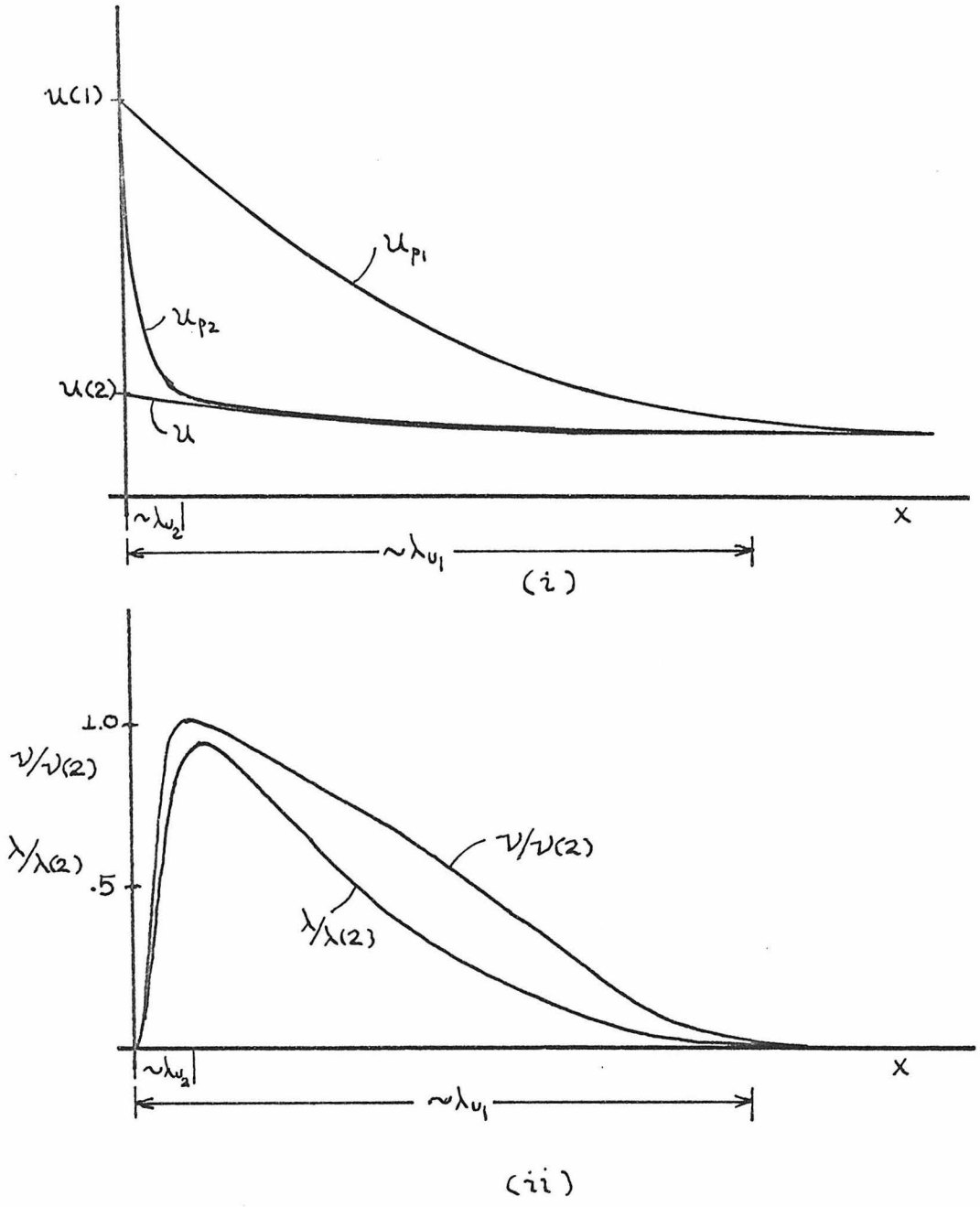

Figure 17. Approximate variation of particle collisional parameters downstream of the shock face

(b) The particle Reynolds number and Mach number is such that the Stokes drag law is valid.

$$Re_2 = \rho \frac{\sigma_2 |u - u_{p2}|}{\mu} \lesssim 1 \qquad \frac{|u - u_{p2}|}{a} << 1 \tag{4.168}$$

$$Re_1 = \rho \frac{\sigma_1 |u - u_{p1}|}{\mu} \lesssim 1 \qquad \frac{|u - u_{p1}|}{a} << 1 \tag{4.169}$$

(c) The time between successive collisions for a given particle must be as large as or larger than the velocity equilibration time of the particles

$$\frac{\tau_{v2}}{\tau_{c2_1}} < 1 \tag{4.170}$$

(d) The velocity equilibration time must be large in comparison with the time required for one particle to pass through the flow field of the other. Analytically, this may be written;

$$\frac{2}{9}\left(\frac{\sigma_2}{\sigma_1}\right)\left(\frac{\rho \sigma_2 |u_{p1} - u_{p2}|}{\mu}\right)\left(\frac{\rho_s}{\rho}\right) >> 1 \tag{4.171}$$

$$\frac{2}{9}\left(\frac{\sigma_2}{\sigma_1}\right)\left(\frac{\rho \sigma_1 |u_{p1} - u_{p2}|}{\mu}\right)\left(\frac{\rho_s}{\rho}\right) >> 1 \tag{4.172}$$

(e) The mass density ρ_{p2} of particles σ_2 is much less than the mass densities ρ_{p1} of particles σ_1 and ρ of the gas;

$$\rho_{p2} << \rho_{p1}, \rho \tag{4.173}$$

(f) The transverse gradients of the density of particles σ_2 are "large"

$$\left(\frac{\lambda_y}{\lambda_{v_1}}\right)^2 \ll 1 \qquad \left(\frac{\lambda_z}{\lambda_{v_1}}\right)^2 \ll 1 \tag{4.174}$$

When Stokes law is violated in the shock relaxation zone, the magnitude of the gas-particle interaction is underestimated. The particle σ_2 range, used to compute the mass flux density Ψ_{p2}, based on Stokes law is therefore too large. Consequently, we may expect our results to be an upper bound on the actual dispersion of particles σ_2. For strong shock waves $M_1 \sim 5$, and particles with $\sigma_1 \sim 10\mu$ the maximum particle σ_1 Reynolds number varies between 10 and several thousand and the maximum particle Mach number is less than or of order unity.

On the other hand, values of elastic collision parameters, (4.171) and (4.172), generally exceed several thousand so that in this regime the effect of the presence of the gas on the collision is negligible. The elasticity of the collision depends on the composition of the particles. The only effects which may be significant are: (1) the effect of the compressibility of the gas since the Mach number of particle σ_1 is of order unity prior to the collision, and (2) the effect of the wake of particle σ_1 on particle σ_2 following the collision. These effects are not well understood at the present time.

Let us now consider condition (4.170) in more detail by writing;

$$\frac{\tau_{v_2}}{\tau_{c_{21}}} = \tau_{v_2}\nu < 1 \tag{4.175}$$

The local collision frequency ν is given by (4.154). Since ν attains a maximum value $\nu(2)$ (4.175) may be expressed more conservatively;

$$\tau_{v_2}(2)\,\nu(2) < 1 \tag{4.176}$$

where $\nu(2)$ is defined by (4.160) and $\tau_{v_2}(2) = \frac{m_2}{6\pi\mu(2)\sigma_2}$, which may be rewritten;

$$\frac{K_1}{6}\left(\frac{\rho(2)\sigma_2\,(u(1)-u(2))}{\mu(2)}\right)\left(\frac{\rho(1)}{\rho(2)}\right)\left(1+\frac{\sigma_2}{\sigma_1}\right)^2 < 1 \tag{4.177}$$

Since $\sigma_2/\sigma_1 << 1$ this condition represents a restriction on the particle σ_2 Reynolds number, $Re_2(2) = \frac{\rho(2)\sigma_2\,(u(1)-u(2))}{\mu(2)}$, immediately downstream of the shock wave, the strength of the shock wave, and the density of particles σ_2.

Alternatively we may rewrite condition (4.176) as $\nu(2) < a(2)/\lambda_{v_2}$ and obtain a restriction on D and $V(2)$ the collisional parameters appearing in (4.161) and (4.162). Using the definitions (4.163) and (4.166) we find

$$D < \frac{1}{6}\left(\frac{\lambda(2)}{\lambda_{v_1}}\right)\left(\frac{\lambda(2)}{\lambda_{v_2}}\right)\left(\frac{a(2)}{a(1)}\right) \tag{4.178}$$

$$V(2) < \left(\frac{\lambda(2)}{\lambda_{v_1}}\right)\left(\frac{a(2)}{a(1)}\right) \tag{4.179}$$

Consequently there is a maximum allowable diffusion velocity and effective diffusion constant. In other words as a consequence of the requirement that particles may only collide while moving at nearly their local slip velocities, there is a limit on the magnitude of the mass flux density of particles σ_2 arising from collisions. In numerical calculations we have found (4.177), (4.178) and (4.179) useful as a guide to guarantee the satisfaction of $\tau_{v_2}\nu < 1$. The limitations imposed by this condition and the variation of $\tau_{v_2}\nu$ in the shock relation zone

are best understood by computing some examples. In general the variation of $\nu\tau_{\omega_2}$ is such that conditions (4.177), (4.178) and (4.179) may be violated without significantly invalidating our results.

The violation of (4.174) results in a correction of order $\left(\sigma_2/\sigma_1\right)^2 << 1$ which, for our purposes, is small. It will become evident from the calculation, however, that this condition is usually satisfied.

6. Results of Numerical Calculations.

By introducing several numerical examples we shall (1) investigate the macroscopic motion of particle cloud σ_2 downstream from the shock wave on the basis of our specific collisional processes, and (2) examine the significance of particle-particle interactions when the present collisional model is valid.

Consider the collisional dispersion of particles σ_2 downstream from the shock wave when their densities upstream are given by;

$$\rho^{(1)}_{p_2}(y) = m_2 \bar{N}_{p_2} \delta(y) \tag{4.180}$$

and

$$\rho^{(1)}_{p_2}(y) = \begin{cases} \rho_{p_2}(1) & |y| \leq y_b \\ 0 & y \text{ otherwise} \end{cases} \tag{4.181}$$

The density distribution of particles σ_2 for $x > 0$, when their upstream density is (4.180), may be determined from (4.155) or (4.161), the fundamental beam solution. This example represents the limiting case of very thin upstream density distributions whose widths are much less than λ_{u_1}, the characteristic dimension of the shock relaxation zone. When the upstream density of particles σ_2 is given by (4.181) their

density downstream of the shock wave may be determined by integration in (4.156) or (4.162) and is

$$\rho_{p_2}(x,y) = \frac{1}{2}\rho_{p_2}(1)\left(\frac{u(1)}{v_{p_2}(x)}\right)\left[\operatorname{erf}\left\{\frac{y_b - y}{\sqrt{4\xi(x)}}\right\} + \operatorname{erf}\left\{\frac{y_b + y}{\sqrt{4\xi(x)}}\right\}\right] \quad (4.182)$$

or introducing dimensionless variables;

$$\tilde{\rho}_{p_2}(\tilde{x},\tilde{y}) = \frac{1}{2}\left(\frac{u(\infty)}{u(1)}\right)\left(\frac{m_1}{\tilde{v}_{p_2}(\tilde{x})}\right)\left[\operatorname{erf}\left\{\frac{\tilde{y}_b - \tilde{y}}{\sqrt{4D\tilde{\xi}(\tilde{x})}}\right\} + \operatorname{erf}\left\{\frac{\tilde{y}_b + \tilde{y}}{\sqrt{4D\tilde{\xi}(\tilde{x})}}\right\}\right] \quad (4.183)$$

where the dimensionless quantities are defined in (4.157)-(4.166), $\rho_{p_2} = \rho_{p_2}(\infty)\tilde{\rho}_{p_2}$ and $\operatorname{erf}(z) = \frac{2}{\sqrt{\pi}}\int_0^z e^{-\eta^2}d\eta$ is the error function of z. This distribution is representative of a distribution whose width is on the same order as the characteristic length of the shock relaxation zone. In the following calculations we will take $y_b = .2\lambda_{v_1}$.

(a) General Variation of $\tilde{\rho}_{p_2}$, $\tilde{\rho}_{p_2}^{(f)}$. As an example of the variation of $\tilde{\rho}_{p_2}^{(f)}(\tilde{x},\tilde{y})$, and $\tilde{\rho}(\tilde{x},\tilde{y})$ throughout the shock relaxation zone consider Figures 18 and 19, respectively. The corresponding variations of u, u_{p_1}, u_{p_2}, λ, ν, K, and $\lambda\nu$, which determine the collisional redistribution of particles σ_2 in the shock relaxation zone, are described in Figure 20. The physical state of the gas-particle mixture upstream of the shock wave is defined by the values of the physical parameters listed in the Figures.

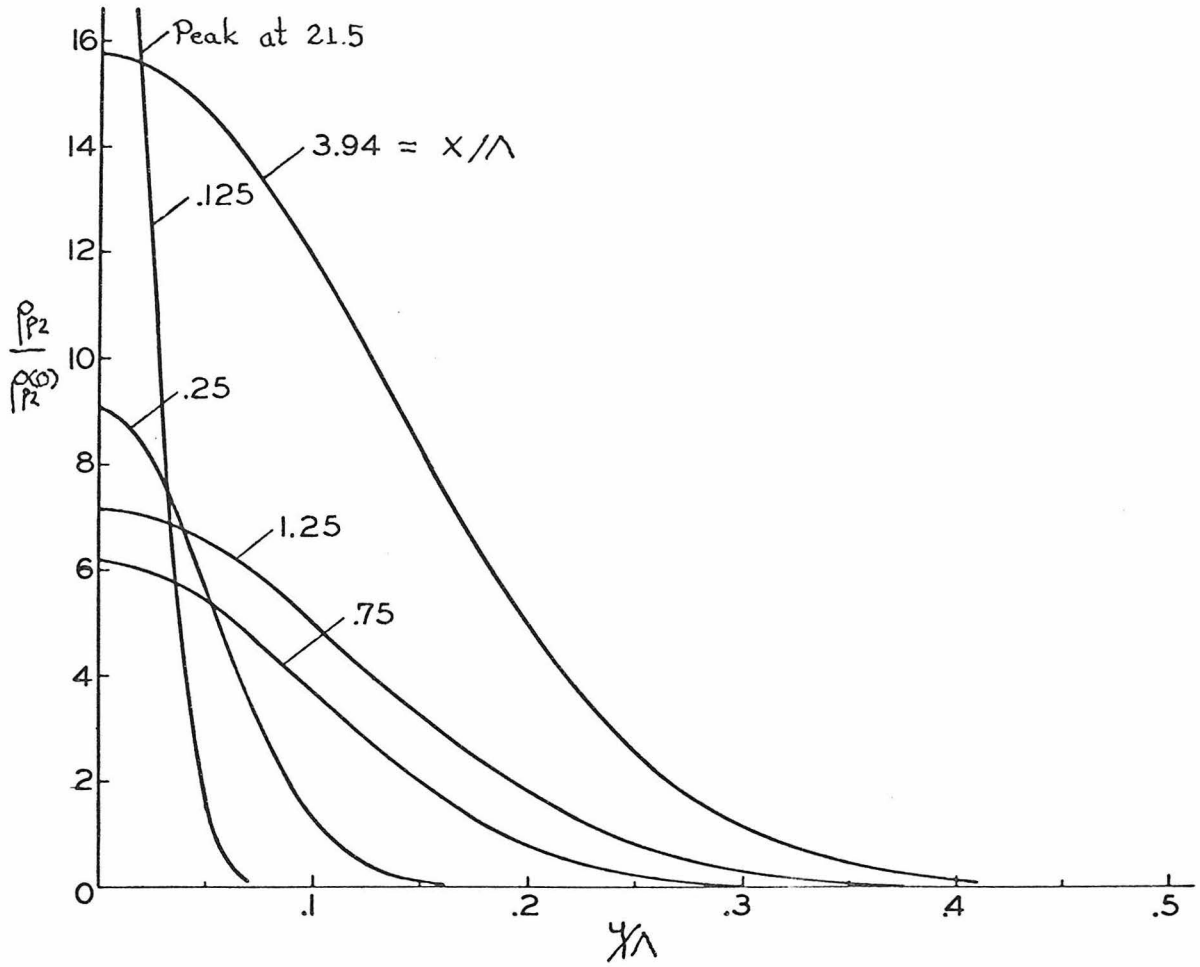

Figure 18. Variation of particle σ_2 fundamental beam density distribution downstream of the shock front. Upstream conditions; Gas-Air, $\rho(1) = 1.3 \times 10^{-3}$ g/cm^3, $T(1) = 20^\circ$C, $M_1 = 3.2$, $\gamma = 1.4$, $K_1 = .25$, $\rho_s/\rho(1) = 10^3$, $\sigma_2/\sigma_1 = 1/4$, $\sigma_1 = 8.0\ \mu$, $\Lambda = \lambda_{v_1} = 31$ cm, $c_s/c_\rho = \lambda_{v_1}/\lambda_{T_1} = 1$.

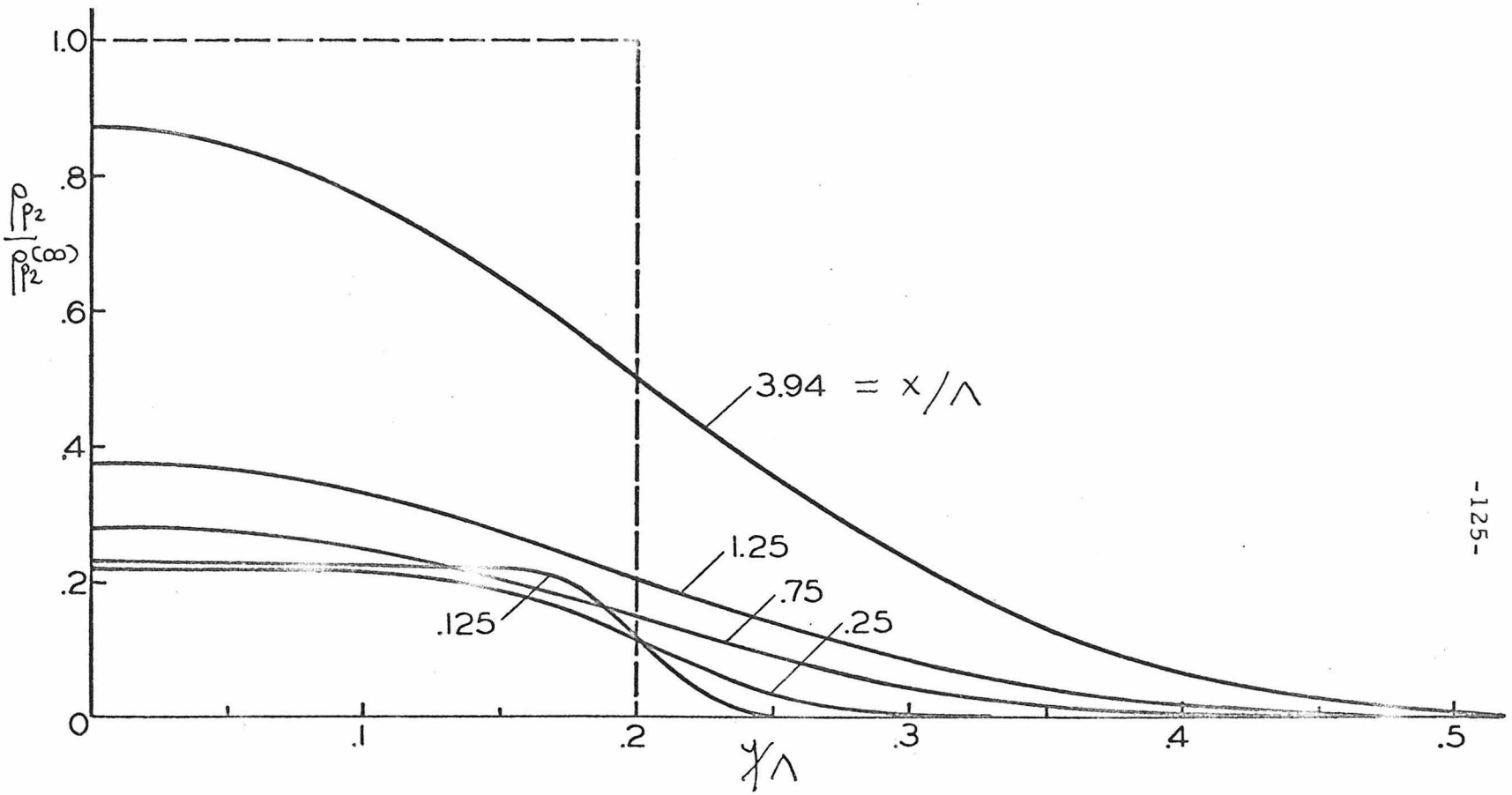

Figure 19. Variation of particle σ_2 uniform beam density distribution downstream of the shock front. Upstream conditions; Gas-Air, $\rho(1) = 1.3 \times 10^{-3}$ g/cm^3, $T(1) = 20°C$, $M_1 = 3.2$, $\gamma = 1.4$, $K_1 = .25$, $\rho_s/\rho(1) = 10^3$, $\sigma_2/\sigma_1 = 1/4$, $\sigma_1 = 8.0\,\mu$, $\Lambda = \lambda_{v_1} = 31$ cm, $c_s/c_p = \lambda_{v_1}/\lambda_{T_1} = 1$.

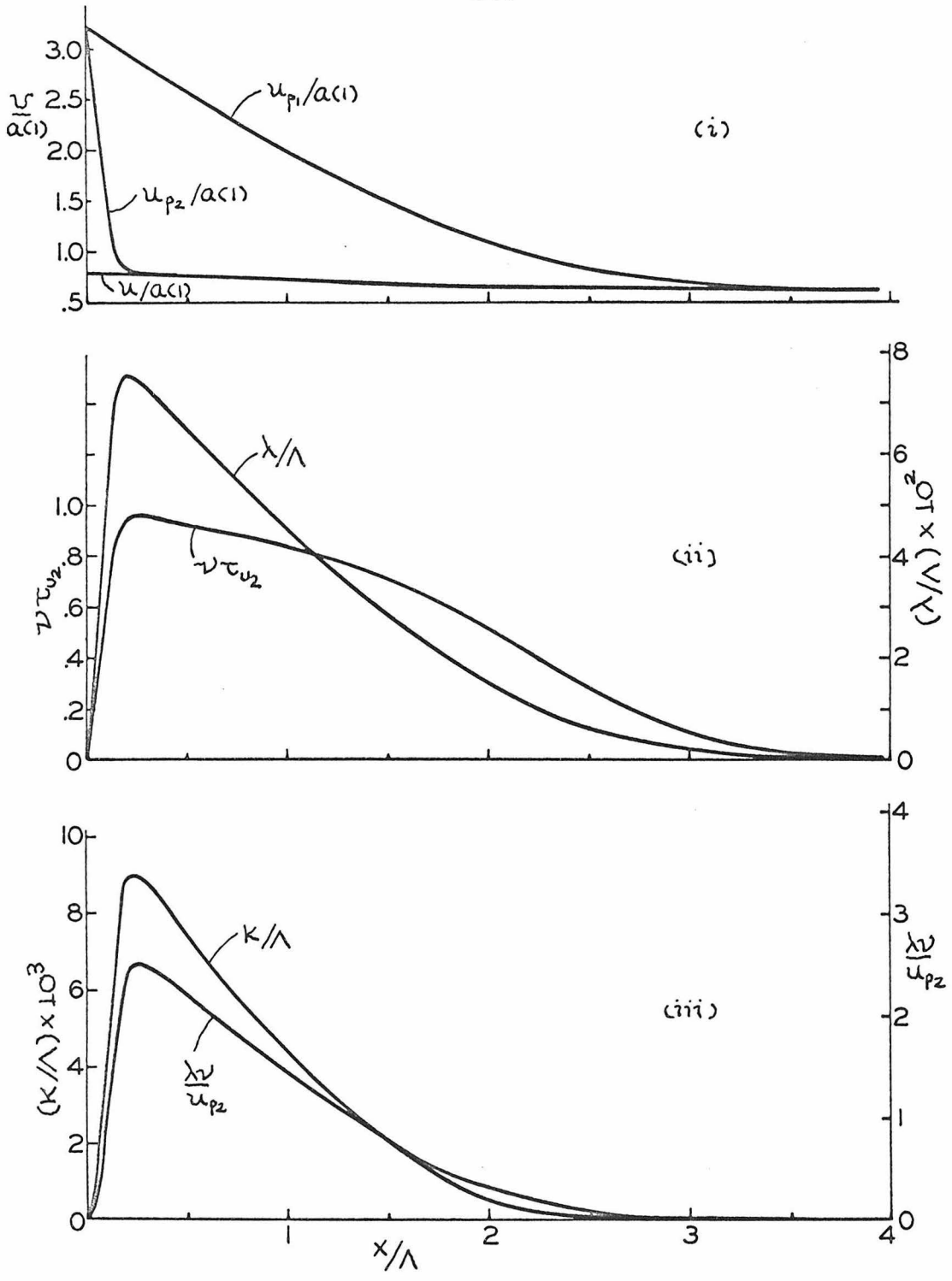

Figure 20. Variation of collisional properties of particles σ_2 downstream of the shock front for density distributions described in Figures 18 and 19.

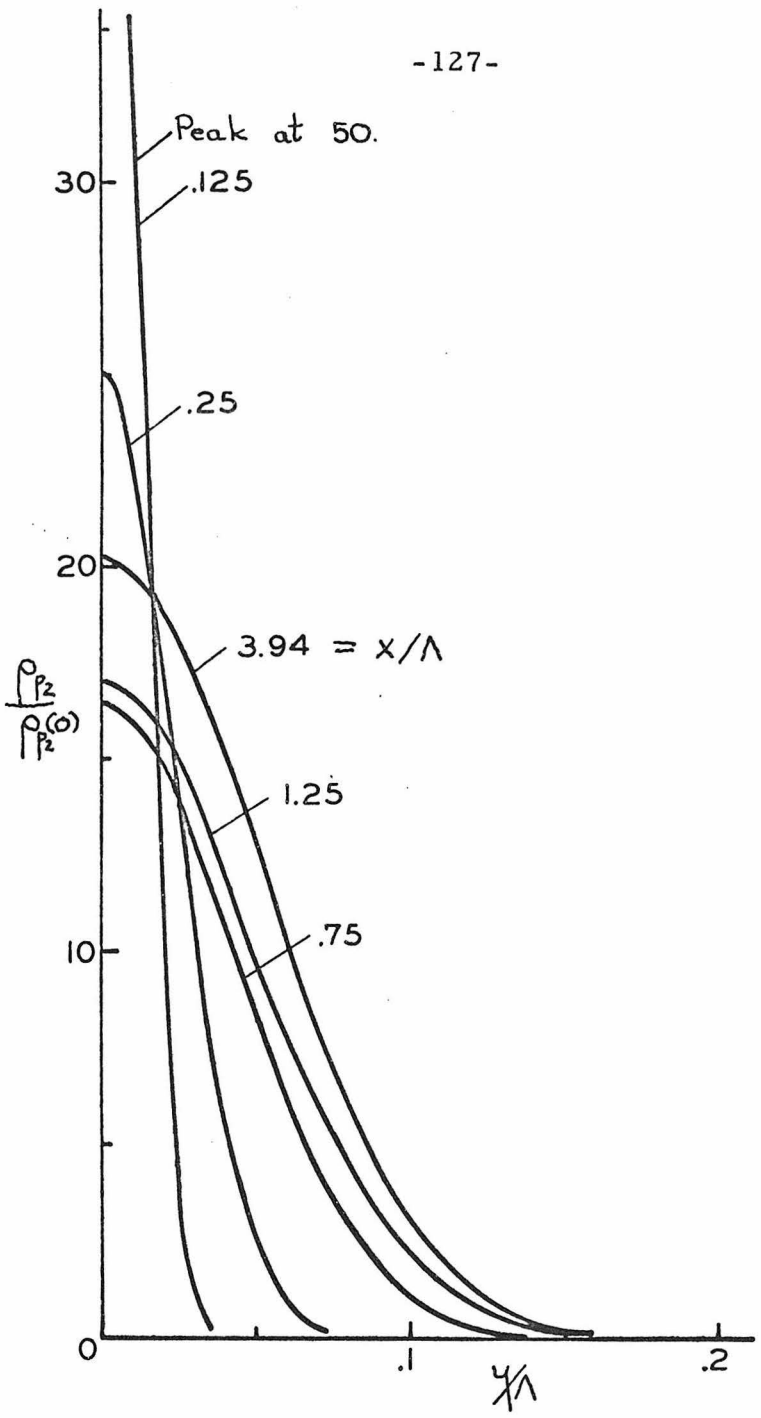

Figure 21. Variation of particle σ_2 fundamental beam density distribution downstream of the shock front. Upstream conditions; Gas-Air, $\rho(1) = 1.3 \times 10^{-3}$ g/cm^3, $T(1) = 20^{\circ}$C, $\gamma = 1.4$, $M_1 = 1.6$, $K_1 = .25$, $\rho_s/\rho(1) = 10^3$, $\sigma_2/\sigma_1 = 1/4$, $\sigma_1 = 8.0\mu$, $\Lambda = \lambda_{v_1} = 31$cm, $c_s/c_p = \lambda_{v_1}/\lambda_{T_1} = 1$.

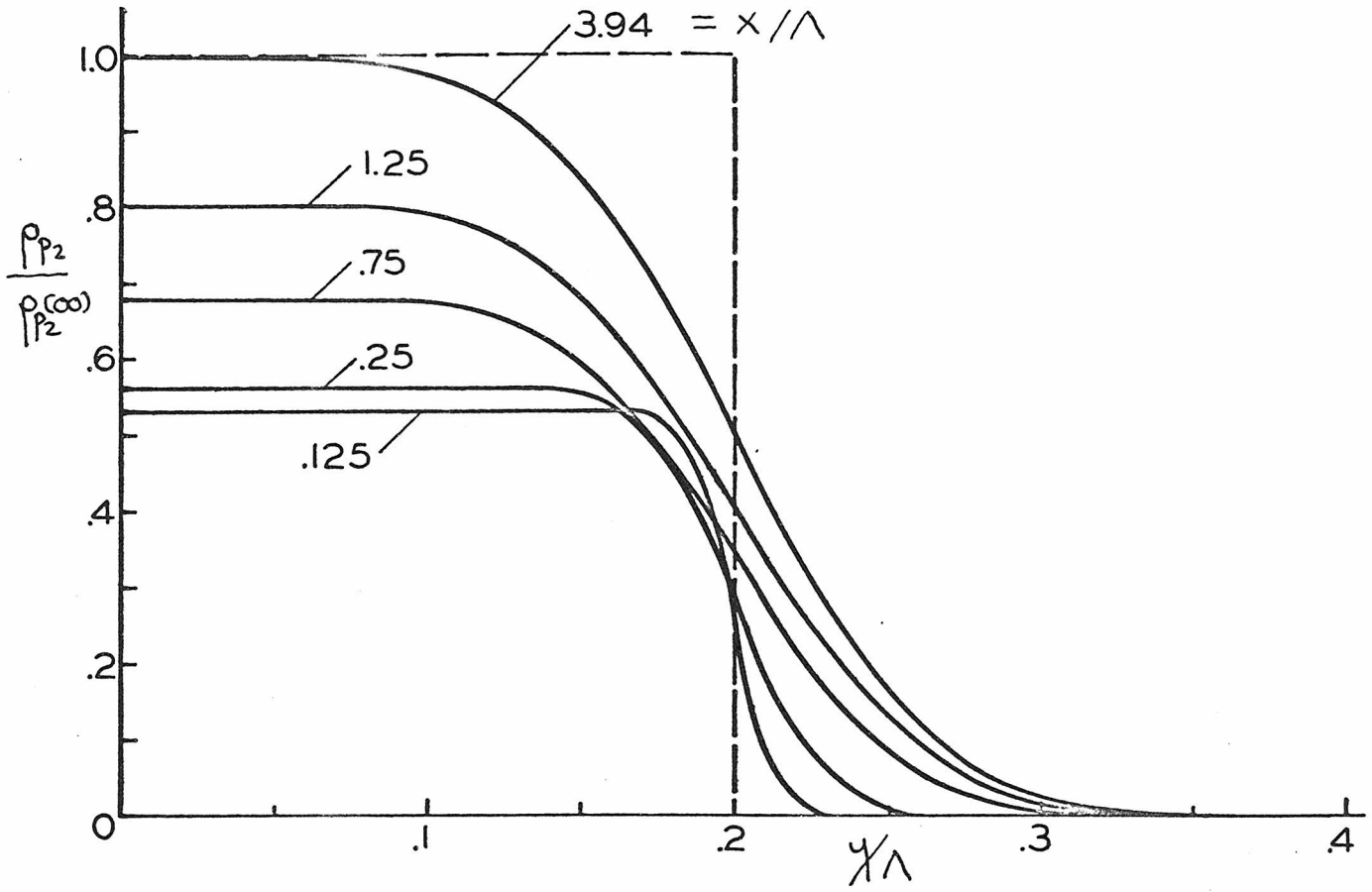

Figure 22. Variation of particle σ_2 uniform beam density distribution downstream of the shock front. Upstream conditions; Gas-Air, $\rho(1) = 1.3 \times 10^{-3}$ g/cm^3, $T(1) = 20^\circ$C, $M_1 = 1.6$, $\gamma = 1.4$, $K_1 = .25$, $\rho_s/\rho(1) = 10^3$, $\sigma_2/\sigma_1 = 1/4$, $\sigma_1 = 8.0\mu$, $\Lambda = \lambda_{u_1} = 31$cm, $c_s/c_p = \lambda_{u_1}/\lambda_{T_1} = 1$.

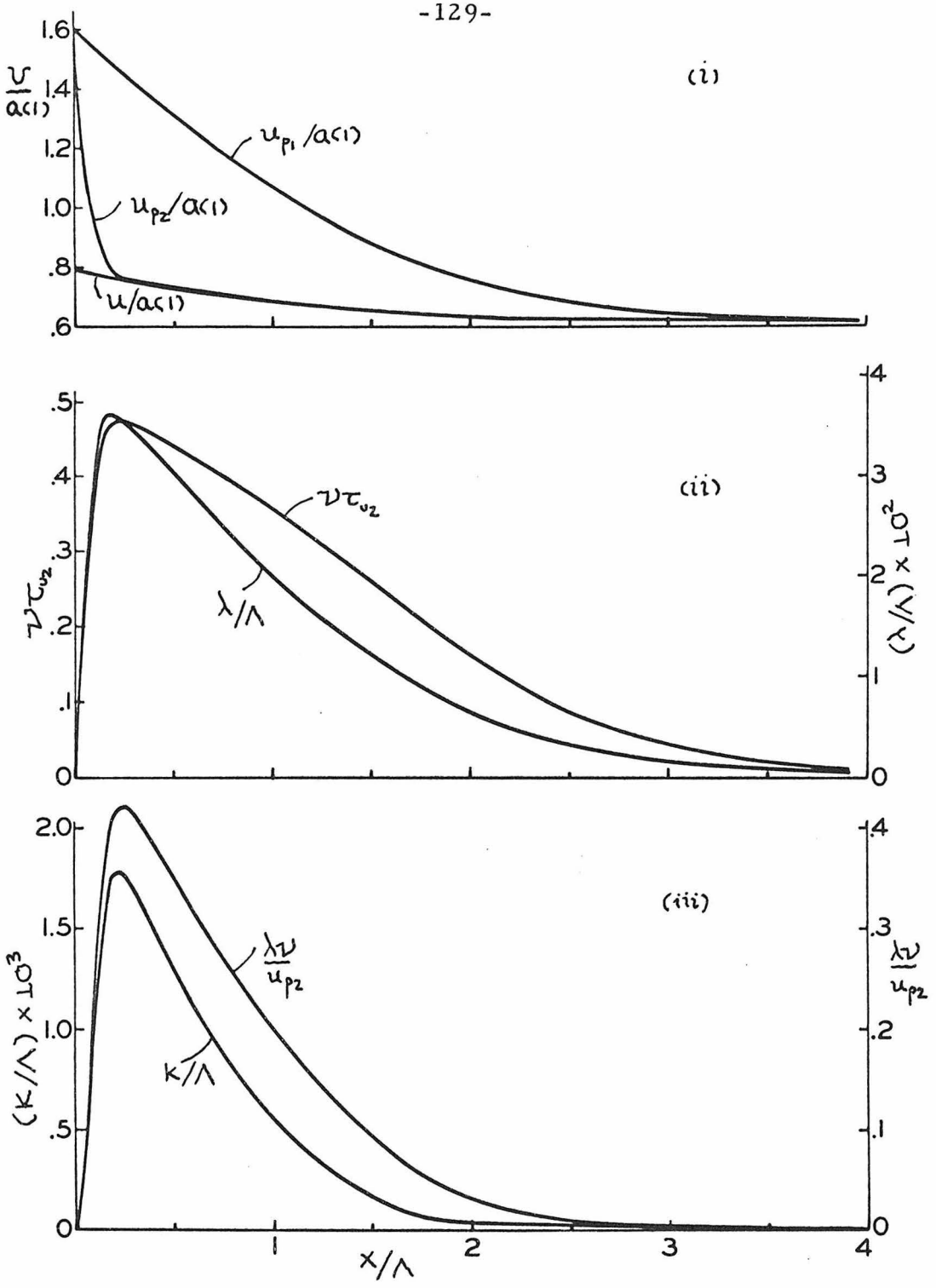

Figure 23. Variation of collisional properties of particles σ_2 downstream of the shock front for density distributions described in Figures 21 and 22.

Upstream of the shock wave the particles σ_2 are distributed in the y = 0 plane. They pass unaffected through the shock wave so that this distribution is retained immediately downstream of the shock wave. Downstream of the shock wave the gas and particles are out of equilibrium, and collisions occur due to the unequal velocity equilibration lengths $\lambda_{v_2} \ll \lambda_{v_1} \simeq \Lambda$. Since, from Figure 20(ii), $\nu(2)\tau_{v_2}(2) < 1$, most of the particles have experienced a collision after moving a distance $x \sim .25\lambda_{v_1}$. Now the maximum transverse range of the particles σ_2 scattered in the region $0 \lesssim x \lesssim .25\lambda_{v_1}$ is, from Figure 20(ii), about $\lambda(2) \sim .075\lambda_{v_1}$. From previous discussions $\lambda(2)$ is the maximum distance a particle σ_2 can move across the gas flow following a collision with a particle σ_1 at position x . Therefore one would expect that at a distance $x \sim .25\lambda_{v_1}$ downstream from the shock wave most of the particles σ_2 would be distributed within a distance $y \sim \lambda(2) \sim .075\lambda_{v_1}$ of the y axis. This assumption is confirmed by the density distribution of particles of radius σ_2 at $x = .25\lambda_{v_1}$ in Figure 18. For $.25\lambda_{v_1} \lesssim x \lesssim 1.25\lambda_{v_1}$ the macroscopic motion of particles σ_2 is primarily diffusive in character. Collisions between particles σ_1 and particles σ_2 determine the form of the density distribution of particles σ_2 in this region. The dispersive effect of collisions for $x \lesssim 1.25\lambda_{v_1}$ may be seen from the following considerations. For $x \gtrsim .25\lambda_{v_1}$ the maximum transverse range of particles σ_2, $\lambda(x)$, due to collisions at x becomes small quite rapidly. Because of the physical significance of λ this greatly reduces the collisional dispersion of particle cloud σ_2 . Consequently in this example the dispersion of particles σ_2 due to

collisions is governed primarly by particle σ_1-particle σ_2 encounters that occur in the neighborhood of $x \sim .25 \lambda_{v_1}$, that is, where $\lambda(x)$ and $\nu(x)$ have maximum values. This point of view is further reinforced by observing the variation of $K(x)$ and $\lambda(x)\nu(x)$ in Figure 20(iii).

On the other hand, for $x \gtrsim 1.25 \lambda_{v_1}$ the form of the distribution of particles σ_2 is governed primarily by the deceleration of the particle cloud as $\lambda\nu \to 0$ and $u_{p2} \to u(\infty)$. There is a piling up of particles σ_2 as a consequence of this deceleration, their density increases, a result that is most apparent near the axis where particles σ_2 are concentrated. Because $\lambda(x)$ is small for $1.25 \lambda_{v_1} \lesssim x$ few particles are scattered beyond $y \sim .3 \lambda_{v_1}$ as they move downstream from $x \sim 1.25 \lambda_{v_1}$. For $x \gtrsim 3.5 \lambda_{v_1}$ the relative velocity, $u_{p1} - u_{p2}$, of particles σ_1 and particles σ_2 is nearly zero and the effect of collisions becomes negligible. The particles reach mechanical equilibrium with the gas and for all practical purposes the density distribution of particles σ_2 freezes. This limiting distribution is given at $x = 3.94 \lambda_{v_1}$. The variation of the density $\tilde{\rho}_{p2}$ may be explained on the basis of our collision model, in a similar manner.

Although the discussion presented here, in order to be specific, has concerned a particular example, the general ideas set forth may be applied with success to the other examples to be presented here. They provide further physical consequences of the collision process and examples of the novel character of the dispersion of particles downstream from the shock wave. To fix the physical magnitudes, it

may be noted that when a shock relaxation zone is over 60 cm in length, the cloud of particles σ_2 spreads out a distance $y \sim .2\lambda_{v_1} = 6.3\text{cm}$ This variation is easily observed experimentally.

Let us now examine the effect of changing several important parameters of the problem. This will also provide physical insight to some of the physical conditions under which the theory may be applied.

(b) Variation of M_1. The effect of the strength of the shock wave on the dispersion of particles σ_2 within the shock relaxation zone may be studied by changing M_1 and holding all the other physical parameters of the problem fixed. This variation of M_1 has been carried out and the results presented in Figures 18-23. The state of the gas-particle mixture upstream of the shock wave is specified in Figures 18, 19 and Figures 21, 22. The shock wave Mach number has been varied from 1.6 to 3.2. By comparing Figures 20 and 23 it appears that the essential effect of increasing M_1 is to increase $(u_{p_1} - u_{p_2})$ and thereby to increase the collision frequency and the momentum transferred from particles σ_1 to particles σ_2. The transverse range of particles σ_2 is increased. The subsequent effect of increasing M_1 then is to significantly increase the dispersion of particles within the shock relaxation zone.

(c) Variation of K_1. When the state of the gas-particle mixture upstream of the shock wave is held fixed, except for the variation of $K_1 = \rho_{p_1}(1)/\rho(1)$, there are two possible effects of importance. The state of the gas-particle σ_1 mixture downstream of the shock wave is altered thus changing $u_{p_1} - u_{p_2}$. In addition, the number

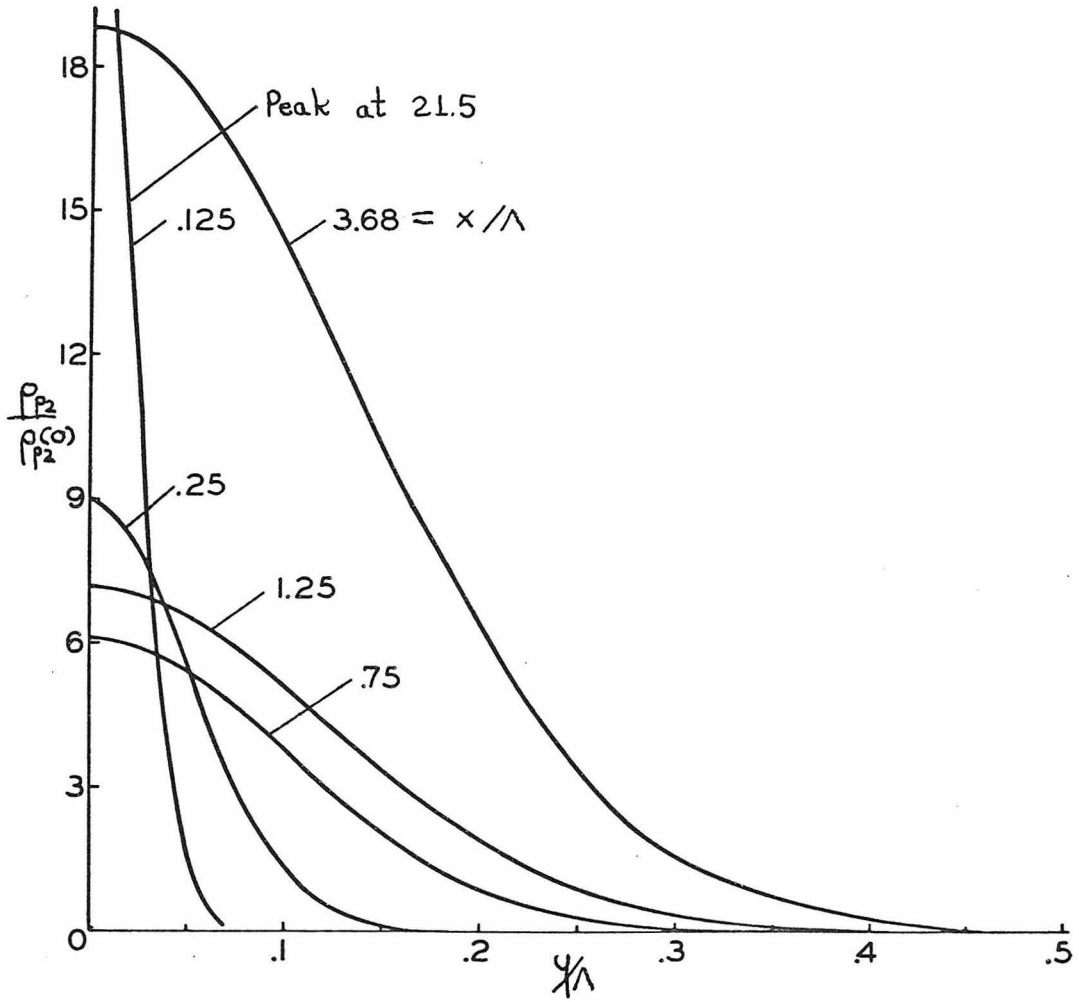

Figure 24. Variation of particle σ_2 fundamental beam density distribution downstream of the shock front. Upstream conditions; Gas-Air, $\rho_{(1)} = 1.3 \times 10^{-3}$ gm/km^3, $T_{(1)} = 20^\circ C$, $M_1 = 3.2$, $\gamma = 1.4$, $K_1 = .50$, $\rho_s/\rho_{(1)} = 10^3$, $\sigma_2/\sigma_1 = 1/4$, $\sigma_1 = 4.0\mu$, $\Lambda_1 = \lambda_{v_1} = 7.9$ cm, $c_s/c_p = \lambda_{v_1}/\lambda_{T_1} = 1$.

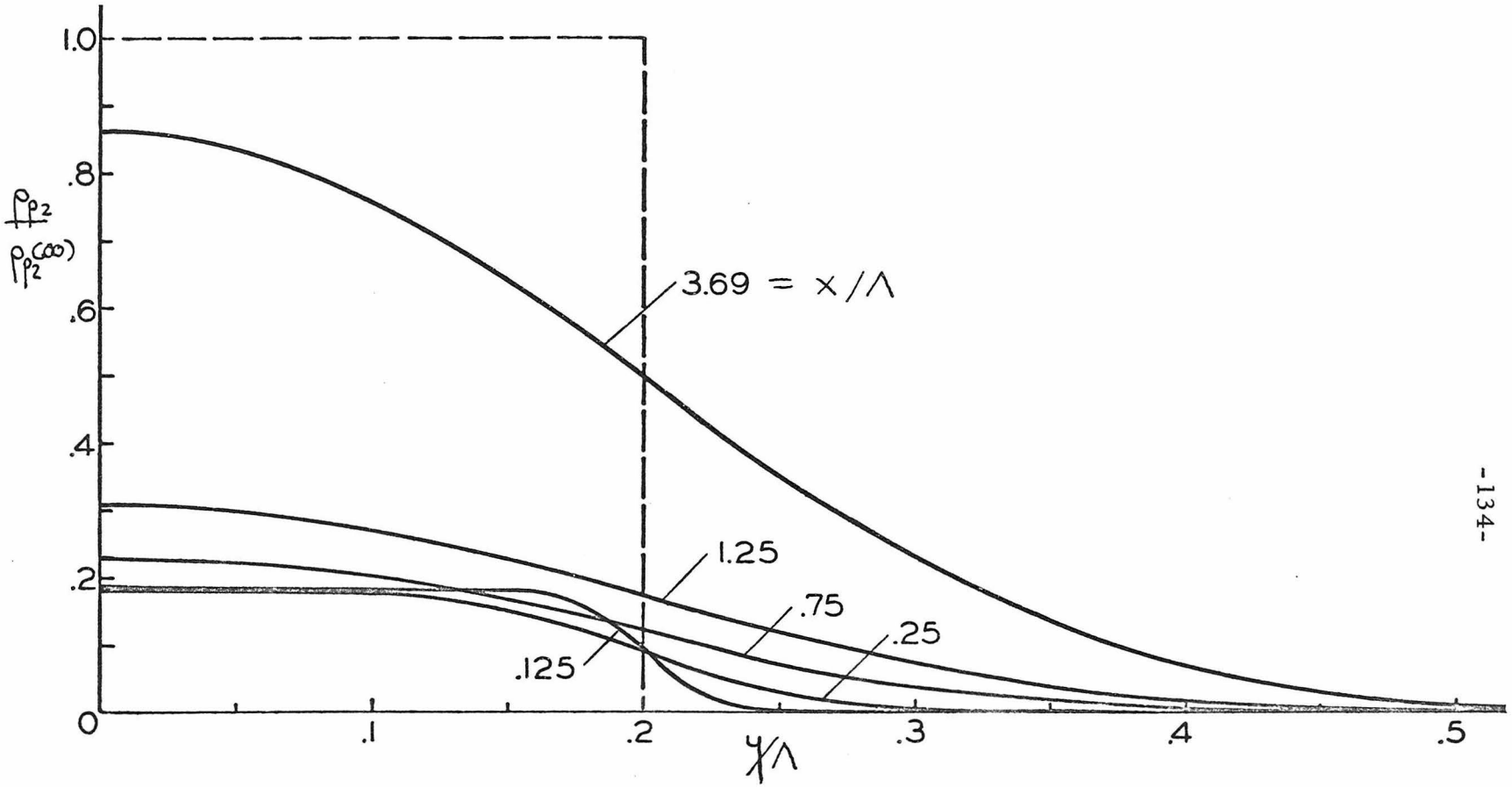

Figure 25. Variation of particle σ_2 uniform beam density distribution downstream of the shock front. Upstream conditions; Gas-Air, $\rho(1) = 1.3 \times 10^{-3}$ gm/cm^3 $T(1) = 20°C$, $M_1 = 3.2$, $\gamma = 1.4$, $K_1 = .50$, $\rho_s/\rho(1) = 10^3$, $\sigma_2/\sigma_1 = 1/4$, $\sigma_1 = 4.0\mu$, $\Lambda = \lambda_{v_1} = 7.9$cm, $c_s/c_p = \lambda_{v_1}/\lambda_{T_1} = 1$.

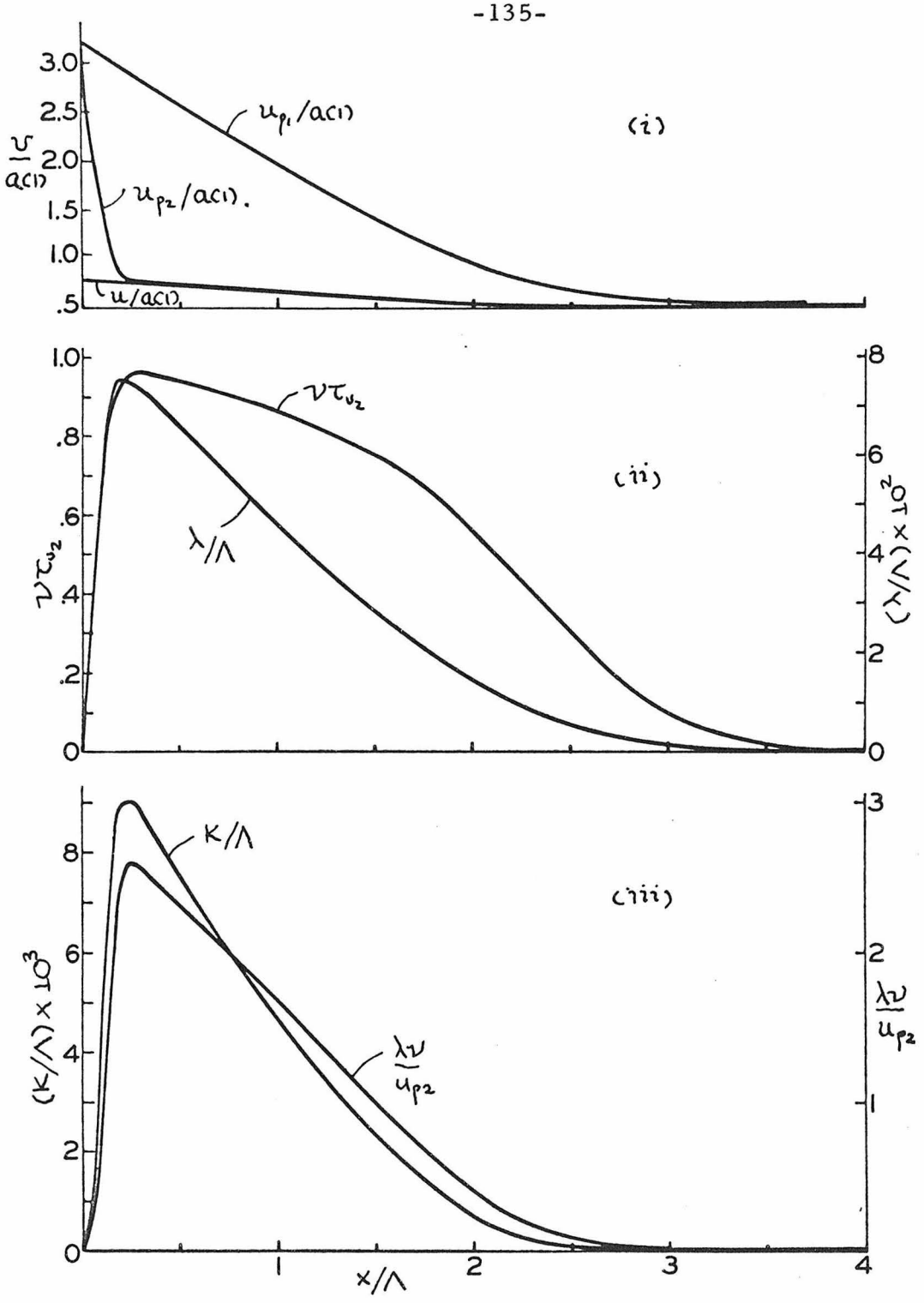

Figure 26. Variation of collisional properties of particles σ_2 downstream of the shock front for the density distributions described in Figures 24 and 25.

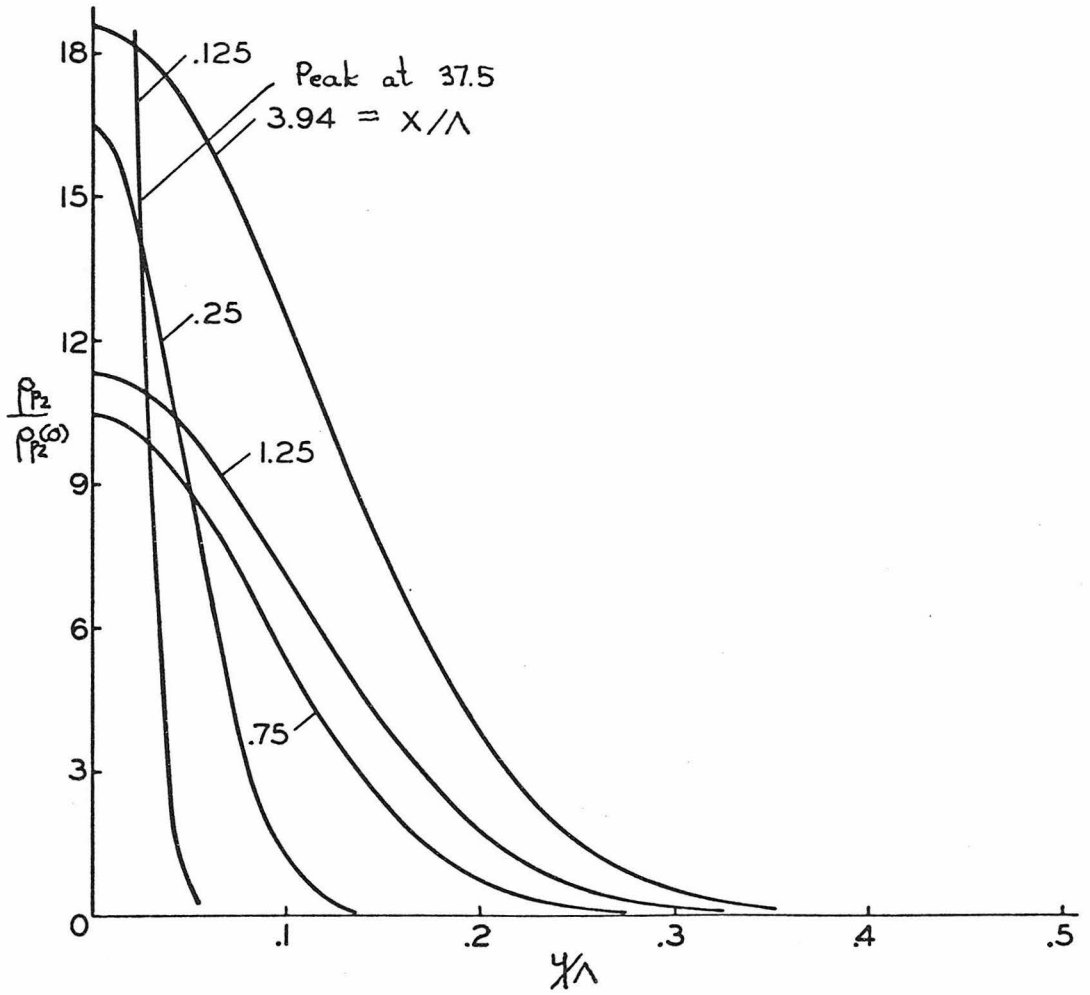

Figure 27. Variation of particle σ_2 fundamental beam density distribution downstream of the shock front. Upstream conditions; Gas-Air, $\rho(1) = 1.3 \times 10^{-3}$ g/cm^3, $T(1) = 20^\circ$C , $M_1 = 3.2$, $\gamma = 1.4$, $K_1 = .25$, $\rho_s/\rho(1) = 10^3$, $\sigma_2/\sigma_1 = 1/4$, $\sigma_1 = 4.0\,\mu$, $\Lambda = \lambda_{v_1} = 7.9$ cm $c_s/c_p = \lambda_{v_1}/\lambda_{T_1} = 1$.

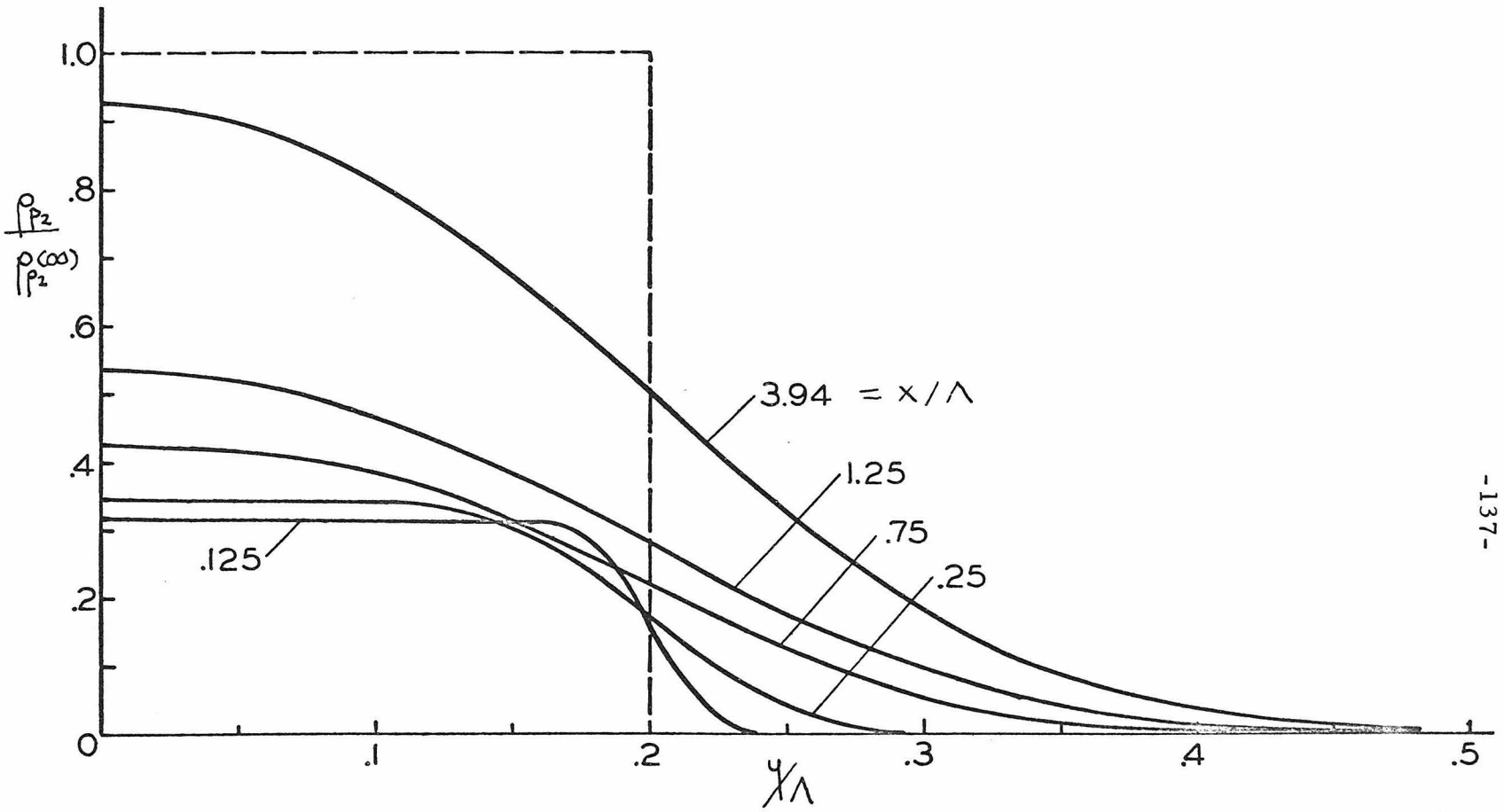

Figure 28. Variation of particle σ_2 fundamental beam density distribution downstream of the shock front. Upstream conditions; Gas-Air, $\rho_{(1)} = 1.3 \times 10^{-3}$ g/cm^3, $T_{(1)} = 20^{\circ}$C, $M_1 = 3.2$, $\gamma = 1.4$, $K_1 = .25$, $\rho_s/\rho_{(1)} = 10^3$, $\sigma_2/\sigma_1 = 1/4$, $\sigma_1 = 4.0\mu$, $\Lambda = \lambda_{v_1} = 7.9$ cm, $c_s/c_p = \lambda_{v_1}/\lambda_{T_1} = 1$.

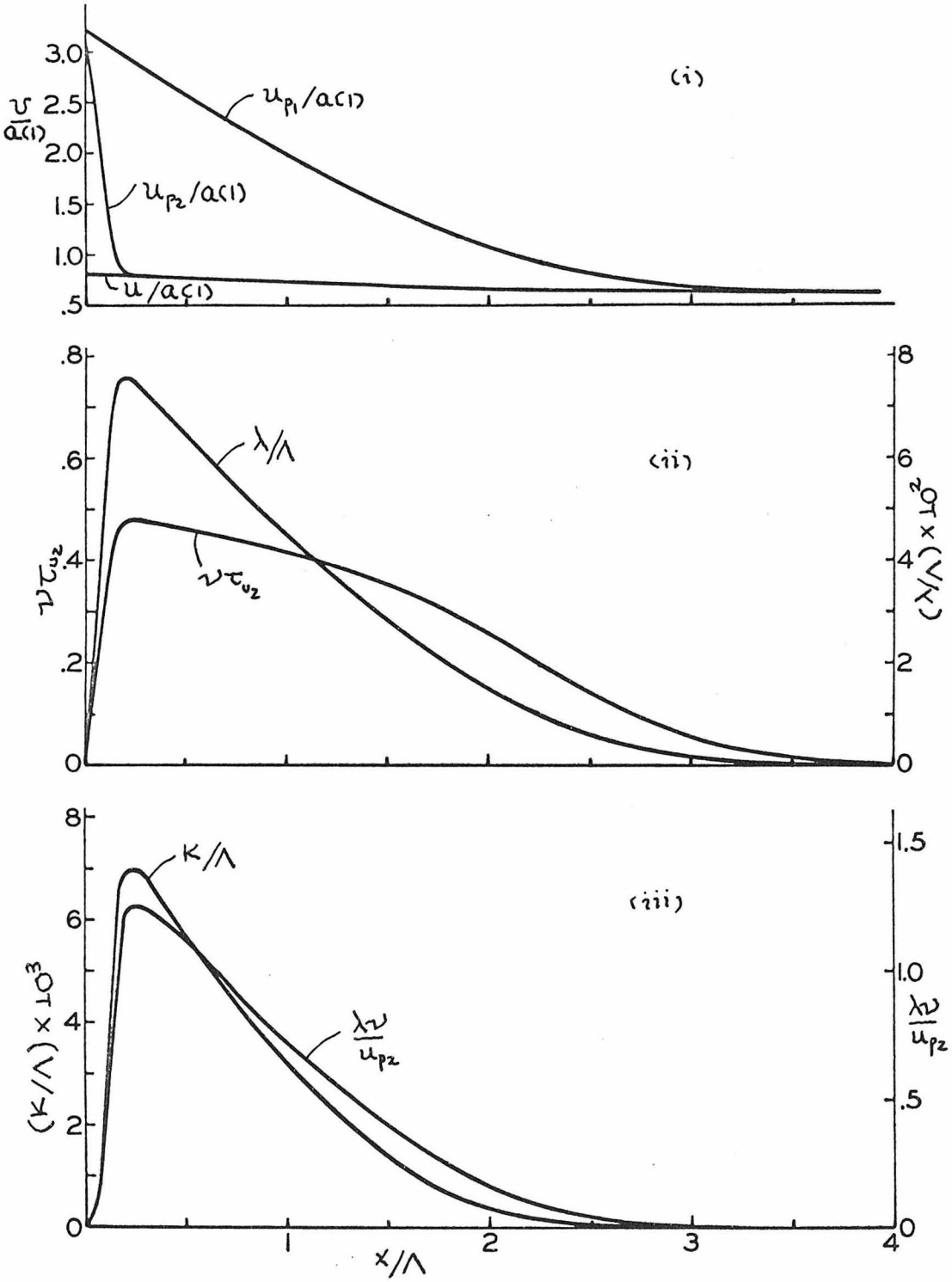

Figure 29. Variation of collisional properties of particles σ_2 downstream of the shock front for the density distributions described in Figures 27 and 28.

density of particles σ_1 is increased. The variation of K_1, holding all other gas-particle properties upstream of the shock fixed, may be studied by comparing Figures 24-26 with Figures 27-29. The parameters describing the gas particle mixture in each case are stated in the Figures and $\Lambda = \lambda_{v_1} = 7.9\,cm$ is the characteristic length of the shock relaxation zone. From Eq. (3.15) we see that $u(\infty)/u(2)$ varies slowly with K_1. Consequently the gas properties downstream of the shock wave are not significantly effected by doubling K_1 as we have done. Therefore $u_{p_1} - u_{p_2}$ is negligibly affected by the variation of K_1. The particle ranges are essentially the same in the two examples.

On the other hand, by increasing K_1 we have increased the density of particles σ_2 proportionally and since the variation of $u_{p_1} - u_{p_2}$ is negligible the collision frequency has also increased proportionally. Therefore increasing K_1 increases the dispersion of particles σ_2. However, because the particle transverse ranges are not significantly altered by the variation of K_1 and the main contribution of collisions comes from $x \sim .25\,\lambda_{v_1}$, the effect is not very important. Because the particle range λ is such a sharply peaked function doubling the frequency of collisions does not effectively alter the spreading of the particle cloud σ_2. Particles σ_2 have at most one collision while traversing the region where λ attains a maximum. The qualitative variation of the distribution of particles σ_2 in Figures 24-25 and 27-28 may be explained on the basis of our model of the collision process by using ideas presented in section (a).

(d) Variation of σ_2. Suppose σ_2 is varied and all other properties of the gas particle mixture upstream of the shock wave are

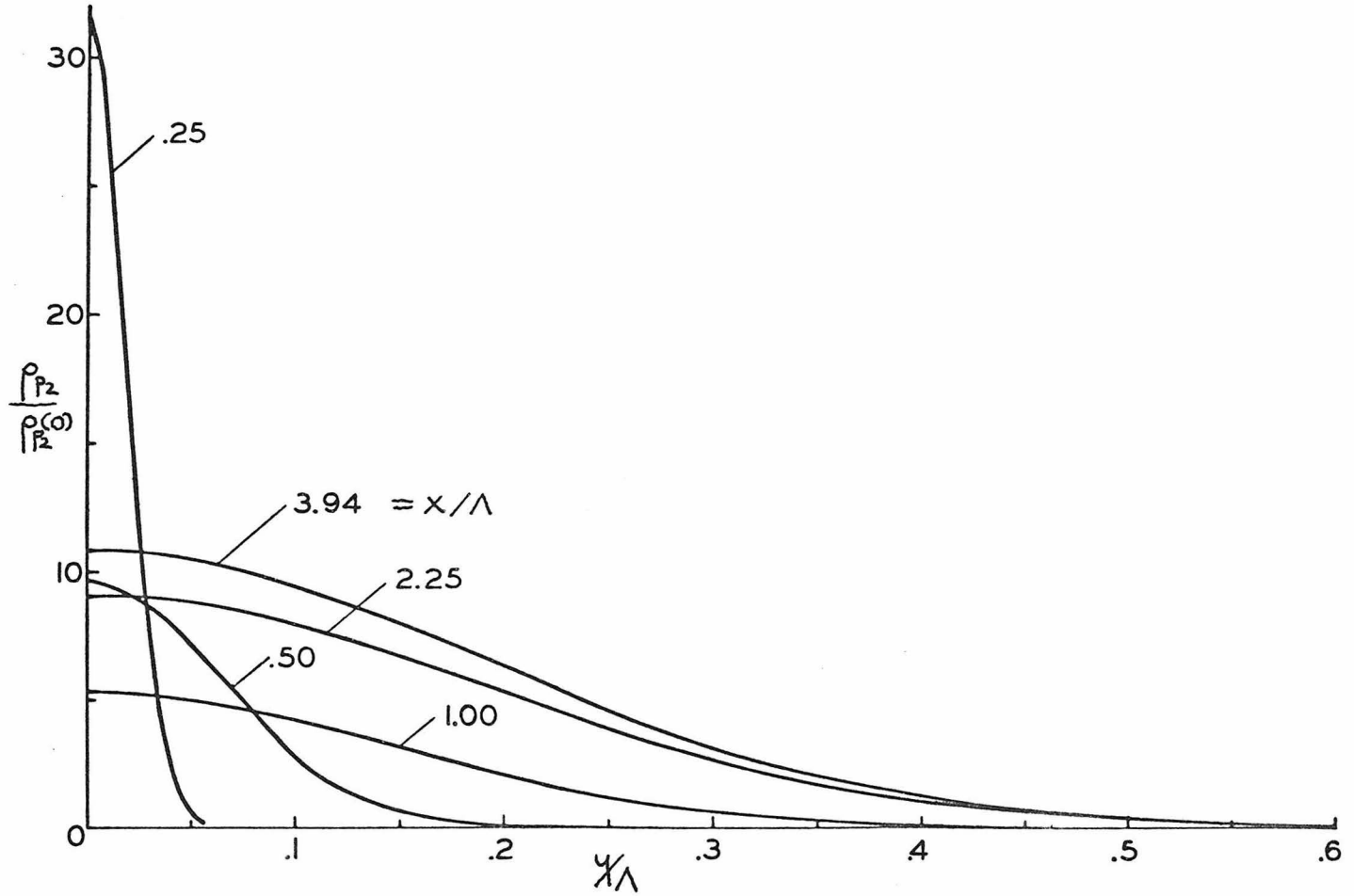

Figure 30. Variation of particle σ_2 fundamental beam density distribution downstream of the shock face. Upstream conditions; Gas-Air, $\rho(1) = 1.3 \times 10^{-4}$ q/cm^3, $T(1) = 20°C$, $M_1 = 3.2$, $\gamma = 1.4$, $K_1 = .25$, $\rho_S/\rho(1) = 10^4$, $\sigma_2/\sigma_1 = 1/2$, $\sigma_1 = 12.8/\mu$, $\Lambda = \lambda_{v_1} = 80$ cm, $c_s/c_p = \lambda_{v_1}/\lambda_{T_1} = 1$.

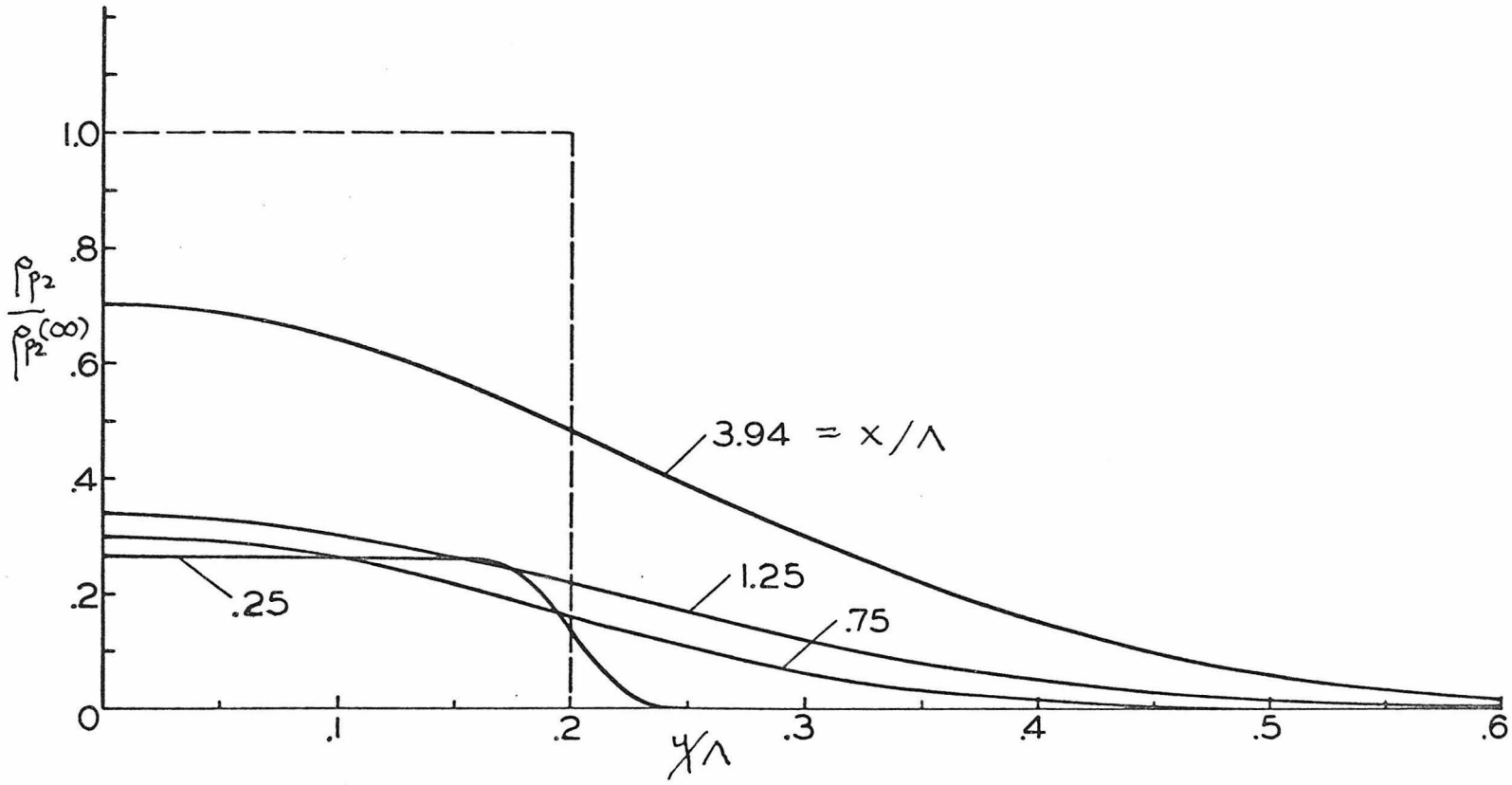

Figure 31. Variation of particle σ_2 uniform beam density distribution downstream of the shock face. Upstream conditions; Gas-Air, $\rho_{(1)} = 1.3 \times 10^{-4}$ g/cm^3, $T_{(1)} = 20^{\circ}$C, $M_1 = 3.2$, $\gamma = 1.4$, $K_1 = .25$, $\rho_s/\rho_{(1)} = 10^4$, $\sigma_2/\sigma_1 = 1/2$, $\sigma_1 = 12.8\,\mu$, $\Lambda = \lambda_{v_1} = 80$ cm, $c_s/c_p = \lambda_{v_1}/\lambda_{T_1} = 1$.

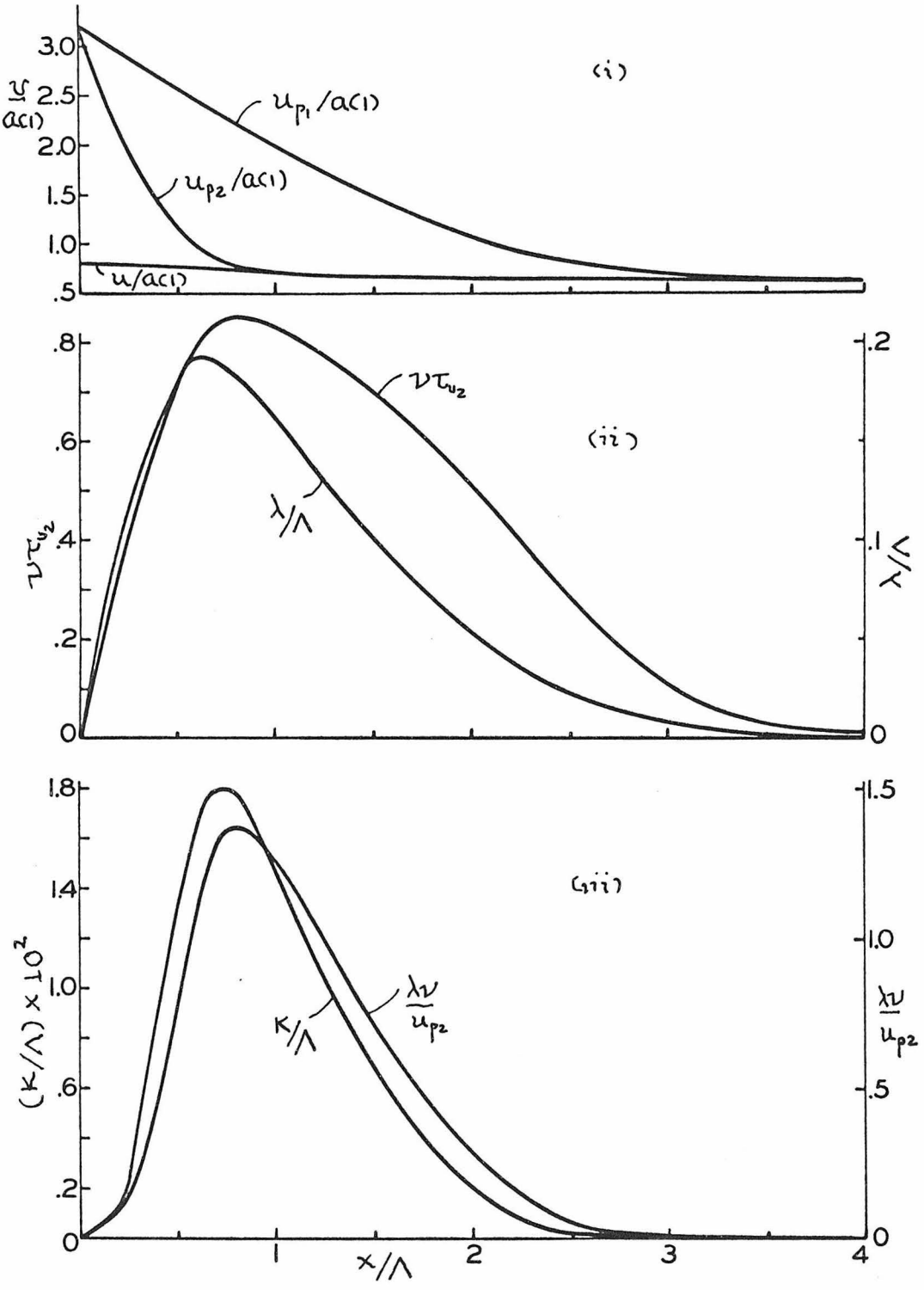

Figure 32. Variation of collisional properties of particles σ_2 downstream of the shock front for the density distributions described in Figures 30 and 31.

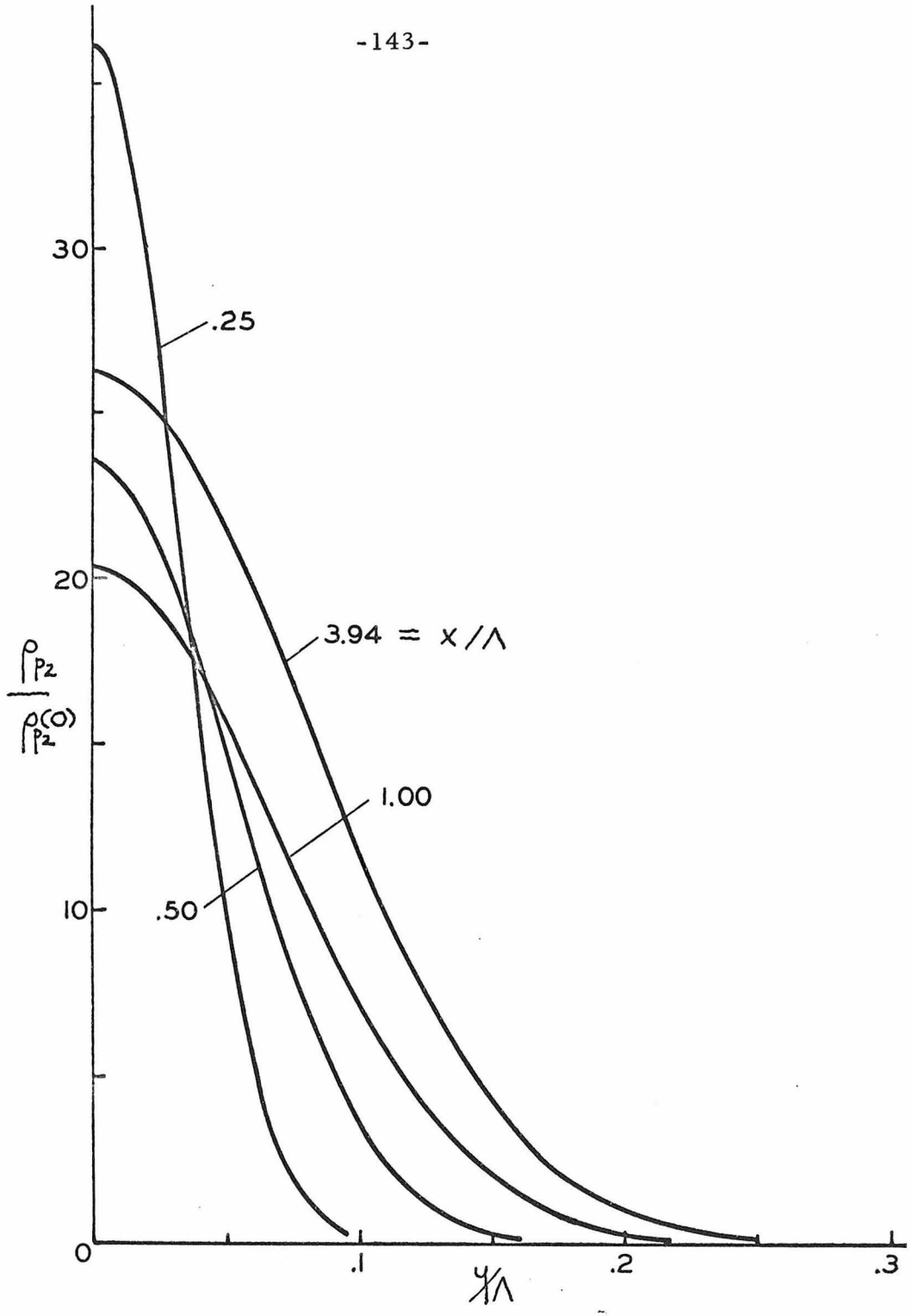

Figure 33. Variation of particle σ_2 fundamental beam density distribution downstream of the shock face. Upstream conditions; Gas-Air, $\rho(1) = 1.3 \times 10^{-4}$ g/cm^3, $T(1) = 20°C$, $M_1 = 3.2$, $\gamma = 1.4$, $K_1 = .25$, $\rho_s/\rho(1) = 10^4$, $\sigma_2/\sigma_1 = 1/4$, $\sigma_1 = 12.8\mu$, $\Lambda = \lambda_{v_1} = 80$cm, $c_s/c_p = \lambda_{v_1}/\lambda_{T_1} = 1$.

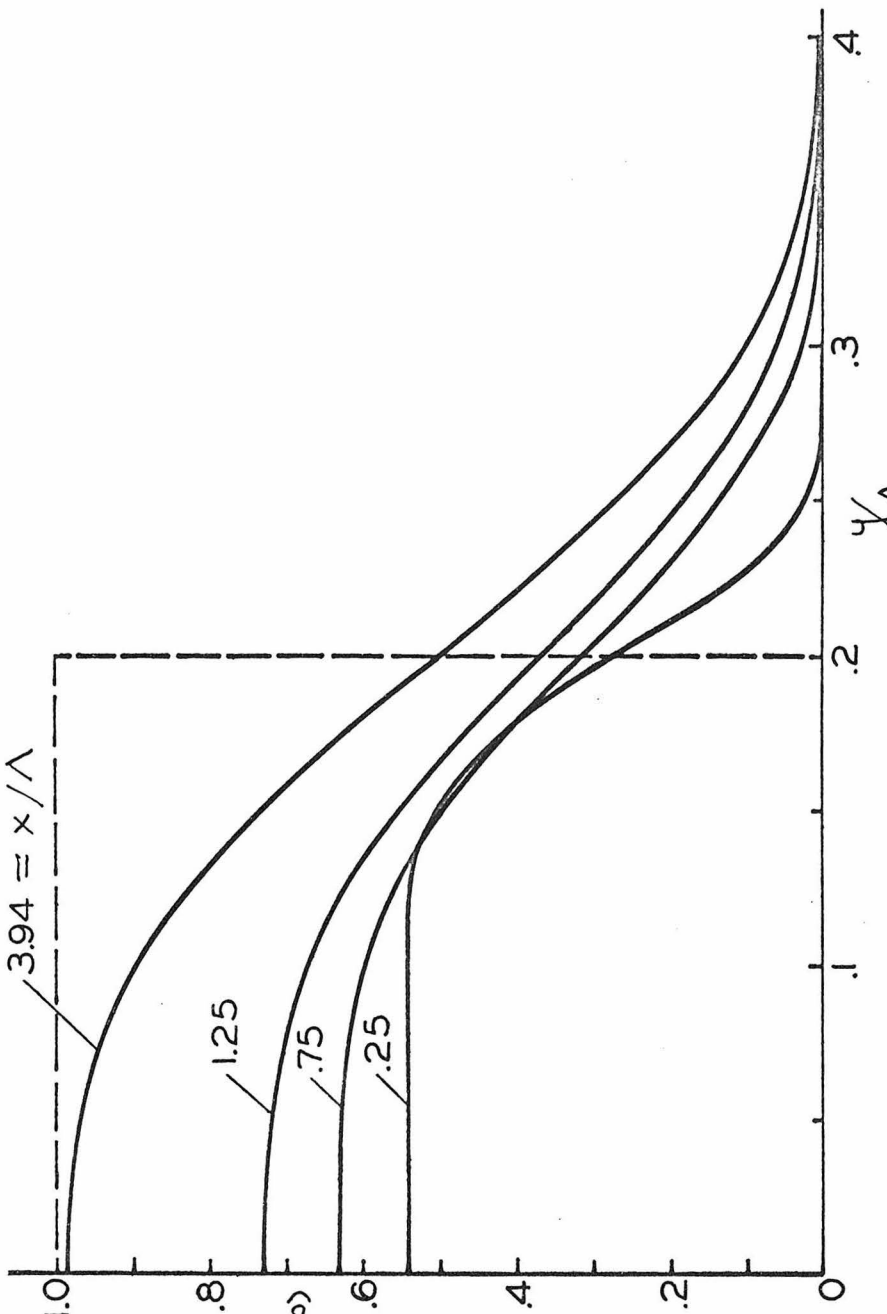

Figure 34. Variation of particle σ_2 uniform beam density distribution downstream of the shock face. Upstream conditions; Gas-Air, $\rho(1) = 1.3 \times 10^{-4}$ gm/cm^3, $T(1) = 20^\circ C$, $M_1 = 3.2$, $\gamma = 1.4$, $K_1 = .25$, $\rho_s/\rho(1) = 10^4$, $\sigma_2/\sigma_1 = 1/4$, $\sigma_1 = 12.8\,\mu$, $\Lambda = \lambda_{v1} = 80$ cm, $c_s/c_p = \lambda_{v1}/\lambda_{T1} = 1$.

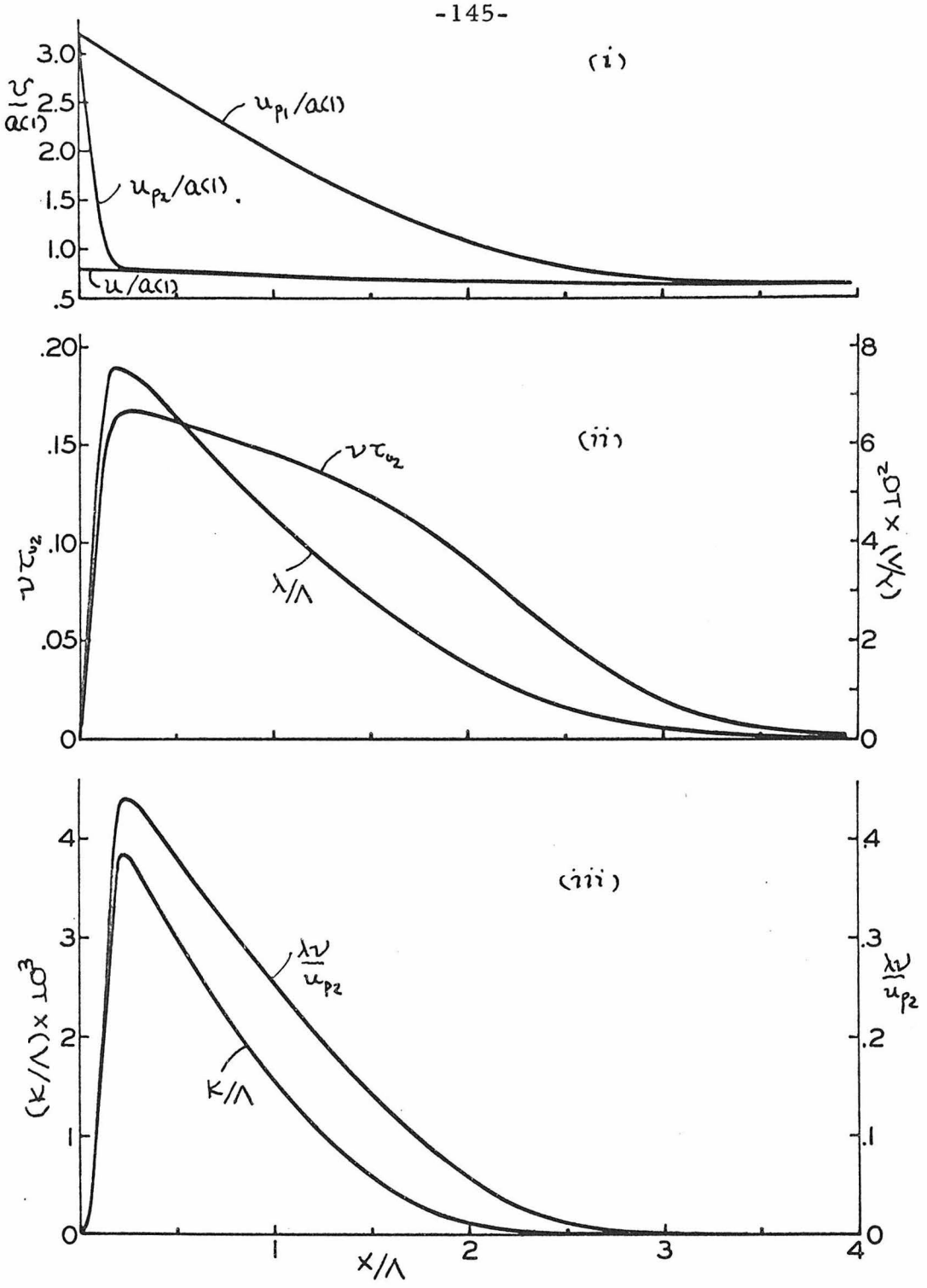

Figure 35. Variation of collisional properties of particles σ_2 downstream of the shock front for the density distributions described in Figures 33 and 34.

unaltered. This dependence may be examined by considering Figures 30-35. Since $\lambda \propto \sigma_2^2$ one expects a substantial effect. In addition to the obvious changes, one should note, from Figure 32(ii) and Figure 35(ii), that increasing σ_2 broadens the variation of λ. This increases the region over which collisions between particles σ_1 and particles σ_2 may substantially affect the dispersion of particle cloud σ_2. When σ_2 is increased, particles σ_2 have fewer collisions in the ratio $\left(\sigma_2^{(i)}/\sigma_2^{(f)}\right)^2$ within the shock relaxation zone. Because of the broadening in $\lambda(x)$, however, the dispersion of particles σ_2 is increased significantly. The details of the variation of $\tilde{\rho}_{p2}^{(f)}$ and $\tilde{\rho}_{p2}$, depicted in Figures 30, 31, 33, and 34, may be studied by extending ideas presented in section (a). It is especially important to note the large magnitude of the dispersion of particles σ_2 under the conditions presented in Figures 30 and 31.

One very interesting observation may be made from the fact that, as the relative size of the particles σ_2/σ_1 was increased, the degree of dispersion of the cloud of particles σ_2 was significantly increased. Thus, if there were a distribution of particle σ_2 sizes present with $\sigma_1 > \sigma_2$, there would be a particle size separation as a consequence of collisions. Relative to the characteristic length of the shock relaxation zone the larger particles would be dispersed the most as a consequence of their larger transverse range. Indeed, the magnitudes of the effects studied here suggest they might be accessible to study by an appropriate experiment. By measuring the dispersion of particle clouds using shock waves, under known conditions, one should be able to measure D and $V(2)$ and thereby study

the particle-particle and particle-gas interaction laws. As indicated, during the calculation of the particle σ_2 fluxes, the kinetic theory method used here may be extended to include more complicated particle-particle and particle-gas interaction laws provided the particles collide while moving at their local collisionless velocities.

(e) Significance of $\lambda\nu$. To complete this discussion of our results we will demonstrate the physical significance of the diffusion velocity $\lambda\nu$. As mentioned earlier, because particles σ_2 are always scattered forward by collisions with particles σ_1, the average convective velocity of the cloud of particles σ_2 is greater than the local collisionless velocity of particles σ_2. The average residence time of a particles σ_2 in the shock relaxation is reduced by collisions. Thus the anisotropy of the particle σ_2-particle σ_1 interaction process tends to reduce the dispersion of particles σ_2. In Figures 36 and 37 the diffusion velocity $\lambda\nu$ has been neglected in the calculations. In Figures 38 and 39 the effect of $\lambda\nu$ has been appropriately accounted for. Clearly the effect of $\lambda\nu$ is to reduce the degree of dispersion of particles σ_2 in the shock relaxation zone.

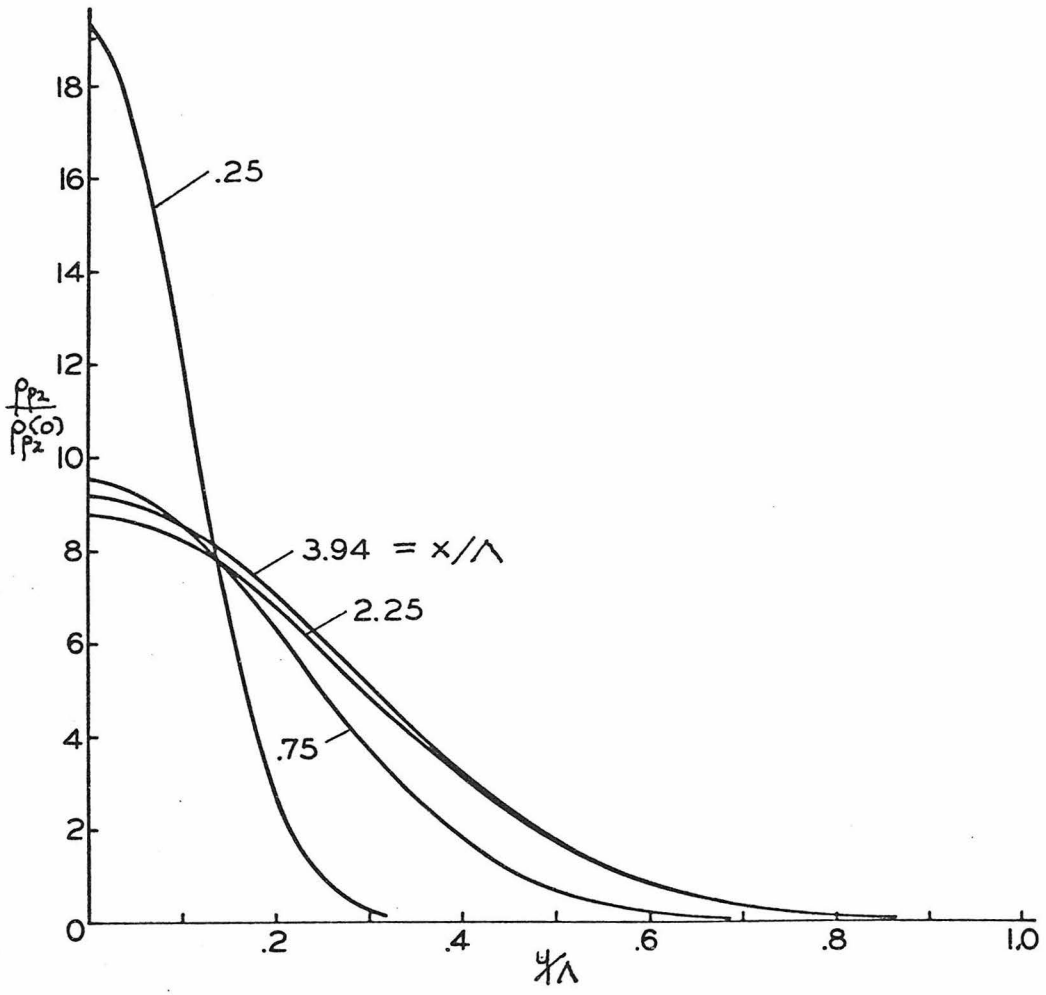

Figure 36. Variation of particle σ_2 fundamental beam density distribution downstream of the shock face, $\lambda v = 0$. Upstream conditions; Gas-Air, $\rho(1) = 1.3 \times 10^{-3}$ gm/cm^3, $T(1) = 20^\circ$C , $M_1 = 4.8$, $\gamma = 1.4$, $K_1 = .25$, $\rho_s/\rho(1) = 10^3$, $\sigma_2/\sigma_1 = 1/4$, $\sigma_1 = 6.2\,\mu$, $\Lambda = \lambda_{v_1} = 19$ cm, $c_s/c_p = \lambda_{v_1}/\lambda_{T_1} = 1$.

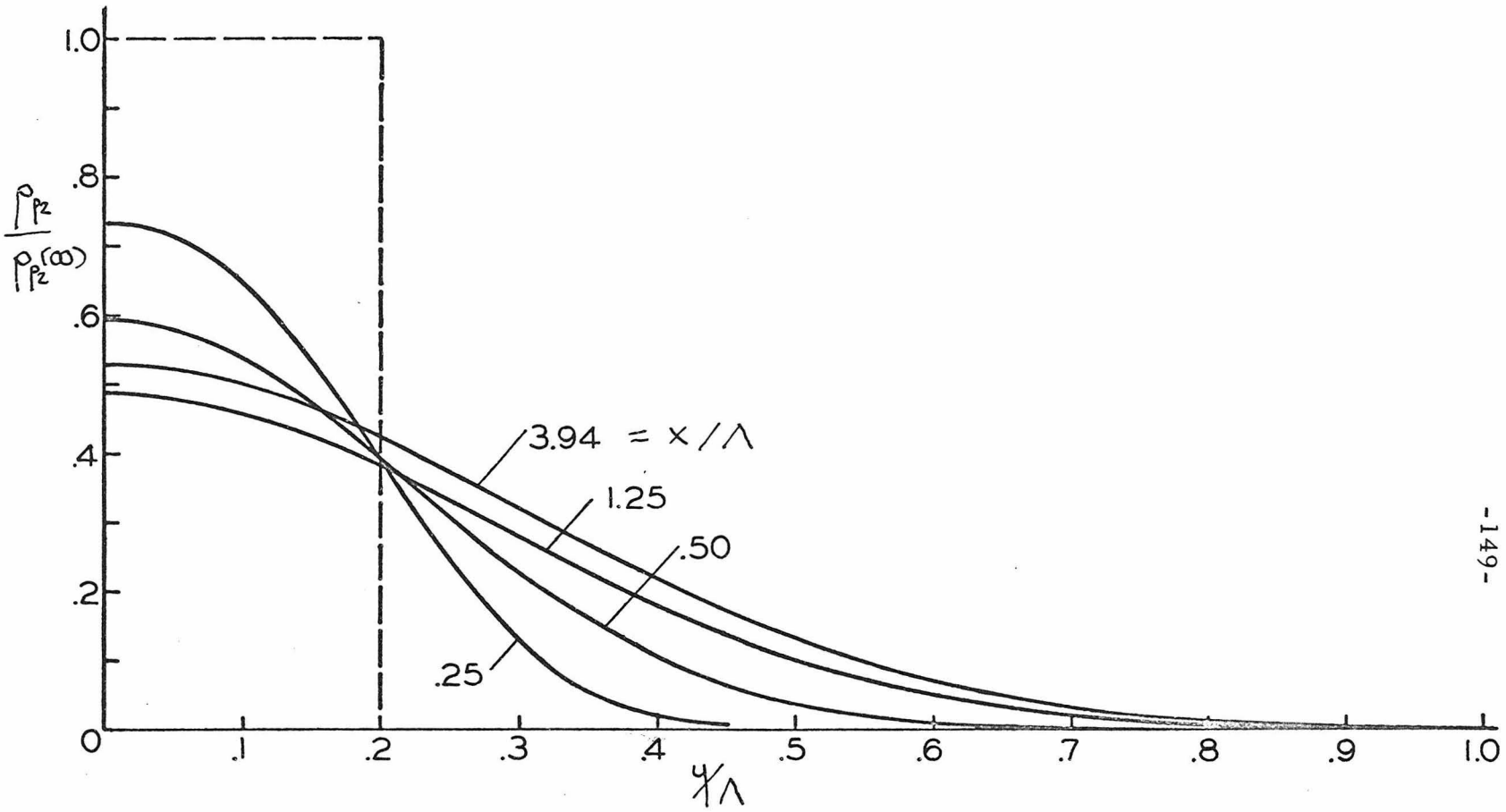

Figure 37. Variation of particle σ_2 uniform beam density distribution downstream of the shock face, $\lambda v = 0$. Upstream conditions; Gas-Air, $\rho(1) = 1.3 \times 10^{-3}$ gm/cm^3, $T(1) = 20^\circ$C, $M_1 = 4.8$, $\gamma = 1.4$, $K_1 = .25$, $\rho_s/\rho(1) = 10^3$, $\sigma_2/\sigma_1 = 1/4$, $\sigma_1 = 6.2\,\mu$, $\Lambda = \lambda_{v_1} = 19$ cm, $c_s/c_p = \lambda_{v_1}/\lambda_{T_1} = 1$.

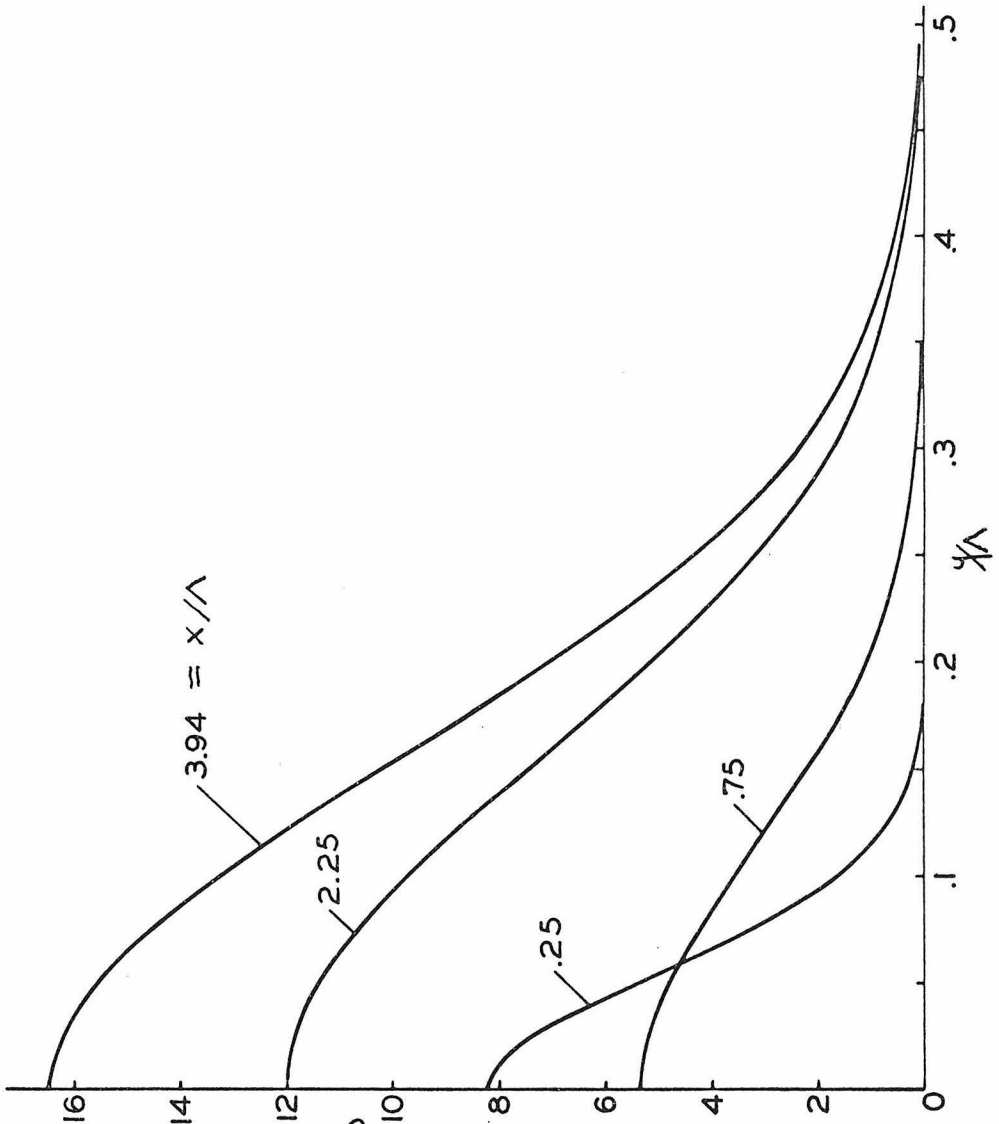

Figure 38. Variation of particle σ_2 fundamental beam density distribution downstream of the shock face. Upstream conditions; Gas-Air, $\rho(1) = 1.3 \times 10^{-3}$ g/cm^3, $T(1) = 20°C$, $M_1 = 4.8$, $\gamma = 1.4$, $\kappa_1 = .25$, $\rho_s/\rho(1) = 10^3$, $\sigma_2/\sigma_1 = 1/4$, $\sigma_1 = 6.2\mu$, $\Lambda = \lambda_{v1} = 19$cm, $c_s/c_p = \lambda_{v1}/\lambda_{T1} = 1$.

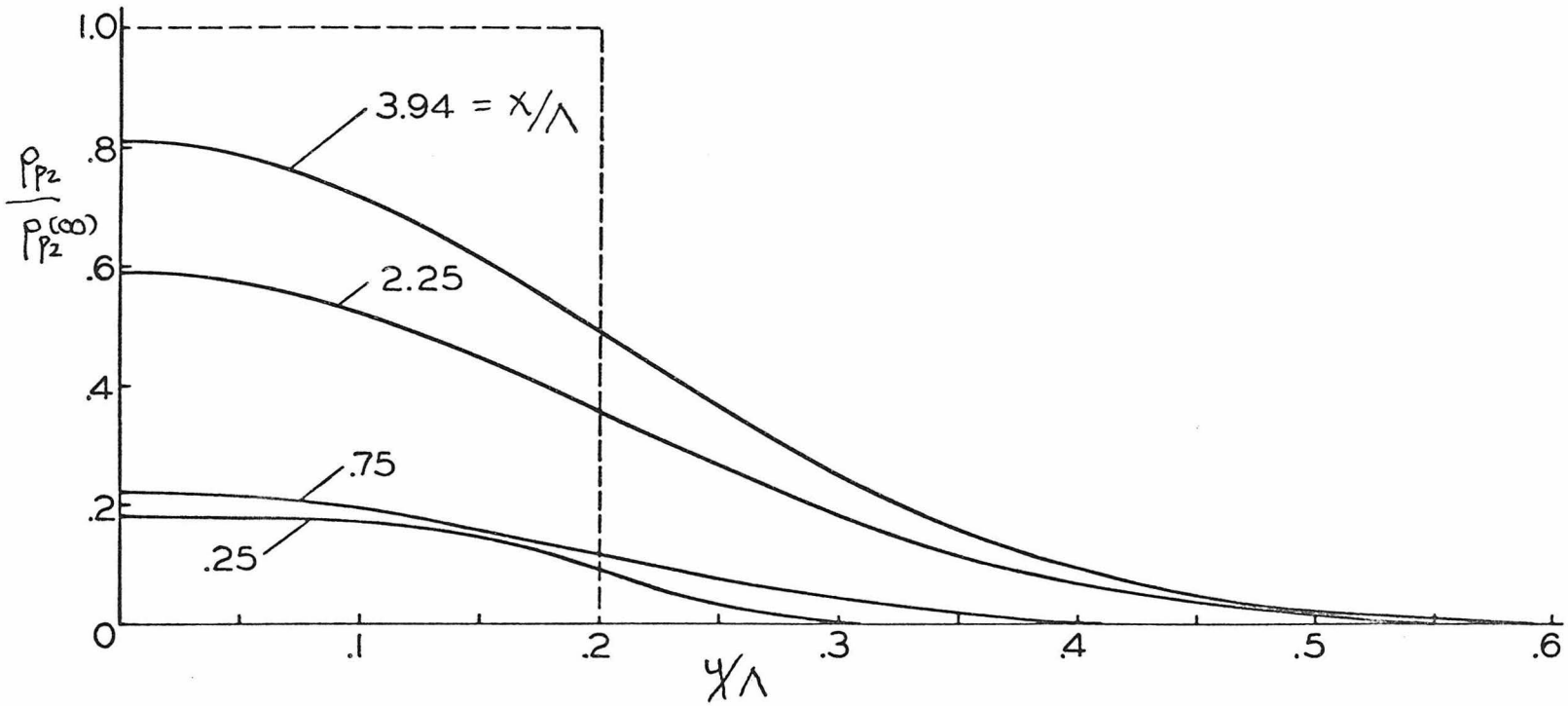

Figure 39. Variation of particle σ_2 uniform beam density distribution downstream of the shock face. Upstream conditions; Gas-Air, $\rho_{(1)} = 1.3 \times 10^{-3}$ gm/cm^3, $T_{(1)} = 20^\circ$C, $M_1 = 4.8$, $\gamma = 1.4$, $K_1 = .25$, $\rho_s/\rho_{(1)} = 10^3$, $\sigma_2/\sigma_1 = 1/4$, $\sigma_1 = 6.2\ \mu$, $\Lambda = \lambda_{v_1} = 19$ cm, $c_s/c_p = \lambda_{v_1}/\lambda_{T_1} = 1$.

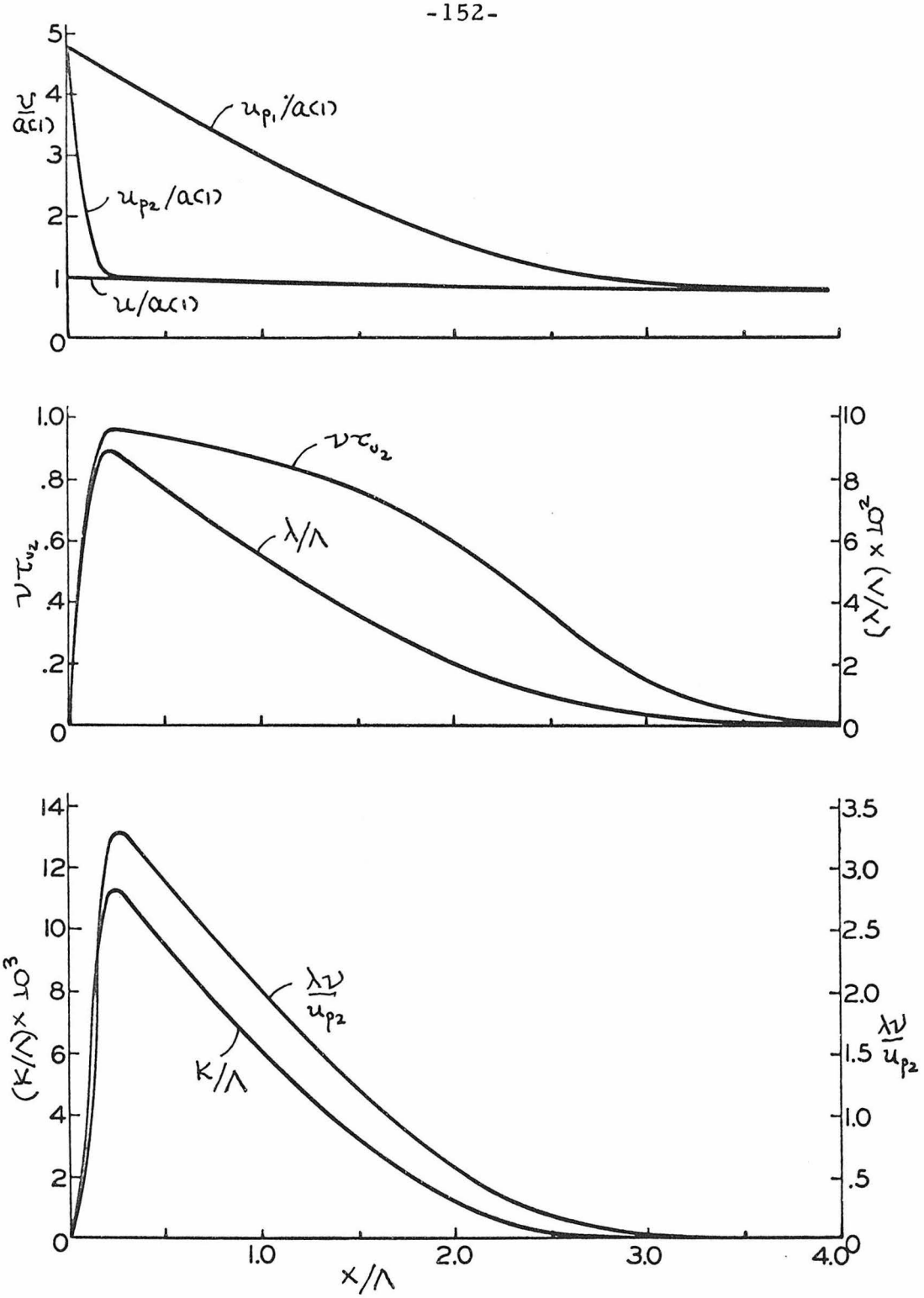

Figure 40. Variation of collisional properties of particles σ_2 downstream of the shock front for the density distributions described in Figures 36, 37, 38, and 39.

V. PARTICLE-PARTICLE SCATTERING IN A SHOCKWAVE; $\sigma_2/\sigma_1 \sim 1$

When $\sigma_2/\sigma_1 \sim 1$ then $\lambda_{v_2}/\lambda_{v_1} = \tau_{v_2}/\tau_{v_1} \sim 1$ and the relative motion of particles σ_1 and σ_2 will be small as can be seen from Figure 41. Provided the particle radii σ_1 and σ_2 and their velocities are sufficiently different that the elastic collision hypothesis, $\tau_{v_2} >> \tau_{o_{21}}$, is satisfied, we may suppose the following conditions are satisfied;

$$\begin{aligned} &\tau_o << \tau_c << \tau_{o_{21}} << \tau_{v_2} \sim \tau_{v_1} < \tau_{c_{21}} \\ &\lambda_o << \lambda_c << \lambda_{o_{21}} << \lambda_{v_2} \sim \lambda_{v_1} < \lambda_{c_{21}} \end{aligned} \tag{5.1}$$

The relative motion and the density of the particles is such that they have at most one collision during their passage through the shock relaxation zone. Therefore the particles σ_1 and σ_2 always collide while moving at their local collisionless velocities u_{p_1} and u_{p_2}, respectively, and only binary encounters are important. As in previous calculations in order to elucidate the essential physical features of the collision process, we will assume $\rho_{p_1}, \rho >> \rho_{p_2}$. Consequently the motion of particles σ_2 has no effect on the gas-particle σ_1 interaction. Upstream and immediately downstream of the shock wave the state of this gas particle mixture is given by conditions (4.2) and (4.3), respectively. The shock relaxation zone is established by the one-dimensional gas-particle σ_1 flow studied in Chapter III. Therefore the macroscopic motion of the nonuniform distribution of particles σ_2, downstream of the gas dynamic shock, may be viewed as the scattering of a beam of particles σ_2 from a known distribution of scattering centers, particles σ_1, distributed within a gas flow whose properties are also known. Following a collision, a particle σ_2 may

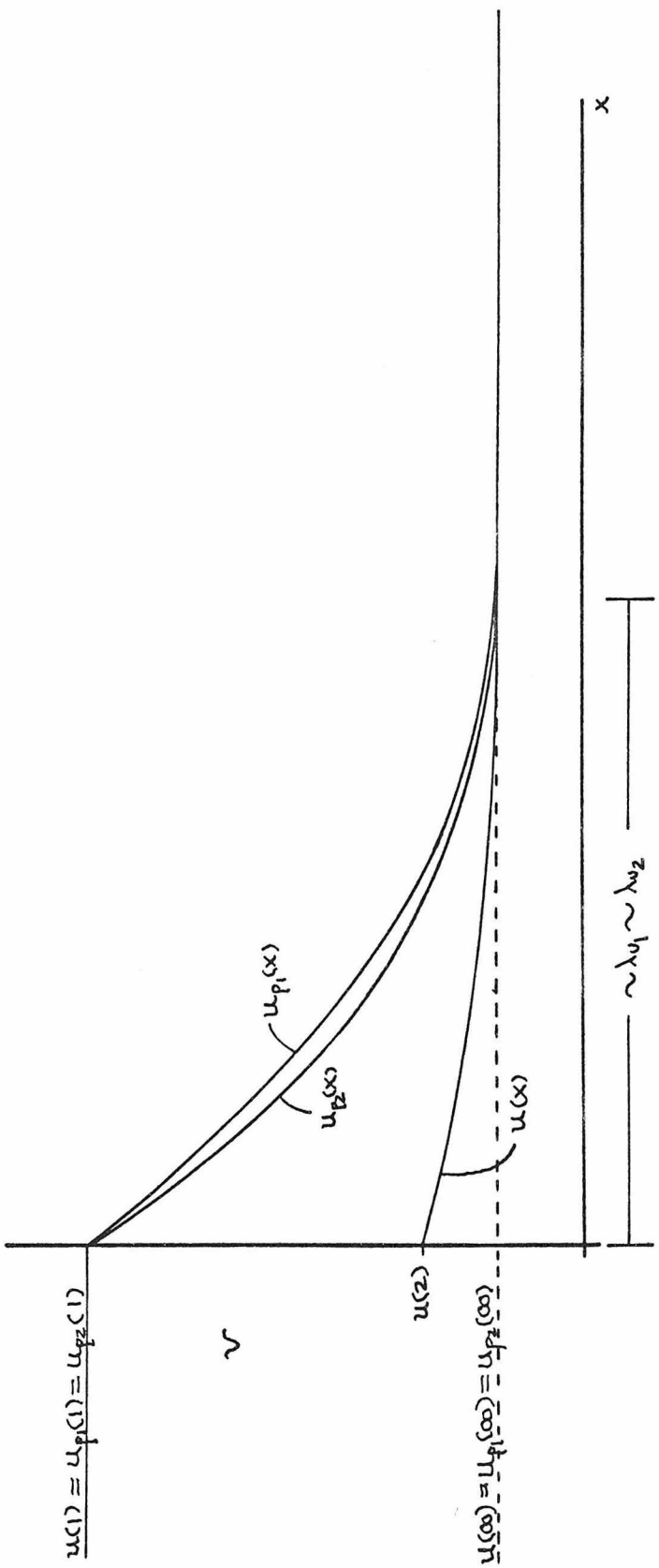

Figure 41. Collisionless velocity relaxation conditions when $\sigma_2/\sigma_1 \sim 1$.

move a distance of order λ_{v_2} across the gas-particle flow field before eventually coming into mechanical and thermal equilibrium with the gas far downstream from the shock wave. Consequently there may be a redistribution of the cloud of particles of radius σ_2 in directions normal to the gas flow. The characteristic length, λ_{v_2}, of this redistribution is of the same order of magnitude as the characteristic length of the shock relaxation zone, λ_{v_1}. We should analyze this process in detail supposing that conditions (5.1) are satisfied throughout the shock relaxation zone and that the particle-gas interaction is governed by Stokes law.

To determine the dynamics of the beam of particles σ_2 downstream of the shock when particles σ_2 have at most one collision in this region we may decompose the beam into two components. One component, hereafter called the primary beam of particles σ_2, consists only of particles σ_2 that have not suffered a collision. The other component, hereafter called the secondary beam of particles σ_2, consists only of particles that have collided with a particle σ_1 at some point within the shock relaxation zone. Far downstream of the relaxation zone both of these streams of particles σ_2 are moving at the local gas velocity $u(\infty)$ parallel to the x axis which is oriented normal to the shock face as in previous chapters. Since the velocity equilibration length λ_{v_2} of particles σ_2 is on the same order of magnitude as the characteristic length, λ_{v_1}, of the gas flow field, the complexity of the motion of particles σ_2 prevents a detailed calculation of the properties of the primary and secondary particle σ_2 beams. However, using the fact that particles σ_2 may only move a finite distance, the transverse

range of particles σ_2, normal to the gas flow following a collision, it is possible to calculate the final density distribution of particles σ_2. The final density distribution is that achieved far downstream of the shock wave where all particles are in mechanical and thermal equilibrium with the gas. Unless specified the notation of this chapter is consistent with the notation of Chapters III and IV.

1. Density distribution of the primary beam.

Particles σ_2 composing the primary beam move through the shock relaxation zone at their local collisionless velocity u_{p_2} given by:

$$u_{p_2}(x)\frac{du_{p_2}(x)}{dx} = \frac{a(x)}{\lambda_{u_2}}\left(u(x) - u_{p_2}(x)\right)$$
$$u_{p_2}(0) = u(1) \qquad (5.2)$$

where a is the local gaseous sound speed, u the local gas velocity, $\lambda_{u_2} = m_2 a / 6\pi\mu\sigma_2$ is the velocity equilibration length of particles σ_2 and is a constant since we will assume the gas viscosity, μ, varies as the square root of the gas temperature. Therefore particles composing the primary beam move in straight lines. Under these circumstances the equation of continuity for particles σ_2 is readily established by considering the motion of the primary beam through two areas $dydz$ oriented perpendicular to the x axis and separated by a distance dx. The distances dx, dy, and dz are small compared to the macroscopic length scales of our problem.

Let the areas be located at x and $x+dx$ where x is any position downstream of the shock wave, Figure 42. The number per second of primary beam particles σ_2 passing through the area

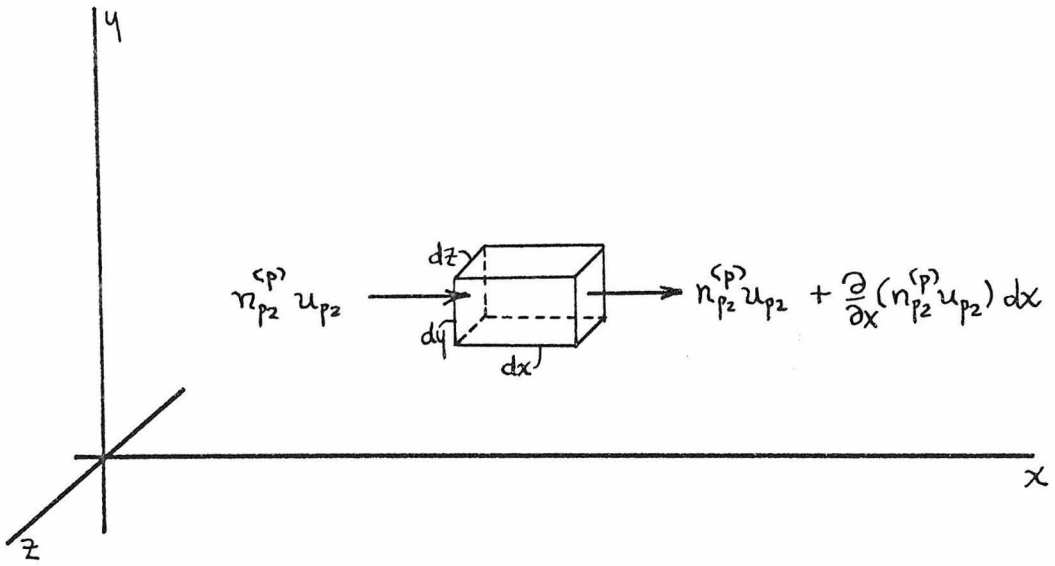
y
z
x
dz
dy
dx
$n_{p_2}^{(p)} u_{p_2}$
$n_{p_2}^{(p)} u_{p_2} + \frac{\partial}{\partial x}(n_{p_2}^{(p)} u_{p_2})\, dx$

Figure 42.

located at x is $n_{p_2}^{(p)}(x,y,z)\,u_{p_2}(x)\,dy\,dz$ and the number per second passing out of the control volume $dx\,dy\,dz$ through the area element $dy\,dz$ at $x+dx$ is $n_{p_2}^{(p)}(x+dx,y,z)\,u_{p_2}(x+dx)\,dy\,dz$. The density of particles σ_2 which compose the primary beam has been denoted by $n_{p_2}^{(p)}$. Collisions between primary beam particles σ_2 and particles σ_1 within $dx\,dy\,dz$ represents a loss to the primary beam and, since particles σ_2 are conserved in collisions, a gain process for the secondary beam. Consequently if $S(x,y,z)\,dx\,dy\,dz$ is the number of particles of radius σ_2 scattered out of the volume element $dx\,dy\,dz$ per second the equation of continuity for particles may be written;

$$n_{p_2}^{(p)}(x+dx,y,z)\,u_{p_2}(x+dx)\,dy\,dz - n_{p_2}^{(p)}(x,y,z)\,u_{p_2}(x)\,dy\,dz = -S(x,y,z)\,dx\,dy\,dz \tag{5.3}$$

To first order in small quantities we obtain the differential form of the equation of continuity for particles σ_2;

$$\frac{\partial}{\partial x}\left(n_{p_2}^{(p)}(\underline{x})\,u_{p_2}(x)\right) = -S(\underline{x}) \tag{5.4}$$

Since only binary encounters are significant and $\tau_{c_{21}} \ll \tau_{c_2}$ encounters are described as elastic collisions between two rigid spheres. Under these conditions $S(\underline{x}) = n_{p_2}^{(p)}(\underline{x})\,\nu(x)$ where $\nu(x) = \pi(\sigma_1+\sigma_2)^2 n_{p_1}(x)\,|u_{p_1}(x)-u_{p_2}(x)|$ is the local collision frequency for particle σ_1 -particle σ_2 collisions; $\nu = \tau_{c_{21}}^{-1}$. Therefore (5.4), the equation of continuity for primary beam particles, may be written;

$$\frac{\partial}{\partial x}\left(n_{p_2}^{(p)}(\underline{x})\,u_{p_2}(x)\right) = -n_{p_2}^{(p)}(\underline{x})\,n_{p_1}(x)\,\pi(\sigma_1+\sigma_2)^2\,|u_{p_1}(x)-u_{p_2}(x)| \qquad (5.5)$$

Since $n_{p_2} << n_{p_1}$ the density of particles σ_1 is known and so is the local collisionless velocity u_{p_1} of particles σ_1. Consequently (5.5) is an equation for $n_{p_2}^{(p)}(\underline{x})$ the density of particles σ_2 contained in the primary beam. To obtain $n_{p_2}^{(p)}$ as a function of $\underline{x}$ we rewrite (5.5) as;

$$\frac{\partial}{\partial x}\left(n_{p_2}^{(p)}(\underline{x})\,u_{p_2}(x)\right) = -\frac{n_{p_2}^{(p)}(\underline{x})\,u_{p_2}(x)}{\lambda_{c_{21}}(x)} \qquad (5.6)$$

where $\lambda_{c_{21}}(x) = u_{p_2}(x)/\nu(x)$ is the local mean free path for particle σ_2-particle σ_1 collisions. Equation(5.6) may be integrated directly since $\lambda_{c_{21}}(x)$ is presumed known;

$$n_{p_2}^{(p)}(x)\,u_{p_2}(x) = C\,e^{-\int_0^x \frac{dx'}{\lambda_{c_{21}}(x')}} \qquad (5.7)$$

where C is a constant with respect to x but may be a function of y and z. Since particles σ_2 are unperturbed by their passage through the gas dynamic shock wave, their flux is continuous through it;

$$n_{p_2}^{(p)}(0,y,z)\,u_{p_2}(0) = \frac{\rho_{p_2}^{(1)}(y,z)\,u(1)}{m_2} \qquad (5.8)$$

where $\rho_{p_2}^{(1)}(y,z)$ is the density distribution of particles σ_2 upstream of the shock wave as defined in Chapter IV. The flux of particles composing the secondary beam vanishes immediately downstream

of the shock wave. Using (5.8) and (5.7) we obtain;

$$n^{(p)}_{p_2}(\underline{x}) = \frac{u(1)}{u_{p_2}(x)} \frac{\rho^{(1)}_{p_2}(y,z)}{m_2} e^{-\int_0^x \frac{dx'}{\lambda_{c_{21}}(x')}} \tag{5.9}$$

or

$$\rho^{(p)}_{p_2}(\underline{x}) = \frac{u(1)}{u_{p_2}(x)} \rho^{(1)}_{p_2}(y,z)\, e^{-\pi(\sigma_1+\sigma_2)^2 \int_0^x n_{p_1}(x') \left| \frac{u_{p_1}(x')}{u_{p_2}(x')} - 1 \right| dx'} \tag{5.10}$$

where $\rho^{(p)}_{p_2}(\underline{x}) = m_2\, n^{(p)}_{p_2}(\underline{x})$ is the mass density of the primary beam of particles σ_2. With (5.9) or (5.10) and (5.2) we have a complete description of the primary beam. We note that far downstream of the shock wave, $X >> \lambda_4$; the gas and particles are in mechanical equilibrium so that

$$u_{p_1}(x) \cong u_{p_2}(x) \cong u(\infty) \tag{5.11}$$

Then for $X >> \lambda_{w_1}$ the integral

$$\int_0^x n_{p_1}(x') \left| \frac{u_{p_1}(x')}{u_{p_2}(x')} - 1 \right| dx' \longrightarrow \text{constant}$$

and consequently the primary beam density reaches a limiting distribution.

$$\rho^{(p)}_{p_2}(x_\infty, y, z) = \frac{u(1)}{u(\infty)} \rho^{(1)}_{p_2}(y,z)\, e^{-\pi(\sigma_1+\sigma_2)^2 \int_0^{x_\infty} n_{p_1}(x') \left| \frac{u_{p_1}(x')}{u_{p_2}(x')} - 1 \right| dx'} \tag{5.12}$$

where $X_\infty >> \lambda_{v_1}$. The form of the initial density distribution $\rho_{p2}^{(1)}$ is preserved but its magnitude has been reduced due to collisions between primary beam particles σ_2 and particles σ_1 .

2. Density distribution of the secondary beam.

The secondary beam of particles σ_2 originates from collisions which occur in the shock relaxation zone. Each member of this beam is presumed to have had only one collision. Now using the notion, established in Chapter II, Section 2, that following a collision a particle σ_2 can move only a finite distance across the gas flow downstream of the shock wave, the final density distribution, $\rho_{p2}^{(s)}(x_\infty, y, z)$, of secondary beam particles may be calculated.

Far downstream, all particles are moving with the gas and consequently the mass flux of secondary beam particles is given by;

$$\varphi_{p2}^{(s)}(x_\infty, y, z) = \rho_{p2}^{(s)}(x_\infty, y, z)\, u(\infty) \qquad (5.13)$$

Then if the mass flux of secondary beam particles σ_2 is known far downstream of the shock wave, the final density distribution of these particles is obtained from (5.13);

$$\rho_{p2}^{(s)}(x_\infty, y, z) = \frac{\varphi_{p2}^{(s)}(x_\infty, y, z)}{u(\infty)} \qquad (5.14)$$

Let us now calculate $\varphi_{p2}^{(s)}(x_\infty, y, z)$ by the methods of kinetic theory. The geometry of this problem is presented in Figure 43.

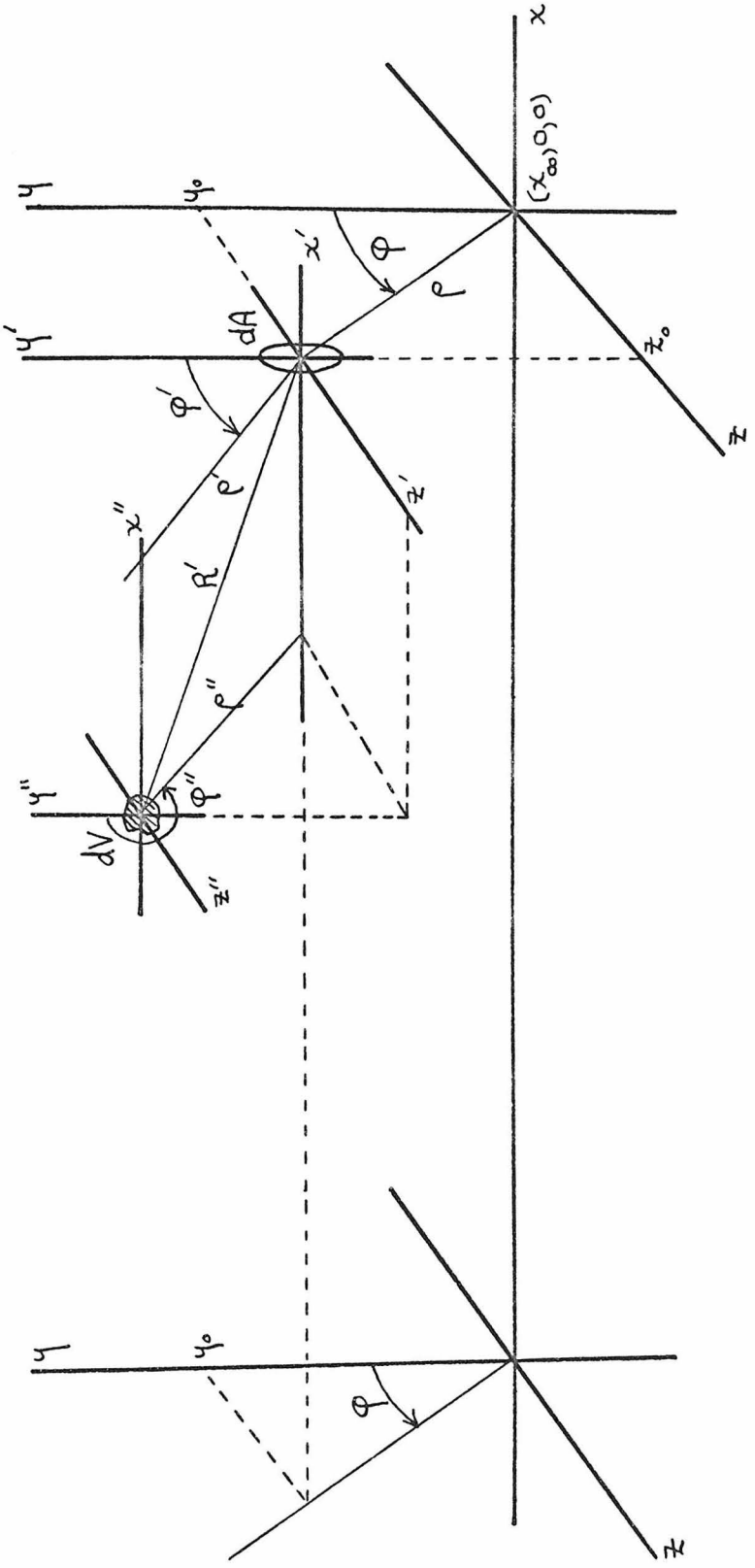

Figure 43.

Consider an element of area dA oriented parallel to the shock face and located far downstream of the shock wave at (x_∞, y_0, z_0). We will assume that x_∞ is so large that all particles scattered in the shock relaxation zone are in mechanical equilibrium with the gas by the time they reach dA. If $\frac{dN_{p2}}{dt}$ is the number per second of particles σ_2 that pass through the area element dA after having a collision in dV, a volume element located within the shock relaxation zone, then the mass flux of secondary beam particles of radius σ_2 at dA is given by

$$\varphi^{(s)}_{p2}(x_\infty, y_0, z_0) = \int_{0<x<x_\infty} m_2 \frac{dN_{p2}}{dt\, dA} \qquad (5.15)$$

The integration in (5.15) extends over all volume elements dV in which particle σ_1-particle σ_2 collisions scatter particles σ_2 into dA. It should be noted that there are no transit time effects since the gas-particle flow is steady and dV is stationary with respect to dA and the shock wave. Denote $\frac{dn_{p2}}{dt}$ as the number per second of particles σ_2 scattered out of dV that have a transverse range, $R_{p2\perp}$, in the interval $\rho''-\rho''+d\rho''$, $\varphi''-\varphi''+d\varphi''$. Where ρ'', φ'' are the polar coordinates of dA relative to the $x''y''z''$ co-ordinate system centered in dV. Then from the physical significance of the transverse range of particles σ_2 we conclude that $\frac{dN_{p2}}{dt} = \frac{dn_{p2}}{dt}$. It should be noted that this result is independent of the details of the shock relaxation zone provided $x_\infty >> \lambda_{01}$.

In calculating $\frac{dn_{p2}}{dt}$ let us assume, for simplicity, that $\sigma_1 > \sigma_2$ and therefore $u_{p1}(x) > u_{p2}(x)$ throughout the shock

relaxation zone. Since the transverse range of a particle σ_2 is independent of the local variation in gas properties along the particle's trajectory $\frac{dn_{p2}}{dt}$ has the same value relative to any reference frame moving parallel to the gas flow whose origin lies in dV at the time of the collision. Therefore, to simplify the calculation, we choose the center of mass frame $\bar{x}\,\bar{y}\,\bar{z}$ whose origin lies in dV at the time of the collision. It is moving parallel to the gas flow with velocity

$$V_{cm} = \frac{m_1 u_{p1} + m_2 u_{p2}}{m_1 + m_2} \tag{5.16}$$

since the particles collide while moving at their local collisionless velocities u_{p1} and u_{p2}. The dynamical conditions for particle σ_1 - particle σ_2 encounters are assumed to satisfy the criteria of Chapter III, Section 3 to insure that the particles collide as rigid elastic spheres. The geometry of a collision, as viewed in the center of mass frame $\bar{x}\,\bar{y}\,\bar{z}$, is depicted in Appendix A, Figure A4. Then from Appendix A, Equation (A4.3), the number per second $\frac{dN_{p2}(d\bar{\Omega})}{dt}$ of particles of radius σ_2 scattered out of the primary beam of density $n_{p2}^{(p)}$ in dV into the solid angle $d\bar{\Omega}$ as viewed in $\bar{x}\bar{y}\bar{z}$ is

$$\begin{aligned}\frac{dN_{p2}(d\bar{\Omega})}{dt} &= n_{p1}\, n_{p2}^{(p)} (u_{p1} - u_{p2}) \frac{(\sigma_1 + \sigma_2)^2}{4} \sin\bar{\vartheta}\, d\bar{\vartheta}\, d\bar{\varphi}\, dV \\ &= \frac{dN_{p2}(d\bar{\vartheta}d\bar{\varphi})}{dt}\end{aligned} \tag{5.17}$$

The quantities n_{p1}, $n_{p2}^{(p)}$, u_{p1}, and u_{p2} are evaluated at dV and the solid angle is $d\bar{\Omega} = \sin\bar{\vartheta}\, d\bar{\vartheta} d\bar{\varphi}$.

The density of primary beam particles, $n_{p2}^{(p)}$, is given by (5.9). As depicted in Figure A4 the scattering or recoil angle of

particles σ_2 relative to the $\bar{x}$ axis is $\bar{\vartheta}$ and the collision occurs in the $\bar{\varphi}=\text{const}$ azimuthal plane. We note that $0 \le \bar{\vartheta} \le \pi$ and $0 \le \bar{\varphi} \le 2\pi$. From the velocity diagram for the collision, Figure A5, since $u_{p_1} > u_{p_2}$ all scattering of particles σ_2 out of dV, as seen in the rest frame of the shock wave, is forward and contained within an angle ψ_{max}. In addition, particles σ_2 scattered into angles $\bar{\vartheta}_1$ and $\bar{\vartheta}_2$, relative to the center of mass frame, have the same radial velocity following the collision and consequently the same transverse range relative to dV. The relationship between the final transverse displacement ρ'' and the scattering angle $\bar{\vartheta}$ is obtained from the magnitude of the transverse range of a particle, $\rho'' = |\underline{u}_{p_2}^{(f)}| \tau_{v_2}$, and Equations (A3.2-A3.4);

$$\rho'' = \frac{m_1 \tau_{v_2}}{m_1+m_2}(u_{p_1}-u_{p_2}) \sin\bar{\vartheta} \qquad (5.18)$$

where u_{p_1} and u_{p_2} are evaluated at dV. Therefore the number of particles σ_2 scattered out of dV in unit time that have a final transverse displacement relative to dV in the interval $\rho''-\rho''+d\rho''$, $\varphi''-\varphi''+d\varphi''$ is;

$$\frac{dn_{p_2}}{dt} = \underset{0 \le \bar{\vartheta}_1 \le \pi/2}{\frac{dN_{p_2}(d\bar{\vartheta}_1 d\varphi'')}{dt}} + \underset{\pi/2 \le \bar{\vartheta}_2 \le \pi}{\frac{dN_{p_2}(d\bar{\vartheta}_2 d\varphi'')}{dt}} \qquad (5.19)$$

Consequently from (5.17) using the fact that $\sin\bar{\vartheta}_1 d\bar{\vartheta}_1 = \sin\bar{\vartheta}_2 d\bar{\vartheta}_2$ we obtain $\frac{dn_{p_2}}{dt}$ in terms of $\bar{\vartheta}_1$ and φ'';

$$\frac{dn_{p_2}}{dt} = n_{p_1} n_{p_2}^{(p)} (u_{p_1}-u_{p_2}) \frac{(\sigma_1+\sigma_2)^2}{2} \sin\bar{\vartheta}_1 d\bar{\vartheta}_1 d\varphi'' dV \qquad (5.20)$$

where $0 \le \bar{\vartheta}_1 \le \pi/2$, $0 \le \varphi'' \le 2\pi$. Then using (5.18) to express $\bar{\vartheta}_1$ in terms of ρ'' we obtain;

$$\frac{dn_{p2}}{dt} = n_{p1}\, n_{p2}^{(p)} (u_{p1}-u_{p2}) \frac{(\sigma_1+\sigma_2)^2}{2} d\left(-\sqrt{1-\lambda^{-2}(\rho'')^2}\right) d\varphi'' dV \tag{5.21}$$

where

$$\lambda \equiv \frac{m_1 \tau_{u2}}{m_1+m_2} (u_{p1}-u_{p2}) \tag{5.22}$$

is the maximum transverse range, relative to dV, of a particle σ_2 scattered out of dV by a collision with a particle of radius σ_1 . Consequently ρ'' satisfies the relation $0 \le \rho'' \le \lambda$. Therefore, from (5.21), the number per second, $\frac{dn_{p2}}{dt}$, of particles of radius σ_2 , scattered out of dV , whose transverse range lies in the interval $\rho'' - \rho'' + d\rho''$, $\varphi'' - \varphi'' + d\varphi''$ is;

$$\frac{dn_{p2}}{dt} = \frac{1}{2} n_{p1}\, n_{p2}^{(p)} (u_{p1}-u_{p2}) \frac{(\sigma_1+\sigma_2)^2 \lambda^{-2} \rho''\, d\rho''\, d\varphi''\, dV}{\sqrt{1-\lambda^{-2}(\rho'')^2}} \tag{5.23}$$

But $\frac{dn_{p2}}{dt} = \frac{dN_{p2}}{dt}$ is also the number of particles of radius σ_2 crossing dA per second;

$$\frac{dN_{p2}}{dt} = \frac{dn_{p2}}{dt} = \frac{1}{2} n_{p1}\, n_{p2}^{(p)} (u_{p1}-u_{p2}) \frac{(\sigma_1+\sigma_2)^2 \lambda^{-2}\, dV\, dA}{\sqrt{1-\lambda^{-2}(\rho'')^2}} \tag{5.24}$$

where the element of area dA is written $dA = \rho''\, d\rho''\, d\varphi''$. Expressing dV in cylindrical coordinates with origin at the area element

$$dV = -\rho' d\rho' d\varphi' dx' \tag{5.25}$$

where the minus sign is required since $dV > 0$ and we are interested in cases where $dx' < 0$. Furthermore, from Figure 43, we have $\rho' = \rho''$. Therefore using (5.24) and (5.25);

$$\frac{dN_{p2}}{dt} = -\frac{1}{2}(\sigma_1+\sigma_2)^2 n_{p_1} n_{p2}^{(\rho)} (u_{p_1} - u_{p2}) \lambda^{-2} \rho' d\rho' d\varphi' dx' dA \Big/ \sqrt{1 - \lambda^{-2}(\rho')^2} \tag{5.26}$$

Where n_{p_1}, $n_{p2}^{(\rho)}$, u_{p_1}, u_{p2}, and λ are evaluated at the location of the source of particles σ_2, the volume element dV; (See Figure 43)

$$\begin{aligned} n_{p_1} &= n_{p_1}(x_\infty + x') \\ n_{p2}^{(\rho)} &= n_{p2}^{(\rho)}(x_\infty + x',\ y_0 + \rho'\cos\varphi',\ z_0 + \rho'\sin\varphi') \\ u_{p_1} &= u_{p_1}(x_\infty + x') \\ u_{p2} &= u_{p2}(x_\infty + x') \end{aligned} \tag{5.27}$$

Using (5.15) and (5.26) the net mass flux of particles of radius σ_2 in the positive x direction at (x_∞, y_0, z_0) due to collisions for $x < x_\infty$ in the relaxation zone, $x_\infty >> \lambda v_1$, may be written

$$\varphi_{p2}^{(s)}(x_\infty, y_0, z_0) = -\frac{n_2}{2}(\sigma_1+\sigma_2)^2 \int_0^{2\pi} d\varphi' \int_0^{-x_\infty} dx' \int_0^{\lambda_m(x_\infty+x')} d\rho' \Big\{ n_{p_1}(x_\infty + x') \tag{5.28}$$

$$n_{p2}^{(\rho)}(x_\infty+x',\ y_0+\rho'\cos\varphi',\ z_0 + \rho'\sin\varphi')(u_{p_1}(x_\infty+x') - u_{p2}(x_\infty+x')) \lambda^{-2}(x_\infty+x')\rho' \Big/ \sqrt{1-\lambda^{-2}(x_\infty+x')(\rho')^2} \Big\}$$

The quantity $\lambda_m(x_\infty+x')$ is the maximum transverse range of particles σ_2 scattered out of a volume element located in the plane $x_\infty + x' = \text{constant}$. Consequently;

$$\lambda_m(x_\infty+x') = \frac{m_1 \tau_{v2}}{m_1+m_2}\left(u_{p_1}(x_\infty+x') - u_{p_2}(x_\infty+x')\right) \tag{5.29}$$

and λ_m is the transverse range of particles corresponding to the limiting scattering angle ψ_{max} observed in the rest frame of the shock wave; $\lambda = \lambda_m$.

The region of integration in (5.28) is sketched in Figure 44 and the physical reasons for its size and shape are easily seen. Only particles σ_2 scattered at points within this region possess enough momentum perpendicular to the gas flow to overcome the viscous force exerted upon them by the gas and thereby reach dA.

The net mass flux of secondary beam particles of radius σ_2, $\varphi^{(s)}_{p2}$, at (x_∞, y_0, z_0) may also be written, using (5.28) as an integral over cartesian coordinates;

$$\varphi^{(s)}_{p2}(x_\infty, y_0, z_0) = -\frac{m_2(\sigma_1+\sigma_2)^2}{2}\int_0^{-x_\infty} dx' \int_{-\lambda(x_\infty+x')}^{\lambda(x_\infty+x')} dy' \int_{-\sqrt{\lambda^2(x_\infty+x')-y'^2}}^{\sqrt{\lambda^2(x_\infty+x')-y'^2}} dz' \left\{ n_{p_1}(x_\infty+x',\right.$$

$$\left. n^{(p)}_{p2}(x_\infty+x', y_0+y', z_0+z')\left(u_{p_1}(x_\infty+x') - u_{p_2}(x_\infty+x')\right)\lambda^{-2}(x_\infty+x')\right\} \Big/ \sqrt{1-\lambda^{-2}(x_\infty+x')(y'^2+z'^2)} \tag{5.30}$$

Introducing the mass densities of particles σ_1 and primary beam particles σ_2, $\rho_{p_1} = m_1 n_{p_1}$ and $\rho^{(p)}_{p2} = m_2 n^{(p)}_{p2}$, we obtain;

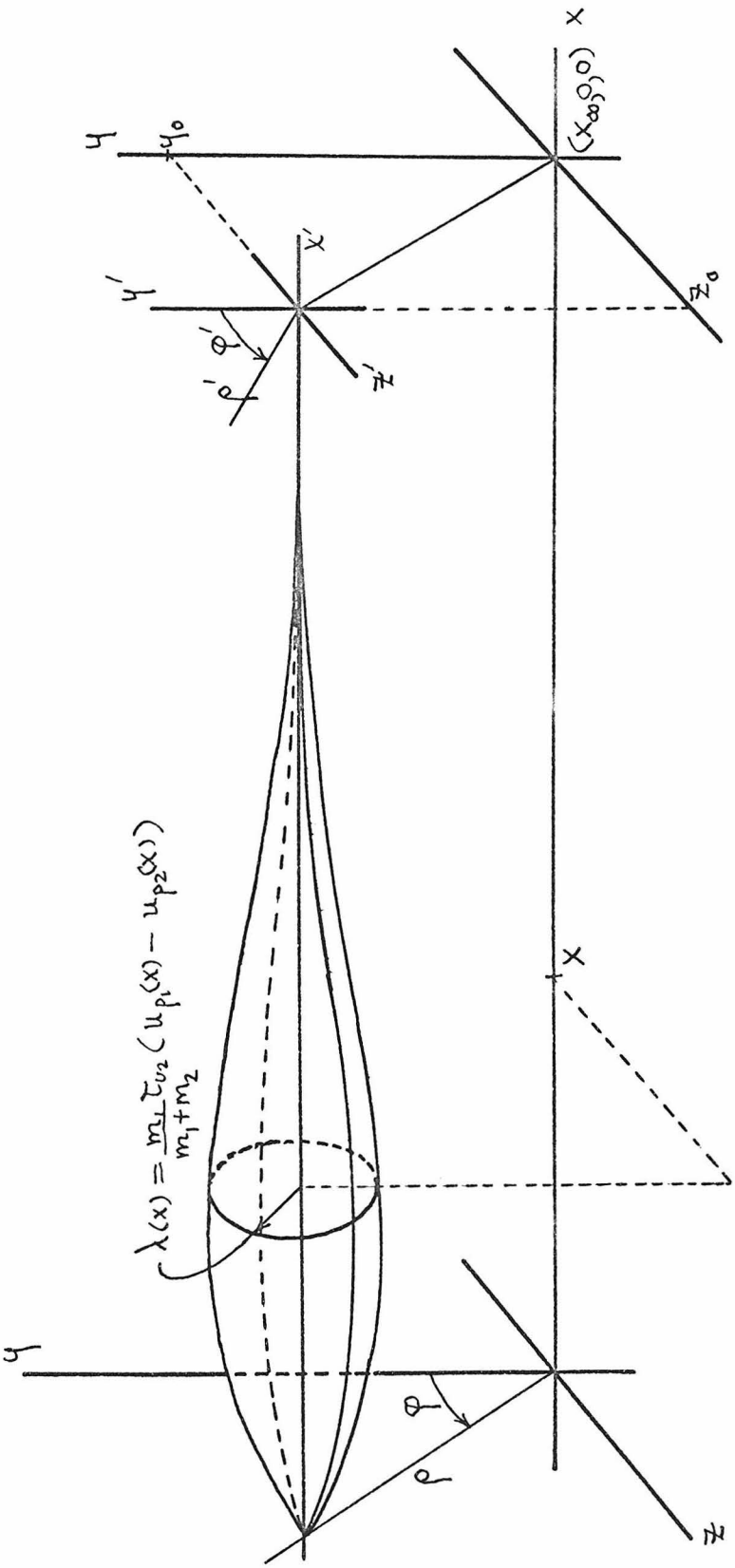
x
$(x_\infty, 0, 0)$
y
y_0
x'
y'
z_0
θ'
ρ'
z'
$\lambda(x) = \frac{m_1}{m_1+m_2} \tau_{v_2} (u_{p_1}(x) - u_{p_2}(x))$
x
y
θ
ρ
z

Figure 44.

$$\varphi^{(s)}_{p_2}(x_\infty, y_0, z_0) = -\frac{(\sigma_1+\sigma_2)^2}{2m_1}\int_0^{-x_\infty} dx' \int_{-\lambda(x_\infty+x')}^{\lambda(x_\infty+x')} dy' \int_{-\sqrt{\lambda^2(x_\infty+x')^2 - y'^2}}^{\sqrt{\lambda^2(x_\infty+x')^2 - y'^2}} dz' \left\{ \rho_{p_1}(x_\infty+x') \right.$$

$$\left. \rho^{(p)}_{p_2}(x_\infty+x', y_0+y', z_0+z') \frac{(u_{p_1}(x_\infty+x') - u_{p_2}(x_\infty+x'))}{\sqrt{1-\lambda^{-2}(x_0+x')(y'^2+z'^2)}} \lambda^{-2}(x_0+x') \right\} \tag{5.31}$$

where the mass density of primary beam particles is given by (5.10);

$$\rho^{(p)}_{p_2}(x) = \frac{u(1)}{u_{p_2}(x)}\, \rho^{(1)}_{p_2}(y,z)\, e^{-\pi(\sigma_1+\sigma_2)^2 \int_0^x n_{p_1}(x') \left| \frac{u_{p_1}(x')}{u_{p_2}(x')} - 1 \right| dx'} \tag{5.32}$$

In general $\rho^{(p)}_{p_2}$ and $\varphi^{(s)}_{p_2}$ must be evaluated numerically. By superposition of primary and secondary beams, the final density distribution of particles σ_2, using (5.14) may be written

$$\rho_{p_2}(x_\infty, y, z) = \rho^{(p)}_{p_2}(x_\infty, y, z) + \frac{\varphi^{(s)}_{p_2}(x_\infty, y, z)}{u(\infty)} \tag{5.33}$$

To simplify the examination of these results we will suppose the distribution of particles σ_2 upstream of the shockwave is uniform in the z direction; $\rho^{(1)}_{p_2}(y,z) = \rho^{(1)}_{p_2}(y)$. This procedure allows us to establish the physical features of the collisional dispersion of particles σ_2 when $\sigma_2/\sigma_1 \sim 1$.

If $\rho^{(1)}_{p_2}$ is independent of z then, from (5.32), $\rho^{(p)}_{p_2}$ is likewise independent of z. Consequently the integration over z' in

(5.31) may be easily carried out. The mass flux of secondary beam particles σ_2 under these conditions becomes

$$\mathcal{F}^{(s)}_{p_2}(x_\infty, y_0) = -\frac{\pi}{2}(\sigma_1+\sigma_2)^2\left(\frac{m_1+m_2}{m_1^2 \tau_{v_2}}\right)\int_0^{-x_\infty} dx' \int_{-\lambda(x_\infty+x')}^{\lambda(x_\infty+x')} dy' \left(\rho_{p_1}(x_\infty+x')\,\rho^{(p)}_{p_2}(x_\infty+x', y_0+y')\right) \quad (5.34)$$

The integration may be simplified by letting $\tilde{x} = x_\infty + x'$ and $\tilde{y} = y_0 + y'$ then;

$$\mathcal{F}^{(s)}_{p_2}(x_\infty, y_0) = \frac{\pi}{2}(\sigma_1+\sigma_2)^2\left(\frac{m_1+m_2}{m_1^2 \tau_{v_2}}\right)\int_0^{x_\infty} d\tilde{x} \int_{y_0-\lambda(\tilde{x})}^{y_0+\lambda(\tilde{x})} d\tilde{y} \left\{\rho_{p_1}(\tilde{x})\,\rho^{(p)}_{p_2}(\tilde{x}, \tilde{y})\right\} \quad (5.35)$$

The domain of integration in (5.35) is described in Figure 45. Once again, because of the finite transverse range of particles σ_2, only those particles scattered at x within a distance $\lambda(x)$ from y_0 parallel to the shock face may reach x_∞, y_0 and contribute to the mass flux $\mathcal{F}^{(s)}_{p_2}(x_\infty, y_0)$.

3. Uniform distribution of particles σ_2; $\rho^{(1)}_{p_2}(y,z) = \rho_0$

It is informative to check the validity of the previous calculation by treating a problem whose solution can be readily obtained by other means. When $\rho^{(1)}_{p_2}(y,z) = \rho_0 = \text{constant}$ and the particles σ_1 are uniformly distributed across the gas flow, there can be no redistribution of particles σ_2 due to collisions with particles σ_1. In addition since particles σ_2 are conserved in collisions the equation of continuity for particles σ_2 may be written;

$$\rho_{p_2}(x)\, v_{p_2}(x) = \rho^{(1)}_{p_2}\, u(1) = \rho_0\, u(1) \quad (5.36)$$

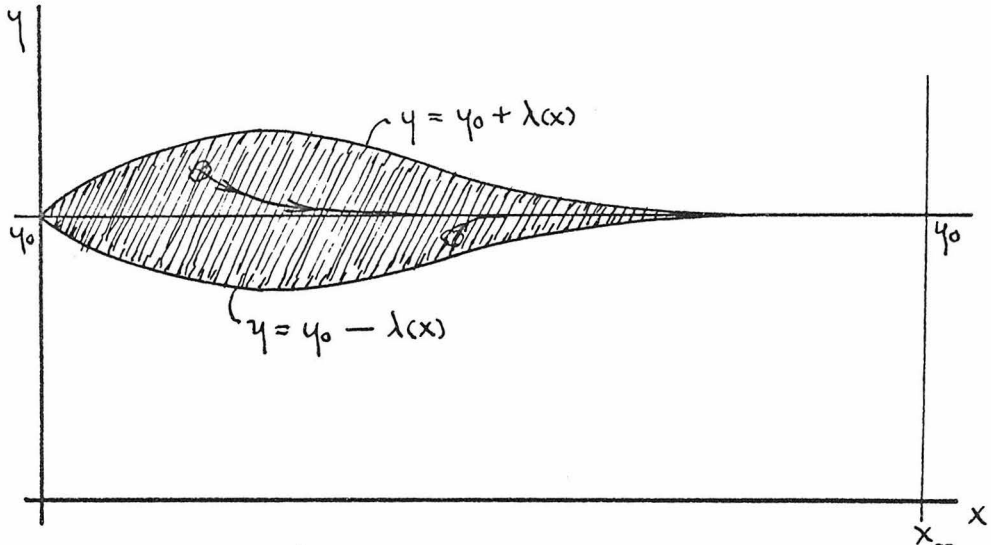

$$\lambda(x) \simeq \frac{m_1 \tau_{v_2}}{m_1 + m_2} \left(u_{p_1}(x) - u_{p_2}(x) \right)$$

//// Region of Integration

Figure 45.

where $v_{p_2}(x)$ is the local average velocity of particles σ_2. Since far downstream of the relaxation zone the particles are in mechanical equilibrium with the gas $v_{p_2}(x_\infty) = u(\infty)$ where $x_\infty >> \lambda_{v_1}$. Then from (5.36) we obtain the limiting density of particles σ_2 when their upstream density is a constant;

$$\rho_{p_2}(x_\infty) = \frac{u(1)}{u(\infty)} \rho_0 \tag{5.37}$$

Let us now compute $\rho_{p_2}(x_\infty, y, z)$ when $\rho_{p_2}^{(1)} = \rho_0$ using the results of the previous section. Writing (5.32), (5.33) and (5.35) for $\rho_{p_2}^{(1)}(y,z) = \rho_0$, the final density distribution of particles σ_2 is;

$$\rho_{p_2}(x_\infty, y, z) = \rho_{p_2}^{(p)}(x_\infty, y, z) + \frac{\varphi_{p_2}^{(s)}(x_\infty, y, z)}{u(\infty)} \tag{5.38}$$

where when $u_{p_1}(x) > u_{p_2}(x)$;

$$\rho_{p_2}^{(p)}(x, y, z) = \rho_0 \left(\frac{u(1)}{u_{p_2}(x)}\right) e^{-\pi(\sigma_1+\sigma_2)^2 \int_0^x n_{p_1}(x') \left(\frac{u_{p_1}(x')}{u_{p_2}(x')} - 1\right) dx'} = \rho_0 \eta(x) \tag{5.39}$$

and

$$\varphi_{p_2}^{(s)}(x_\infty, y, z) = \frac{\pi}{2}(\sigma_1+\sigma_2)^2 \left(\frac{m_1+m_2}{m_1^2 \tau_{v_2}}\right) \int_0^{x_\infty} d\tilde{x} \int_{y-\lambda(x)}^{y+\lambda(x)} d\tilde{y} \left\{ \rho_{p_1}(\tilde{x}) \rho_{p_2}^{(p)}(\tilde{x}, \tilde{y}) \right\} \tag{5.40}$$

Substituting $\rho_{p_2}^{(p)}(\tilde{x}, \tilde{y})$ into (5.40)

$$\mathcal{F}^{(s)}_{p_2}(x_\infty,y,z) = \frac{\pi}{2}(\sigma_1+\sigma_2)^2\left(\frac{m_1+m_2}{m_1^2\tau_{v_2}}\right)\int_0^{x_\infty} d\tilde{x}\left\{\rho_{p_1}(\tilde{x})\,\eta(\tilde{x})\int_{y-\lambda(\tilde{x})}^{y+\lambda(\tilde{x})} d\tilde{y}\right\} \tag{5.41}$$

Integrating over $\tilde{y}$ and using (5.35), the definition of $\lambda(\tilde{x})$,

$$\mathcal{F}^{(s)}_{p_2}(x_\infty,y,z) = \pi\frac{(\sigma_1+\sigma_2)^2}{m_1}\int_0^{x_\infty} d\tilde{x}\left\{\rho_{p_1}(\tilde{x})\,\eta(\tilde{x})\left(u_{p_1}(\tilde{x})-u_{p_2}(\tilde{x})\right)\right\} \tag{5.42}$$

Substituting (5.39) into (5.42) and using

$$-\frac{d}{dx}\left(e^{-\int_0^x \frac{dx'}{\lambda(x')}}\right) = \frac{1}{\lambda(x)}\,e^{-\int_0^x \frac{dx'}{\lambda(x')}}$$

we have,

$$\mathcal{F}^{(s)}_{p_2}(x_\infty,y,z) = \rho_0 u(1)\int_0^{x_\infty} d\tilde{x}\left\{\frac{-d}{d\tilde{x}}\left[e^{-\pi(\sigma_1+\sigma_2)^2\int_0^{\tilde{x}} n_{p_1}\left(\frac{u_{p_1}}{u_{p_2}}-1\right)d\tilde{x}'}\right]\right\} \tag{5.43}$$

which may be integrated directly

$$\mathcal{F}^{(s)}_{p_2}(x_\infty,y,z) = \rho_0 u(1)\left\{1-e^{-\pi(\sigma_1+\sigma_2)^2\int_0^{x_\infty} n_{p_1}\left(\frac{u_{p_1}}{u_{p_2}}-1\right)d\tilde{x}'}\right\} \tag{5.44}$$

Using (5.44), (5.39) and (5.38), the final density distribution of particles σ_2 may be expressed

$$\rho_{p_2}(x_\infty,y,z) = \rho_0\left(\frac{u(1)}{u(\infty)}\right)e^{-\pi(\sigma_1+\sigma_2)^2\int_0^{x_\infty} n_{p_1}\left(\frac{u_{p_1}}{u_{p_2}}-1\right)d\tilde{x}'} + \rho_0\left(\frac{u(1)}{u(\infty)}\right)\left\{1-e^{-\pi(\sigma_1+\sigma_2)^2\int_0^{x_\infty} n_{p_1}\left(\frac{u_{p_1}}{u_{p_2}}-1\right)d\tilde{x}'}\right\} \tag{5.45}$$

or

$$\rho_{p_2}(x_\infty) = \left(\frac{u(1)}{u(\infty)}\right)\rho_0 \tag{5.46}$$

Since this result checks with (5.37) we have demonstrated the consistency of our formulation.

4. Fundamental Beam Solution, $\rho^{(1)}_{p_2}(y) = m_2 N_{p_2}\delta(y)$.

During their passage through the relaxation zone of the shock wave, particles σ_2 interact only with the gas and particles σ_1. Therefore the particles σ_2 are non interacting and their density distribution satisfies the principal of superposition. Then if $\rho^{(1)}_{p_2}(y,z)_1$ and $\rho^{(1)}_{p_2}(y,z)_2$ are two distinct upstream density distributions of particles σ_2 and $\rho_{p_2}(x_\infty, y, z)_1$ and $\rho_{p_2}(x_\infty, y, z)_2$ are their corresponding final density distributions, respectively, then the final density distribution corresponding to the composite upstream density $\rho^{(1)}_{p_2}(y,z) = \rho^{(1)}_{p_2}(y,z)_1 + \rho^{(1)}_{p_2}(y,z)_2$ is simply $\rho_{p_2}(x_\infty, y, z) = \rho_{p_2}(x_\infty, y, z)_1 + \rho_{p_2}(x_\infty, y, z)_2$. Therefore the fundamental beam solution has its usual physical significance, for from it and the principle of superposition we can construct the final density distribution corresponding to any upstream density distribution $\rho^{(1)}_{p_2}(y,z)$. This formulation provides an alternative to that of Section 2.

Suppose that the upstream density distribution of particles is given by

$$\rho^{(1)}_{p_2}(y) = m_2 N_{p_2}\delta(y) \tag{5.47}$$

where $\delta(y)$ is the Dirac delta function and $N_{p_2} = \frac{1}{m_2}\int_{-\infty}^{\infty} \rho_{p_2}(y)\,dy$ is the number of particles σ_2 contained within a cross section of unit thickness in the x and z directions upstream of the shock wave. From (5.32) the primary beam part of the fundamental beam solution is simply;

$$\rho_{p_2}^{(p)}(x,y) = m_2 N_{p_2}\left(\frac{u(1)}{u_{p_2}(x)}\right)\delta(y)\, e^{-\pi(\sigma_1+\sigma_2)^2\int_0^x n_{p_1}\left(\frac{u_{p_1}}{u_{p_2}}-1\right)dx'} \tag{5.48}$$

Substituting (5.47) into (5.35) the secondary beam mass flux density at (x_∞, y_0) for all z may be written;

$$\rho_{p_2}^{(s)}(x_\infty, y_0) = \frac{\pi}{2}(\sigma_1+\sigma_2)^2\left(\frac{m_2}{m_1}\right)\left(\frac{m_1+m_2}{m_1 v_2}\right)\int_0^{x_\infty} d\tilde{x}\int_{y_0-\lambda(\tilde{x})}^{y_0+\lambda(\tilde{x})} d\tilde{y}\left\{\rho_{p_1}(\tilde{x})\,\eta(\tilde{x})\,\delta(\tilde{y})\right\} \tag{5.49}$$

where

$$\eta(x) = N_{p_2}\left(\frac{u(1)}{u_{p_2}(x)}\right) e^{-\pi(\sigma_1+\sigma_2)^2\int_0^x n_{p_1}\left(\frac{u_{p_1}}{u_{p_2}}-1\right)dx'} \tag{5.50}$$

and

$$\lambda(x) = \frac{m_1 v_2}{m_1+m_2}\left(u_{p_1}(x) - u_{p_2}(x)\right) \tag{5.51}$$

is the maximum transverse range of particles σ_2 scattered at x.

Because of the singular nature of the integrand care must be taken during the integration in (5.49). There are essentially four distinct cases corresponding to the value of y_0. Because of the variation of $u_{p_1} - u_{p_2}$ in the shock relaxation zone $\lambda(x)$ has a

single maximum at $X = X_m$ and decreases monotonically on either side of this maximum. If we let;

$$y_m \equiv \lambda(x_m) = \frac{m_1 \tau_{02}}{m_1 + m_2} \left(u_{p_1}(x_m) - u_{p_2}(x_m)\right) \tag{5.52}$$

be the maximum value of $\lambda(x)$ in the shock relaxation zone, the integration in (5.49) is straight forward. Suppose $y_0 > y_m$ or $y_0 < -y_m$. Then, because of the nature of $\delta(y)$, we have $f^{(s)}_{p_2}(x_\infty, y_0) \equiv 0$. This result is a simple consequence of the transverse range of particles σ_2. The secondary beam of particles σ_2 is composed of particles σ_2 scattered out of the primary beam which, in the present problem, is distributed in the $y=0$ plane. Therefore, since y_m is the maximum transverse range of particles σ_2 scattered within the shock relaxation zone, none of the particles σ_2 scattered out of the primary beam may reach $|y_0| > y_m$. Consequently the flux of secondary beam particles σ_2 vanishes for $|y_0| > y_m$.

From Figure 46 when $0 < |y_0| < y_m$, $f^{(s)}_{p_2}(x_\infty, y_0) \neq 0$ and is given by

$$f_{p_2}(x_\infty, y_0) = \frac{\pi}{2}(\sigma_1 + \sigma_2)^2 \left(\frac{m_2}{m_1}\right)\left(\frac{m_1 + m_2}{m_1 \tau_{02}}\right) \int_{X_1(y_0)}^{X_2(y_0)} \rho_{p_1}(\tilde{x})\eta(\tilde{x})\, d\tilde{x} \tag{5.53}$$

where $X_1(y_0)$ and $X_2(y_0)$ are points where the curve $y = y_0 - \lambda(x)$ or $y = y_0 + \lambda(x)$ crosses the x axis depending on whether $y_0 > 0$ or $y_0 < 0$, respectively. Then $X_1(|y_0|)$ and $X_2(|y_0|)$ are solutions of the transcendental relation;

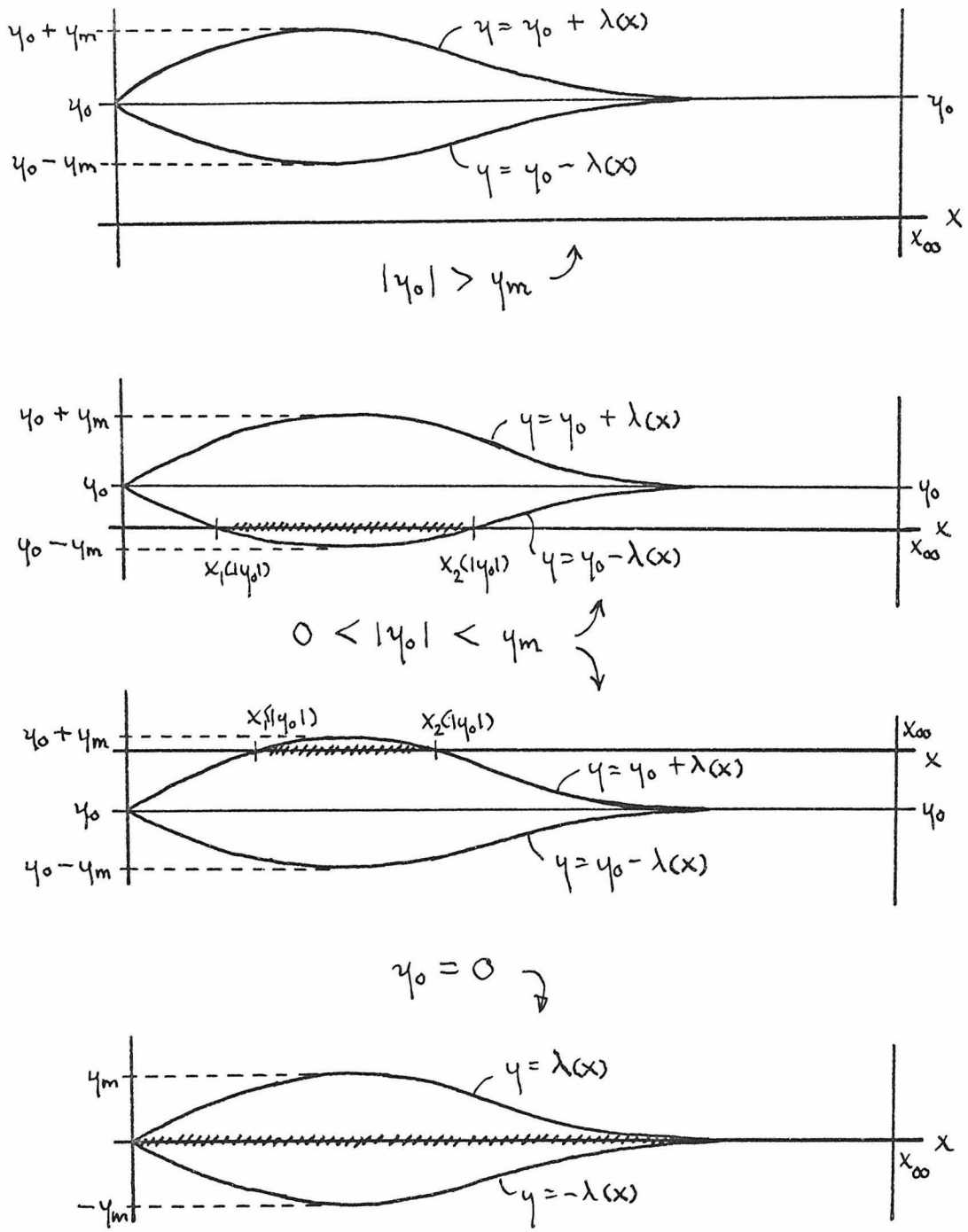

$$\lambda(x) = \frac{m_1 \tau_{v_2}}{m_1 + m_2} \left(u_{p_1}(x) - u_{p_2}(x) \right)$$

Figure 46.

$$|y_0| = \lambda(x) = \frac{m_1 \tau_{v2}}{m_1 + m_2}\left(u_{p_1}(x) - u_{p_2}(x)\right) \qquad (5.54)$$

It is to be expected that the fundamental beam solution is symmetrical in y_0. In collisions all impact parameters have been assumed equally probable. Physically (5.53) results because only between $x_1(y_0)$ and $x_2(y_0)$ is $u_{p_1}(x) - u_{p_2}(x)$ sufficiently large that particles σ_2 scattered from this region possess enough momentum normal to the gas flow to reach y_0 at $x_\infty >> \lambda_{v_1}$. Finally, when $y_0 = 0$ from (5.49) we have

$$f^{(s)}_{p_2}(x_\infty, y_0) = \frac{\pi}{2}(\sigma_1+\sigma_2)^2\left(\frac{m_2}{m_1}\right)\left(\frac{m_1+m_2}{m_1\tau_{v_2}}\right)\int_0^{x_\infty} \rho_{p_1}(\tilde{x})\,\eta(\tilde{x})\,d\tilde{x} \qquad (5.55)$$

Collecting results (5.48), (5.50, (5.53) and (5.55) together with (5.33) we may write down the final density distribution, $\rho^{(f)}_{p_2}$, for the fundamental beam, since y_0 was arbitrary.

For $|y| > y_m$:

$$\rho^{(f)}_{p_2}(x_\infty, y) = 0 \qquad (5.56)$$

For $0 \le |y| \le y_m$:

$$\rho^{(f)}_{p_2}(x_\infty, y) = m_2\eta(x_\infty)\delta(y) + \frac{\pi}{2}\frac{(\sigma_1+\sigma_2)^2}{u(\infty)}\left(\frac{m_2}{m_1}\right)\left(\frac{m_1+m_2}{m_1\tau_{v_2}}\right)\int_{x_1(|y|)}^{x_2(|y|)} \rho_{p_1}(\tilde{x})\,\eta(\tilde{x})\,d\tilde{x} \qquad (5.57)$$

where;

$$\eta(x) = N_{p2}\left(\frac{u_{(1)}}{u_{p2}(x)}\right) e^{-\pi(\sigma_1+\sigma_2)^2 \int_0^x n_{p1}\left(\frac{u_{p1}}{u_{p2}} - 1\right) dx'} \tag{5.58}$$

and $X_1(|y|)$, $X_2(|y|)$ are solutions of the transcendental equation

$$|y| = \frac{m_1 \tau_{v2}}{m_1 + m_2}\left(u_{p1}(x) - u_{p2}(x)\right) \tag{5.59}$$

When $|y| = 0$, as an approximation, $X_1(0) = 0$, $X_2(0) = X_\infty$. In addition, $y_m = \frac{m_1 \tau_{v2}}{m_1 + m_2}\left(u_{p1}(x_m) - u_{p2}(x_m)\right)$ is the maximum transverse range for particles σ_2 in the shock relaxation zone.

5. General Beam Solution by Superposition

Suppose the upstream density distribution of particles σ_2 is given by $\rho_{p2}^{(1)}(y)$. By an appropriate superposition of fundamental beams we can construct the final density distribution for $\rho_{p2}^{(1)}(y)$.

Take $m_2 N_{p2} = 1$ in the fundamental beam solution. Then from Figure 47 at $X = X_\infty$ the contribution to the particle σ_2 density at y due to a fundamental beam of strength $\rho_{p2}^{(1)}(y')\, dy'$ at y' is $d\rho_{p2}(y) = \rho_{p2}^{(1)}(y')\, \rho_{ffb}(y - y')\, dy'$. Where $\rho_{ffb} = \rho_{p2}^{(f)}$ with $m_2 N_{p2} = 1$. Summing over all contributions from $\rho_{p2}^{(1)}(y')$ we obtain the final density distribution of particles σ_2 ;

$$\rho_{p2}(x_\infty, y) = \int d\rho_{p2}(x_\infty, y) = \int_{-\infty}^{\infty} \rho_{p2}^{(1)}(y')\, \rho_{ffb}(x_\infty, y - y')\, dy' \tag{5.60}$$

Since $\rho_{ffb}(y) \neq 0$ only when $0 \leq |y| \leq y_m$, we have

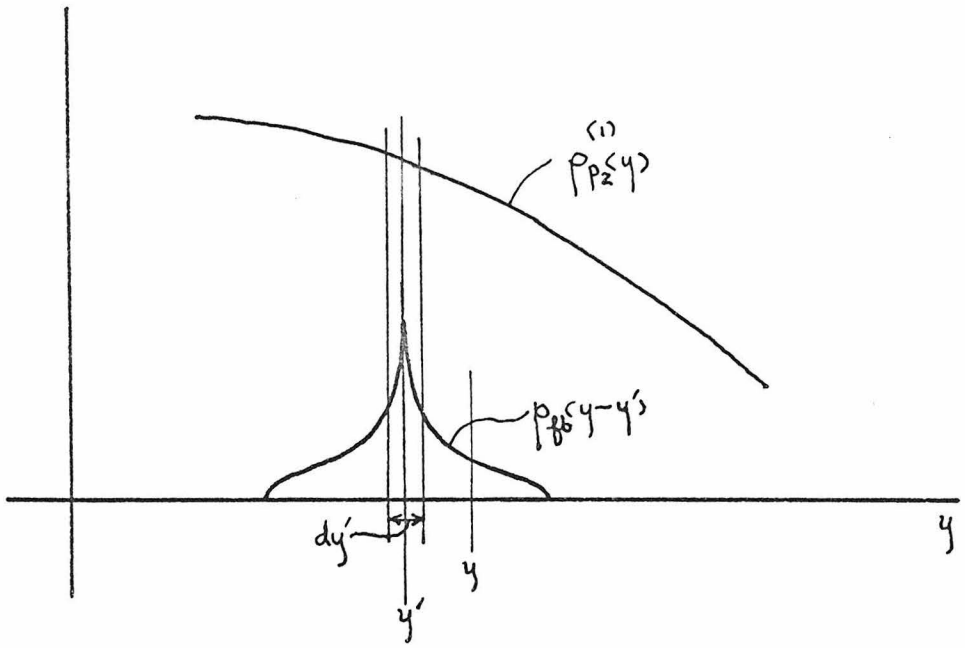

Figure 47.

$$\rho_{p_2}(x_\infty, y) = \int_{y-y_m}^{y+y_m} \rho_{p_2}^{(1)}(y')\, \rho_{ff_b}(x_\infty, y-y')\, dy' \tag{5.61}$$

Introducing the variables $\zeta = y - y'$ and $d\zeta = -dy'$ we may rewrite (5.61) as;

$$\rho_{p_2}(x_\infty, y) = \int_{-y_m}^{y_m} \rho_{p_2}^{(1)}(y-\zeta)\, \rho_{ff_b}(\zeta)\, d\zeta \tag{5.62}$$

Then substituting (5.57) and (5.58) into (5.60) with $m_2 N_{p_2} = 1$ and using the properties of the Dirac delta function, we obtain

$$\rho_{p_2}(x_\infty, y) = \rho_{p_2}^{(1)}(y)\left(\frac{u(1)}{u(\infty)}\right) e^{-\pi\frac{(\sigma_1+\sigma_2)^2}{m_1}\int_0^{x_\infty} \rho_{p_1}\left(\frac{u_{p_1}}{u_{p_2}} - 1\right) dx'}$$

$$+ \int_{-y_m}^{y_m} \rho_{p_2}^{(1)}(y-\zeta)\, \rho_{ff_b}^{(s)}(x_\infty, \zeta)\, d\zeta \tag{5.63}$$

where $\rho_{ff_b}^{(s)}(x_\infty, \zeta)$ is the secondary beam contribution to the fundamental beam solution;

$$\rho_{ff}^{(s)}(x_\infty, \zeta) = \frac{\pi}{2}\frac{(\sigma_1+\sigma_2)^2}{u(\infty)}\left(\frac{m_1+m_2}{m_1^2\tau_{v2}}\right)\int_{x_1(|\zeta|)}^{x_2(|\zeta|)} \rho_{p_1}(\tilde{x})\left(\frac{u(1)}{u_{p_2}(\tilde{x})}\right) e^{-\pi\frac{(\sigma_1+\sigma_2)^2}{m_1}\int_0^{\tilde{x}} \rho_{p_1}\left(\frac{u_{p_1}}{u_{p_2}} - 1\right) dx'} d\tilde{x} \tag{5.64}$$

The evaluation of (5.63) and (5.64) must usually be done numerically. Introducing the dimensionless variables defined in Chapter IV, Equation (4.157) the previous results (5.63) and (5.64) may be written;

$$\tilde{\rho}_{p_2}(\tilde{x}_\infty,\tilde{y}) = \rho_{p_2}^{(1)}(\tilde{y})\left(\frac{u(1)}{u(\infty)}\right) e^{-\left(\frac{\lambda_{v_2}}{\ell}\right)\left(\frac{\lambda_{v_1}}{\lambda_{v_2}}\right)\left(1+\frac{m_2}{m_1}\right)\int_0^{\tilde{x}_\infty}\left(\frac{M_1}{\tilde{u}_{p_1}}\right)\left(\frac{\tilde{u}_{p_1}}{\tilde{u}_{p_2}}-1\right)d\tilde{x}'}$$

$$+\frac{1}{2}\left(\frac{\lambda_{v_2}}{\ell}\right)\left(\frac{\lambda_{v_1}}{\lambda_{v_2}}\right)^2\left(\frac{u(1)}{u(\infty)}\right)\left(\frac{a(2)}{a(1)}\right)\left(1+\frac{m_2}{m_1}\right)^2\int_{-\tilde{y}_m}^{\tilde{y}_m}\tilde{\rho}_{p_2}^{(1)}(\tilde{y}-\tilde{s})\,\tilde{\rho}_{ff}^{(s)}(\tilde{x}_\infty,\tilde{s})\,d\tilde{s} \qquad (5.65)$$

In this relation

$$\tilde{\rho}_{ff_0}^{(s)}(\tilde{x}_\infty,\tilde{s}) = \int_{\tilde{x}_1(|\tilde{s}|)}^{\tilde{x}_2(|\tilde{s}|)}\left(\frac{M_1}{\tilde{u}_{p_1}}\right)\left(\frac{1}{\tilde{u}_{p_2}}\right) e^{-\left(\frac{\lambda_{v_2}}{\ell}\right)\left(\frac{\lambda_{v_1}}{\lambda_{v_2}}\right)\left(1+\frac{m_2}{m_1}\right)\int_0^{\tilde{x}}\left(\frac{M_1}{\tilde{u}_{p_1}}\right)\left(\frac{\tilde{u}_{p_1}}{\tilde{u}_{p_2}}-1\right)d\tilde{x}'} d\tilde{x} \qquad (5.66)$$

and

$$\tilde{y}_m = \frac{1}{(1+m_2/m_1)}\left(\frac{\lambda_{v_2}}{\lambda_{v_1}}\right)\left(\frac{a(1)}{a(2)}\right)\left(\tilde{u}_{p_1}(\tilde{x}_m)-\tilde{u}_{p_2}(\tilde{x}_m)\right) \qquad (5.67)$$

The quantities $\tilde{x}_1(|\tilde{s}|)$ and $\tilde{x}_2(|\tilde{s}|)$ are solutions of

$$|\tilde{s}| = \frac{1}{(1+m_2/m_1)}\left(\frac{\lambda_{v_2}}{\lambda_{v_1}}\right)\left(\frac{a(1)}{a(2)}\right)\left(\tilde{u}_{p_1}(\tilde{x})-\tilde{u}_{p_2}(\tilde{x})\right) \qquad (5.68)$$

We have used the continuity equation for particles σ_1 to eliminate ρ_{p_1}.

Finally the characteristic length ℓ is

$$\ell = \frac{m_1+m_2}{\pi(\sigma_1+\sigma_2)^2 K_1 \rho(1)} \qquad (5.69)$$

Let us now examine the physical significance of the dimensionless parameter $\left(\frac{\lambda_{u_2}}{\ell}\right)$. As discussed in Chapter IV, the results of collisions may be interpreted as a dynamical friction force between the two clouds of particles. Since $\rho_{p1}, \rho >> \rho_{p2}$ this force has a negligible effect on particles σ_1. However, it plays an important role in the macroscopic motion of particles σ_2. From Eq. (4.114) of Chapter IV the dynamical friction force, $F_{DF}\,\underline{e}_x$, exerted on particle cloud σ_2 due to collisions with particles σ_1 is given by;

$$F_{DF}(\underline{x}) = \rho_{p_1}(x)\,\rho_{p_2}(\underline{x})\,\pi\,\frac{(\sigma_1+\sigma_2)^2}{(m_1+m_2)}\,(u_{p_1}(x)-u_{p_2}(x))\,|u_{p_1}(x)-u_{p_2}(x)| \qquad (5.70)$$

The relative importance of collisions may be measured by the ratio of F_{DF} to F_S, the Stokes drag force exerted on the particle cloud by the gas. Using the definition (5.69) we obtain

$$\frac{F_{DF}}{F_S} = \left(\frac{\rho_{p1}}{K_1\rho(1)}\right)\left(\frac{\lambda_{u_2}}{\ell}\right)\frac{(u_{p_1}-u_{p_2})\,|u_{p_1}-u_{p_2}|}{a(u-u_{p_2})} \qquad (5.71)$$

Since $\sigma_1 \sim \sigma_2$ the term $(u_{p_1}-u_{p_2})\,|u_{p_1}-u_{p_2}|/(a(u-u_{p_2}))$ as less than or of order unity except at the two ends of the shock relaxation zone. This is in contrast to the situation of Chapter IV where $u-u_{p2}$ was small over most of the shock relaxation zone and the ratio F_{DF}/F_S was dominated by the velocity term. Since $(\rho_{p1}/K\rho(1)) \sim 1$, when $\sigma_2/\sigma_1 \sim 1$, we find that the magnitude of (λ_{u_2}/ℓ) characterizes the effect of collisions on the macroscopic motion of particle cloud σ_2. This point of view is reinforced if we take the limit $\frac{\lambda_{u_2}}{\ell} \to 0$, corresponding to $\frac{F_{DF}}{F_S} \to 0$, in (5.65) we find

$$\tilde{\rho}_{p2}(\tilde{x}_\infty, \tilde{y}) = \rho_{p2}^{(1)}(\tilde{y}) \left(\frac{u(1)}{u(\infty)}\right) \tag{5.72}$$

the effect of collisions has vanished. In addition, we may write the dynamical friction force F_{DF} as;

$$F_{DF} = \rho_{p2} \left(\frac{\rho_{p1}}{K_1 \rho(1)}\right) \frac{(u_{p1} - u_{p2}) | u_{p1} - u_{p2} |}{\ell} \tag{5.73}$$

Therefore ℓ is the characteristic length of the dynamical friction force. Note that λ_{u_2} is the characteristic length of the Stokes drag force.

Before proceeding with numerical solution of (5.65)-(5.69) for a particular upstream density distribution of particles σ_2 let us review the assumptions that underlie the previous calculations;

(a) The particles are nearly the same size

$$\frac{\lambda_{u_2}}{\lambda_{u_1}} = \frac{\tau_{u_2}}{\tau_{u_1}} = \left(\frac{\sigma_2}{\sigma_1}\right)^2 \sim 1 \tag{5.74}$$

(b) The particle-gas interaction is governed by Stokes Law;

$$Re_1 = \frac{\rho \sigma_1 | u - u_{p1} |}{\mu} \lesssim 1 \qquad \frac{|u - u_{p1}|}{a} \ll 1 \tag{5.75}$$

$$Re_2 = \frac{\rho \sigma_2 | u - u_{p2} |}{\mu} \lesssim 1 \qquad \frac{|u - u_{p2}|}{a} \ll 1 \tag{5.76}$$

As discussed in Chapter IV this assumption is frequently violated. As a consequence, our results represent an upper bound on the degree of dispersion of particles σ_2 due to collisions in the shock relaxation zone. However, our results are expected to describe

the essential physical features of the collision process.

(c) The velocity equilibration time must be large in comparison with the time required for one particle to pass through the Stokes flow field of the other;

$$\left(\frac{\sigma_1}{\sigma_2}\right)\left(\frac{\rho\sigma_1 |u_{p1}-u_{p2}|}{\mu}\right)\left(\frac{\rho_s}{\rho}\right) >> 1 \tag{5.77}$$

$$\left(\frac{\sigma_2}{\sigma_1}\right)\left(\frac{\rho\sigma_2 |u_{p1}-u_{p2}|}{\mu}\right)\left(\frac{\rho_s}{\rho}\right) >> 1 \tag{5.78}$$

In the present problem this condition is generally satisfied as required by McLaughlin's results except if σ_1 is very nearly equal to σ_2. When this is the case, however, collisions will be unimportant because of the finite length of the shock relaxation zone.

(d) The particles σ_2 have at most one collision during their passage through the shock relaxation zone. Consequently they collide while moving at their local collisionless velocities u_{p1} and u_{p2}. The restriction introduced by this assumption may be explored in the following manner. The length $\lambda_{c_{21}}(x)$ is the average distance traveled by a particle σ_2 between collisions with particles of radius σ_1. If $P(x)$ is defined as the probability, a particle σ_2 will travel a distance x downstream from the shock wave without collision then[15]

$$P(x) = e^{-\int_0^x \frac{dx'}{\lambda_{c_{21}}(x')}} \tag{5.79}$$

Using $\lambda_{c_{21}}(x)$ for rigid sphere collisions we have;

$$P(x) = e^{-\pi(\sigma_1+\sigma_2)^2 \int_0^x \rho_{p_1}(x') \left| \frac{u_{p_1}(x')}{u_{p_2}(x')} - 1 \right| dx'} \qquad (5.80)$$

In the present problem for the single collision assumption to be valid we must impose a condition which assures that most of the particles σ_2 have only one collision in traversing the region $0 \le x \le x_\infty$; we take this to be $P(x_\infty) \gtrsim e^{-1}$. Consequently the single collision assumption requires;

$$\frac{\pi(\sigma_1+\sigma_2)^2}{m_1} \int_0^{x_\infty} \rho_{p_1}(x') \left| \frac{u_{p_1}(x')}{u_{p_2}(x')} - 1 \right| dx' \lesssim 1 \qquad (5.81)$$

Introducing the dimensionless variables used to obtain (5.68)-(5.69) , the single collision condition may be rewritten

$$\left(\frac{\lambda_{v_2}}{\ell}\right)\left(\frac{\lambda_{v_1}}{\lambda_{v_2}}\right)\left(1 + \frac{m_2}{m_1}\right) \int_0^{\tilde{x}_\infty} \left(\frac{M_1}{\tilde{u}_{p_1}}\right) \left| \frac{u_{p_1}}{u_{p_2}} - 1 \right| d\tilde{x}' \lesssim 1 \qquad (5.82)$$

or

$$\left(\frac{\lambda_{v_2}}{\ell}\right) \lesssim \left\{ \left(\frac{\lambda_{v_1}}{\lambda_{v_2}}\right)\left(1 + \frac{m_2}{m_1}\right) \int_0^{\tilde{x}_\infty} \left(\frac{M_1}{\tilde{u}_{p_1}}\right) \left| \frac{\tilde{u}_{p_1}}{\tilde{u}_{p_2}} - 1 \right| d\tilde{x}' \right\}^{-1} \qquad (5.83)$$

Whether a given solution satisfies this condition must be explored numerically. It is not surprising, however, that it places an upper bound on (λ_{v_2}/ℓ) . If the dynamical friction force exerted on particle cloud σ_2 due to collisions with particles σ_1 is too large, the single collision hypothesis is invalidated.

The previous results may be extended to the case $u_{p_1} < u_{p_2}$ by replacing $u_{p_1}(x) - u_{p_2}(x)$ by $|u_{p_1}(x) - u_{p_2}(x)|$.

6. Results

By treating several specific examples, our purpose in this section is; (1) to illustrate the physical features of the final density distribution of particles σ_2 when the single collision hypothesis is valid and (2) to establish the possible significance of particle-particle interactions when $\sigma_2/\sigma_1 \sim 1$.

As a first example, consider the collisional dispersion of particles σ_2 downstream from the shock wave when their density upstream is given by;

$$\rho_{p_2}^{(1)}(y) = \begin{cases} \rho_{p_2}^{(1)} & |y| \le y_b \\ 0 & \text{otherwise} \end{cases} \tag{5.84}$$

This is chosen to examine the behavior of any distribution of particles σ_2 whose width is of the same order as the characteristic length of the shock relaxation zone. The limiting case of very narrow upstream density distributions may be examined by taking $y_b \ll \lambda_{v_1}$. The final density distribution for particles σ_2 , in dimensionless variables, may be obtained from (5.65)-(5.66);

$$\tilde{\rho}_{p_2}(\tilde{x}_\infty, \tilde{y}) = H(\tilde{y}_b+\tilde{y})\,H(\tilde{y}_b-\tilde{y})\,e^{-\left(\frac{\lambda_{v_1}}{\ell}\right)\left(1+\frac{m_2}{m_1}\right)\int_0^{\tilde{x}_\infty}\left(\frac{m_1}{m_2}\right)\left|\frac{\tilde{u}_{p_1}}{\tilde{u}_{p_2}}-1\right| d\tilde{x}'} + \frac{1}{2}\left(\frac{\lambda_{v_1}}{\ell}\right)\left(\frac{\lambda_{v_1}}{\lambda_{v_2}}\right)\left(\frac{a_{(2)}}{a_{(1)}}\right)\left(1+\frac{m_2}{m_1}\right)^2 \int_{-\tilde{y}_m}^{\tilde{y}_m} H(\tilde{y}_b+(\tilde{y}-\tilde{s}))\,H(\tilde{y}_b-(\tilde{y}-\tilde{s}))\,\tilde{\rho}_{fb}^{(s)}(\tilde{x}_\infty)\,\tilde{s}\,d\tilde{s} \tag{5.85}$$

In this relation

$$\tilde{\rho}_{fb}^{(2)}(\tilde{x}_\infty, \tilde{s}) = \int_{\tilde{x}_1(|\tilde{s}|)}^{\tilde{x}_2(|\tilde{s}|)} \left(\frac{M_1}{\tilde{u}_{p1}}\right)\left(\frac{1}{\tilde{u}_{p2}}\right) e^{-\left(\frac{\lambda_{v1}}{q}\right)\left(1+\frac{m_2}{m_1}\right)\int_0^{\tilde{x}} \left(\frac{M_1}{\tilde{u}_{p1}}\right)\left|\frac{\tilde{u}_{p1}}{\tilde{u}_{p2}} - 1\right| d\tilde{x}'} \tag{5.86}$$

and

$$\tilde{y}_m = \frac{1}{\left(1+\frac{m_2}{m_1}\right)}\left(\frac{\lambda_{v2}}{\lambda_{v1}}\right)\left(\frac{a(1)}{a(2)}\right)\left|\tilde{u}_{p1}(\tilde{x}_m) - \tilde{u}_{p2}(\tilde{x}_m)\right| \tag{5.87}$$

The quantities $\tilde{x}_1(|\tilde{s}|)$ and $\tilde{x}_2(|\tilde{s}|)$ are solutions of;

$$|\tilde{s}| = \frac{1}{\left(1+\frac{m_2}{m_1}\right)}\left(\frac{\lambda_{v2}}{\lambda_{v1}}\right)\left(\frac{a(1)}{a(2)}\right)\left|\tilde{u}_{p1}(\tilde{x}) - \tilde{u}_{p2}(\tilde{x})\right| \tag{5.88}$$

$H(t)$ is the Heaviside step function;

$$H(t) = \begin{cases} 0 & t<0 \\ 1 & t\geq 0 \end{cases} \tag{5.89}$$

and $\rho_{p2} = \rho_{p2}(\infty)\tilde{\rho}_{p2} = (\rho_{p2}(1)u(1)/u(\infty))\tilde{\rho}_{p2}$.

Because particles σ_2 can move at most a distance y_m across the gas flow due to a collision, far downstream of the shock wave all particles σ_2 will be distributed within a distance $(y_b + y_m)$ of the X axis. This result is independent of the magnitude of y_b. Furthermore if $y_b > y_m$, only the edge of the beam $|y_b - y_m| < |y|$ will be affected by the collisions. Since all impact parameters are equally probable, the density of a finite width uniform beam can only be redistributed within a distance y_m of its sides. When $y_m > y_b$ the entire beam cross section will be dispersed due to collisions. These effects are illustrated in Figures 48-51.

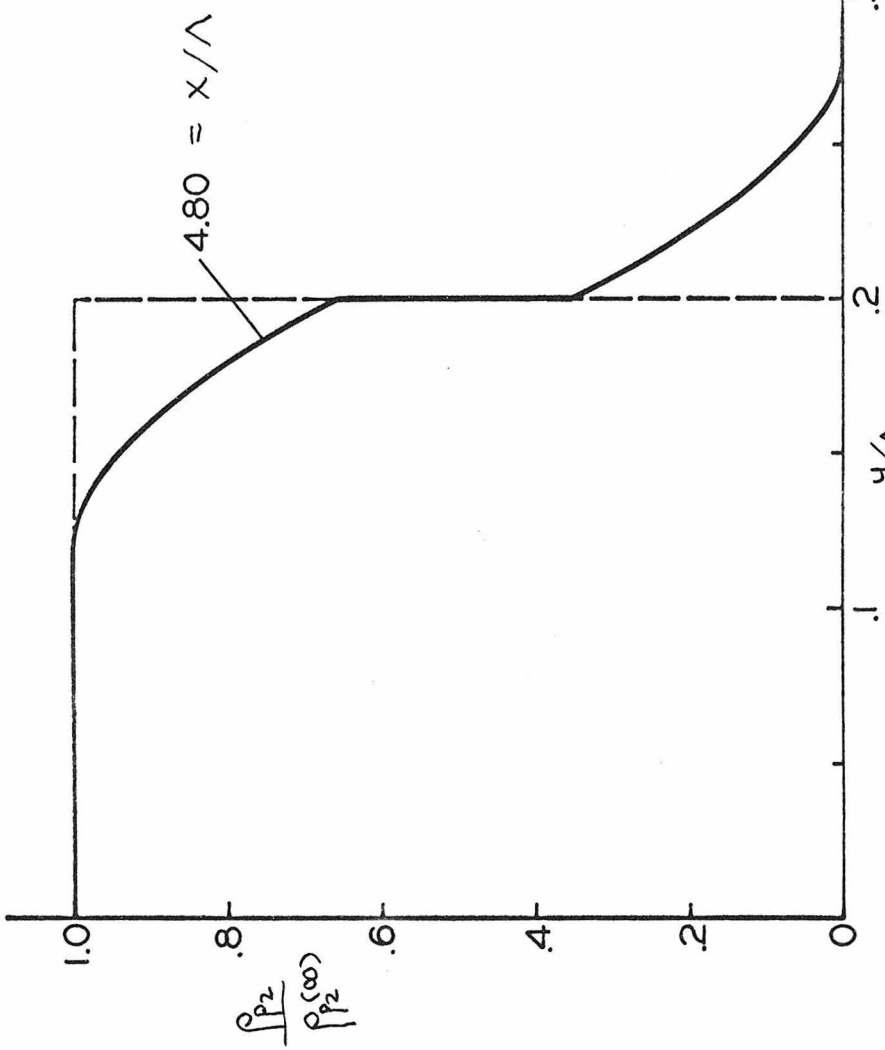

Figure 48. Final particle σ_2 uniform beam density distribution downstream of the shock face. Upstream conditions; Gas-Air, $\rho(1) = 1.3 \times 10^{-4}$ g/cm^3, $T(1) \approx 20°C$, $M_1 = 3.2$, $\gamma = 1.4$, $K_1 = .25$, $\rho_s/\rho(1) \approx 10^4$, $\sigma_2/\sigma_1 \approx 0.9$, $\sigma_1 \approx 2.8\,\mu$, $\Lambda = \lambda_{v1} = 3.9$cm, $c_s/c_p = \lambda_{v1}/\lambda_{T1} = 1$.

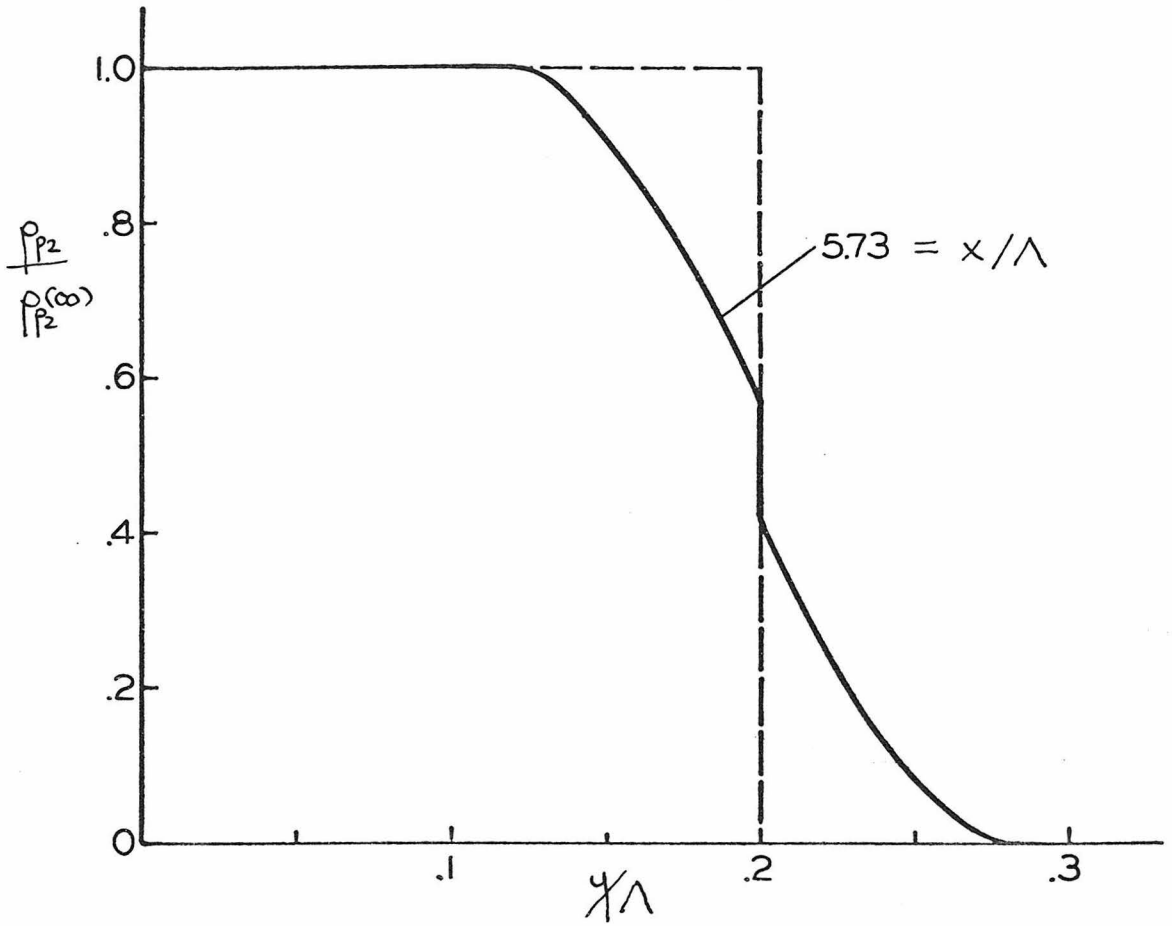

Figure 49. Final particle σ_2 uniform beam density distribution downstream of the shock face. Upstream conditions; Gas-Air, $\rho(1) = 1.3 \times 10^{-4}$ gm/cm^3 $T(1) = 20°C$, $M_1 = 3.2$, $\gamma = 1.4$, $K_1 = .25$, $\rho_s/\rho(1) = 10^4$, $\sigma_2/\sigma_1 = 1.1$, $\sigma_1 = 2.8\,\mu$, $\Lambda = \lambda_{u_1} = 3.9$ cm, $c_s/c_p = \lambda_{u_1}/\lambda_{T_1} = 1$,

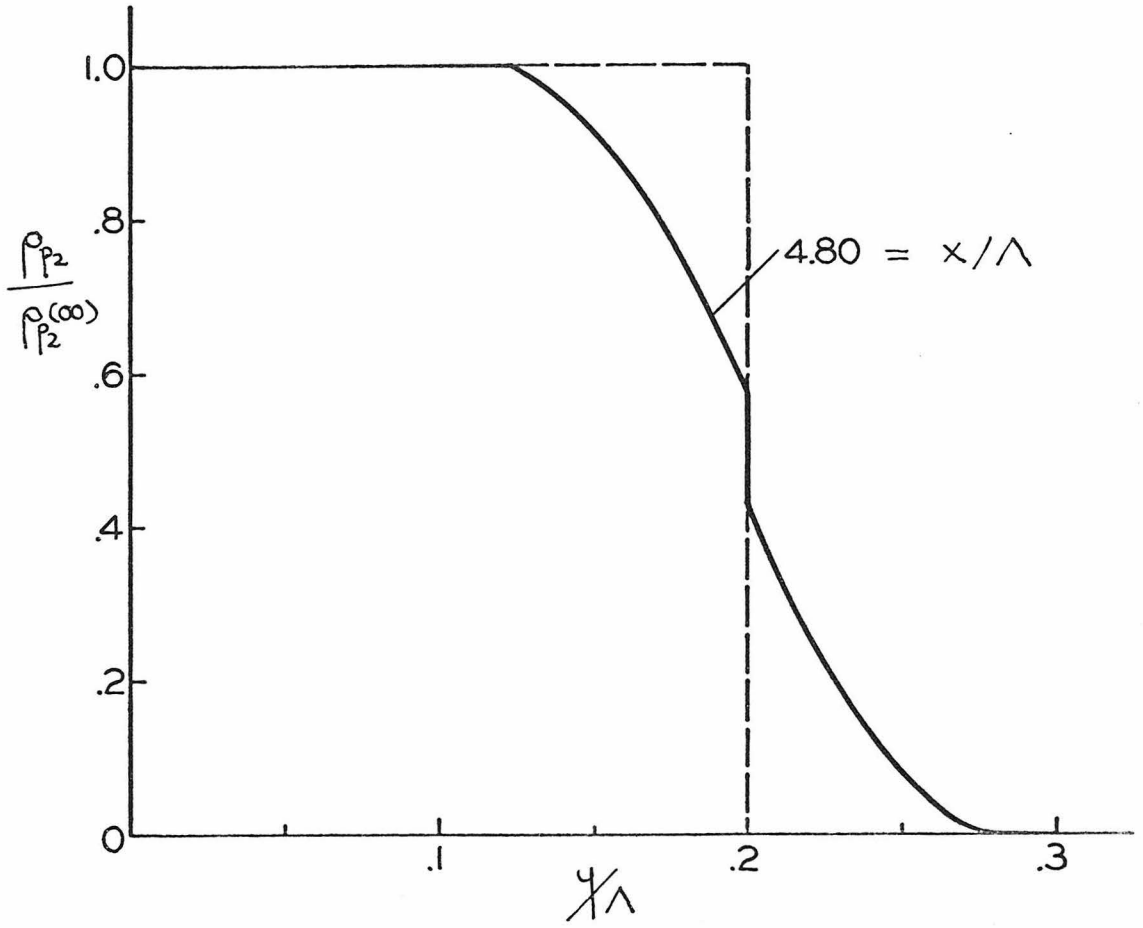

Figure 50. Final particle σ_2 uniform beam density distribution downstream of shock face. Upstream conditions; Gas-Air, $\rho(1) = 1.3 \times 10^{-4}$ g/cm^3, $T(1) = 20^\circ$C, $M_1 = 3.2$, $\gamma = 1.4$, $K_1 = .25$, $\rho_s/\rho(1) = 10^4$, $\sigma_2/\sigma_1 = 0.9$, $\sigma_1 = 4.3\,\mu$, $\Lambda = \lambda_{u_1} = 9.2$ cm, $c_s/c_p = \lambda_{u_1}/\lambda_{T_1} = 1$.

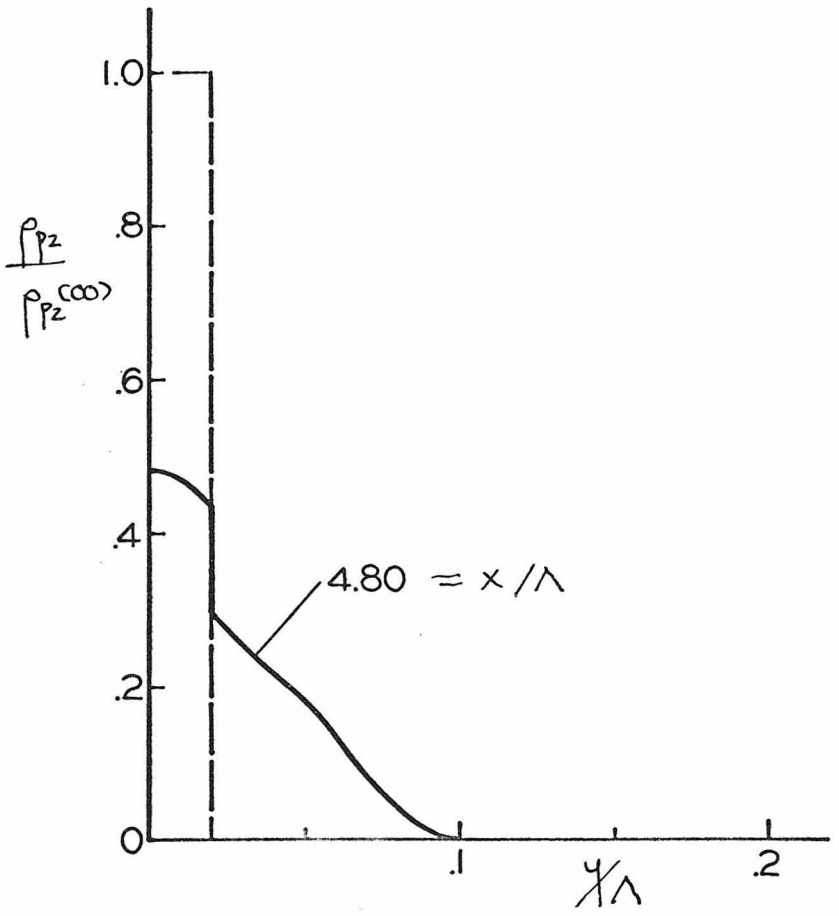

Figure 51. Final particle σ_2 uniform beam density distribution downstream of shock face. Upstream conditions; Gas-Air, $\rho(1) = 1.3 \times 10^{-4}$ g/cm^3 $T(1) = 20°C$, $M_1 = 3.2$, $\gamma = 1.4$, $\kappa_1 = .25$, $\rho_s/\rho(1) \approx 10^4$, $\sigma_2/\sigma_1 = 0.9$, $\sigma_1 = 4.3\,\mu$, $\Lambda = \lambda_{v_1} = 9.2$ cm, $c_s/c_p = \lambda_{v_1}/\lambda_{T_1} = 1$.

In Figures 48 and 49 the size of particles σ_2 has been varied keeping all other properties of the gas-particle mixture upstream of the shock wave constant. In Figures 50 and 51 the beam width has been varied holding other upstream properties fixed. For strong shock waves the relative velocity of the particles σ_1 and σ_2 may be large consequently the single collision condition is violated unless $\sigma_2/\sigma_1 \cong 1$ or K_1 is small. Since $u(2)/u(\infty)$ is a slowly varying function of K_1, in the region of interest, changing has little effect on $\tilde{y}_m$.

In Figure 52 $\tilde{p}_{ff_b}^{\nu(s)}$, calculated from Eq. (5.92), has been plotted for upstream gas-particle mixture conditions stated in the figure. A finite width uniform distribution related to this secondary fundamental beam by (5.91) appears as curve 1 in Figure 53. As discussed earlier, $\tilde{p}_{ff_b}^{\nu(s)}$ must vanish for $|\tilde{y}| > \tilde{y}_m$ since particles σ_2 can move only a finite distance across the gas flow following an encounter. The manner in which $\tilde{p}_{ff_b}^{\nu(s)}$ goes to zero as $|\tilde{y}| \to |\tilde{y}_m|$ may be accounted for by noting that $\lambda(x)$, the transverse range of particles σ_2, has a single peak at $x = x_m$ within the shock relaxation zone. Collisions that occur in the neighborhood of this peak contribute to $\tilde{p}_{ff_b}^{\nu(s)}$ near $\tilde{y}_m$. The sharp peak in $\tilde{p}_{ff_b}^{\nu(s)}$ at $\tilde{y} = 0$ is due to forward scattering of particles σ_2 and the fact that $\lambda(x) \to 0$ at the ends of the shock relaxation zone. The results shown in Figure 52 are representative of those corresponding to more general variations of $\tilde{p}_{ff_b}^{\nu(s)}$.

Consider curves 2 and 3 in Figure 53. For the same upstream state of the gas-particle mixture, the final density distribution of particles σ_2 has been computed using the single collision formalism,

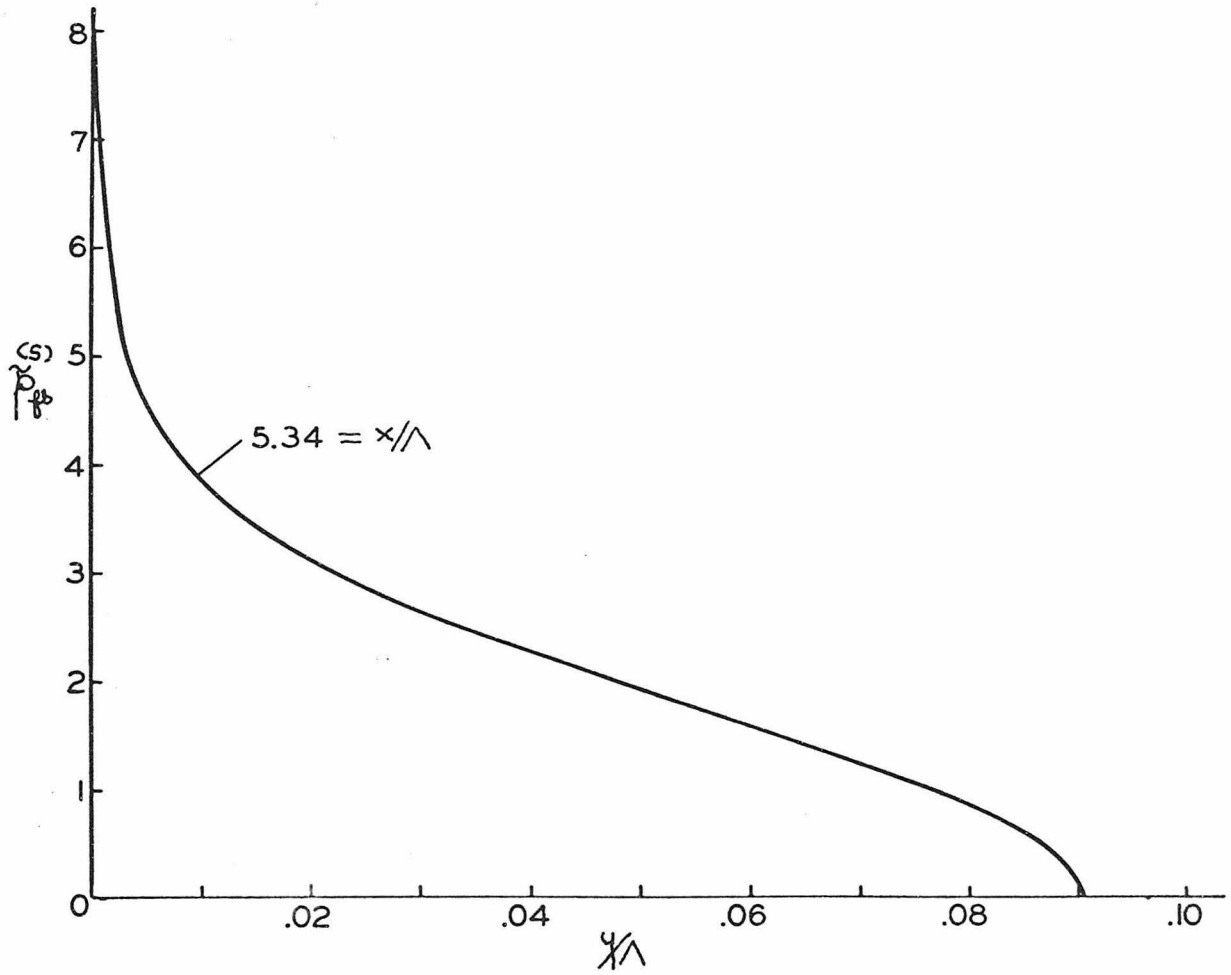

Figure 52. Final particle σ_2 secondary beam contribution to fundamental beam downstream of shock front. Upstream conditions; Gas-Air, $\rho(1) = 1.3 \times 10^{-4}$ gm/cm^3, $T(1) = 20°C$, $M_1 = 1.6$, $\gamma = 1.4$, $K_1 = .25$, $\rho_s/\rho(1) = 10^4$, $\sigma_2/\sigma_1 = 2/3$, $\sigma_1 = 3.5\,\mu$, $\Lambda = \lambda_{v_1} = 6.0$ cm, $c_s/c_p = \lambda_{v_1}/\lambda_{T_1} = 1$.

Eqs. (5.85)-(5.89), and the multiple collision or diffusion result, Eq. (4.183), of Chapter IV, respectively. In the calculation of curve 2 it was found that e^{-2} of the particles σ_2 passed through the shock relaxation zone without having a collision. In this case the diffusion model result, curve 3, may well afford the better approximation to the final density distribution. These results are so similar, however, as to suggest that the entire range of collision problems may be covered by the single collision and diffusion models and that no treatment of the difficult intermediate case is required.

On the basis of our results it appears that for upstream gas density greater than atmospheric density and $k_1 \sim O(.25)$, the single collision condition (5.82) is violated unless particles σ_2 and σ_1 are very small or very nearly the same size. Under these conditions their relative velocity is so small that the transverse range, $\lambda(x)$, of particles σ_2 is not large enough to cause a substantial redistribution of the cloud of particles σ_2. On the other hand, at lower pressures with the same particle loading, the restrictions on the particle sizes due to (5.82) are relaxed. The relative velocity of the particles is no longer small and their transverse range is such that important redistributions of particles σ_2 may result under single collision conditions. Further study is needed to examine all possible conditions of physical interest.

Rewriting (5.82) the essential condition for single collisions becomes;

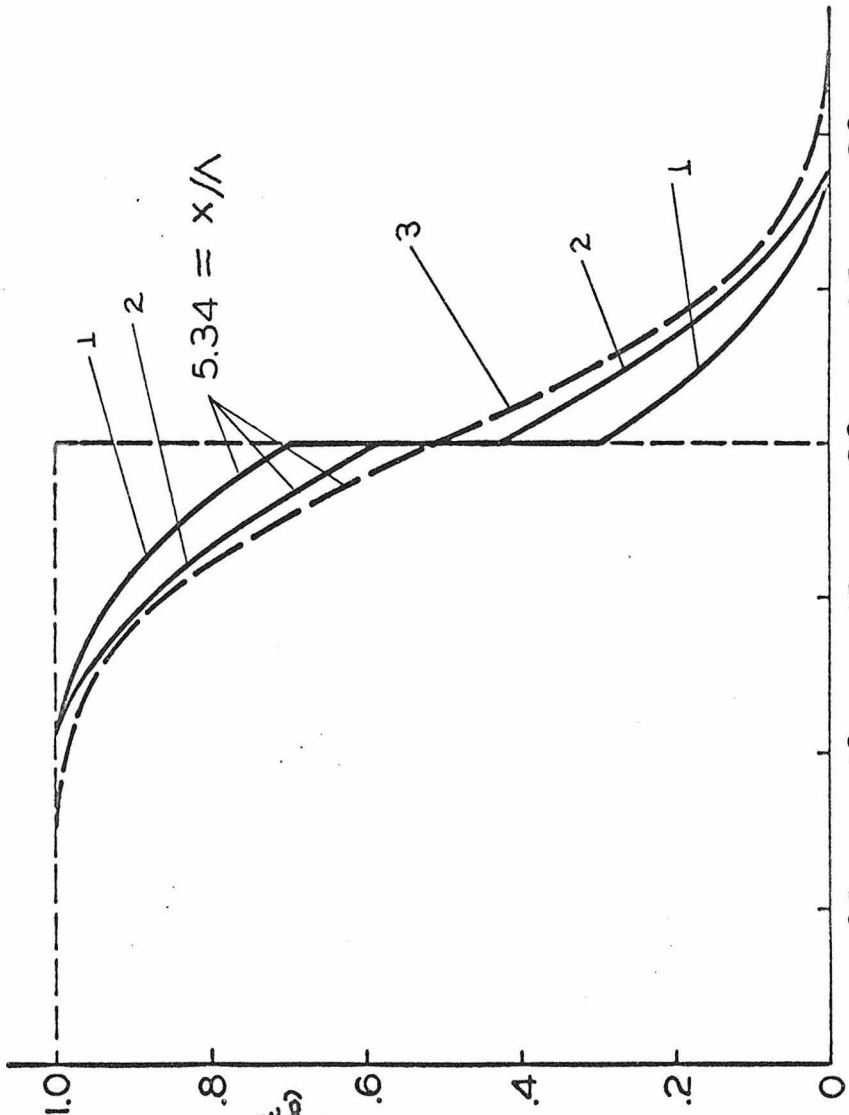

Figure 53. Final particle σ_z uniform beam density distributions downstream of shock front. Upstream conditions; Gas-Air; ((Curve 1; $\rho(1)=2.6\times10^{-4}$ gm/cm^3 $\rho_s/\rho(1)=.5\times10^4$, ((2) Curve 2 and 3; $\rho(1)=1.3\times10^{-4}$ gm/cm^3 $\rho_s/\rho(1)=10^4$, $T(1)=20^\circ C$, $M=1.6$, $\gamma=1.4$, $K_1=.25$, $\sigma_2/\sigma_1=2/3$, $\sigma_1=3.5\mu$, $\Lambda=\lambda_{w_1}=6.0\mu$, $c_s/c_p=\lambda_{w_1}/\lambda_{T_1}=1$.

$$\frac{K_1}{6}\left(\frac{\rho(1)\,\sigma_1\,a(1)}{\mu(1)}\right)\left(1+\frac{\sigma_2}{\sigma_1}\right)^2 \leq \left\{\int_0^{\tilde{\chi}_\infty}\left(\frac{M_1}{\tilde{u}_{p_1}}\right)\left(\frac{\tilde{u}_{p_1}}{\tilde{u}_{p_2}}-1\right)\left|\frac{d\tilde{\nu}}{d\tilde{x}}\right|\right\}^{-1} \tag{5.90}$$

It appears possible to study experimentally the interaction of a shock wave with a very thin stream of two particles sizes whose density is such that single collision conditions exist. By studying the redistribution of these particles due to collisions, it is possible to obtain direct evidence of the particle-particle interaction law.

VI. SUMMARY AND CONCLUSIONS

In this thesis the interaction of a normal gas dynamic shock wave with a gas containing a distribution of small solid spherical particles of two distinct radii, σ_1 and σ_2, was studied. In order to elucidate the essential physical features of the particle-particle and particle-gas interaction processes upstream of the shock wave particles σ_1 were assumed uniformly distributed with mass density ρ_{p1} and particles σ_2 were nonuniformly distributed parallel to the shock face with mass density ρ_{p2}. Ahead of the shock, particles and the gas were in mechanical and thermal equilibrium and $\rho_{p1} > \rho >> \rho_{p2}$. Under these conditions the gas-particle σ_1 flow downstream of the shock wave is one-dimensional and independent of the presence of particles σ_2. The usual shock relaxation zone is established by the interaction of particles σ_1 and the gas downstream of the shock wave.

By considering in some detail the effect of the particle σ_1-particle σ_2 and particle σ_2-gas interactions on the macroscopic motion of particles σ_2 in the shock relaxation zone, under the previous conditions, it has been the three-fold aim of this thesis (1) to demonstrate that the methods of kinetic theory can be extended to treat solid particle collision phenomena in multidimensional gas-particle flows; (2) to elucidate some of the essential physical characteristics of the dispersion of particles in a gas-particle flow field due to particle-particle encounters; and (3) to assess the importance of particle collisions in particle-laden gas flows.

To render the problem tractable, the scope of the investigation was restricted to physical conditions which allowed the collisional model proposed by Marble[3] to be extended to treat the three-dimensional motion of particles σ_2 downstream of the shock wave. This model is particularly important for two reasons. The criteria for its application are fairly straightforward and easy to handle. Secondly, particularly in the present problem, the model admits a wide class of physically interesting situations.

The essential feature of model is that the random velocity imparted to a particle σ_2 by a collision is damped by its viscous interaction with the gas before the particle σ_2 suffers another collision. The model used here also assumes the particle motion is governed by Stokes law and the viscous flow fields about each particle do not interfere during collision. Within the framework of the kinetic theory method used in this thesis, the last two conditions may be relaxed to include more general particle-particle and particle-gas interaction laws when necessary.

Within the previous restrictions the mean free path method of kinetic theory was extended to derive the macroscopic properties of particles σ_2 including particle σ_1-particle σ_2 and particle σ_2 -gas interactions. The gas-particle σ_1 relaxation zone was calculated in manner of references 4 and 6 . Within the restrictions of the collision model it was possible to analyze the macroscopic motion of particles σ_2 for the three important limiting cases: $(\sigma_2/\sigma_1)^2 >> 1$, $(\sigma_2/\sigma_1)^2 << 1$, and $(\sigma_2/\sigma_1)^2 \sim 1$.

When $(\sigma_2/\sigma_1)^2 >> 1$ the length of the shock relaxation zone,

established by the interaction of particles σ_1 and the gas, is small compared to the relaxation length of particles σ_2. Then downstream of the shock wave particles σ_2 are moving through a uniform distribution of particles σ_1. Consequently there is essentially no redistribution of particles σ_2 normal to the gas flow. The only effect of particle σ_1 - particle σ_2 encounters is a drag force acting to retard particles σ_2.

When $(\sigma_2/\sigma_1)^2 \ll 1$ the large difference between velocities of particles σ_2 and particles σ_1 results in many collisions for each particle σ_2 while traversing the relaxation zone. As a consequence of these collisions there is a force of interaction between the two particle clouds which opposes the viscous force exerted on the particles σ_2 by the gas and tends to accelerate particles σ_2. It was found this force may significantly exceed the viscous force exerted on the particles by the gas.

In addition the collisions cause a diffusion of particles σ_2 across the gas flow. The characteristic stepsize of this diffusion process is the local maximum transverse range of particles σ_2. The transverse range is defined as the maximum distance a particle can move across the gas flow as the result of a local collision. Although the dispersion of particles σ_2 is inhibited by the viscous force, there exists a wide range of physically interesting conditions for which collisional effects dominate the viscous forces. Under such circumstances there may be a substantial redistribution of particles σ_2 downstream of the shock wave.

As an example, consider a normal gas dynamic shock with

Mach number 3.2 passing through a gas-particles suspension with the following properties; atmospheric air at 20°C, metal particles with $\frac{\rho_s}{\rho} = 10^3$, $\frac{c_s}{c_p} \simeq 1$, $\frac{\rho_{p1}}{\rho} = .25$, $\frac{\sigma_2}{\sigma_1} = \frac{1}{4}$ and $\sigma_1 = 8.0\mu$. If particles σ_2 are distributed over a beam of 1cm wide upstream of the shock wave then, far downstream, collisions will have diffused the beam into one about 12.6 cm wide. The characteristic dimension of the density distribution of particles σ_2 has been increased by a factor of 12.6 due to particle-particle collisions. In addition it has been found that increasing the shock Mach number and the particle loading increases the degree of dispersion of particles σ_2. However, moderate increases in the particle σ_1 loading do not result in corresponding increases in particle σ_2 dispersion. One of the most significant factors affecting the degree of dispersion of particles σ_2 is the radius ratio σ_2/σ_1. When $\sigma_2/\sigma_1 \to 0$ the transverse range of particles σ_2 is significantly reduced. On the other hand, as σ_2/σ_1 approaches unity but stays different from it, the degree of dispersion of particles σ_2, due to several scattering events in the shock relaxation zone, was found to increase considerably. The appropriate conclusion here is that the collisional dispersion of particles σ_2 is most important when the particle radii σ_2 and σ_1 are the same order of magnitude. Clearly, however, thedispersion vanishes when $\sigma_1 = \sigma_2$.

To examine the case when $\sigma_2/\sigma_1 \simeq 1$ it was assumed that particles σ_2 had at most one collision during their passage through the shock relaxation zone. It was found again that the redistribution of particles σ_2 due to collision with particles σ_1 was limited by the maximum value of the transverse range of particles σ_2 which is

attained within the shock relaxation zone. A rigorous condition was established under which the single collision model is valid. The results of these calculations showed that for low particle σ_1 loadings or upstream gas densities less than atmospheric, and permissible values of σ_2/σ_1, single collision events may result in an important redistribution of particles σ_2.

The general results that have been obtained indicate the significant results associated with particle collisions in dusty gases may be examined by extending the methods of kinetic theory. On the basis of the similarity between shock relaxation flow and other gas-particle flow problems of interest, it is expected that the general kinetic theory calculation procedures established here should have a relatively wide range of applicability. Certainly as our theoretical and experimental understanding of the effects of particle-particle interactions on gas-particle flows increases a more comprehensive kinetic theory treatment will evolve.

One of the most substantial obstacles to extending our analysis is the lack of good experiment regarding the particle-particle and particle-gas interaction laws. Definitive experiments to establish these laws are needed.

The calculations which have been described indicate that the experimental study of shock waves passing through gas-particle suspensions, may be particularly well suited for investigating particle-particle interactions and other non-equilibrium phenomena in solid particle-gas flows. By controlling σ_2/σ_1 and upstream gas-particle conditions the results obtained make it possible to study both the

collisional regime, $\tau_{v_2} < \tau_{c_{21}}$, and the single collision regime of the particle-gas relaxation flow. By measuring the dispersion of the particle σ_2 cloud downstream of the shock wave, the important physical constants for given particle-particle and particle-gas interaction laws may be measured.

REFERENCES

(1) Zenz, F. A. and Othmer, D. F., Fluidization and Fluid-Particle Systems, Reinhold Publishing Corp., New York (1960).

(2) Soo, S. L., Fluid Dynamics of Multiphase Systems, Blaisdell Publishing Company, Massachusetts (1967).

(3) Marble, F. E., "Mechanism of Particle Collision in the One-Dimensional Dynamics of Gas-Particle Mixtures," The Physics of Fluids, 7, 1270 (1964).

(4) Marble, F. E., "Dynamics of a Gas Containing Small Solid Particles," Proceedings of the Fifth AGARD Combustion and Propulsion Colloquium, Pergamon Press, New York (1963).

(5) Carrier, G. F., "Shock Waves in a Dusty Gas," J. Fluid Mechanics, 4, 376 (1955).

(6) Rudinger, G., "Some Properties of Shock Relaxation in Gas Flows Carrying Small Particles," The Physics of Fluids, 7, 658 (1964).

(7) Kriebel, A. R., "Analysis of Normal Shock Waves in Particle-Laden Gas," Journal of Basic Engineering, Transactions of ASME, 655, (December, 1964).

(8) Hoglund, R. F., "Recent Advances in Gas-Particle Nozzle Flows," J. American Rocket Society, 32, 662 (1962).

(9) McLaughlin, M. H., "Experimental Study of Particle-Wall Collision Relating to Flow of Solid Particles in a Fluid," Thesis, California Institute of Technology (1968).

(10) Torobin, L. B. and Gauvin, W. H., "Fundamental Aspects of Solids-Gas Flow," Canadian Journal of Chemical Engineering, Part I, p. 129 (Aug. 1959); Part II, p. 167 (Oct. 1959); Part III, p. 224 (Dec. 1959); Part IV, p. 142 (Oct. 1960); Part V, p. 189 (Dec. 1960).

(11) Fuks, N. A., The Mechanics of Aerosols, Revised Edition, Pergamon Press (1964).

(12) Present, R. D., Kinetic Theory of Gases, McGraw-Hill Book Company, Inc. (1958).

(13) Chandrasekhar, S., "Stochastic Problems in Physics and Astronomy," Rev. Mod. Phys., 15, p. 1 (1943).

(14) Courant, R. and Hilbert, D., Methods of Mathematical Physics, Vol. II, Interscience, New York (1965).

(15) Jeans, J., The Dynamical Theory of Gases, Dover Publications, 4th Edition (1954), p. 293.

(16) Rudinger, G., Multi Phase Symposium, edited by N. J. Lipstein (American Society of Mechanical Engineers, New York, 1963), p. 55.

APPENDIX A

DYNAMICS OF THE COLLISION PROCESS

On the basis of the results presented in Chapter II, Section 3 the collision process has been treated as the interaction of two rigid elastic spheres. The effect of the gas on the particle-particle interaction has been neglected. In this Appendix we consider the collision of two elastic spheres of radius σ_1 and σ_2 in sufficient detail to establish the results required in the calculations of Chapters IV and V. Prior to the collision the spheres are assumed to be moving parallel to the x axis at the local collisionless velocities, u_{p_1} and u_{p_2}, of particles σ_1 and σ_2 respectively.

1. Collision of particles σ_1 and σ_2 as viewed in the local collisionless velocity frame of particles σ_2.

The reference frame, $x'y'z'$, is moving at the local collisionless velocity, u_{p_2}, of particles σ_2. The appropriate geometrical description of the collision is presented in Figure A1. Since $\lambda_{v_1}, \lambda_{v_2} >> \sigma_1$, σ_2 then $\frac{\partial}{\partial x}(u_{p_1} - u_{p_2}) << \frac{(u_{p_1} - u_{p_2})}{(\sigma_1 + \sigma_2)}$ and consequently the velocities of the particles used to analyze the collision process may be evaluated at the same value of x. Prior to the collision, as indicated in Figure (A1-i), particle σ_2 is at rest and particle σ_1 is approaching from the negative x' direction with impact parameter b' and azimuthal angle φ'. We have assumed, without loss of generality, that $u_{p_1}(x) > u_{p_2}(x)$. The spheres are considered to interact only at the instant of contact. Then the momentum of particle σ_2 immediately before impact is $m_1(u_{p_1}(x) - u_{p_2}(x))$ where x is the position of the origin of $x'y'z'$ downstream of the shock wave which

(i) Immediately before collision (ψ' is contact angle)

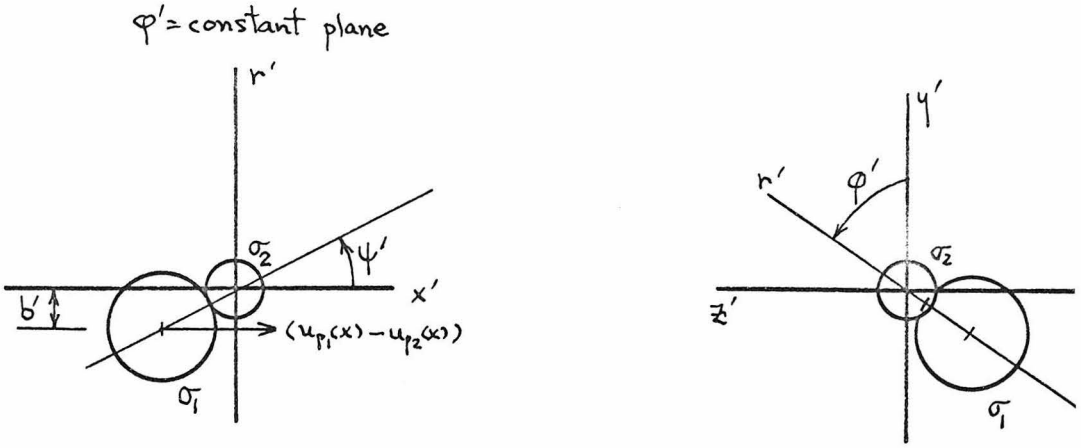

(ii) Immediately after collision

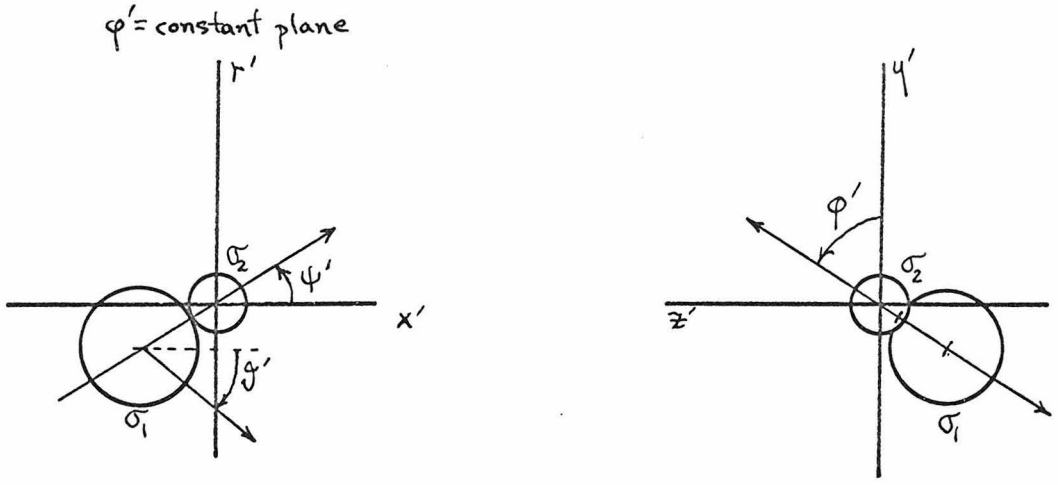

Figure A1.

is also the center of particle σ_2. For smooth elastic spheres during the instant of contact, see Figure (A1-ii), the force of interaction is along their line of centers, described by the contact angle ψ and azimuthal angle φ'. Consequently the total angular momentum of the particles is conserved and the entire collision event takes place in the φ' = constant plane. Furthermore, during the collision the spheres exchange momentum only along their line of centers which, as mentioned, is denoted by ψ' in the φ' = constant plane. Consequently, referring to Figure (A1-ii), after the collision, particle σ_2 recoils in the direction ψ' and particle σ_1 is scattered into angle ϑ' both particles remaining in the φ' = constant plane. By conservation of momentum and energy;

$$m_1(u_{p_1}(x) - u_{p_2}(x)) = m_1 |\underline{u}_{p_1}^{(f)}(x)| \cos\vartheta' + m_2 |\underline{u}_{p_2}^{(f)}(x)| \cos\psi' \qquad (A1.1)$$

$$0 = m_1 |\underline{u}_{p_1}^{(f)}(x)| \sin\vartheta' + m_2 |\underline{u}_{p_2}^{(f)}(x)| \sin\psi' \qquad (A1.2)$$

$$\frac{m_1}{2}(u_{p_1}(x) - u_{p_2}(x))^2 = \frac{m_1}{2} |\underline{u}_{p_1}^{(f)}(x)|^2 + \frac{m_2}{2} |\underline{u}_{p_2}^{(f)}(x)|^2 \qquad (A1.3)$$

we obtain three equations in three unknowns; $|\underline{u}_{p_1}^{(f)}(x)|$, $|\underline{u}_{p_2}^{(f)}(x)|$, and ϑ'. The contact angle ψ' is related to the impact parameter b' by simple geometry,

$$b' = (\sigma_1 + \sigma_2) \sin\psi' \qquad (A1.4)$$

Since in the calculations we are only interested in the motion of particle σ_2 following the collision if we let:

$$\underline{u}^{(f)}_{p_2}(x) = u^{(f)}_{p_2}(x)\,\underline{e}_{x'} + v^{(f)}_{p_2}(x)\,\underline{e}_{y'} + w^{(f)}_{p_2}(x)\,\underline{e}_{z'}$$

$$= u^{(f)}_{p_2}(x)\,\underline{e}_{x'} + u^{(f)}_{p_2 r}(x)\,\underline{e}_{r'}$$, where $\underline{e}_{x'}$, $\underline{e}_{y'}$, $\underline{e}_{z'}$, and $\underline{e}_{r'}$ are unit vectors in the x', y', z' and r' directions, respectively, then the solution of Equations (A1.1-A1.3) for the velocity of particle σ_2 after the collision is;

$$u^{(f)}_{p_2}(x) = |\underline{u}^{(f)}_{p_2}(x)| \cos\psi' = \frac{m_1}{m_1+m_2}(u_{p_1}(x) - u_{p_2}(x))(1+\cos 2\psi') \quad \text{(A1.5)}$$

$$u^{(f)}_{p_2 r}(x) = |u^{(f)}_{p_2}(x)| \sin\psi' = \frac{m_1}{m_1+m_2}(u_{p_1}(x) - u_{p_2}(x)) \sin\psi' \quad \text{(A1.6)}$$

The y' and z' components of velocity are derivable from the radial velocity component $u^{(f)}_{p_2 r}(x)$ and are given by;

$$v^{(f)}_{p_2}(x) = \frac{m_1}{m_1+m_2}(u_{p_1}(x) - u_{p_2}(x)) \cos\varphi' \sin 2\psi' \quad \text{(A1.7)}$$

$$w^{(f)}_{p_2}(x) = \frac{m_1}{m_1+m_2}(u_{p_1}(x) - u_{p_2}(x)) \sin\varphi' \sin 2\psi' \quad \text{(A1.8)}$$

Immediately following the collision the tip of the velocity vector of particle σ_2 lies on a sphere in the velocity space, for the $x'y'z'$ reference frame, that is displaced from the origin by an amount $\frac{m_1}{m_1+m_2}(u_{p_1}(x) - u_{p_2}(x))$. The situation is sketched in Figure A2. In the present case where $u_{p_1}(x) > u_{p_2}(x)$ the scattering is entirely forward as viewed in $x'y'z'$ frame of reference; Figure (A2-i). However, formulas (A1.5-A1.8) are also valid if $u_{p_1}(x) < u_{p_2}(x)$ provided ψ', φ' and b' retain their meaning. When $u_{p_1}(x) < u_{p_2}(x)$

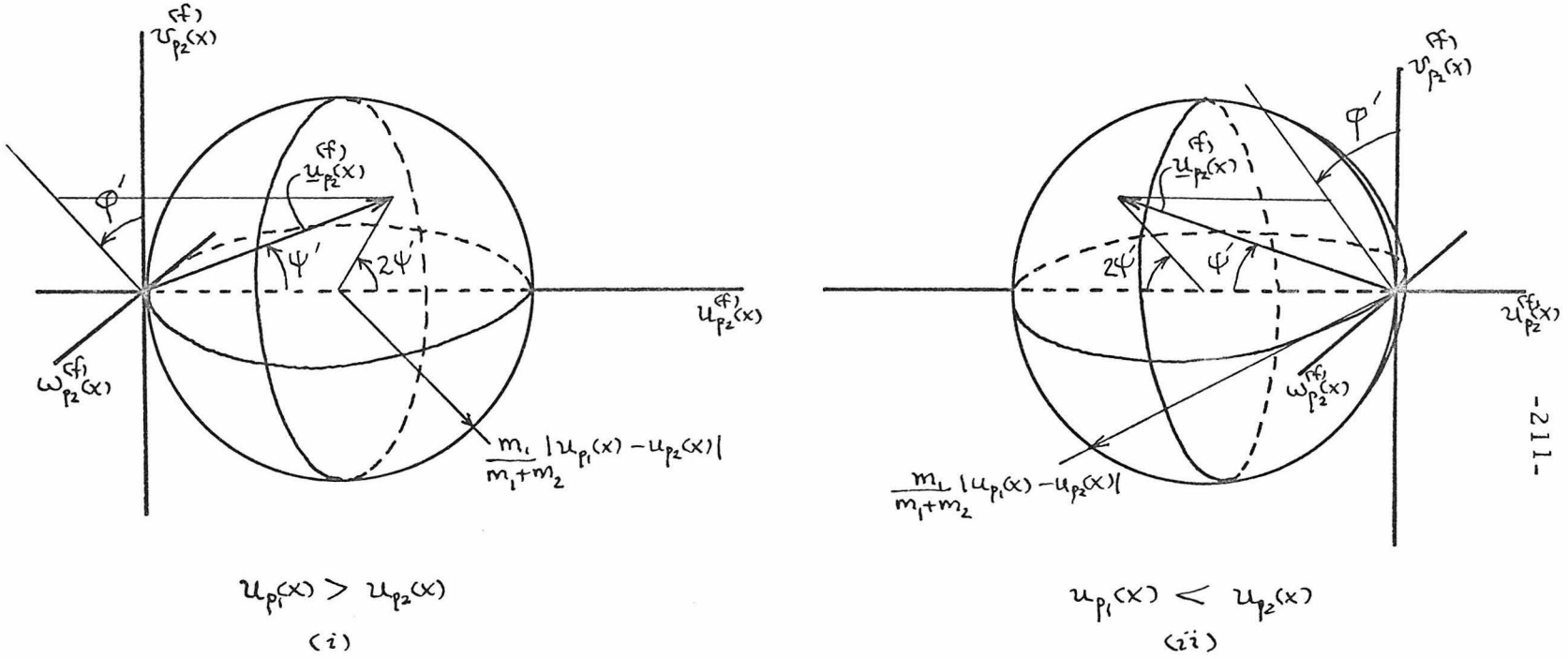

Figure A2. Recoil velocity sphere for particles σ_2

and particles σ_2 overtake particles σ_1 in the local collisionless velocity frame $x'y'z'$ of particles σ_2 the scattering is all backward; Figure (A2-ii).

2. Statistics of encounter for particle σ_2 relative to reference frame $x'y'z'$.

Consider a small volume element dV' centered at the origin of the reference frame $x'y'z'$ which is moving at the local collisionless velocity of particles σ_2. We wish to calculate dN_{p_2}, the average number of particles of radius σ_2 that are scattered, due to collisions with particles σ_1, out of dV in a time interval $t - t + dt$ and into a solid angle $d\Omega' = \sin\psi' d\psi' d\varphi'$ which is centered in dV'. The angles ψ' and φ' are defined, as in the previous section, as the contact angle and azimuthal angle, respectively, for a collision between a particle of radius σ_2 with a particle σ_1 that occurs within dV'. Variation of ψ' and φ' for collision events throughout dV' is neglected. We suppose that encounters in which more than two particles take part are negligible in number and effect, compared with binary encounters. This is consistent with the previous assumption that the distribution of particles is dilute. Collisions occupy only a small fraction of the life of a particle σ_2.

In considering such encounters within dV' it will be assumed that both sets of particles are moving at their local collisionless velocities before impact and that they are randomly distributed across dV'. Particles σ_2 are essentially at rest in dV while particles approach them along the negative x' direction. During the calculation

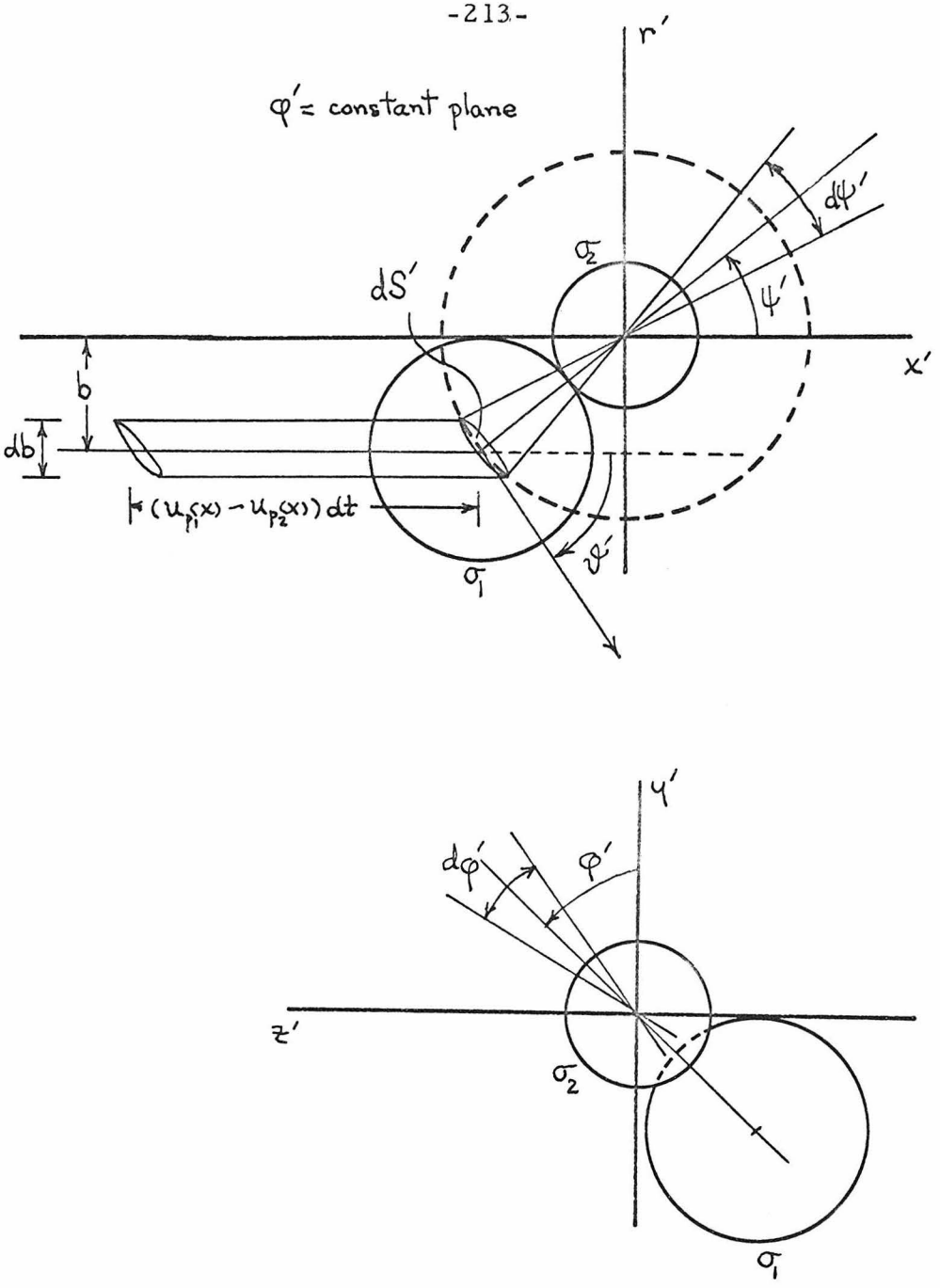

Figure 13. Collision diagram

we will assume $u_{p_1}(x) > u_{p_2}(x)$. Then there is no correlation between their position in dV' and their velocity. Also the interval of time dt will be taken to be small compared to the time scales governing the motion of the particles between successive encounters, but large compared to the duration of an encounter which in the present case involving hard spheres is quite short.

Now since the contact angle ψ' is related to the impact parameter b' of particle σ_1 prior to collision by (A1.4) then dN_{p_2} is also the number of collisions between particles σ_1 and σ_2 within dV' in a time $t \sim t+dt$ where the geometric encounter variables b' and φ' of particle σ_2 are located in the range $b'-b'+db'$ and $\varphi'-\varphi'+d\varphi'$. This is apparent from Figure A3. Let us now compute dN_{p_2} from this point of view. Consider Figure A3, the number of collisions that occur in time dt , between a given particle σ_2 and particles σ_1 , is equal to the number of incident particles of radius σ_1 whose centers are to be found in the oblique cylinder of base area $dS' = (\sigma_1+\sigma_2)^2 \sin\psi' d\psi' d\varphi'$ and slant length $(u_{p_1}(x) - u_{p_2}(x))dt$. This number is simply the volume of the cylinder $(u_{p_1}(x) - u_{p_2}(x))dt \cos\psi' dS'$ multiplied by the local number density, $n_{p_1}(x)$, of particles σ_1 . This gives the number of particles of radius σ_1 scattered from a single particle of radius σ_2 in dV' during time dt , such that particle σ_2 recoils into solid angle $d\Omega'$;

$$n_{p_1}(x)\,(u_{p_1}(x) - u_{p_2}(x))\,(\sigma_1+\sigma_2)^2 \cos\psi' d\Omega' dt \qquad \text{(A2.1)}$$

This follows because particles exchange momentum only along their line of centers and hence particles σ_2 recoil into the angle $\psi'-\psi'+d\psi'$ on each collision where particle σ_1 has impact parameter $b'-b'+db'$. Multiplying (A2.1) by $n_{p_2}(\underline{x})\,dV'$ the total number of scattering centers, particles σ_2, in dV' we obtain dN_{p_2} ;

$$dN_{p_2} = n_{p_1}(x)\, n_{p_2}(\underline{x})\,(u_{p_1}(x)-u_{p_2}(x))(\sigma_1+\sigma_2)^2\cos\psi'\sin\psi'\,d\psi'd\varphi'dV\,dt \qquad \text{(A2.2)}$$

Strictly speaking $n_{p_2}(\underline{x})$ should be the density of particles in dV' that are essentially at rest awaiting a collision. This is not the average density since there will be particles of radius σ_2 passing through that are not eligible, under assumption $\tau_{u_2} < \tau_{c21}$, for a collision. As an approximation we will neglect this discrepancy and assume $n_{p_2}(\underline{x})$ is, indeed, the average density of particles σ_2 within dV' . This approximation becomes less accurate as the velocity equilibration time, τ_{u_2} , of particles σ_2 approaches the average time between successive collisions, $\tau_{c_{21}}$, for a particle σ_2 .

Then from (A2.2) the number $\frac{dN}{dt}p_2(\underline{x})$ of particles of radius σ_2 scattered per unit time $d\Omega'$ due to collisions in dV' at a position $\underline{x}$ relative to the shock face, is;

$$\frac{dN}{dt}p_2(\underline{x}) = n_{p_1}(x)\, n_{p_2}(\underline{x})\,(u_{p_1}(x)-u_{p_2}(x))(\sigma_1+\sigma_2)^2\cos\psi'\,d\Omega'dV' \qquad \text{(A2.3)}$$

If $u_{p_2}(x) > u_{p_1}(x)$, appropriate redefinition of ψ', φ' and b' as in Figure (A2-ii) leads to

$$\frac{dN_{p2}(\underline{x})}{dt} = n_{p_1}(x)\, n_{p_2}(\underline{x})(u_{p_2}(x) - u_{p_1}(x))(\sigma_1+\sigma_2)^2 \cos\psi' d\Omega' dV' \quad \text{(A2.4)}$$

Therefore if ψ' and φ' are appropriately defined as the contact angle and azimuthal angle, respectively, for a collision in dV' that in general;

$$\frac{dN_{p2}(\underline{x})}{dt} = n_{p_1}(x)\, n_{p_2}(\underline{x})\,|u_{p_1}(x) - u_{p_2}(x)|(\sigma_1+\sigma_2)^2 \cos\psi' d\Omega' dV' \quad \text{(A2.5)}$$

Alternatively Eq. (A2.5) may be expressed in terms of the pre collision coordinates of particle σ_2. Using (A1.4);

$$\frac{dN_{p2}(\underline{x})}{dt} = n_{p_1}(x)\, n_{p_2}(\underline{x})\,|u_{p_1}(x) - u_{p_2}(x)|\, b' db' d\varphi' dV' \quad \text{(A2.6)}$$

Since the impact parameter (b', φ') of the collision are the same in all reference frames moving parallel to the x' or x axis (A2.6) is the same in these reference frames.

3. Collision of particles σ_1 and σ_2 as viewed in their center of mass reference frame.

Consider the collision process discussed in the last two sections as viewed in the center of mass reference frame $\bar{x}\,\bar{y}\,\bar{z}$ where the total momentum of the colliding particles is zero. The velocity of this frame relative to the rest frame of the shock wave is;

$$\underline{V}_{cm} = V_{cm}\, e_x = \left(\frac{m_1 u_{p_1} + m_2 u_{p_2}}{m_1+m_2}\right) e_x \quad \text{(A3.1)}$$

The geometry of the collision for $u_{p_1}(x) > u_{p_2}(x)$ is given in Figure A4. In contrast to normal convention we define the scattering

(i) Immediately before collision (Contact angle $\bar{\Psi}$)

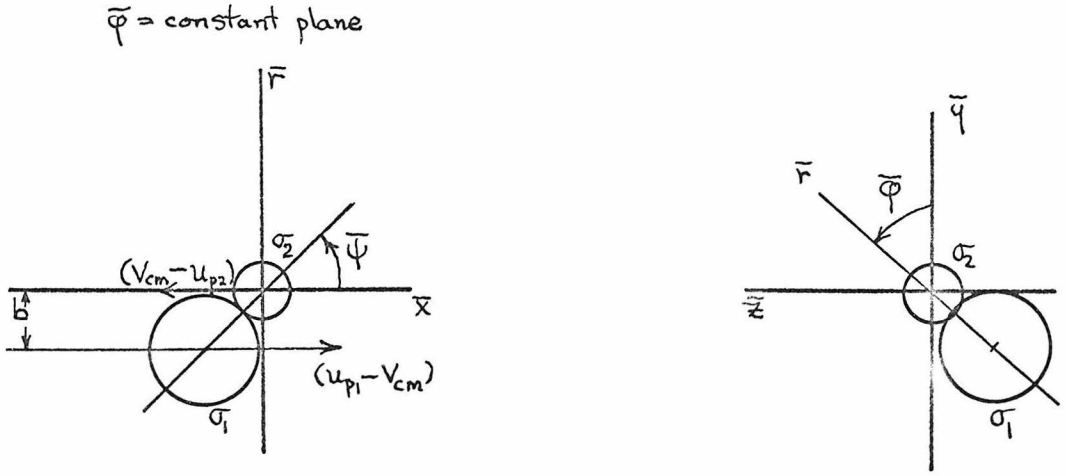

(ii) Immediately after collision

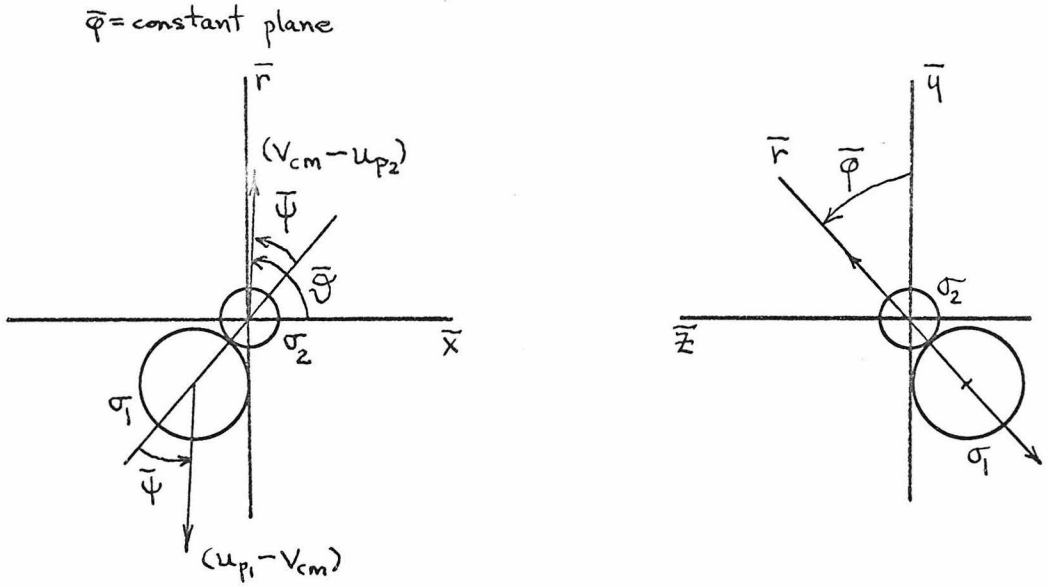

Figure A4.

or recoil angle of particle σ_2 as $\bar{\vartheta} = 2\bar{\Psi}$ since in the present case $\bar{\vartheta}$ is measured with respect to the positive $\bar{x}$ axis. We note the collision in this frame preserves the magnitudes of the particle velocities. The velocity components of the particle σ_2 in this frame after the collision can be written using Figure A4;

$$u_{p_2}^{(f)}(x) = (V_{cm} - u_{p_2})\cos\bar{\vartheta} = \frac{m_1}{m_1+m_2}(u_{p_1} - u_{p_2})\cos\bar{\vartheta} \qquad \text{(A3.2)}$$

$$v_{p_2}^{(f)}(x) = (V_{cm} - u_{p_2})\sin\bar{\vartheta}\cos\bar{\varphi} = \frac{m_1}{m_1+m_2}(u_{p_1} - u_{p_2})\sin\bar{\vartheta}\cos\bar{\varphi} \qquad \text{(A3.3)}$$

$$w_{p_2}^{(f)}(x) = (V_{cm} - u_{p_2})\sin\bar{\vartheta}\sin\bar{\varphi} = \frac{m_1}{m_1+m_2}(u_{p_1} - u_{p_2})\sin\bar{\vartheta}\sin\bar{\varphi} \qquad \text{(A3.4)}$$

where $\underline{u}_{p_2}^{(f)} = u_{p_2}^{(f)}\underline{e}_x + v_{p_2}^{(f)}\underline{e}_y + w_{p_2}^{(f)}\underline{e}_z$

The impace parameter is related to the contact angle $\bar{\Psi}$ by;

$$b = (\sigma_1 + \sigma_2)\sin\bar{\Psi} \qquad \text{(A3.5)}$$

The velocity diagram for this collision relative to the rest frame of the shock wave is given in Figure A5.

4. Statistice of encounters for particles σ_2 as viewed in the center of mass frame.

Referring to Section 2 for some of the details the number per second of particles σ_2 scattered in a volume element dV relative to the center of mass frame is;

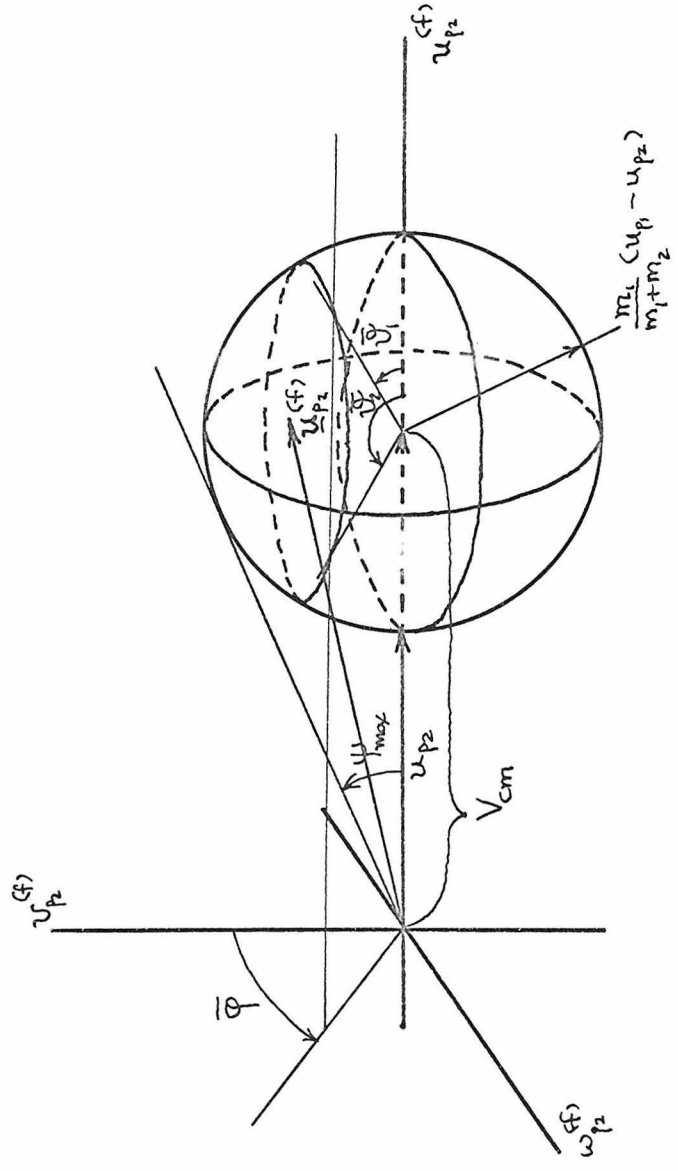
$u_{pz}^{(f)}$
$\frac{m_1}{m_1+m_2}(u_{pi}-u_{pz})$
$u_{pz}^{(f)}$
θ_{max}
u_{pz}
V_{cm}
$u_{pz}^{(f)}$
θ
$u_{pz}^{(f)}$

Figure A5.

$$\frac{dN_{p_2}(\underline{x})}{dt} = n_{p_1}(x)\, n_{p_2}(\underline{x})\, |u_{p_1}(x) - u_{p_2}(x)|\, b\, db\, d\bar{\varphi}\, dV \qquad \text{(A4. 1)}$$

where $(b, \bar{\varphi})$ are the impact variables of the collision. Using (A3. 5) this may be expressed in terms of the contact angle $\bar{\Psi}$ as;

$$\frac{dN_{p_2}(\underline{x})}{dt} = n_{p_1}(x)\, n_{p_2}(\underline{x})\, |u_{p_1}(x) - u_{p_2}(x)|\, (\sigma_1+\sigma_2)^2 \sin\bar{\Psi}\cos\bar{\Psi}\, d\bar{\Psi}\, d\bar{\varphi}\, dV \qquad \text{(A4. 2)}$$

or in terms of the recoil angle $\bar{\vartheta}$;

$$\frac{dN_{p_2}(d\bar{\Omega})}{dt} = n_{p_1}(x)\, n_{p_2}(\underline{x})\, |u_{p_1}(x) - u_{p_2}(x)|\, \frac{(\sigma_1+\sigma_2)^2}{4} \sin\bar{\vartheta}\, d\bar{\vartheta}\, d\bar{\varphi}\, dV \qquad \text{(A4. 3)}$$

where $0 \le \bar{\vartheta} \le \pi$ and $0 \le \bar{\varphi} \le 2\pi$. Then (A4. 3) is the number per second of particles σ_2 scattered out of dV into the solid angle $d\Omega = \sin\bar{\Psi}\, d\bar{\Psi}\, d\bar{\varphi}$.

APPENDIX B

CYLINDRICAL SYMMETRY - $\sigma_2/\sigma_1 \ll 1$

Within the assumptions set forth in Chapter IV, consider the collisional dispersion of particles downstream from the shock wave when their densities upstream are given by;

$$\rho_{p_2}^{(1)}(y,z) = m_2 N_{p_2}\, \delta(y)\, \delta(z) \tag{B. 1}$$

and

$$\rho_{p_2}^{(1)}(r) = \begin{cases} \rho_{p_2}(1) & |r| \le r_b \\ 0 & r \text{ otherwise} \end{cases} \tag{B. 2}$$

The independent variable r is the radial coordinate of a polar coordinate system (r, θ, x) with the $r\theta$ plane on the downstream face of the shock wave.

When the density of particles σ_2 upstream of the shock wave is given by the delta function distribution (B. 1) then downstream of the shock wave their density is given by the fundamental beam solution, Eq. (4. 149);

$$\rho_{p_2}^{(f)}(x,r) = m_2 N_{p_2}\left(\frac{u_{(1)}}{v_{p_2}(x)}\right)\frac{e^{-r^2/4S(x)}}{4\pi S(x)} \tag{B. 3}$$

The notation of Chapter IV is used throughout Appendix B. Introducing the dimensionless variables in Equations (4. 157) and (4. 158)

$$\tilde{\rho}^{(f)}_{\rho_2}(\tilde{x},\tilde{r}) = \left(\frac{M_1}{\tilde{v}_{\rho_2}(\tilde{x})}\right)\frac{e^{-\tilde{r}^2/4D\tilde{\xi}(\tilde{x})}}{4\pi D\tilde{\xi}(\tilde{x})} \qquad \text{(B. 4)}$$

where $r = \lambda_{v_1}\tilde{r}$ and $\rho^{(f)}_{\rho_2} = \rho_{\rho_2(0)}\tilde{\rho}^{(f)}_{\rho_2} = m_2\left(N_{\rho_2}/\lambda^2_{v_1}\right)\tilde{\rho}^{(f)}_{\rho_2}$.

The fundamental beam solutions (B. 3) and (B. 4) represent the limiting case of very narrow upstream density distributions whose radial dimensions are much less than λ_{v_1}.

The density of particles σ_2 downstream from the shock wave for a general density distribution, $\rho^{(1)}_{\rho_2}(y,z)$, of particles σ_2 upstream of the shock wave is given by Eq. (4.150);

$$\rho_{\rho_2}(x,y,z) = \left(\frac{u_{(1)}}{v_{\rho_2(x)}}\right)\frac{1}{4\pi\xi(x)}\int_{-\infty}^{\infty}\int \rho^{(1)}_{\rho_2}(y',z')\, e^{-\{(y-y')^2+(z-z')^2\}/4\xi(x)}\, dy'dz' \qquad \text{(B. 5)}$$

Changing variables in (B. 5) from cartesian coordinates to cylindrical coordinates and using the upstream density distribution (B. 2) we obtain;

$$\rho_{\rho_2}(r) = \rho_{\rho_2(1)}\left(\frac{u_{(1)}}{v_{\rho_2(x)}}\right)\frac{e^{-r^2/4\xi(x)}}{4\pi\xi(x)}\int_0^{r_b} R(r,r',\theta)\, e^{-r'^2/4\xi(x)}\, r'dr' \qquad \text{(B. 6)}$$

where;

$$R(r,r',\theta) = \int_0^{2\pi} e^{rr'\cos(\theta'-\theta)/2\xi(x)}\, d\theta' \qquad \text{(B. 7)}$$

The integral of B. 7 may be rewritten, using the relation

$$e^{z\cos\vartheta} = I_0(z) + 2\sum_{k=1}^{\infty} I_k(z)\cos k\vartheta \qquad \text{(B. 8)}$$

where $I_n(z)$ is the n^{th} order modified Bessel function. Substituting (B. 8) into (B. 7) and carrying out the integration in Θ we obtain;

$$R(r,r',\theta) = 2\pi I_0\left(\frac{rr'}{2s(x)}\right) \qquad \text{(B. 9)}$$

a result that is independent of Θ as expected by symmetry considerations. Substituting (B. 9) into (B. 6) we obtain;

$$\rho_{p_2}(x,r) = \rho_{p_2}(1)\left(\frac{u(1)}{v_{p_2}(x)}\right)\frac{e^{-r^2/4s(x)}}{2s(x)}\int_0^{r_b} I_0\left(\frac{rr'}{2s(x)}\right)e^{-r'^2/4s(x)}\,r'dr' \qquad \text{(B. 10)}$$

Introduce dimensionless variables;

$$\tilde{\rho}_{p_2}(\tilde{x},\tilde{r}) = \frac{u(\infty)}{u(1)}\left(\frac{m_1}{\tilde{v}_{p_2}(\tilde{x})}\right)\frac{e^{-\tilde{r}^2/4D\tilde{s}(\tilde{x})}}{2D\tilde{s}(\tilde{x})}\int_0^{\tilde{r}_b} I_0\left(\frac{\tilde{r}\tilde{r}'}{2D\tilde{s}(\tilde{x})}\right)e^{-\tilde{r}^2/4D\tilde{s}(\tilde{x})}\,\tilde{r}'d\tilde{r}' \qquad \text{(B. 11)}$$

where $\rho_{p_2} = \rho_{p_2}(\infty)\,\tilde{\rho}_{p_2}$. The density $\rho_{p_2}(\infty)$ is the final density if there are no collisions; $\rho_{p_2}(\infty) = (u(1)/u(\infty))\,\rho_{p_2}(1)$.

The density distributions (B. 4) and (B. 11) have been computed numerically and typical solutions are given in Figures B1 and B2. Except for the upstream density distribution of particles σ_2 the state of the gas-particle mixture upstream of the shock wave is the same as that used in the calculations for Figures (18-20). Therefore the

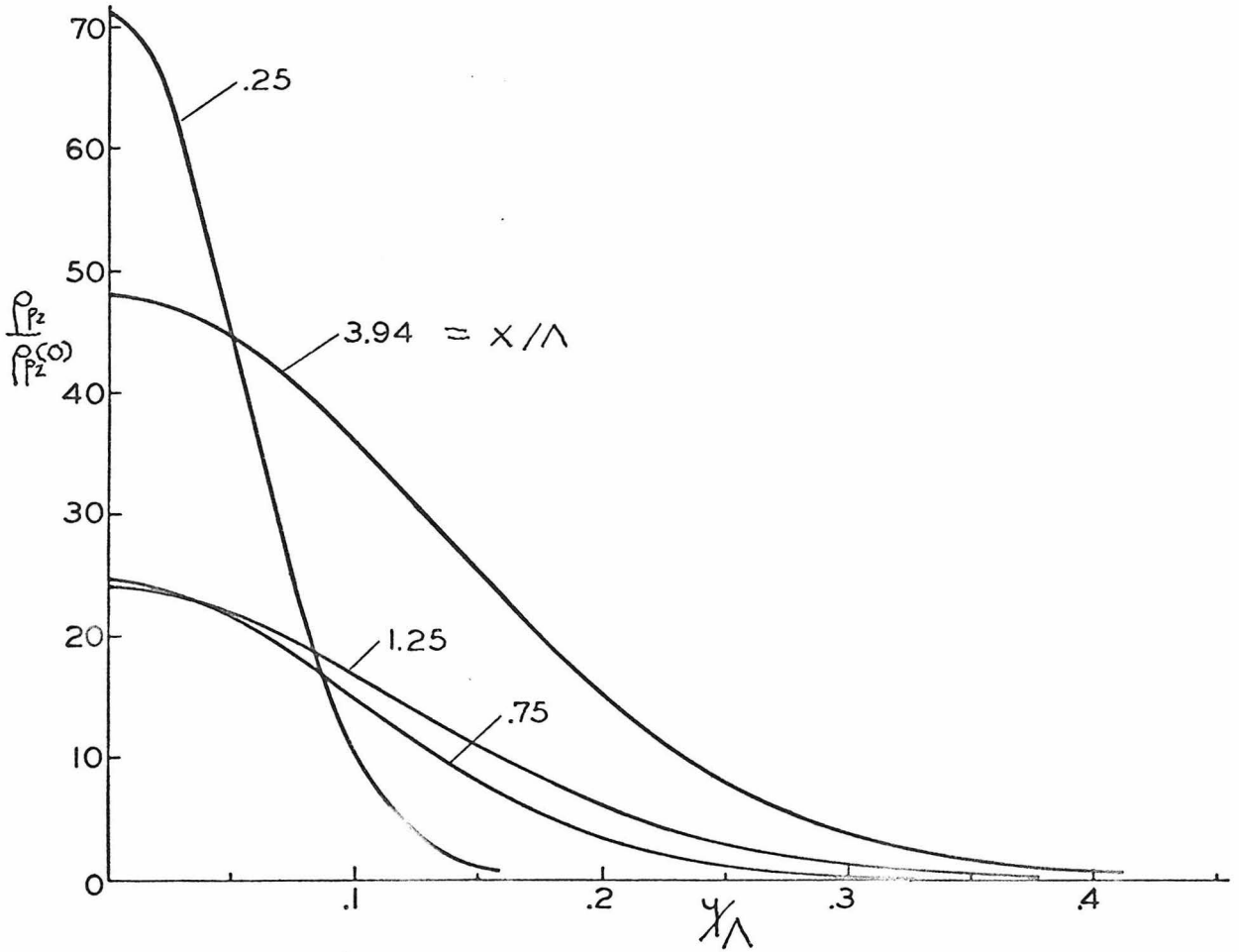

Figure B1. Variation of particle σ_2 cylindrical fundamental beam density distribution downstream of the shock front. Upstream conditions; Gas-Air, $\rho(1) = 1.3 \times 10^{-3}$ gm/cm^3 $T(1) = 20^\circ$C , $M_1 = 3.2$, $\gamma = 1.4$, $K_1 = .25$, $\rho_s/\rho(1) = 10^3$, $\sigma_2/\sigma_1 = 1/4$, $\sigma_1 = 8.0\ \mu$, $\Lambda = \lambda_{v_1} = 31$ cm , $c_s/c_p = \lambda_{v_1}/\lambda_{T_1} = 1$.

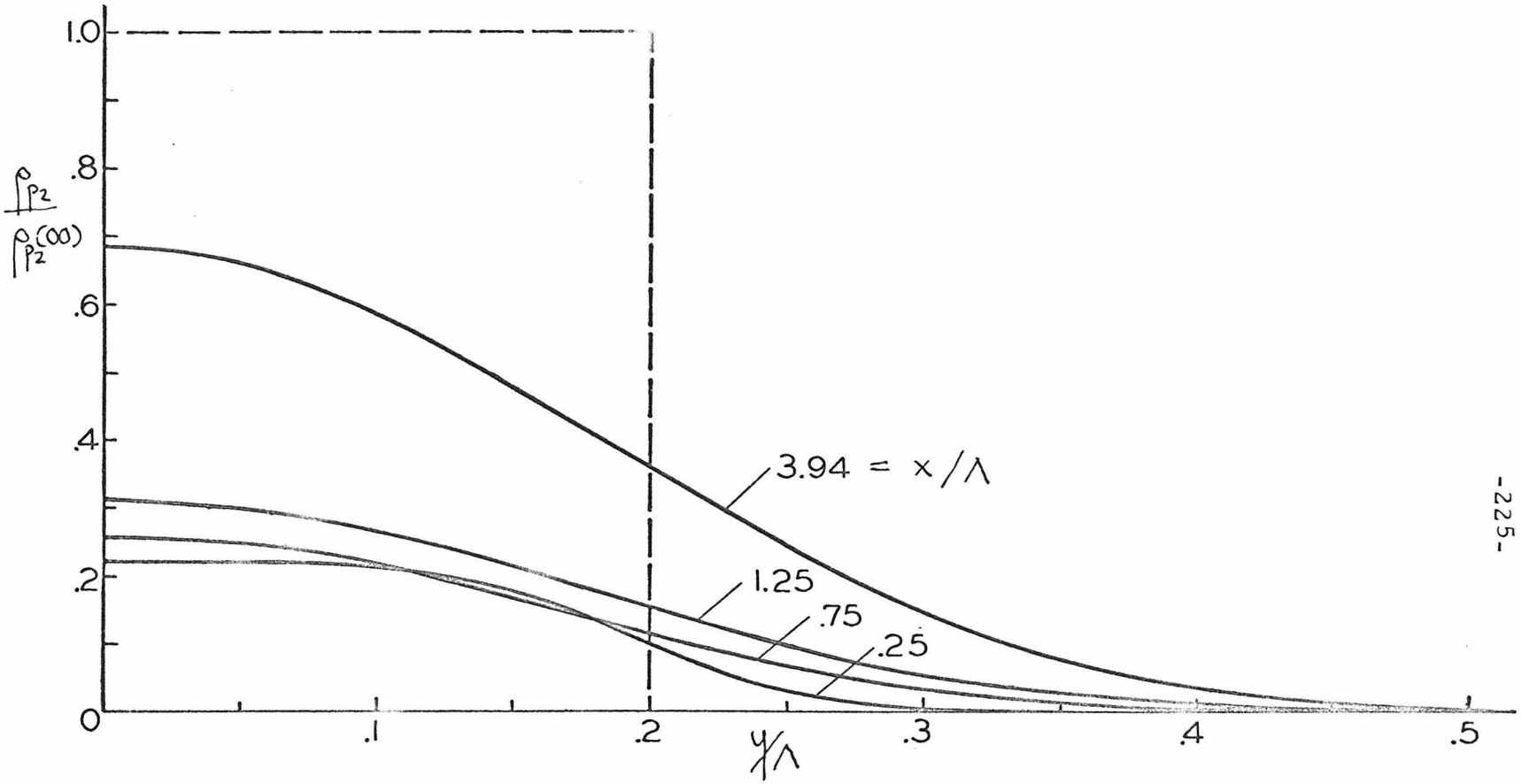

Figure B2. Variation of particle σ_2 cylindrical uniform beam density distribution downstream of the shock front. Upstream conditions; Gas-Air, $\rho(1) = 1.3 \times 10^{-3}$ g/km^3, $T(1) = 20°C$, $M_1 = 3.2$, $\gamma = 1.4$, $K_1 = .25$, $\rho_s/\rho(1) = 10^3$, $\sigma_2/\sigma_1 = 1/4$, $\sigma_1 = 8.0\,\mu$, $\Lambda = \lambda_{u_1} = 31$cm, $\varsigma/\varsigma_p = \lambda_{u_1}/\lambda_{T_1} = 1$.

collision parameters presented in Figure 20 also apply to the present case. Comparison of the results presented in Figures 18 and 19 with corresponding results plotted in Figures B1 and B2 reveals that the essential physical features of the collisional dispersion of particles σ_2 downstream of the shock wave are independent of the cross sectional geometry. The only differences may be accounted for by the fact that, in the cylindrical case, the particles σ_2 are scattered over a larger cross sectional area.